# RADIOLOGY AND ONCOLOGY

vol.55 no.2
june 2021

RADIOLOGY AND ONCOLOGY

*June 2021*
*Vol. 55 No. 2*
*Pages 121-246*
*ISSN 1318-2099*
*UDC 616-006*
*CODEN: RONCEM*

**Publisher**
Association of Radiology and Oncology

**Aims and Scope**
*Radiology and Oncology is a multidisciplinary journal devoted to the publishing original and high quality scientific papers and review articles, pertinent to diagnostic and interventional radiology, computerized tomography, magnetic resonance, ultrasound, nuclear medicine, radiotherapy, clinical and experimental oncology, radiobiology, medical physics and radiation protection. Therefore, the scope of the journal is to cover beside radiology the diagnostic and therapeutic aspects in oncology, which distinguishes it from other journals in the field.*

Editorial office

**Radiology and Oncology**
Zaloška cesta 2
P. O. Box 2217
SI-1000 Ljubljana
Slovenia
Phone: +386 1 5879 369
Phone/Fax: +386 1 5879 434
E-mail: gsersa@onko-i.si



Reader for English
**Vida Kološa**

Secretary
**Mira Klemenčič**
**Zvezdana Vukmirović**

Design
**Monika Fink-Serša, Samo Rovan, Ivana Ljubanović**

Layout
**Matjaž Lužar**

Printed by
**Tiskarna Ozimek,** Slovenia

Published quarterly in 400 copies

*Beneficiary name: DRUŠTVO RADIOLOGIJE IN ONKOLOGIJE*
*Zaloška cesta 2*
*1000 Ljubljana*
*Slovenia*

*Beneficiary bank account number: SI56 02010-0090006751*
*IBAN: SI56 0201 0009 0006 751*
*Our bank name: Nova Ljubljanska banka, d.d.,*
*Ljubljana, Trg republike 2,*
*1520 Ljubljana; Slovenia*

*SWIFT: LJBASI2X*

*Subscription fee for institutions EUR 100, individuals EUR 50*

*The publication of this journal is subsidized by the Slovenian Research Agency.*

Indexed and abstracted by:

- *Baidu Scholar*
- *Case*
- *Chemical Abstracts Service (CAS) - CAplus*
- *Chemical Abstracts Service (CAS) - SciFinder*
- *CNKI Scholar (China National Knowledge Infrastructure)*
- *CNPIEC - cnpLINKer*
- *Dimensions*
- *DOAJ (Directory of Open Access Journals)*
- *EBSCO (relevant databases)*
- *EBSCO Discovery Service*
- *Embase*
- *Genamics JournalSeek*
- *Google Scholar*
- *Japan Science and Technology Agency (JST)*
- *J-Gate*
- *Journal Citation Reports/Science Edition*
- *JournalGuide*
- *JournalTOCs*
- *KESLI-NDSL (Korean National Discovery for Science Leaders)*
- *Medline*
- *Meta*
- *Microsoft Academic*
- *Naviga (Softweco)*
- *Primo Central (ExLibris)*
- *ProQuest (relevant databases)*
- *Publons*
- *PubMed*
- *PubMed Central*
- *PubsHub*
- *QOAM (Quality Open Access Market)*
- *ReadCube*
- *Reaxys*
- *SCImago (SJR)*
- *SCOPUS*
- *Sherpa/RoMEO*
- *Summon (Serials Solutions/ProQuest)*
- *TDNet*
- *Ulrich's Periodicals Directory/ulrichsweb*
- *WanFang Data*
- *Web of Science - Current Contents/Clinical Medicine*
- *Web of Science - Science Citation Index Expanded*
- *WorldCat (OCLC)*

*This journal is printed on acid- free paper*

On the web: ISSN 1581-3207
*https://content.sciendo.com/raon*
*http://www.radioloncol.com*

# contents

*review*

# Covid-19 infection in cancer patients: the management in a diagnostic unit

Vincenza Granata[1], Roberta Fusco[1], Francesco Izzo[2], Sergio Venanzio Setola[1], Michele Coppola[3], Roberta Grassi[4], Alfonso Reginelli[4], Salvatore Cappabianca[4], Roberto Grassi[4,5], Antonella Petrillo[1]

[1] Radiology Division, Istituto Nazionale Tumori IRCCS Fondazione Pascale – IRCCS di Napoli, Naples, Italy
[2] Hepatobiliary Surgical Oncology Division, Istituto Nazionale Tumori IRCCS Fondazione Pascale – IRCCS di Napoli, Naples, Italy
[3] Division of Radiology, Cotugno Hospitals, Naples, Italy
[4] Division of Radiology, University of Campania Luigi Vanvitelli, Naples, Italy
[5] Foundation SIRM, Milan, Italy

Radiol Oncol 2021; 55(2): 121-129.

Received 17 September 2020
Accepted 19 December 2020

Correspondence to: Roberta Fusco, M.D., Radiology Division, Istituto Nazionale Tumori Fondazione Pascale, Naples, Italy.
E-mail: r.fusco@istitutotumori.na.it

Disclosure: No potential conflicts of interest were disclosed.

**Background.** COVID-19 infection is particularly aggressive in frail patients, as cancer patients. Therefore, the more suitable management of the oncological patient requires a multidisciplinary assessment, to identify which patients should be treated, as inpatients or outpatients, and which treatments can be procrastinated.

**Conclusions.** The role of radiologist is crucial, and, all cancer patients who need an imaging evaluation will need to be studied, using the most appropriate imaging tools related to the clinical question and paying a special attention to preserve public health. Guidelines are necessary in the correct organization of a radiology unit to manage patients with suspected or confirmed COVID-19 infection, and whenever possible, a satellite radiography center with dedicated equipment should be used to decrease the transmission risk.

Key words: COVID-19 infection; cancer patients, diagnostic unit; management; guideline

## Introduction

In December 2019, health authorities in Wuhan, China, identified a cluster of acute respiratory disease of unknown etiology.[1] Subsequently the researchers identified a new viral agent, SARS-CoV-2, as responsible for the heart of an international outbreak centred on Hubei. On 30 January 2020, World Health Organization (WHO) confirmed the COVID-19 epidemic as a public health emergency and on 11 March 2020 demarcated the rapid spread of infection as a pandemic in the world.[1,2] Globally, at the time of writing (15 September 2020), there have been 29,525,571 confirmed cases of COVID-19, including 934,192 deaths. In Italy, there have been 289,990 confirmed cases, including 35,633 deaths, reported to WHO.[2] According to the data reported by the Italian authorities, the fatality rates, related to COVID-19 infection, increase exponentially after the age of 70 years, and the presence of an oncological pathology increases the risk of mortality.[3] According to Liang *et al*., cancer patients have a higher risk of getting COVID-19 infection.[4] This data may be correlated to a higher rate of screening, higher risks for nosocomial contaminations and decreased immune defence. Moreover, the rate of pulmonary complications, requiring resuscitation, is higher in cancer patients than in non-cancer patients (39% *vs.* 8%), especially when a treatment was performed in the months before the infection.[4] During epidemic of COVID-19, a guideline for the optimal management of oncological patients urgently needs and the cancer patients should be treated as outpatients if possible

at the nearest medical centre.[5] Conversely, patients who need to be hospitalized for oncological therapies should have COVID-19 infection excluded prior being admitted and more attention should be paid to COVID-19 symptoms identification and of adverse reactions caused by the malignancy or antitumor treatments.[5] However, an intentional postponing of antitumor treatment should be considered according to patient performance status.[5] Therefore, the more suitable management of the cancer patient requires a multidisciplinary assessment, to identify which patients should be treated, as inpatients or outpatients, and which treatments can be procrastinated. It is clear that in this decision the role of radiologist is primary, for a correct staging of the disease as well as for identifying complications from radio- or chemo- therapy. Therefore, in this pandemic condition, all cancer patients who need an imaging evaluation will still need to be studied, using the most appropriate imaging tools related to the clinical question and taking attention to preserve public health.

## Methods

This document is based upon oncological panel of expert opinions by 9 radiologists, 1 cancer surgeon, and 1 radiotherapist, as well as additional expert in statistic. The panel included members of Italian Society of Radiology and Interventional Radiology (SIRM), including the President, the oncology diagnostic imaging section president-elect and the SIRM board. The panel identified four possible scenarios on how to manage a cancer patient during the COVID-19 pandemic in a radiology unit. The entire panel was convened during a single session using a live audio and video interface. The four scenarios were presented, discussed, and refined. These scenarios are intended to support the management of adults only. Children merit separate consideration and are beyond the scope of this document.

We accorded to the "*Grading of Recommendations Assessment, Development and Evaluation (GRADE) basic approaches and rules, and particularly considered experts' evidence to assess the quality of a body of evidence to make recommendations. The level of evidence was categorized as "high quality", "moderate quality", "low quality", or "very low quality". Recommendations were classified as "strong" or "weak". The strong recommendation does not always mean there is sufficient intervention effectiveness. Besides the effectiveness of intervention, the forming of recommendations is based on the severity of the disease, patient willingness, safety, and economics*".[6] "*Once the evidence has been identified and assessed, recommendations were formulated based on the evidence by a face-to-face meeting of panel members and supplemented by experts participating in the panel meeting*".[6]

The document derived also by a comprehensive literature search. Using the following terms "COVID-19 OR SARS-CoV 2" AND "Cancer Patients" AND "Management" and "Imaging" we found a total of 148 articles published between Dec 1st, 2019 and Sept 15th, 2020. Each article was evaluated for relevance to the primary endpoint and a summary of key findings from relevant articles was created. The panel assessed 39 papers that met the document criteria.[7-46]

## Overview of clinical scenarios

Four scenarios can be defined in the radiological management of cancer patient:

1. Non-COVID-19 cancer patient
2. Suspected COVID-19 cancer patient
3. Confirmed COVID-19 cancer patient
4. Cancer Patients with incidental COVID-19 diagnosis

Although each scenario requires different management, however all should be performed with the intent of avoiding contamination for health workers and other patients.

### First scenario: non COVID-19 cancer patient

Patients, with laboratory non confirmed COVID-19 infection by using reverse transcriptase-polymerase chain reaction (RT-PCR) test of nasopharyngeal swab to SARS-CoV-2, are defined as non COVID-19 patients. However, since laboratory tests are not yet used as a screening tool to identify COVID-19 patients, and many people may be asymptomatic or *pauci*-symptomatic it would be appropriate for health professionals to consider all patients as potential infected.[7] Therefore, according to Jin *et al.*[7], all patients should wear N95 (strong recommendation) or surgical mask (weak recommendation), although the Centers for Disease Control and Prevention recommend that patients wear a facemask which can also be just a cloth mask, it is appropriate that a cancer patient, because he is fragile, should wear at least one surgical mask. In addition, while waiting for a radiological procedure,

**TABLE 1.** Recommendations for first scenario – non COVID-19 cancer patient, according to Italian Society of Radiology and Interventional Radiology (SIRM) guidelines[10]

| Patients | Health care staff |
|---|---|
| Wear<br>• N95 mask [strong recommendation]<br>• or surgical mask [weak recommendation] | Wear<br>• N95 mask [strong recommendation]<br>• goggles or face shield [strong recommendation]<br>• gloves [strong recommendation]<br>• surgical cap [weak recommendation]<br>• shoe covers [weak recommendation] |
| Stay away from other people (at least 6 feet of distance) [strong recommendation] | Clean and disinfect with 500 mg/L chlorine-containing disinfectant the radiological equipment used, clean their hands properly, and the room should be opened for appropriate ventilation [strong recommendation] |

the patient should stay away from other people (at least 6 feet of distance). The family members, accompanying patient, should follow the same recommendations.

The healthcare staff should wear N95 mask, avoids direct contact with patient's secretions, especially oral or respiratory, wear goggles or face shield, wear gloves, wash or disinfect hands before wearing gloves and after removing the gloves. A surgical cap and shoe covers may be added. After each radiological procedure, the community hospital should clean and disinfect with 500 mg/L chlorine-containing disinfectant the radiological equipment used, clean their hands properly, and the room should be opened for appropriate ventilation. The isolation times of the section in which the person has stayed depend on the number of air parts insured for the environment (about 6/h with related 69 minutes of isolation), according to SIRM guidelines (Table 1).[7-10]

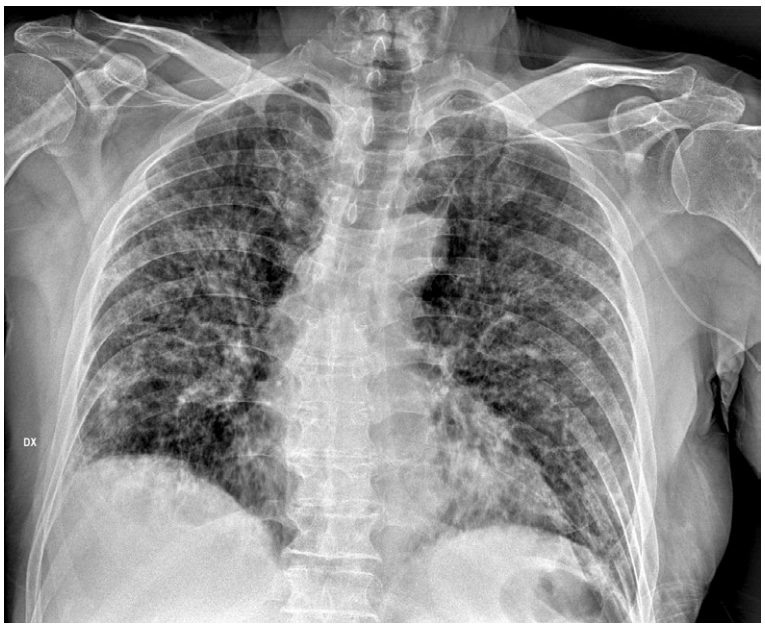


**FIGURE 1.** Man, 64 year. Chest x-ray shows patchy consolidation and strip-like opacities in a patient with confirmed COVID-19 infection by reverse transcriptase-polymerase chain reaction (RT-PCR).

## Second scenario: suspected covid-19 cancer patient

Suspected infected patient should be isolated, controlled, and diagnostic confirmation should be as quick as possible. Patients with mild symptoms should remain in home isolation, while patients with severe symptoms should be hospitalized, following the isolation guidelines.[7] As for the first scenario, also in this case patient and healthcare staff should follow the same procedures concerning the use of masks, wear goggles or face shield, gloves and the distance of at least 6 feet if possible, avoiding direct contact with respiratory secretions, so as disinfection procedures for radiological equipment and rooms. In this scenario, it asks the radiologist to confirm the diagnosis of COVID-19. COVID-19 diagnosis is made by RT-PCR test, however radiological test is suggested for medical triage of suspected patients with moderate-severe clinical symptoms and with higher pre-test infection probability.[8] The reported sensitivity of chest x-ray (CXR) for COVID-19 pneumonia is relatively low in the early phase of the disease and in mild cases (69%).[48] Conversely, chest computed tomography (CT) shows greater sensitivity for early pneumonic change, disease progression, and alternative diagnoses; the administration of the intravenous contrast medium, is essential for the diagnosis of pulmonary thromboembolism.[9] However, in Italy, to reduce the possibility of the spread of the infection, in accordance with the Italian Society of Radiology and Interventional Radiology (SIRM) guidelines, CXR is the first tool to be used in patients with suspected COVID-19 (see Figure 1 that shown a patchy consolidation and strip-like opacity in a

**TABLE 2.** Recommendations for second scenario – suspected COVID-19 cancer patient, according to Italian Society of Radiology and Interventional Radiology (SIRM) guidelines[10]

| Patients | Healthcare staff |
|---|---|
| Isolated, controlled, and diagnostic confirmation should be as quick as possible | |
| Wear<br>• N95 mask [strong recommendation]<br>• or surgical mask [weak recommendation] | Wear<br>• N95 mask [strong recommendation]<br>• goggles or face shield [strong recommendation]<br>• gloves [strong recommendation]<br>• surgical cap [weak recommendation]<br>• shoe covers [weak recommendation] |
| Stay away from other people (at least 6 feet of distance) [strong recommendation] | Clean and disinfect with 500 mg/L chlorine-containing disinfectant the radiological equipment used, clean their hands properly, and the room should be opened for appropriate ventilation [strong recommendation] |
| | Diagnostic tool<br>• Chest radiography (CXR; not very sensitive), with portable equipment in the isolation room [strong recommendation]<br>• Computed tomography (CT; greater sensitivity) for early pneumonic change, disease progression, and alternative diagnoses;<br>the administration of the intravenous contrast medium for the diagnosis of pulmonary thromboembolism |

patient with confirmed COVID-19 disease by RT-PCR).[10] Since, portable equipment for performing the diagnostic investigation in the patient 's isolation room is the element that might favour CXR in selected patients, reducing the risk of COVID-19 infection and eliminating the risk related to the transport route to a CT scanner (Table 2).[8]

## Third scenario: confirmed COVID-19 cancer patient

*"The COVID-19 infected patients show symptoms as fatigue, fever, dry cough, dyspnoea, with or without nasal congestion, runny nose or other upper respiratory symptoms. Patients with mild symptoms may have no signs, conversely in patients with severe symptoms, we could find breath shortness, moist rales in lungs, weakened breath sounds, dullness in percussion, and increased or decreased tactile speech tremor. During the early stage of COVID-19 disease, the leukocytes number in peripheral blood was normal or decreased and the lymphocyte count decreased. In some patients, liver enzyme, creatine kinase and myoglobin increased. In severe case, the increase of D-dimer was reported. The typical CT/CXR imaging findings were multiple, patchy, sub-segmental or segmental ground-glass opacities in both lungs. They were classified as "paving stone-like" changes by fine-grid or small honeycomb-like thickening of interlobular septa. In the elderly or severe condition patients more common features are multiple, patchy or large patches*

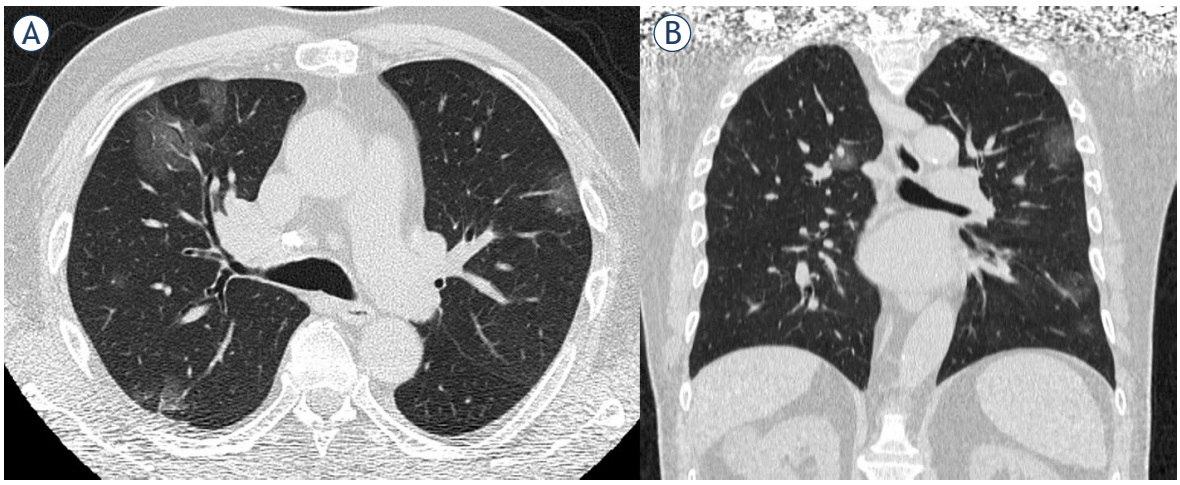


**FIGURE 2.** Man, 53 year. CT shows multiple focal ground-glass opacities. **(A)** Axial plane, **(B)** multiplanar reconstruction in coronal plane.

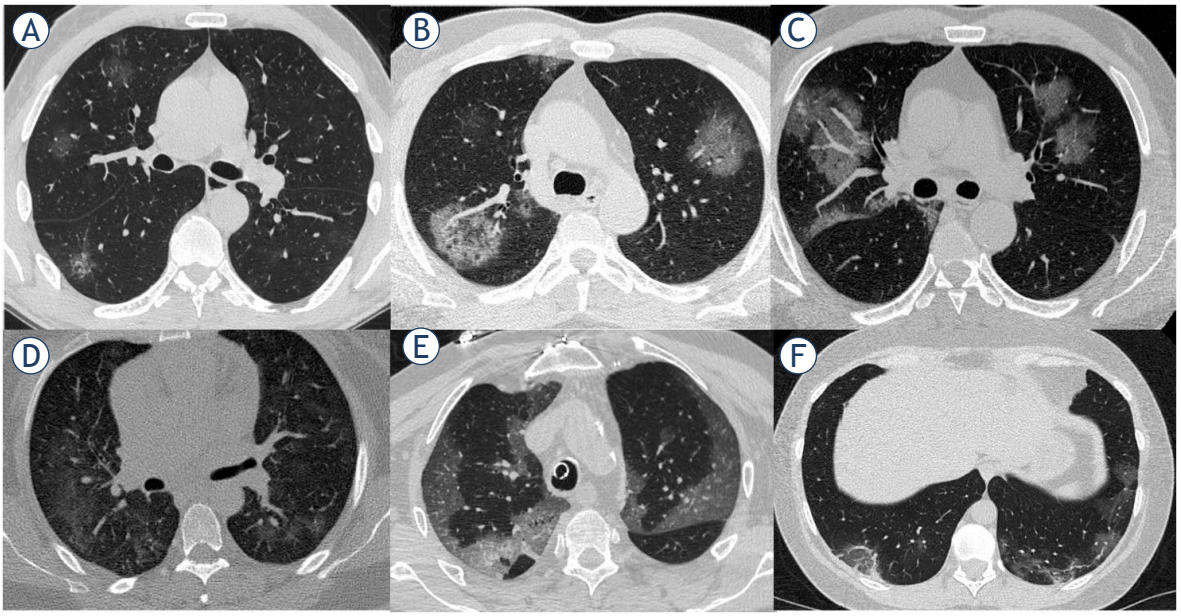


**FIGURE 3.** Man, 61 year. CT shows ground-glass opacities separated by thickened interlobular septa. **(A-F)** Axial planes.

*of consolidation in both lungs, with a little grid-like or honeycomb-shaped interlobular septal thickening, especially in the middle and lower lobes. Based on CT image we find 5 stages according to the time of onset and the response of body to the virus"*[7]:

1. *Ultra-early stage*. The stage without clinical symptoms, within 1–2 weeks after the infection. *"The typical imaging features are single, double or scattered focal ground-glass opacity, nodules located in central lobule surrounded by patchy ground-glass opacities, patchy consolidation and sign of intrabronchial air-bronchogram, which was dominant in the middle and lower pleura"*[7] (Figure 2).
2. *Early stage*. One-three days after clinical manifestations. *"CT scan shows single or multiple scattered patchy or agglomerated ground-glass opacities, separated by honeycomb-like or grid-like thickened of interlobular septa"* [7] – crazy paving (Figure 3).

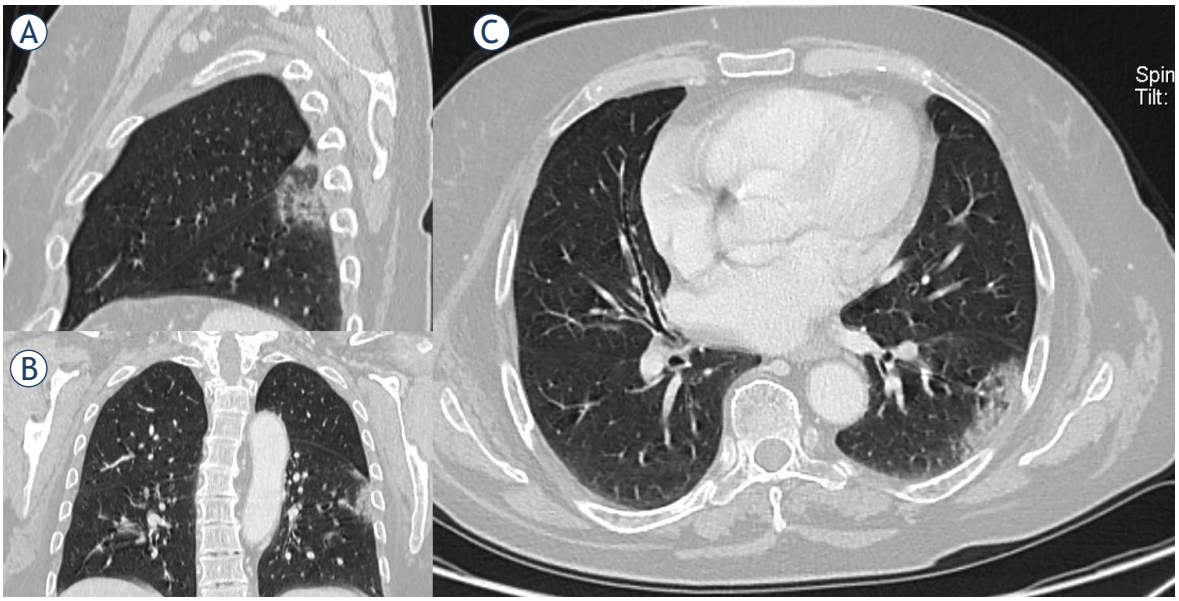


**FIGURE 4.** Woman, 54 year. CT shows patchy consolidation in apical segment of left lower lung. **(A)** Multiplanar reconstruction in sagittal plane; **(B)** multiplanar reconstruction in coronal plane; **(C)** axial plane.

**TABLE 3.** Recommendations for third scenario - confirmed Covid-19 cancer patient, according to Italian Society of Radiology and Interventional Radiology (SIRM) guidelines[10]

| Patients | Healthcare staff |
|---|---|
| Isolated and controlled<br>• treated in designated hospitals with isolation and protection conditions<br>[strong recommendation] | Medical personnel enter into the isolation area through designated channels<br>(strongrecommendation] |
| Wear<br>• N95 mask [strong recommendation]<br>• or surgical mask [weak recommendation] | Wear<br>• N95 mask (strong recommendation]<br>• goggles or face shield (strong recommendation]<br>• gloves (strong recommendation]<br>• surgical cap (weak recommendation]<br>• shoe covers(weak recommendation] |
| Stay away from other people<br>(at least 6 feet of distance)<br>[strong recommendation] | Clean and disinfect with 500 mg/L chlorine-containing disinfectant the radiological equipment used, clean their hands properly, and the room should be opened for appropriate ventilation<br>[strong recommendation] |
| | Diagnostic tool<br>• daily chest radiographs are not indicated<br>• CT scan is indicated for the evaluation of the stage of infection, for defining complications and for a correct differential diagnosis<br>• The chest ultrasound (POCUS – point-of-care ultrasound) a monitoring tool to evaluate the effectiveness of the prono-supination manoeuvres |

3. *Rapid progression stage*. Three-seven days after clinical manifestations started. "*CT features are a fused and large-scale light consolidation sometimes with air-bronchogram inside*".[7]
4. *Consolidation stage*. Seven- fourteen days after clinical symptoms appeared. "*CT shows multiple patchy consolidations in slighter density and smaller range than that of the previous stage*"[7] (Figure 4).
5. *Dissipation stage*. Two and 3weeks after the onset of clinical symptoms. "*CT shows patchy consolidation or strip-like opacity. As time goes on, it showed grid-like thickening of interlobular septa, thickening and strip-like twist of bronchial walls and a few scattered patchy consolidations*"[7] (Figure 5).

"*Confirmed infected patients should be treated in designated hospitals with isolation and protection conditions. Medical personnel enter into the isolation area with proper self-protection through designated channels*".[7]

Several features should be considered in for imaging methods in the COVID-19 patient. First, daily chest radiographs are not indicated in stable intubated patients with COVID-19, so it is possible also to reduce exposure risk of radiology technicians.[8] Second, CT scan is indicated for the evaluation of the stage of infection, for defining complications and for a correct differential diagnosis.[8] Third, the chest ultrasound (POCUS – point-of-care ultrasound), performed by the intensivists at the patient's bed, can also represent a monitoring tool to evaluate the effectiveness of the prono-supination manoeuvres. Systematic application of the POCUS can reduce the use of diagnostic imaging resources, also reducing staff exposure to possible contamination and helping to optimize therapies especially in critically ill patients (Table 3).[10-12]

## Fourth scenario: Cancer patients with incidental COVID-19 diagnosis

We defined cancer patient with incidental COVID-19 diagnosis, when the diagnosis is random, during examination by staging or follow-up for oncological disease. CT features of COVID-19 infection are non-specific, however, the detection of these in an asymptomatic patient allows to identify that group of asymptomatic patients who can favour the spread of the infection in the community. It is reported that asymptomatic carriers of COVID-19 are 17.9%–33.3% of all infected cases.[13,14] The undetected infected patients are responsible for a rapid spread of SARS-CoV2.[15] RT-PCR test in this scenario is important to identify an occult infection and limit further transmission within the community. Therefore, although in the cancer patient, especially when undergoing immunotherapy, interstitial pneumonia may be a complication of treatment, in a pandemic phase it is essential to exclude COVID-19 infection, so that the patient, even asymptomatic, must be considered infected before laboratory tests (Table 4).

**TABLE 4.** Fourth scenario -Cancer Patients with incidental COVID-19 diagnosis, according to Italian Society of Radiology and Interventional Radiology (SIRM) guidelines[10]

| Patients | Healthcare staff |
|---|---|
| Controlled<br>• diagnostic confirmation should be as quick as possible [strong recommendation] | |
| Wear<br>• N95 mask [strong recommendation]<br>• or surgical mask [weak recommendation] | Wear<br>• N95 mask [strong recommendation]<br>• goggles or face shield [strong recommendation]<br>• gloves [strong recommendation]<br>• surgical cap [weak recommendation]<br>• shoe covers [weak recommendation] |
| Stay away from other people (at least 6 feet of distance) [strong recommendation] | Clean and disinfect with 500 mg/L chlorine-containing disinfectant the radiological equipment used, clean their hands properly, and the room should be opened for appropriate ventilation [strong recommendation] |

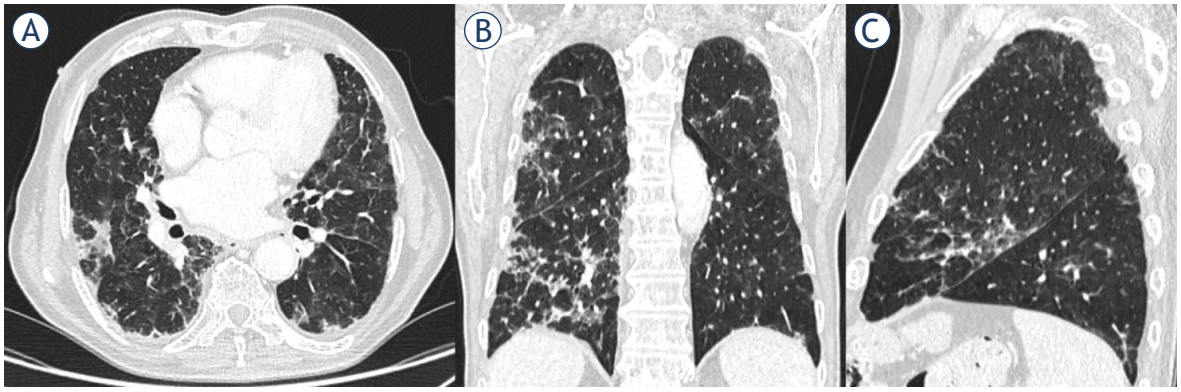


**FIGURE 5.** Man, 76 year. CT shows strip-like opacity, grid-like thickening of interlobular septa, thickening and strip-like twist of bronchial walls and patchy consolidations. **(A)** Axial plane; **(B)** multiplanar reconstruction in coronal plane; **(C)** multiplanar reconstruction in sagittal plane.

## Infection prevention in a radiology unit

Up to day, it is known that the main source of COVID-19 infection are patients during the first week of infection, later the viral load diminishes and in some studies live virus was not isolated past 8th day post infection. Respiratory droplet is the main route of transmission, so as strict contact. Although, several data, as the source of the virus and its ability to spread between people is unknown, however it is clear that it is possible a human-to-human transmission.[16]

"*For healthcare providers, the centers for disease control (CDC) groups medical-related exposures into low, medium, and high-risk*".[17] Within a radiology unit, a brief, without protection interaction with an infected patient, so as a prolonged close contact with a masked, are classified as low-risk exposures.[17,18] However, the radiographers, since exposed continuously, might be infected to COVID-19. Therefore, guidelines are necessary in the correct organization of a radiology unit to manage patients with suspected or confirmed COVID-19 infection, and if possible, portable diagnostic equipment should be employed to reduce the patient's movements. Moreover, it would also be appropriate to use a satellite radiography centre with dedicated equipment to decrease the risk of transmission. The Centers for Disease Control and Prevention guidelines for SARS COVID-19 recommended that the healthcare staff should wear N95 mask, avoid direct contact with patient's secretions, especially oral or respiratory, wear goggles or face shield, wear gloves, wash or disinfect hands before wearing gloves and after removing the gloves. A surgical cap and shoe covers may be added.[17,46] Radiological equipment, such as CT and Magnetic Resonance (MR), ultrasound probes, and image viewing station should

be disinfected after every contact with suspected patients. Health personnel with suspicious exposure, without adequate personal protective equipment, should be observed for 14-day, starting from the last day of contact with the COVID-19 infected patients. If properly trained, the can avoid contamination of equipment, staff and other patients.[19]

## Conclusions

COVID-19 infection is particularly aggressive in frail patients, as cancer patients. Therefore, the more suitable management of the cancer patient requires a multidisciplinary assessment, to identify which patients should be treated, as inpatients or outpatients, and which treatments can be procrastinated. It is clear that the role of radiologist is crucial, and, all cancer patients who need an imaging evaluation will still need to be studied, using the most appropriate imaging tools related to the clinical question and taking attention to preserve public health. Therefore, guidelines are necessary in the correct organization of a radiology unit to manage patients with suspected or confirmed COVID-19 infection, and whenever possible, a satellite radiography center with dedicated equipment should be used to decrease the risk of transmission.

## References


1. Lake MA. What we know so far: COVID-19 current clinical knowledge and research. *Clin Med* 2020; **20:** 124-7. doi: 10.7861/clinmed.2019-coron
2. World Health Organization. Rolling updates on coronavirus disease (COVID-19). [cited 2020 Sep 3]. Available at: https://www.who.int/emergencies/diseases/novel-coronavirus-2019/events-as-they-happen
3. Falandry C, Filteau C, Ravot C, Le Saux O. Challenges with the management of older patients with cancer during the COVID-19 pandemic. *J Geriatr Oncol* 2020. **11:** 747-9. doi: 10.1016/j.jgo.2020.03.020
4. Liang W, Guan W, Chen R, Wang W, Li J, Xu K, et al. Cancer patients in SARS-CoV-2 infection: a nationwide analysis in China. *Lancet Oncol* 2020; **2:** 335-7. doi: 10.1016/S1470-2045(20)30096-6
5. Lung Cancer Study Group, Chinese Thoracic Society, Chinese Medical Association; Chinese Respiratory Oncology Collaboration. [Expert recommendations on the management of patients with advanced non-small cell lung cancer during epidemic of COVID-19 (Trial version)]. [Article in Chinese]. *ZhonghuaJie He He Hu Xi ZaZhi* 2020; **43:** 297-301. doi: 10.3760/cma.j.cn112147-20200221-00138
6. Mendoza C, Kraemer P, Herrera P, Burdiles P, Sepúlveda D, Núñez E, et al. [Clinical guidelines using the GRADE system (Grading of recommendations assessment, development and evaluation)]. *Rev Med Chil* 2017; **145:** 1463-70. doi: 10.4067/s0034-98872017001101463
7. Jin YH, Cai L, Cheng ZS, Cheng H, Deng T, Fan YP, et al; for the Zhongnan Hospital of Wuhan University Novel Coronavirus Management and Research Team, Evidence-Based Medicine Chapter of China International Exchange and Promotive Association for Medical and Health Care (CPAM). A rapid advice guideline for the diagnosis and treatment of 2019 novel coronavirus (2019-nCoV) infected pneumonia (standard version). *Mil Med Res* 2020; **7:** 4. doi: 10.1186/s40779-020-0233-6
8. Rubin GD, Ryerson CJ, Haramati LB, Sverzellati N, Kanne JP, Raoof S, et al. The role of chest imaging in patient management during the COVID-19 pandemic: a multinational consensus statement from the Fleischner Society. *Chest* 2020; **158:** 106-16. doi: 10.1016/j.chest.2020.04.003
9. Wong HYF, Lam HYS, Fong AH, Leung ST, Chin TW, Lo CSY, et al. Frequency and distribution of chest radiographic findings in COVID-19 positive patients. *Radiology* 2020; **296:** E72-8. doi: 10.1148/radiol.2020201160
10. Italian Society of Radiology – SIRM. Covid-19 database. [cited 2020 Oct 25]. Available at: https://www.sirm.org
11. Peng QY, Wang XT, Zhang LN, Chinese Critical Care Ultrasound Study Group (CCUSG). Findings of lung ultrasonography of novel corona virus pneumonia during the 2019-2020 epidemic. *Intensive Care Med* 2020; **46:** 849-50. doi: 10.1007/s00134-020-05996-6
12. See KC, Ong V, Tan YL, Sahagun J, Taculod J. Chest radiography versus lung ultrasound for identification of acute respiratory distress syndrome: a retrospective observational study. *Crit Care* 2018; **22:** 1-9. doi: 10.1186/s13054-018-2105-y
13. Mizumoto K, Kagaya K, Zarebski A, Chowell G. Estimating the asymptomatic proportion of coronavirus disease 2019 (COVID-19) cases on board the Diamond Princess cruise ship, Yokohama, Japan, 2020. *Euro Surveill* 2020; **25:** 2000180. doi: 10.2807/1560-7917.ES.2020.25.10.2000180
14. Nishiura H, Kobayashi T, Miyama T, Suzuki A, Jung SM, Hayashi K, et al. Estimation of the asymptomatic ratio of novel coronavirus infections (COVID-19). *Int J Infect Dis* 2020; **94:** 154-55. doi: 10.1016/j.ijid.2020.03.020
15. Li R, Pei S, Chen B, Song Y, Zhang T, Yang W, et al. Substantial undocumented infection facilitates the rapid dissemination of novel coronavirus (SARS-CoV2). *Science* 2020; **368:** 489-93. doi: 10.1126/science.abb3221
16. Zhou P, Yang XL, Wang XG, Hu B, Zhang L, Zhang W, et al. A pneumonia outbreak associated with a new coronavirus of probable bat origin. *Nature* 2020; **579:** 270-3. doi: 10.1038/s41586-020-2012-7
17. Center for Disease Control and Prevention. Interim U.S. Guidance for risk assessment and public health management of healthcare personnel with potential exposure in a healthcare setting to patients with coronavirus disease (COVID-19); 2020. [cited 2020 Apr 01]. Available at: https://www.cdc.gov/coronavirus/2019-ncov/hcp/guidance-risk-assesment-hcp.html
18. Center for Disease Control and Prevention. Coronavirus disease 2019 (COVID-19) public health recommendations for community-Related exposure; 2020. [cited 2020 Apr 01]. Available at: https://www.cdc.gov/coronavirus/2019-ncov/php/public-health-recommendations.html
19. Kooraki S, Hosseiny M, Myers L, Gholamrezanezhad A. Coronavirus (COVID-19) outbreak: what the department of radiology should know. *J Am Coll Radiol* 2020; **17:** 447-51. doi: 10.1016/j.jacr.2020.02.008
20. Belfiore MP, Urraro F, Grassi R, Giacobbe G, Patelli G, Cappabianca S, et al. Artificial intelligence to codify lung CT in Covid-19 patients. *Radiol Med* 2020; **125:** 500-4. doi: 10.1007/s11547-020-01195-x
21. Borghesi A, Zigliani A, Masciullo R, Golemi S, Maculotti P, Farina D, et al. Radiographic severity index in COVID-19 pneumonia: relationship to age and sex in 783 Italian patients. *Radiol Med* 2020; **125:** 461-4. doi: 10.1007/s11547-020-01202-1
22. Borghesi A, Maroldi R. COVID-19 outbreak in Italy: experimental chest X-ray scoring system for quantifying and monitoring disease progression. *Radiol Med* 2020; **125:** 509-13. doi: 10.1007/s11547-020-01200-3
23. Fichera G, Stramare R, De Conti G, Motta R, Giraudo C. It's not over until it's over: the chameleonic behaviour of COVID-19 over a six-day period. *Radiol Med* 2020; **125:** 514-6. doi: 10.1007/s11547-020-01203-0
24. Neri E, Miele V, Coppola F, Grassi R. Use of CT and artificial intelligence in suspected or COVID-19 positive patients: statement of the Italian Society of Medical and Interventional Radiology. *Radiol Med* 2020; **125:** 505-8. doi: 10.1007/s11547-020-01197-9
25. Agostini A, Floridi C, Borgheresi A, Badaloni M, Esposto Pirani P, Terilli F, et al. Proposal of a low-dose, long-pitch, dual-source chest CT protocol on third-generation dual-source CT using a tin filter for spectral shaping at 100 kVp for Corona Virus Disease 2019 (COVID-19) patients: a feasibility study. *Radiol Med* 2020; **125:** 365-73. doi: 10.1007/s11547-020-01179-x
26. Giovagnoni A. Facing the COVID-19 emergency: we can and we do. *Radiol Med* 2020; **125:** 337-8. doi: 10.1007/s11547-020-01178-y

27. Pediconi F, Galati F, Bernardi D, Belli P, Brancato B, Calabrese M, et al. Breast imaging and cancer diagnosis during the COVID-19 pandemic: recommendations from the Italian College of Breast Radiologists by SIRM. *Radiol Med* 2020; **125:** 926-30. doi: 10.1007/s11547-020-01254-3

28. Neri E, Miele V, Coppola F, Grassi R. Use of CT and artificial intelligence in suspected or COVID-19 positive patients: statement of the Italian Society of Medical and Interventional Radiology. *Radiol Med* 2020; **125:** 505-8. doi:10.1007/s11547-020-01197-9

29. Neri E, Coppola F, Larici AR, Sverzellati N, Mazzei MA, Sacco P, et al. Structured reporting of chest CT in COVID-19 pneumonia: a consensus proposal. *Insights Imaging* 2020; **11:** 92. doi: 10.1186/s13244-020-00901-7

30. Byrne D, O'Neill SB, Müller NL, Jalal S, Parker W, Nicolaou S, et al. RSNA Expert consensus Statement on reporting chest CT findings related to COVID-19: interobserver agreement between chest radiologists. *Can Assoc Radiol J* 2020, Jul 2; 846537120938328. [Ahead of print]. doi:10.1177/0846537120938328

31. Huang Z, Zhao S, Li Z, Chen W, Zhao L, Deng L, et al. The battle against coronavirus disease 2019 (COVID-19): emergency management and infection control in a radiology department. *J AmColl Radiol* 2020; **17:** 710-6. doi: 10.1016/j.jacr.2020.03.011

32. Rubin GD, Ryerson CJ, Haramati LB, Sverzellati N, Kanne JP, Raoof S, et al. The role of chest imaging in patient management during the COVID-19 pandemic: a multinational consensus statement from the Fleischner Society. *Radiology* 2020; **296:** 172-80. doi: 10.1148/radiol.2020201365

33. Albano D, Bruno A, Bruno F, Calandri M, Caruso D, Clemente A, et al. Impact of coronavirus disease 2019 (COVID-19) emergency on Italian radiologists: a national survey. *Eur Radiol* 2020; **30:** 6635-44. 1-10. doi: 10.1007/s00330-020-07046-7

34. Belfiore MP, Urraro F, Grassi R, Giacobbe G, Patelli G, Cappabianca S, et al. Artificial intelligence to codify lung CT in Covid-19 patients. *Radiol Med* 2020; **125:** 500-4. doi: 10.1007/s11547-020-01195-x

35. Laghi A, Grassi R. Italian radiology's response to the COVID-19 outbreak. *J Am Coll Radiol* 2020; **17:** 699-700. doi: 10.1016/j.jacr.2020.04.012

36. Duggan NM, Liteplo AS, Shokoohi H, Goldsmith AJ. Using lung point-of-care ultrasound in suspected COVID-19: case series and proposed triage algorithm. *Clin Pract Cases Emerg Med* 2020; **4:** 289-94. doi: 10.5811/cpcem.2020.7.47912

37. Di Serafino M, Notaro M, Rea G, Iacobellis F, Paoli VD, Acampora C, et al. The lung ultrasound: facts or artifacts? In the era of COVID-19 outbreak. *Radiol Med* 2020; **125:** 738-53. doi: 10.1007/s11547-020-01236-5

38. Alilio PM, Ebeling-Koning NE, Roth KR, Desai T. Lung point-of-care (POCUS) ultrasound in a pediatric COVID-19 case. *Radiol Case Rep* 2020; **15:** 2314-8. doi: 10.1016/j.radcr.2020.09.007

39. Shen C, Yu N, Cai S, Zhou J, Sheng J, Liu K, et al. Evaluation of dynamic lung changes during coronavirus disease 2019 (COVID-19) by quantitative computed tomography. *J Xray Sci Technol* 2020; **28:** 863-73. doi: 10.3233/XST-200721

40. Pakdemirli E, Mandalia U, Monib S. Characteristics of chest CT images in patients with COVID-19 pneumonia in London, UK. *Cureus* 2020; **12:** e10289. doi: 10.7759/cureus.10289

41. Gatti M, Calandri M, Barba M, Biondo A, Geninatti C, Gentile S, et al. Baseline chest X-ray in coronavirus disease 19 (COVID-19) patients: association with clinical and laboratory data. *Radiol Med* 2020; **125;** 1271-9. doi: 10.1007/s11547-020-01272-1

42. Giannitto C, Sposta FM, Repici A, Vatteroni G, Casiraghi E, Casari E, et al. Chest CT in patients with a moderate or high pretest probability of COVID-19 and negative swab. *Radiol Med* 2020; **125:** 1260-70. doi:10.1007/s11547-020-01269-w

43. Cartocci G, Colaiacomo MC, Lanciotti S, Andreoli C, De Cicco ML, Brachetti G, et al. Chest CT for early detection and management of coronavirus disease (COVID-19): a report of 314 patients admitted to emergency department with suspected pneumonia. *Radiol Med* 2020; **125:** 931-42. doi: 10.1007/s11547-020-01256-1

44. Ierardi AM, Wood BJ, Arrichiello A, Bottino N, Bracchi L, Forzenigo L, et al. Preparation of a radiology department in an Italian hospital dedicated to COVID-19 patients. *Radiol Med* 2020; **125:** 894-901. doi: 10.1007/s11547-020-01248-1

45. Cozzi D, Albanesi M, Cavigli E, Moroni C, Bindi A, Luvarà S, et al. Chest X-ray in new coronavirus disease 2019 (COVID-19) infection: findings and correlation with clinical outcome. *Radiol Med* 2020; **125:** 730-7. doi: 10.1007/s11547-020-01232-9

46. Rawashdeh MA, Saade C. Radiation dose reduction considerations and imaging patterns of ground glass opacities in coronavirus: risk of over exposure in computed tomography. *Radiol Med* 2020, Sep 8; [Ahead of print]. doi:10.1007/s11547-020-01271-2

47. Larici AR, Cicchetti G, Marano R, Merlino B, Elia L, Calandriello L, et al. Multimodality imaging of COVID-19 pneumonia: from diagnosis to follow-up. A comprehensive review. *Eur J Radiol* 2020; **131:** 109217. doi: 10.1016/j.ejrad.2020.109217

48. Carlos RC, Lowry KP, Sadigh G. The coronavirus disease 2019 (COVID-19) pandemic: a patient-centered model of systemic shock and cancer care adherence. *J Am Coll Radiol* 2020; **17:** 927-30. doi: 10.1016/j.jacr.2020.05.032

review

# An overview of hepatocellular carcinoma with atypical enhancement pattern: spectrum of magnetic resonance imaging findings with pathologic correlation

Jelena Djokic Kovac[1], Aleksandar Ivanovic[1], Tamara Milovanovic[2], Marjan Micev[3], Francesco Alessandrino[4], Richard M. Gore[5]

[1] Center for Radiology and MRI, Clinical Center Serbia, School of Medicine, University of Belgrade; Belgrade, Serbia
[2] Clinic for Gastroenterology and Hepatology, Clinical Center of Serbia School of Medicine, University of Belgrade; Belgrade, Serbia
[3] Departament of Digestive Pathology, Clinical Center of Serbia, Belgrade, Serbia
[4] Division of Abdominal Imaging, Department of Radiology, Beth Israel Deaconess Medical Center, Harvard Medical School, Boston, USA
[5] Department of Gastrointestinal Radiology, NorthShore University, Evanston, Pritzker School of Medicine at the University of Chicago, USA

Radiol Oncol 2021; 55(2): 130-143.

Received 9 October 2020
Accepted 15 December 2020

Correspondence to: Jelena Djokic Kovac, M.D., Ph.D., Associate Professor, Center for Radiology and Magnetic Resonance Imaging, Clinical Center of Serbia, School of Medicine, University of Belgrade, Pasterova 2, 11000 Belgrade, Serbia. E-mail: jelenadjokickovac@gmail.com

Disclosure: No potential conflicts of interest were disclosed.

**Background.** In the setting of cirrhotic liver, the diagnosis of hepatocellular carcinoma (HCC) is straightforward when typical imaging findings consisting of arterial hypervascularity followed by portal-venous washout are present in nodules larger than 1 cm. However, due to the complexity of hepatocarcinogenesis, not all HCCs present with typical vascular behaviour. Atypical forms such as hypervascular HCC without washout, isovascular or even hypovascular HCC can pose diagnostic dilemmas. In such cases, it is important to consider also the appearance of the nodules on diffusion-weighted imaging and hepatobiliary phase. In this regard, diffusion restriction and hypointensity on hepatobiliary phase are suggestive of malignancy. If both findings are present in hypervascular lesion without washout, or even in iso- or hypovascular lesion in cirrhotic liver, HCC should be considered. Moreover, other ancillary imaging findings such as the presence of the capsule, fat content, signal intensity on T2-weighted image favour the diagnosis of HCC. Another form of atypical HCCs are lesions which show hyperintensity on hepatobiliary phase. Therefore, the aim of the present study was to provide an overview of HCCs with atypical enhancement pattern, and focus on their magnetic resonance imaging (MRI) features.

**Conclusions.** In order to correctly characterize atypical HCC lesions in cirrhotic liver it is important to consider not only vascular behaviour of the nodule, but also ancillary MRI features, such as diffusion restriction, hepatobiliary phase hypointensity, and T2-weighted hyperintensity. Fat content, corona enhancement, mosaic architecture are other MRI feautures which favour the diagnosis of HCC even in the absence of typical vascular profile.

Key words: hepatocellular carcinoma; liver cirrhosis; magnetic resonance imaging; diffusion magnetic resonance imaging

## Introduction

Hepatocellular carcinoma (HCC) is the most common primary hepatic malignancy, and the fifth cause of cancer mortality worldwide.[1,2] In more than 90% of cases, HCC occurrs in a cirrhotic liver.[3,4] The diagnosis of HCC at an early stage is of great clinical importance since curative treatments

such as resection, transplantation, or local ablation therapy are possible.[5,6] In order to achieve this goal American Association for the Study of Liver Disease (AASLD) recommends ultrasound follow-up every six months for high risk patients.[7,8] In case nodule larger than 1cm is detected, the patient should undergo further examination with computed tomography (CT) or magnetic resonance imaging (MRI). The presence of arterial hyperenhancement, followed by washout in the portal-venous or delayed phase, is sufficient for the diagnosis of HCC in the setting of cirrhotic liver without the need for tissue biopsy.[7,9] In addition to CT and MRI, contrast-enhanced ultrasound (CEUS) is relatively new imaging modality, which allows real-time depiction of the typical vascular profile of HCC.[10] CEUS is used in several indications in cirrhotic liver: to characterize nodules detected on surveillance US allowing prompt evaluation, and thus avoiding unnecessary further imaging in case of benign lesions; to add additional information to CT and MRI in case of suspected arterioportal shunts; and to provide more information for indeterminate nodules on CT and MRI prior to considration of liver biopsy.[11] Nevertheless CEUS has some limitations including inability for HCC staging. Thus, once malignancy is detected CT or MRI is necessary for staging disease.[12]

If nodules detected in cirrhotic liver are smaller than 1cm, an ultrasound follow-up at 3-months intervals is adviced, in order to detect lesion growth.[8] Although typical enhancement pattern is highly specific (97-99%), it has low sensitivity, as 30% of HCCs have an atypical enhancement due to immature neovascularization.[13] According to previous publications, the incidence of atypical enhancement pattern was most frequent among small and well-differentiated HCCs.[9,13] Thus, some HCCs are misdiagnosed, since they do not exhibit these specific imaging criteria, presenting as either iso/hypovascular lesions, rim-enhancing lesions, or hypervascular lesions without washout.[14]

Therefore, we sought herein to provide an overview of atypical manifestations of HCC in term of vascular behaviour, and focus on their MRI features that might be used for establishing an accurate diagnosis.

## Hepatocarcinogenesis

Cirrhosis may be caused by chronic viral hepatitis, chronic alcohol abuse, different inherited and acquired metabolic diseases with nonalcoholic fatty liver disease (NAFLD) arising as a new epidemic liver disease in modern world.[15] Among all etiologies, the risk for HCC development is highest in patients with chronic viral hepatitis.[16] Many recent studies have shown that the risk of HCC is reduced among patients with hepatitis C viral infection who achieve sustained virological response (SVR) with interferon-based antiviral therapy.[17] However contradictory data exist on the risk of HCC in patients receiving new direct-acting antivirals (DAA).[18] Namely in contrast to interferon, these drugs can also be used in patients with advanced liver disease in whom cirrhosis has already developed.[19] Additionally, DAA lead to distortion of immune system which not only cause rapid decrease in viral overload but also alters inflammatory profile which can accelerate the growth of already existing preclinical cancer.[20] The role of imaging in these subset of patients is early detection of HCC as the most important complication of longstanding cirrhosis.

It is widely accepted that in cirrhotic liver HCC develops through multistep process of hepatocarcinogenesis starting from low grade dysplastic nodules (DN), followed by high grade DN, early HCC, and finally progressed HCC.[21,22] Low grade DNs are vaguely or distinctly nodular lesions with mild increase in cell density, no cytologic atypia, and morphologically indistinguishable from surrounding regenerative nodules.[23] However, this distinction is clinically not so important as low grade DN have only slightly elevated risk of further dedifferentiation.[23] In contrast, high grade DNs are premalignant lesions with cellular and architectural atypia. Rare unpaired arteries are also found in most of high grade DNs. Early HCC is defined as well-differentiated lesion, lacking fibrous pseudocapsule, characterized by five major histological features: (1) increased cell density; (2) various number of portal tracts within the nodule; (3) frequent acinar and/or pseudoglandular pattern; (4) common diffuse fatty change; and (5) varying number of unpaired arteries.[24] Diffuse fatty change is seen in 40% of tumors less than 2 cm in diameter.[15] Nevertheless, all these features may also be present in high grade DNs, thereby an accurate differentiation among these lesions and early HCC is very difficult, even on pathological examination.[25] To date, the presence of stromal invasion is regarded to be the most important pathological finding for distinction of early HCC from dysplastic nodule.[25] Progressed HCC are distinctly nodular lesions, which in contrast to early HCC, have a propensity for microvascular invasion and

metastasis.[23] Although pathologists have reached the consensus on histological characteristics of cirrhotic nodules, precise radiological criteria for identification of early atypically enhancing HCC are still missing.[26]

The hallmark of hepatocarcinogenesis are changes in nodule vascularization. At the beginning of hepatocarcinogenesis the nodules show arterial hypovascularity with portal perfusion still present.[27] Subsequently, both arterial and portal blood perfusion decrease.[27,28] This step is followed by an increase of arterial vascularity to an isovascular pattern, and at the end to a hypervascular pattern.[29] Hypervascularity is a result of formation of numerous unpaired arteries.[22] Nodule-in-nodule type is specific hemodynamic pattern, characterized by development of spots of arterial hypervascularity in a hypovascular background.[30] Due to insufficient number of unpaired arteries, typical vascular enhancement including arterial hypervascularity, and portal-venous washout is frequently absent in early HCCs.[31] Therefore, the detection of these nodules on conventional MRI remains very difficult. Previous studies have shown that early HCCs are biologically less aggressive lesions, with much lower incidence of microvascular invasion compared to small hypervascular HCCs.[32] Since early HCC has a great chance for surgical cure and low risk of recurrence, it is of great clinical importance to detect these lesions, and correctly characterize them.[33-35]

## Imaging diagnosis of hepatocellular carcinoma

### Current guidelines for HCC diagnosis

According to international guidelines published by AASLD and European Association for the Study of Liver (EASL), non-invasive diagnosis of HCC in cirrhotic patients is based on the detection of arterial hyperenhancement followed by washout in portal-venous phase.[36] Although this vascular behavior is recognized as radiological hallmark for HCC diagnosis, it has low sensitivity, as 30% of HCCs have an atypical enhancement due to immature neovascularization.[37,38] Atypical enhancement pattern is usually present in small and well-differentiated HCCs.[39,40] These results indicate that current guidelines for noninvasive diagnosis of HCC may have limited value for early HCC, and may lead to many false negative findings.[41] Therefore, there is an obvious need for new imaging criteria in the diagnosis of early HCC, since liver biopsy recommended for all atypical nodules has many drawbacks, such as bleeding, infection, and inadequate sampling.[42] In this regard recent studies have stressed the utility of ancillary features such as T2-weighted hyperintensity, increased fat content, hypointensity in hepatobiliary phase (HBP), and diffusion weighted imaging (DWI) hyperintensity for the detection of early HCCs.[43-45] The presence of three or more positive findings among above mentioned ancillary MRI features in nodules with diameter of 1-2 cm without typical vascular profile, has shown to significantly improve sensitivity (77%) without reduction of specificity (95%).[46]

Liver Imaging Reporting and Data System (LI-RADS) was developed by American College of Radiology in order to standardize diagnosis and reporting of lesions and pseudolesions identified in patients who are at risk for hepatocellular carcinoma.[47,48] Moreover, imaging criteria for various benign and malignant hepatic tumors, including non-HCC malignancies like cholangiocarcinoma are discussed. LI-RADS categorizes hepatic lesions from LR-1 to LR-5 depending on their imaging features, reflecting probability of being HCC. Categories LR-1 and LR-2 include definitely (LR-1) or probably benign lesions (LR-2). LR-3 are lesions with intermediate risk of being HCC, LR-4 include observations that are probably HCC, while LR-5 are considered definitely HCC.[49] LI-RADS algorithm can be applied to both CT and MRI examinations in patients with cirrhosis, chronic hepatitis B infection, and in patients with prior HCC.[49,50] The categorization of the lesions using LI-RADS is based on major imaging criteria with arterial phase hyperenhancement and washout appearance, being the most important.[47-50] However, there are a few others major features which favor the diagnosis of HCC. In this regard, enhancing capsule has a strong predictive value for HCC. Histologically, it correlates to either a true capsule or pseudocapsule.[51] It is seen as peripheral rim of smooth hyperenhancement on portal-venous, delayed or transitional phase. In addition, threshold growth defined as increase of ≥50% in diameter over ≤6 months, or ≥100% of diameter increase over >6 months, with minimal increase of at least 5 mm, is a strong indicator of malignancy.[52] Moreover, the use of ancillary features to further define final category is highly recommended.[48]

The current European Association for the study of the Liver favours the use of Barcelona-Clinic Liver Cancer (BCLC) staging system for clinical classification of HCC.[53,54] In this system prognosis

prediction is defined by variables related to tumor status, liver function and health status.[54,55] The role of imaging in this classification system is to accurately assess the number of tumor nodules, their size, the presence of portal vein invasion and extrahepatic spread of disease. In cases of single HCC nodules less than 2 cm, or 2-3 HCC nodules up to 3 cm, the radical treatment such as resection, ablation and transplantation are possible in cases of preserved liver function.[56] In contrast, for advanced cases chemoembolization or systemic therapy are methods of choice.[56]

One of the preconditions associated with a higher rate of complications in patients with cirrhosis and HCC is sarcopenia, defined as the loss of skeletal muscle mass, quality and function.[57] In this regard, many studies have been published trying to assess the real clinical impact of sarcopenia on the outcome of HCC patients undergoing treatment.[58,59] However, to date there is no standardization of methodology for sarcopenia evaluation. There are many different CT approaches for assessment of sarcopenia such as measurement of total bilateral psoas muscle area at the middle of the third lumbar vertebra, or measurement of psoas mass thickness at the level of umbilicus, and many others.[60,61] The lack of standardization and unified cut-off values indicate the need of further studies to clarify the impact of sarcopenia on therapeutic outcome in cirrhotic patients with HCC.

## Ancillary MRI features for the diagnosis of HCC

Hepatocarcinogenesis is a complex process that includes not only changes in vascularity, but also changes in architecture, cellular density, hepatocyte function, and Kupffer cell number or function.[62] Therefore, development of hepatoselective contrast agents, such as gadoxetic acid, or gadobenate-dimeglumine, and introduction of DWI into abdominal MRI protocols, allowed evaluation not only of neovascularization, but also of other processes occurring during hepatocarcinogenesis.[45,63,64]

The hepatocyte-specific contrast agent gadolinium-ethoxybenzyl-diethylenetriamine pentaacetic acid (Gd-EOB-DTPA) is a dual contrast agent, which combines the properties of conventional extracellular contrast agents with hepatobiliary phase.[65] It is transported into hepatocytes using organic anion-transporting polypeptide OATP1B1 (synonymous with OATP8) and OATP1B3 receptors.[66] Multiple resistance-associated Protein 2 (MRP2) located in the canalicular membrane of hepatocytes or tumour cells is responsible for excretion of hepatobiliary agents into bile ducts.[65] OATP transporters are typically inhibited, while MRP2 are overexpressed in malignant liver lesions such as HCC, which therefore show hypointensity on hepatobiliary phase.[67] The importance of OATP receptors not only for detection of HCC, but also for prediction of recurrence rate and overall prognosis has been recently shown.[66] In this context, it was demonstrated that progressive loss in OATP immunoreactivity correlates well with the gain of biliary phenotype by neoplastic hepatocytes, which indicates high risk for faster recurrence and overall worse prognosis in patients with HCC.[66,68] The importance of assessment of correlation between MRI features of HCC on hepatobiliary phase and different morphovascular patterns of HCC defined on histology was also outlined in the recent study by Vasuri *et al*.[69] The results of this study and similar future studies could allow more accurate preoperative sub classification of HCC in order to discriminate patients with good and poor prognostic outcome.

Many previous studies have shown that reduction of OATP1B/B3 expression occurs early in the course of hepatocarcinogenesis, even before development of neovascularization.[63,70] On the other hand, regenerative nodules, or low grade dysplastic nodules retain normal expression of uptake OATP1B/B3 transporter and excretory transporter MRP2.[67] Therefore, the first sign of malignancy in cirrhotic nodules could be hypointensity in HBP, which is later followed by development of arterial hypervascularity. The utility of Gd-EOB-DTPA in the detection and characterization of atypically enhancing HCCs has been demonstrated in many recent reports.[45,46,71-74] In this regard, Golfieri *et al*. tested 111 atypical cirrhotic nodules and shown that HBP hypointensity was the strongest marker of malignancy with 88% of sensitivity, 91% negative predictive value and 93% diagnostic accuracy.[75] The same group of authors have shown that after addition of HBP phase in MRI protocol, sensitivity and specificity for the detection of small HCCs significantly increased, from 88.4% up to 99.4%, and from 88% to 95%, respectively.[73] The high incidence of atypical nodules particularly among small lesions, and their frequent malignancy indicate the need to incorporate Gd-EOB-DTPA in standard MRI protocols for evaluation of cirrhotic liver.[74] Nevertheless, it should be kept in mind that hepatic dysfunction or hyperbilirubinemia can result in diminished uptake of hepatospecific contrast

agent, leading to reduced conspicuity of HCC lesions on HBP.[76]

The value of DWI in the characterization of cirrhotic nodules could be explained by progressive cellular changes occurring during hepatocarcinogenesis.[77] It is well known that DWI signal intensity is influenced by cellular density, architectural changes, as well as vascular changes during malignant transformation of cirrhotic nodules. As one of the major differences between dysplastic nodules and early HCCs is the degree of cellular density, DWI might provide a good insight into histological changes of hepatocellular nodules irrespective of vascularity.[78] Notably, since RN and low grade DN are usually histologically identical to the surrounding hepatic tissue, they are isointense on DWI.[79,80] On the other hand, HCC and high grade DN, show a progressive increase in cellular density, thickening of cellular plates, leading to progressive restriction of water mobility, which results in increased signal intensity on DWI.[80] Since at an earlier stage, the degree of neovascularization may be insufficient for depiction on contrast-enhanced images, small lesions could sometimes be detected only on DWI.[81] Opposite to the signal intensity on DWI, the calculation of apparent diffusion coefficient (ADC) values was not shown to be usefull for differentiation of benign from malignant cirrhotic nodules.[44,82] The subtle cellular changes, and variable presence of fat, necrosis, and vascular changes result in strong overlap of ADC values between malignant and benign nodules. In addition, DWI hyperintensity could be also found in high grade DN, and even in a few low grade DN.[83] These results could be explained by heterogeneity of cirrhotic liver which also shows diffusion restriction, thus making it difficult to identify hepatocellular nodules with increased signal intensity on DWI.[84] In addition, HCCs are less cellular than metastases, and sometimes difficult to detect on DWI.[64] Furthermore, DWI also has other limitations, including limited spatial resolution, susceptibility to motion artifacts, especially for lesions located in the left lateral segment, and close to the diaphragm because of cardiac motion.[77] Thus, in general DWI is not used alone in clinical scenarios, but only as a part of MRI protocol.[85]

The value of signal intensity on T2-weighted images in the identification of HCC lesions was stressed in many previous reports.[41] Namely, T2-weighted hyperintensity is considered to be strong predictor of malignancy, and subsequent hypervascularization in hypovascular nodules.[40,43] Higher signal intensity on T2-weighted images could partly be explained by peliotic changes in the intratumoral sinusoids of HCC.[86] In this regard, Channual *et al*. have shown that relative signal intensity on T2-weighted images is significantly different between low grade DN on one side, and high grade DN with HCC on the other side.[87] Moreover, when T2-weighted hyperintensity was combined with arterial hypervascularity, differentiation could be possible with the sensitivity of 88.6%, and positive predictive value of 99.2%.[87] The value of T2-weighted hyperintensity was also shown in the study by Hwang *et al.*, who reported that this feature was present in 76% of hypovascular HCC, and in only 12.9% of dysplastic nodules.[88] Although T2-weighted hyperintensity can also occur in dysplastic nodules, probably due to infarction, the signal intensity is usually lower than in HCCs.[89]

Besides above mentioned imaging characteristics, there are also other ancillary features which could help in characterization of the lesions in cirrhotic liver. One of them is corona enhancement which refers to an ill-defined perilesional enhancement in late arterial phase.[48] It develops as a consequence of an early drainage of blood from a tumor into the surrounding hepatic sinusoids and portal venules.[90] This occurs due to the obstruction of intranodular hepatic veins by neoplastic cells.[90] While capsular appearance is obvious on portal-venous phase, corona enhancement is present in late arterial phase.[91] If iron sparing solid mass is seen in the setting of cirrhotic liver with multiple siderotic nodules, this finding should indicate the presence of malignancy.[48] It is well known that during hepatocarcinogenesis neoplastic cells loose their capability of iron accumulation.[48] Non-enhancing capsule has recently been introduced as another ancillary feature that in particular favors HCC.[48] It refers to uniformly thin, sharply demarcated, non-enhancing rim surrounding the lesion.[48] Furthermore, mosaic architecture and "nodule-in-nodule" appearance are very well known ancillary features of HCC.[30,92] While mosaic architecture is usually seen in large lesions, nodule-in-nodule often represents development of early HCC in high grade dysplastic nodule. The presence of fat inside the cirrhotic nodule is also considered to be ancillary feature of HCC.[93] Although the exact underlying mechanism of intralesional fat accumulation is not known, hypoxia which occurs during hepatocarcinogenesis is considered to be the most probable reason.[93] Intralesional fat is usually seen in small HCCs (less than 1.5 cm) with decreasing frequency in larger lesions.[48] Nevertheless, this finding should not be confused with fat accumula-

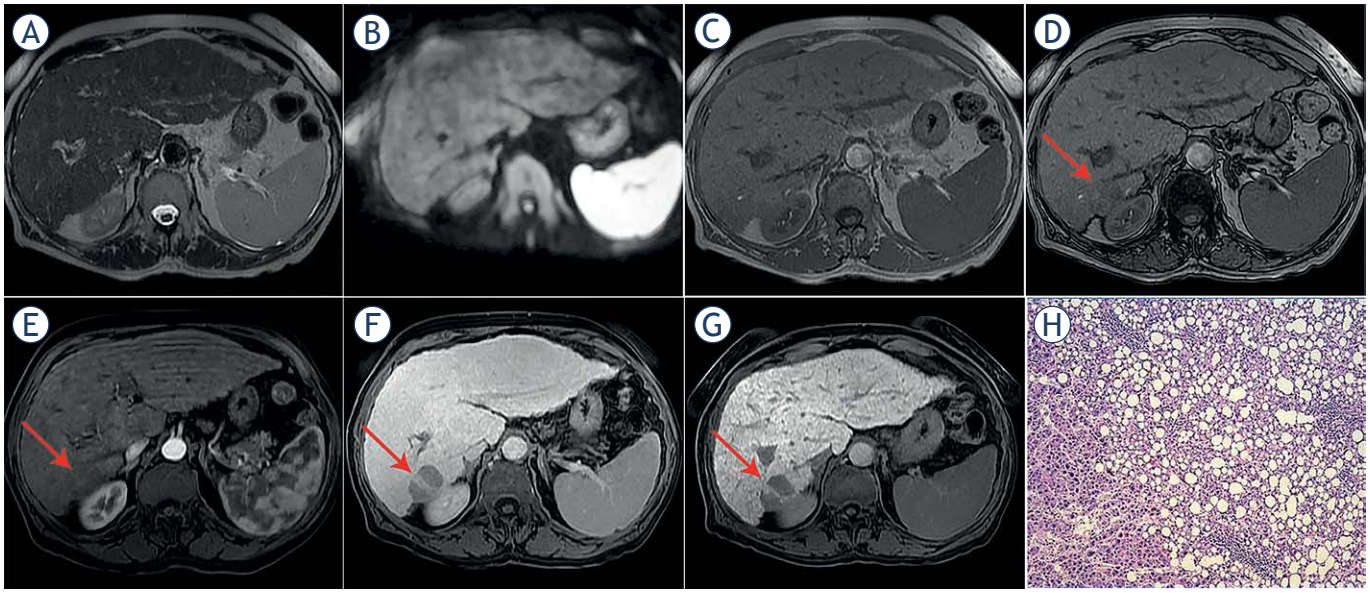


**FIGURE 1.** Hypovascular hepatocellular carcinoma (HCC) in 58-year old woman with cirrhosis. On axial T2-weighted image **(A)**, diffusion-weighted image **(B)** and on in-phase image **(C)** tumor is isointense with surrounding liver parenchyma. On opposed-phase image there is a partial drop of signal intensity in the lesion (*arrow*) corresponding to the fatty component **(D)**. The lesion (*arrow*) is slightly hypointense on arterial phase **(E)**, while it is clearly hypovascular on portal-venous phase **(F)**. On hepatobiliary phase after administration of gadoxetic acid the lesion (*arrow*) is hypointense **(G)**. Hematoxylin and eosin (H&E) staining showed well-differentiated HCC with fat deposition; original magnification x 200 **(H)**.

tion seen in steatotic HCC which represents specific hystological variant of HCC.[39] Some other features, such as subtreshold growth, fat sparing in solid mass, blood products in mass, and transitional phase hypointensity have also been included as ancillary features for HCC diagnosis in latest LI-RADS algorithm.[48,49]

Since early HCC detection is crucial for appropriate clinical management of patients, the establishemnet of predictive markers for primary HCC occurance in the setting of compensated advanced chronic liver disease is in focus of many recent studies.[94] Among different non-invasive tests for the prediction of primary HCC, Marasco *et al*. have found that the liver stiffness measurement is the most reliable, allowing evaluation of liver fibrosis degree, inflammation and portal hypertension.[95] However further studies are needed to determine specific optimal cut-off values able to assess the risk for HCC development in different etiologies.

## Atypically enhanced hepatocellular carcinoma

### Iso- or hypovascular HCC

Iso- or hypovascular HCCs are defined as lesions without arterial phase hypervascularity. As the reduction of portal vascularization precedes development of new unpaired arteries, iso- or hypovascularity in arterial phase, with hypointensity in portal-venous phase could be the first sign of early HCC (Figure 1,2).[27] The prevalence of hypovascular HCC varies among different studies, ranging from 14% in the study by Leoni *et al.* [96], to 19.5% by Choi *et al.*[97] If this vascular pattern is identified at dynamic CT, further examination with MRI using hepatospecific contrast agents is necessary. Hypointensity on HBP in nodules hypovascular in arterial phase, indicates that loss of metabolic hepatocyte function occurs before development of neovascularization.[65,70] There are many recent studies which pointed out that hypointensity on HBP is one of the imaging findings with highest diagnostic accuracy for detection of early HCC.[45,46,71-74] Accordingly, in the study by Sano *et al.*[41] the sensitivity of HBP hypointensity for the detection of early HCC was 97%, while specificity reached 100%. Although several other imaging features, such as nodule-in-nodule appearance, washout in portal-venous phase, and fat content also had specificity of 100%, none of these findings had sufficient sensitivity for HCC detection. Similar results were published by Choi *et al.* who have shown that 96.6% of hypovascular HCCs were hypointense on HBP, indicating that HBP hypointensity must be considered as imaging biomarker of malignancy.[97]

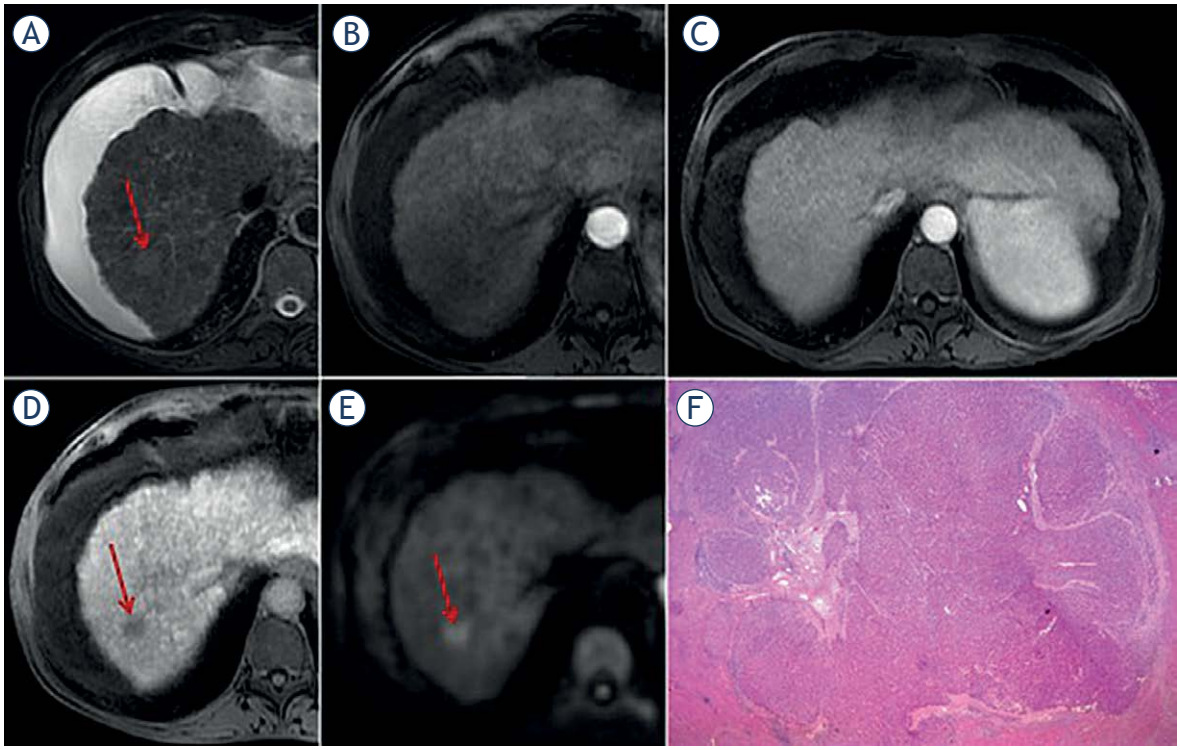


**FIGURE 2.** Isovascular hepatocellular carcinoma (HCC) in 55-year old woman with cirrhosis. On T2-weighted image slightly hyperintense nodule (arrow) is seen in liver segment VII **(A)**. No lesion is seen on arterial **(B)** and portal venous phase **(C)**. On hepatobiliary phase after administration of gadoxetic acid the lesion (arrow) is hypointense **(D)**. Diffusion-weighted image shows diffusion restriction of the lesion (arrow) **(E)**. Hematoxylin and eosin (H&E) staining showed well-differentiated HCC; original magnification x 200 **(F)**.

On the basis of these results, it could be concluded that double hypointensity, including hypointensity in the portal-venous phase, and hypointensity in hepatobiliary phase is highly suggestive of hypovascular HCC.[72] On the other hand, Bartolozzi *et al.* reported that 70% of high grades DNs were also hypointense on HBP, indicating that using only this sign, precise distinction among high grade DN and HCC is not possible.[63] However, differentiation among high grade DNs and early HCC is not crucial from clinical point of view. Namely, in many institutions high grade DN are considered to be early HCCs.[72] Taking into account that high grade DN are premalignant lesions, it is questionable whether exact radiological distinction among these two pathological entities is indeed necessary. If not treated immediately, HBP hypointense nodules should be rigorously monitored as was stressed by many previous studies.[98-101] The cumulative risk of hypervascularization in these lesions varies from 31-35% in the study by Kim *et al.*[98], and Hyodo *et al.*[99], up to 77% in the study by Kumada *et al.*[100]. Similar results were also reported in other studies.[98-102] Considering that a significant percent of non-hypervascular HBP hypointense cirrhotic nodules are already HCCs, or will develop typical radiological features of HCC in follow-up, they must be characterized as high risk nodules, and if possible should be subject to liver biopsy. However, care should be taken when interpreting HBP phase imaging findings in cirrhotic liver. Namely, in patients with worse Child Pugh class, the uptake of Gd-EOB-DTPA can be very reduced and delayed, affecting relative signal intensity of HCCs.[65] In this regard, the diagnosis of HCC with atypical enhancement pattern may be very challenging in cirrhotic liver, indicating the importance of multiparametric assessment.

Besides hepatospecific contrast agents, further characterization of iso-, or hypovascular nodules could be done with DWI. In this context, Hwang *et al.* reported high diagnostic accuracy of DWI in differentiation between hypovascular HCC and dysplastic nodules, as hyperintensity on DWI was observed in 92% of HCC, in contrast to 16.1% of dysplastic nodules.[88] In the study by Kim *et al.* DWI restriction was present in 56% of 139 hypovascular, HBP hypointense nodules which subsequently progressed to hypervascular HCC, indicating that DWI hyperintensity is a strong predictor of devel-

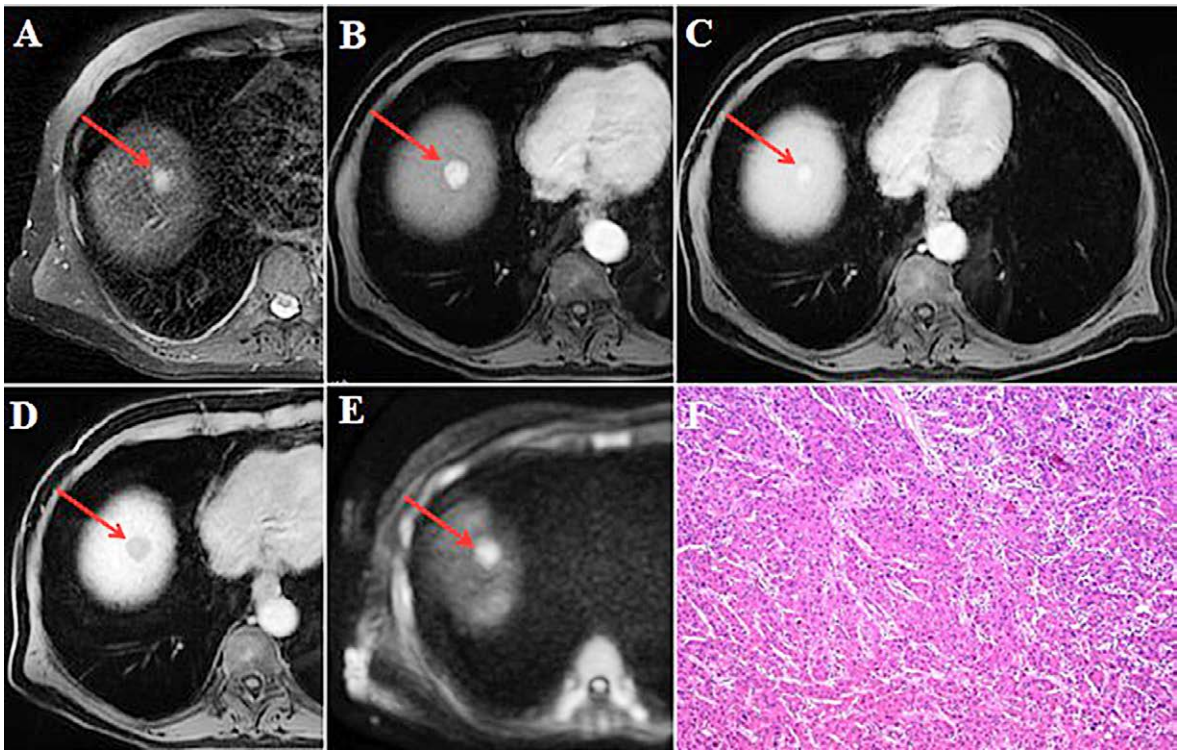


**FIGURE 3.** Hypervascular hepatocellular carcinoma (HCC) without washout in 64-year old man with cirrhosis. Axial T2-weighted fat-suppressed image shows hyperintense nodule (arrow) in liver segment VIII **(A)**. On arterial phase the nodule (arrow) is hypervascular **(B)** without washout on portal-venous phase **(C)**. On hepatobiliary phase the nodule (arrow) is hypointense **(D)** and on diffusion-weighted image it is hyperintense **(E)**. Hematoxylin and eosin (H&E) staining showed moderately-differentiated HCC; original magnification x 200 **(F)**.

opment of hypervascularity.[98] Moreover, on the basis of these results, it could be concluded that iso- or hypovascular nodules, which show hypointenyity on HBP and high signal intensity on DWI, could already be considered as early HCC. Additionally, according to some authors hypovascular nodules, hypointense in the HBP, not hyperintense on DWI, should be further investigated by contrast enhanced ultrasound (CEUS), as this method allows depiction of early arterial phase enhancement, which could be missed on dynamic CT and MRI.[74]

## Hypervascular HCC without washout in portal-venous phase

Many small HCCs are depicted only during arterial phase imaging as hypervascular lesions, lacking washout on portal-venous and delayed phase (Figure 3).[103] Actually, in HCCs ≤ 1 cm, arterial enhancement is the most frequent MRI finding (79%) in comparison to other features, such as wash-out in the portal-venous or delayed phase (50%).[104] This can raise a diagnostic dilemma, as it is often difficult to differentiate these lesions from non-neoplastic hypervascular pseudolesions, such as small arterioportal shunts, or atypical cirrhosis related nodules.[105,106] Moreover, the majority of these small hypervascular nodules detected in cirrhotic liver are benign lesions.[105,106] Differential diagnosis is usually made using T2-weighted images, DWI, and signal intensity on HBP. Concerning the value of T2-weighted signal intensity there are discrepant results in the previous literature.[87,88,107] Thus, Hussain *et al.* concluded that T2-weighted hyperintesity has no additional value in the identification of small HCC, due to very heterogeneous signal intensity of surrounding liver parenchyma.[107] In contrast, many other investigators reported that addition of T2-weighted images to dynamic contrast enhanced images significantly improves detection of HCC.[87,88] In this regard, HCCs are seen as slightly hyperintense lesions, while arterioportal shunts are isointense with surrounding liver tissue.[43] Additionally, the majority of these atypical HCCs are hypointense on HBP phase indicating the lack of functional hepatocytes. Very rarely this atypical vascular profile can occur in large HCCs (Figure 4). In such cases hypointensity on HBP is

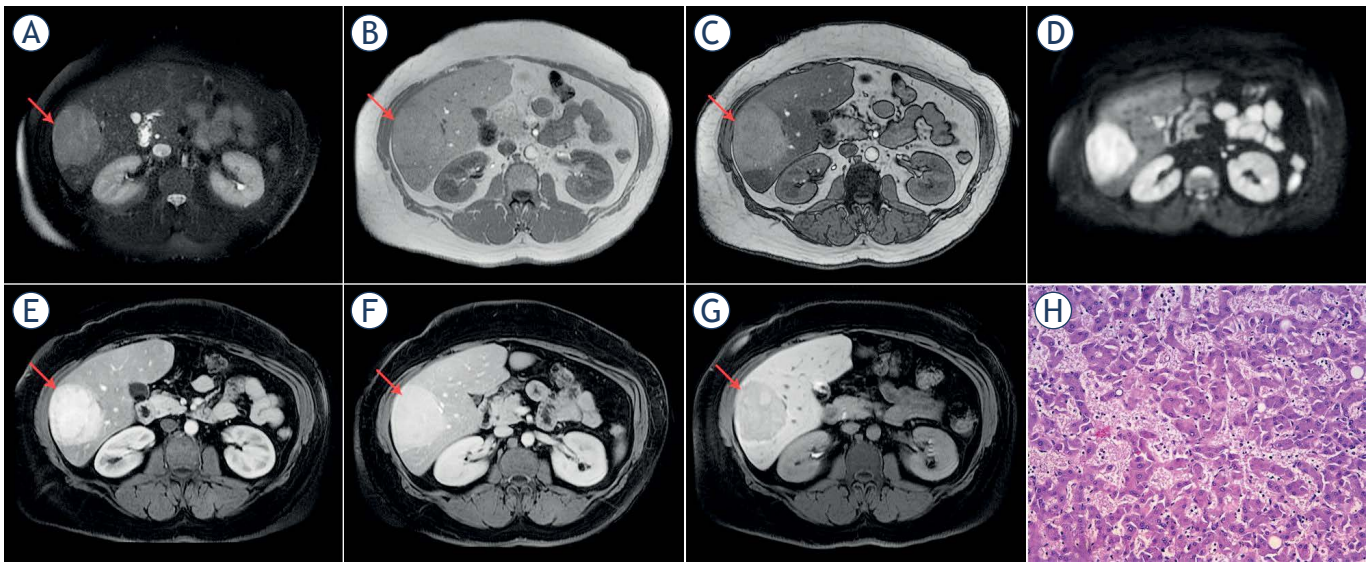


**FIGURE 4.** Hypervascular hepatocellular carcinoma (HCC) without washout in 44-year old man with non alcoholic fatty liver disease. Axial T2-weighted fat-suppressed image shows moderately hyperintense lesion (arrow) in segment VI **(A)**. Dual-echo images show that tumor (arrows) is isointense on in-phase image **(B)** without signal drop on opposed-phase image, while background liver parenchyma shows diffuse signal drop as a consequence of fatty liver disease **(C)**. The lesion (arrows) is hyperintense on diffusion-weighted image **(D)**, hypevascular on arterial phase **(E)** without washout on portal-venous phase **(F)**. On hepatobiliary phase the tumor (arrow) is hypointense **(G)**. Hematoxylin and eosin (H&E) staining showed moderately-differentiated HCC with very dilatated sinusoidal network; original magnification x 200 **(H)**.

the most useful sequence for distinction from other hypervascular benign lesions, such as focal nodular hyperplasia. Since arterial enhancement and HBP hypointensity are two strongest markers of malignancy in cirrhotic patients, a nodule with arterial hypervascularity, even without wash-out in portal-venous or delayed phase, but hypointense in the HBP, should be highly suspicious of HCC. Another diagnostic problem could be the distinction between these atypically enhancing HCCs, and small hemangiomas in liver cirrhosis.[108] Namely, in cirrhotic parenchyma small hemangiomas can shrink, and become fibrotic and hyalinized, which influences their signal intensity on T2-weighted images. Moreover, similar to HCCs, hemangiomas are hypointense in HBP. In this context Semelka *et al.* reported that accurate differential diagnosis among small HCCs and hepatic hemangioma less than 15 mm can not be made on the basis of imaging criteria.[109]

## HBP hyperintense hepatocellular carcinoma

According to molecular changes during hepatocarcinogenesis, HCCs should typically show hypointensity on HBP. The signal intensity of HCC on HBP is strongly correlated to the expression of uptake transporter OATP8.[110] It is well known that during hepatocarcinogenesis the progressive decrease in OATP8 expression occurs, thus influencing the enhancement ratio of cirrhotic nodules in the HBP.[70,111] Nevertheless, in 10% of HCCs paradoxical uptake of hepatospecific contrast agent may occur.[70] This can partly be explained by residual functional hepatocytes expressing OATP8 receptors in well-differentiated lesions.[70] However, in the study by Asayama *et al.* Gd-EOB-DTPA uptake did not correlate with tumor differentiation.[112] In addition, these authors have shown that uptake of Gd-EOB-DTPA was significantly correlated with the maintenance of bile production. Similar results were published by Choi *et al.* who have shown that among 28 tumors showing iso- or hyperintensity on HBP, only 10 were well-differentiated HCCs (35.7%), while 16 were moderately (57.1%), and two were poorly differentiated lesions (7.1%).[97] A few recent studies have shown that gadoxetic acid uptake in HCCs can be the result of genetic mutations and reversion to their original hepatocyte nature during neoplastic transformation.[113,114] Namely, in some moderately or even poorly differentiated lesions OATP8 receptor expression can increase due to genetic alterations, followed by decrease in MRP expression.[115-117] In contrast to normal hepatocytes where excretion of gadoxetic acid occurs via MRP2 transporters localized on canalicular side, in hepatobiliary phase iso- orhy-

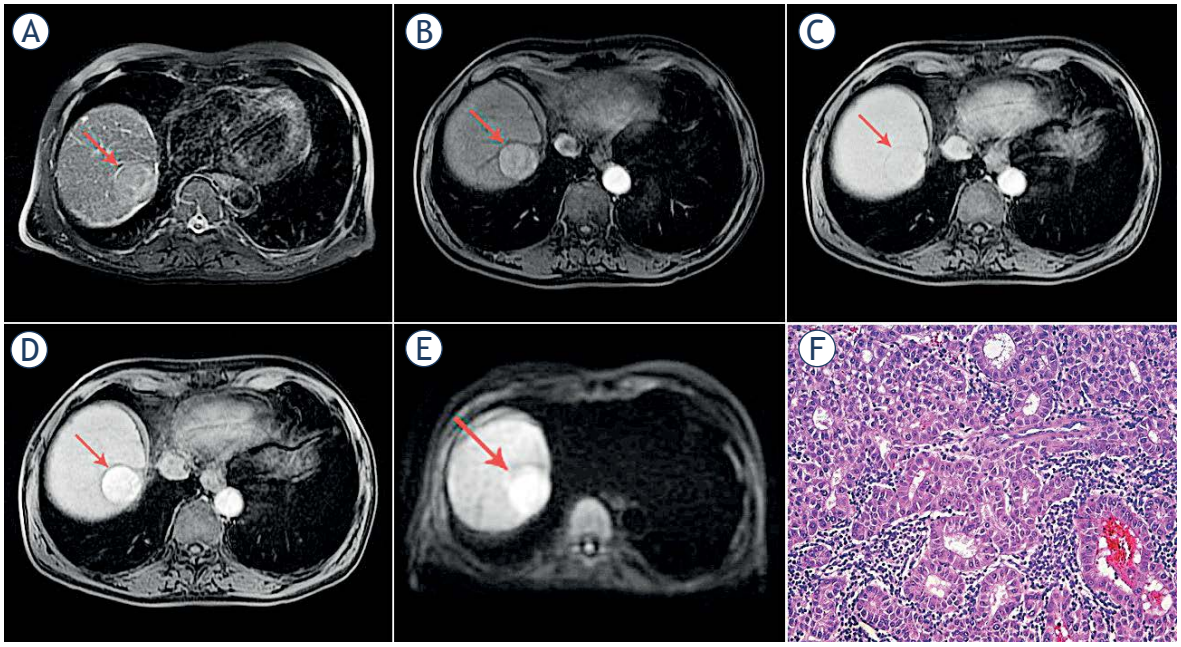


**FIGURE 5.** Hepatocellular carcinoma (HCC) in 73-year old man with alcoholic cirrhosis. Axial T2-weighted fat-suppressed image shows slightly hyperintense well-defined nodular lesion (arrow) in segment VII **(A)**. The lesion (arrows) is hypervascular on arterial phase **(B)** without washout on portal-venous phase **(C)**. On hepatobiliary phase the tumor (arrow) is strongly hyperintense **(D)** with hyperintensity on diffusion-weighted image **(E)**. Hematoxylin and eosin (H&E) staining showed well-differentiated HCC; original magnification x 200 **(F)**.

perintense HCCs the main pathway of excretion is through MRP3 on sinusoidal side.[116] Therefore, HBP iso- or hyperintensity in HCCs does not indicate well-differentiated lesion, but rather suggest different genetic subtype of HCC.[66,69] Although differentiation of the tumor cannot be predicted by signal intensity on hepatobiliary phase, Choi *et al.* have demonstrated that HBP hyperintense HCCs showed significantly higher differentiation grades, less frequent portal vein invasion, and lower recurrence rate.[97] Moreover, patients with hyperintense HCCs showed longer survival than those with hypointense HCCs.[97] All these findings suggest that HBP hyperintense HCCs are probably a particular form of HCC with biologically less aggressive features in comparison to HBP hypointense HCCs.[118,119] Interestingly, the AFP levels were shown to be significantly higher in hypointense HCCs than in hyperintense HCCs.[110,116]

However, there are no data in the previous literature about behaviour of HBP hyperintense HCCs in portal venous phase, whether they demonstrate washout or not. Although most reported cases show typical vascular profile, rarely HCCs hyperintense in HBP lack portal-venous or delayed phase washout (Figure 5).[74] The incidence of such nodules is very low, less than 3%.[74] In such cases differential diagnosis towards benign lesions, such as large regenerative nodules (LRNs), and focal nodular hyperplasia is very challenging.[120] LRNs are hyperplastic lesions, 5 mm to 5 cm in diameter, associated with cirrhosis, Budd–Chiari syndrome, certain forms of congenital heart disease, and other conditions.[121,122] LRNs are typically hypervascular in arterial phase, without washout in portal-venous or delayed phase, iso- or hyperintense in HBP.[121] The distinction between LRNs and atypically enhancing HCCs showing hyperintensity on HBP, requires detailed analysis of other MRI features, such as T2-weighted, T1-weighted, and DWI signal intensity.[122] While HCCs are usually slightly hyperintense on T2-weighted images, hypointense on T1-weighted images with restricted diffusion, LRN and FNH are isointense on both T2- and T1-weighted images, without DWI hyperintensity.[120,121] If there is any doubt, rigorous follow-up is required, and if nodule grows a biopsy is recommended.

## Conclusions

The diagnosis of HCC is straightforward when typical imaging features are present. Nonetheless,

due to complexity of hepatocarcinogenesis, HCC can present with atypical vascular profile, especially in small lesions, including iso- or hypovascular nodules without arterial hypervascularity, and hypervascular lesions without washout in portal-venous phase. Additionally, there are HCCs with high signal intensity in HBP. In order to correctly characterize these lesions ancillary features such as T2-weighted hyperintensity, diffusion restriction, hepatobiliary phase hypointensity together with other MRI characteristics should be carefully examined. Even though these atypical presentations are rare, it is important to recognize them in order to provide the patients optimal and timely treatment.

## References


1. Mittal S, El-Serag HB. Epidemiology of hepatocellular carcinoma: consider the population. *J Clin Gastroenterol* 2013; **47:** S2-6. doi: 10.1097/MCG.0b013e3182872f29
2. Yang JD, Hainaut P, Gores GJ, Amadou A, Plymoth A, Roberts LR. A global view of hepatocellular carcinoma: trends, risk, prevention and management. *Nat Rev Gastroenterol Hepatol* 2019; **16:** 589-604. doi: 10.1038/s41575-019-0186-y
3. Degos F, Christidis C, Ganne-Carrie N, Farmachidi JP, Degott C, Guettier C, et al. Hepatitis C virus related cirrhosis: time to occurrence of hepatocellular carcinoma and death. *Gut* 2000; **47:** 131-6. doi: 10.1136/gut.47.1.131
4. Tang A, Hallouch O, Chernyak V, Kamaya A, Sirlin CB. Epidemiology of hepatocellular carcinoma: Target population for surveillance and diagnosis. *Abdom Radiol* 2018; **43:** 13-25. doi: 10.1007/s00261-017-1209-1
5. Marrero JA, Kulik LM, Sirlin CB, Zhu AX, Finn RS, Abecassis MM, et al. Diagnosis, staging, and management of hepatocellular carcinoma: 2018 practice guidance by the American Association for the Study of Liver Diseases. *Hepatology* 2018; **68:** 723-50. doi: 10.1002/hep.29913
6. Hartke J, Johnson M, Ghabril M. The diagnosis and treatment of hepatocellular carcinoma. *Semin Diagn Pathol* 2017; **34:** 153-9. doi: 10.1053/j.semdp.2016.12.011
7. Furlan A, Marin D, Cabassa P, Taibbi A, Brunelli E, Agnello F, et al. Enhancement pattern of small hepatocellular carcinoma (HCC) at contrast-enhanced US (CEUS), MDCT, and MRI: intermodality agreement and comparison of diagnostic sensitivity between 2005 and 2010 American Association for the Study of Liver Diseases (AASLD) guidelines. *Eur J Radiol* 2012; **81:** 2099-105. doi: 10.1016/j.ejrad.2011.07.010
8. Harris PS, Hansen RM, Gray ME, Massoud OI, McGuire BM, Shoreibah MG. Hepatocellular carcinoma surveillance: an evidence-based approach. *World J Gastroenterol* 2019; **25:** 1550-9. doi: 10.3748/wjg.v25.i13.1550
9. Anis M, Irshad A. Imaging of hepatocellular carcinoma: practical guide to differential diagnosis. *Clin Liver Dis* 2011; **15:** 335-52. doi: 10.1016/j.cld.2011.03.014
10. Claudon M, Dietrich CF, Choi BI, Cosgrove DO, Kudo M, Nolsøe CP. Guidelines and good clinical practice recommendations for Contrast Enhanced Ultrasound (CEUS) in the liver - update 2012: A WFUMB-EFSUMB initiative in cooperation with representatives of AFSUMB, AIUM, ASUM, FLAUS and ICUS. *Ultrasound Med Biol* 2013; **39:** 187-210. doi: 10.1016/j.ultrasmedbio.2012.09.002
11. Wilson SR, Lyshchik A, Piscaglia F, Cosgrove D, Jang HJ, Sirlin C, et al. CEUS LI-RADS: algorithm, implementation, and key differences from CT/MRI. *Abdom Radiol* 2018; **43:** 127-42. doi: 10.1007/s00261-017-1250-0
12. Jo PC, Jang H, Burns PN, Burak KW, Kim TK, Wilson SR. Integration of contrast-enhanced US into a multimodality approach to imaging of nodules in a cirrhotic liver: how I do It. *Radiology* 2017; **282:** 317-31. doi: 10.1148/radiol.2016151732
13. Bruix J, Reig M, Rimola J, Forner A, Burrel M, Vilana R, et al. Clinical decision making and research in hepatocellular carcinoma: pivotal role of imaging techniques. *Hepatology* 2011; **54:** 2238-44. doi: 10.1002/hep.24670
14. Forner A, Vilana R, Ayuso C, Bianchi L, Solé M, Ayuso JR, et al. Diffusion-weighted imaging of surgically resected hepatocellular carcinoma: imaging characteristics and relationship among signal intensity, apparent diffusion coefficient, and histopathologic grade. *Hepatology* 2008; **47:** 97-104. doi: 10.1002/hep.21966
15. European Association for the Study of the Liver. EASL Clinical Practice Guidelines: Management of hepatocellular carcinoma. *J Hepatol* 2018; **69:** 182-236. doi: 10.1016/j.jhep.2018.03.019
16. Lok AS, Seeff LB, Morgan TR, di Bisceglie AM, Sterling RK, Curto TM, et al. Incidence of hepatocellular carcinoma and associated risk factors. *Gastroenterology* 2009; **136:** 138-48. doi: 10.10153/j.gastro.2008.09.014
17. van der Meer AJ, Veldt BJ, Feld JJ, Wedemeyer H, Dufour J-F, Lammert F, et al. Association between sustained virological response and all-cause mortality among patients with chronic hepatitis C and advanced hepatic fibrosis. *JAMA* 2012; **308:** 2584-93. doi: 10.1001/jama.2012.144878
18. Guarino M, Sessa A, Cossiga V, Morando F, Caporaso N, Morisco F. Direct-acting antivirals and hepatocellular carcinoma in chronic hepatitis C: A few lights and many shadows. *World J Gastroenterol* 2018; **24:** 2582-95. doi: 10.3478/wjg.v24.i24.2582
19. Reig M, Marino Z, Perello C, Inarrairaegui M, Ribeiro A, Lens S, et al. Unexpected high rate of early tumor recurrence in patients with HCVrelated HCC undergoing interferon-free therapy. *J Hepatol* 2016; **65:** 719-26. doi: 10.1016/j.jhep.2016.04.008
20. Conti F, Buonfiglioli F, Scuteri A, Crespi C, Bolondi L, Caraceni P, et al. Early occurrence and recurrence of hepatocellular carcinoma in HCVrelated cirrhosis treated with direct-acting antivirals. *J Hepatol* 2016; **65:** 727-33. doi: 10.1016/j.jhep.2016.06.015
21. Kudo M. Multistep human hepatocarcinogenesis: correlation of imaging with pathology. *J Gastroenterol* 2009; **44:** 112-8. doi: 10.1007/s00535-008-2274-6
22. Matsui O, Kobayashi S, Sanada J, Kouda W, Ryu Y, Kozaka K, et al. Hepatocelluar nodules in liver cirrhosis: hemodynamic evaluation (angiography-assisted CT) with special reference to multi-step hepatocarcinogenesis. *Abdom Imaging* 2011; **36:** 264-72. doi: 10.1007/s00261-011-9685-1
23. The International Consensus Group for Hepatocellular Neoplasia. Pathologic diagnosis of early hepatocellular carcinoma: a report of the International Consensus Group for Hepatocellular Neoplasia. *Hepatology* 2009; **49:** 658-64. doi: 10.1002/hep.22709
24. Hytiroglou P, Park YN, Krinsky G, Theise ND. Hepatic precancerous lesions and small hepatocellular carcinoma. *Gastroenterol Clin North Am* 2007; **36:** 867-87. doi: 10.1016/j.gtc.2007.08.010
25. Sakamoto M, Hirohashi S, Shimosato Y. Early stages of multistep hepatocarcinogenesis: adenomatous hyperplasia and early hepatocellular carcinoma. *Hum Pathol* 1991; **22:** 172-8. doi: 10.1016/0046-8177(91)90039-r
26. Gupta M, Gabriel H, Miller FH. Role of imaging in surveillance and diagnosis of hepatocellular carcinoma. *Gastroenterol Clin North Am* 2018; **47:** 585-602. doi: 10.1016/j.gtc.2018.04.013
27. Kudo M. Imaging blood flow characteristics of hepatocellular carcinoma. *Oncology* 2002; **62:** 48-56. doi: 10.1159/000048276
28. Takayasu K, Muramatsu Y, Mizuguchi Y, Moriyama N, Ojima H. Imaging of early hepatocellular carcinoma and adenomatous hyperplasia (dysplastic nodules) with dynamic ct and a combination of CT and angiography: experience with resected liver specimens. *Intervirology* 2004; **47:** 199-208. doi: 10.1159/000078473
29. Tajima T, Honda H, Taguchi K, Asayama Y, Kuroiwa T, Yoshimitsu K, et al. Sequential hemodynamic change in hepatocellular carcinoma and dysplastic nodules: CT angiography and pathologic correlation. *AJR Am J Roentgenol* 2002; **178:** 885-97. doi: 10.2214/ajr.178.4.1780885
30. Kojiro M. 'Nodule-in-nodule' appearance in hepatocellular carcinoma: its significance as a morphologic marker of dedifferentiation. *Intervirology* 2004; **47:** 179-83. doi: 10.1159/000078470
31. Nakashima Y, Nakashima O, Hsia CC, Kojiro M, Tabor E. Vascularization of small hepatocellular carcinomas: correlation with differentiation. *Liver* 1999; **19:** 12-8. doi: 10.1111/j.1478-3231.1999.tb00003.x

32. Kojiro M. Pathological diagnosis at early stage: reaching international consensus. *Oncology* 2010; **78:** 31-5. doi: org/10.1159/000315227

33. Inoue K, Takayama T, Higaki T, Watanabe Y, Makuuchi M. Clinical significance of early hepatocellular carcinoma. *Liver Transpl* 2004; **10:** S16-9. doi: 10.1002/lt.20049

34. Takayama T, Makuuchi M, Kojiro M, Lauwers GY, Adams RB, Wilson SR, et al. Early hepatocellular carcinoma: pathology, imaging, and therapy. *Ann Surg Oncol* 2008; **15:** 972-8. doi: 10.1245/s10434-007-9685-0

35. Yamamoto M, Takasaki K, Otsubo T, Katsuragawa H, Katagiri S, Yoshitoshi K, et al. Favorable surgical outcomes in patients with early hepatocellular carcinoma. *Ann Surg* 2004; **239:** 395-9. doi: 10.1097/01.sla.0000114215.03112.e0

36. Kim TH, Kim SY, Tang A, Lee JM. Comparison of international guidelines for noninvasive diagnosis of hepatocellular carcinoma: 2018 update. *Clin Mol Hepatol* 2019; **25:** 245-63. doi: 10.3350/cmh.2018.0090

37. Choi JW, Lee JM, Kim SJ, Yoon JH, Baek JH, Han JK, et al. Hepatocellular carcinoma: imaging patterns on gadoxetic acid-enhanced MR Images and their value as an imaging biomarker. *Radiology* 2013; **267:** 776-86. doi: 10.1148/radiol.13120775

38. Bartolozzi C, Battaglia V, Bargellini I, Bozzi E, Campani D, Pollina LE, et al. Contrast-enhanced magnetic resonance imaging of 102 nodules in cirrhosis: correlation with histological findings on explanted livers. *Abdom Imaging* 2013; **38:** 290-6. doi: 10.1007/s00261-012-9952-9

39. Kim JH, Joo I, Lee JM. Atypical appearance of hepatocellular carcinoma and its mimickers: How to solve challenging cases using gadoxetic acid-enhanced liver magnetic resonance imaging. *Korean J Radiol* 2019; **20:** 1019-41. doi: 10.3348/kjr.2018.0636

40. Willatt JM, Hussain HK, Adusumilli S, Marrero JA. MR Imaging of hepatocellular carcinoma in the cirrhotic liver: challenges and controversies. *Radiology* 2008; **247:** 311-30. doi: 10.1148/radiol.2472061331

41. Sano K, Ichikawa T, Motosugi U, Sou H, Muhi AM, Matsuda M, et al. Imaging study of early hepatocellular carcinoma: usefulness of gadoxetic acid-enhanced MR imaging. *Radiology* 2011; **261:** 834-44. doi: 10.1148/radiol.11101840

42. Robert M. A comparison of hepatopathologists' and community pathologists' review of liver biopsy specimens from patients with hepatitis C. *Clin Gastroenterol Hepatol* 2009; **7:** 335-8. doi: 10.1016/j.cgh.2008.11.029

43. Kim YK, Lee YH, Kim CS, Han YM. Added diagnostic value of T2-weighted MR imaging to gadolinium-enhanced three-dimensional dynamic MR imaging for the detection of small hepatocellular carcinomas. *Eur J Radiol* 2008; **67:** 304-10. doi: 10.1016/j.ejrad.2007.07.001

44. Piana G, Trinquart L, Meskine N, Barrau V, Beers BV, Vilgrain V. New MR imaging criteria with a diffusion-weighted sequence for the diagnosis of hepatocellular carcinoma in chronic liver diseases. *J Hepatol* 2011; **55:** 126-32. doi: 10.1016/j.jhep.2010.10.023

45. Ahn SS, Kim MJ, Lim JS, Hong HS, Chung YE, Choi JY. Added value of gadoxetic acid-enhanced hepatobiliary phase MR imaging in the diagnosis of hepatocellular carcinoma. *Radiology* 2010; **255:** 459-66. doi: 10.1148/radiol.10091388

46. Kim TK, Lee KH, Jang HJ, Haider MA, Jacks LM, Menezes RJ, et al. Analysis of gadobenate dimeglumine-enhanced MR findings for characterizing small (1-2-cm) hepatic nodules in patients at high risk for hepatocellular carcinoma. *Radiology* 2011; **259:** 730-8. doi: 10.1148/radiol.11101549

47. Kierans AS, Makkar J, Guniganti P, Kierans AS, Makkar J, Guniganti P, et al. Validation of Liver Imaging Reporting and Data System 2017 (LI-RADS) criteria for imaging diagnosis of hepatocellular carcinoma. *J Magn Reson Imaging* 2019; **49:** e205-e15. doi: 10.1002/jmri.26329

48. Chernyak V, Fowler KJ, Kamaya A, Chernyak V, Fowler KJ, Kamaya A, et al. Liver Imaging Reporting and Data System (LI-RADS) Version 2018: Imaging of hepatocellular carcinoma in at-risk patients. *Radiology* 2018; **289:** 816-30. doi: 10.1148/radiol.2018181494

49. Kamath A, Roudenko A, Hecht E, Sirlin C, Chernyak V, Fowler K, et al. CT/MR LI-RADS 2018: Clinical implications and management recommendations. *Abdom Radiol* 2019; **44:** 1306-22. doi: 10.1007/s00261-018-1868-6

50. Cannella R, Fowler KJ, Borhani AA, Minervini MI, Heller M, Furlan A. Common pitfalls when using the Liver Imaging Reporting and Data System (LI-RADS): lessons learned from a multi-year experience. *Abdom Radiol* 2019; **44:** 43-53. doi: 10.1007/s00261-018-1720-z

51. Ishigami K, Yoshimitsu K, Nishihara Y, Irie H, Asayama Y, Tajima T, et al. Hepatocellular carcinoma with a pseudocapsule on gadolinium-enhanced MR images: correlation with histopathologic findings. *Radiology* 2009; **250:** 435-43. doi: 10.1148/radiol.2501071702

52. Narsinh KH, Cui J, Papadatos D, Sirlin CB, Santillan CS. Hepatocarcinogenesis and LI-RADS. *Abdom Radiol* 2018; **43:** 158-68. doi: 10.1007/s00261-017-1409-8

53. Cabibbo G, Enea M, Attanasio M, Bruix J, Craxi A, Camma C. A meta-analysis of survival rates of untreated patients in randomized clinical trials of hepatocellular carcinoma. *Hepatology* 2010; **51:** 1274-83. doi: 10.1002/hep.23485

54. Marrero JA, Fontana RJ, Barrat A, Askari F, Conjeevaram HS, Su GL, et al. Prognosis of hepatocellular carcinoma: comparison of 7 staging systems in an American cohort. *Hepatology* 2005; **41:** 707-16. doi: 10.1002/hep.20636

55. Cillo U, Bassanello M, Vitale A, Grigoletto FA, Burra P, Fagiuoli S, et al. The critical issue of hepatocellular carcinoma prognostic classification: which is the best tool available? *J Hepatol* 2004; **40:** 124-31. doi:10.1016/j.jhep.2003.09.027

56. Forner A, Reig M, Bruix J. Hepatocellular carcinoma. *Lancet* 2018; **391:** 1301-14. doi: 10.1016/S0140-6736(18)30010-2

57. Marasco G, Serenari M, Renzulli M, Alemanni LV, Rossini B, Pettinari I, et al. Clinical impact of sarcopenia assessment in patients with hepatocellular carcinoma undergoing treatments. *J Gastroenterol* 2020; **55:** 927-943. doi: 10.1007/s00535-020-01711-w

58. Harimoto N, Yoshizumi T, Shimokawa M, Sakata K, Kimura K, Itoh S, et al. Sarcopenia is a poor prognostic factor following hepatic resection in patients aged 70 years and older with hepatocellular carcinoma. *Hepatol Res* 2016; **46:**1247-55. doi: 10.1111/hepr.12674

59. Loosen SH, Schulze-Hagen M, Bruners P, Tacke F, Trautwein C, Kuhl C, et al. Sarcopenia is a negative prognostic factor in patients undergoing transarterial chemoembolization (TACE) for hepatic malignancies. *Cancers* 2019; **11:** 1503. doi: 10.3390/cancers11101503.

60. Harimoto N, Shirabe K, Yamashita Y-I, Ikegami T, Yoshizumi T, Soejima Y, et al. Sarcopenia as a predictor of prognosis in patients following hepatectomy for hepatocellular carcinoma. *Br J Surg* 2013; **100:** 1523-30. doi: 10.1002/bjs.9258

61. Voron T, Tselikas L, Pietrasz D, Pigneur F, Laurent A, Compagnon P, et al. Sarcopenia impacts on short- and long-term results of hepatectomy for hepatocellular carcinoma. *Ann Surg* 2015; **261:** 1173-83. doi: 10.1097/SLA.0000000000000743

62. Kojiro M. Pathological evolution of early hepatocellular carcinoma. *Oncology* 2002; **62:** 43-7. doi: 10.1159/000048275

63. Bartolozzi C, Crocetti L, Lencioni R, Cioni D, Della Pina C, Campani D. Biliary and reticuloendothelial impairment in hepatocarcinogenesis: the diagnostic role of tissue-specific MR contrast media. *Eur Radiol* 2007; **17:** 2519-30. doi: 10.1007/s00330-007-0602-5

64. Nasu K, Kuroki Y, Tsukamoto T, Nakajima H, Mori K, Minami M. Diffusion-weighted imaging of surgically resected hepatocellular carcinoma: imaging characteristics and relationship among signal intensity, apparent diffusion coefficient, and histopathologic grade. *AJR Am J Roentgenol* 2009; **193:** 438-44. doi: 10.2214/AJR.08.1424

65. Cruite I, Schroeder M, Merkle EM, Sirlin CB. Gadoxetate disodium-enhanced MRI of the liver: part 2, protocol optimization and lesion appearance in the cirrhotic liver. *AJR Am J Roentgenol* 2010; **195:** 29-41. doi: 10.2214/AJR.10.4538

66. Vasuri F, Golfieri R, Fiorentino M, Capizzi E, Renzulli M, Pinna AD, et al. OATP 1B1/1B3 expression in hepatocellular carcinomas treated with orthotopic liver transplantation. *Virchows Arch* 2011; **459:** 141-6. doi: 10.1007/s00428-011-1099-5.

67. Golfieri R, Garzillo G, Ascanio S, Renzulli M. Focal lesions in the cirrhotic liver: their pivotal role in gadoxetic acid-enhanced MRI and recognition by the Western guidelines. *Dig Dis* 2014; **32:** 696-704. doi: 10.1159/000368002

68. Durnez A, Verslype C, Nevens F, Fevery J, Aerts R, Pirenne J, et al. The clinicopathological and prognostic relevance of cytokeratin 7 and 19 expression in hepatocellular carcinoma. A possible progenitor cell origin. *Histopathology* 2006; **49:** 138-51. doi: 10.1111/j.1365-2559.2006.02468.x

69. Vasuri F, Renzulli M, Fittipaldi S, Brocchi S, Clemente A, Cappabianca S, et al. Pathobiological and radiological approach for hepatocellular carcinoma subclassification. *Sci Rep* 2019; **9:** 14749. doi: 10.1038/s41598-019-51303-9

70. Narita M, Hatano E, Arizono S, Miyagawa-Hayashino A, Isoda H, Kitamura K, et al. Expression of OATP1B3 determines uptake of Gd-EOB-DTPA in hepatocellular carcinoma. *J Gastroenterol* 2009; **44:** 793-8. doi: 10.1007/s00535-009-0056-4

71. Granito A, Galassi M, Piscaglia F, Romanini L, Lucidi V, Renzulli M, et al. Impact of gadoxetic acid (Gd-EOB-DTPA)-enhanced magnetic resonance on the non-invasivediagnosis of small hepatocellular carcinoma: a prospective study. *Aliment Pharmacol Ther* 2013; **37:** 355-63. doi: 10.1111/apt.12166

72. Ichikawa T, Sano K, Morisaka H. Diagnosis of pathologically early HCC with EOB-MRI: experiences and current consensus. *Liver Cancer* 2014; **3:** 97-107. doi: 10.1159/000343865

73. Golfieri R, Renzulli M, Lucidi V, Corcioni B, Trevisani F, Bolondi L. Contribution of the hepatobiliary phase of Gd-EOB-DTPA-enhanced MRI to Dynamic MRI in the detection of hypovascular small (≤ 2 cm) HCC in cirrhosis. *Eur Radiol* 2011; **21:** 1233-42. doi: 10.1007/s00330-010-2030-1

74. Renzulli M, Golfieri R, Bologna Liver Oncology Group (BLOG). Proposal of a new diagnostic algorithm for hepatocellular carcinoma based on the Japanese guidelines but adapted to the Western world for patients under surveillance for chronic liver disease. *J Gastroenterol Hepatol* 2016; **31:** 69-80. doi: 10.1111/jgh.13150

75. Golfieri R, Grazioli L, Orlando E, Dormi A, Lucidi L, Corcioni B, et al. Which is the best MRI marker of malignancy for atypical cirrhotic nodules: hypointensity in hepatobiliary phase alone or combined with other features? Classification after Gd-EOB-DTPA administration. *J Magn Reson Imaging* 2012; **36:** 648-57. doi: 10.1002/jmri.23685

76. Kim T, Murakami T, Hasuike Y, Gotoh M, Kato N, Takahashi M, et al. Experimental hepatic dysfunction: evaluation by MRI with Gd-EOB-DTPA. *J Magn Reson Imaging* 1997; **7:** 683-8. doi: 10.1002/jmri.1880070413

77. Taouli B. Diffusion-weighted MR imaging for liver lesion characterization: a critical look. *Radiology* 2012; **262:** 378-80. doi: 10.1148/radiol.11112417

78. Takayama T, Makuuchi M, Hirohashi S, Sakamoto M, Okazaki N, Takayasu K, et al. Malignant transformation of adenomatous hyperplasia to hepatocellular carcinoma. *Lancet* 1990; **336:** 1150-3. doi: 10.1016/0140-6736(90)92768-d

79. Roncalli M, Roz E, Coggi G, Di Rocco MG, Bossi P, Minola E, et al. The vascular profile of regenerative and dysplastic nodules of the cirrhotic liver: implications for diagnosis and classification. *Hepatology* 1999; **30:** 1174-8. doi: 10.1002/hep.510300507

80. Koh DM, Collins DJ. Diffusion-weighted MRI in the body: applications and challenges in oncology. *AJR Am J Roentgenol* 2007; **188:** 1622-35. doi: 10.2214/AJR.06.1403

81. van den Bos IC, Hussain SM, Dwarkasing RS, Hop WCJ, Zondervan PE, de Man RA, et al. MR imaging of hepatocellular carcinoma: relationship between lesion size and imaging findings, including signal intensity and dynamic enhancement patterns. *J Magn Reson Imaging* 2007; **26:** 1548-55. doi: 10.1002/jmri.21046

82. Bruegel M, Holzapfel K, Gaa J, Bruegel M, Holzapfel K, Gaa J, et al. Characterization of focal liver lesions by ADC measurements using a respiratory triggered diffusion-weighted single-shot echo-planar MR imaging technique. *Eur Radiol* 2008; **18:** 477-85. doi: 10.1007/s00330-007-0785-9

83. Lee MH, Kim SH, Park MJ, Park CK, Rhim H. Gadoxetic acid-enhanced hepatobiliary phase MRI and high-b-value diffusion-weighted imaging to distinguish well-differentiated hepatocellular carcinomas from benign nodules in patients with chronic liver disease. *AJR Am J Roentgenol* 2011; **197:** W868-75. doi: 10.2214/AJR.10.6237

84. Sandrasegaran K, Akisik FM, Lin C, Tahir B, Rajan J, Saxena R, et al. Value of diffusion-weighted MRI for assessing liver fibrosis and cirrhosis. *AJR Am J Roentgenol* 2009; **193:** 1556-60. doi: 10.2214/AJR.09.2436

85. Park MJ, Kim YK, Lee MW, Lee WJ, Kim YS, Kim SH, et al. Small hepatocellular carcinomas: improved sensitivity by combining gadoxetic acid-enhanced and diffusion-weighted MR imaging patterns. *Radiology* 2012; **264:** 761-70. doi: 10.1148/radiol.12112517

86. Kadoya M, Matsui O, Takashima T, Nonomura A. Hepatocellular carcinoma: correlation of MR imaging and histopathologic findings. *Radiology* 1992; **183:** 819-25. doi: 10.1148/radiology.183.3.1316622

87. Channual S, Tan N, Siripongsakun S, Lassman C, Lu DS, Raman SS. Gadoxetate disodium-enhanced MRI to differentiate dysplastic nodules and grade of hepatocellular carcinoma: Correlation with histopathology. *AJR Am J Roentgenol* 2015; **205:** 546-53. doi: 10.2214/AJR.14.12716

88. Hwang J, Kim YK, Jeong WK, Choi D, Rhim H, Lee WJ. Nonhypervascular hypointense nodules at gadoxetic acid-enhanced MR imaging in chronic liver disease: Diffusion-weighted imaging for characterization. *Radiology* 2015; **276:** 137-46. doi: 10.1148/radiol.15141350

89. Kim T, Baron RL, Nalesnik MA. Infarcted regenerative nodules in cirrhosis: CT and MR imaging findings with pathologic correlation. *AJR Am J Roentgenol* 2000; **175:** 1121-5. doi: 10.2214/ajr.175.4.1751121

90. Miyayama S, Yamashiro M, Okuda M, Yoshie Y, Nakashima Y, Ikeno H, et al. Detection of corona enhancement of hypervascular hepatocellular carcinoma by C-arm dual-phase cone-beam CT during hepatic arteriography. *Cardiovasc Intervent Radiol* 2011; **34:** 81-6. doi: 10.1007/s00270-010-9835-9

91. Santillan C, Fowler K, Kono Y, Chernyak V. LI-RADS major features: CT, MRI with extracellular agents, and MRI with hepatobiliary agents. *Abdom Radiol* 2018; **43:** 75-81. doi: 10.1007/s00261-017-1291-4

92. Stevens WR, Gulino SP, Batts KP, Stephens DH, Johnson CD. Mosaic pattern of hepatocellular carcinoma: Histologic basis for a characteristic CT appearance. *J Comput Assist Tomogr* 1996; **20:** 337-42. doi: 10.1097/00004728-199605000-00001

93. Park HJ, Jang KM, Kang TW, Song KD, Kim SH, Kim YK, et al. Identification of imaging predictors discriminating different primary liver tumours in patients with chronic liver disease on gadoxetic acid-enhanced MRI: a classification tree analysis. *Eur Radiol* 2016; **26:** 3102-11. doi: 10.1007/s00330-015-4136-y

94. Paik N, Sinn DH, Lee JH, Oh IS, Kim JH, Kang W, et al. Non-invasive tests for liver disease severity and the hepatocellular carcinoma risk in chronic hepatitis B patients with low-level viremia. *Liver Int* 2018; **38:** 68-75. doi: 10.1111/liv.13489

95. Marasco G, Colecchia A, Silva G, Rossini B, Eusebi LH, Ravaioli F, et al. Non-invasive tests for the prediction of primary hepatocellular carcinoma. *World J Gastroenterol* 2020; **26:** 3326-43. doi: 10.3748/wjg.v26.i24.3326

96. Leoni S, Piscaglia F, Golfieri R, Camaggi V, Vidili G, Pini P, et al. The impact of vascular and nonvascular findings on the noninvasive diagnosis of small hepatocellular carcinoma based on the EASL and AASLD criteria. *Am J Gastroenterol* 2010; **105:** 599-609. doi: 10.1038/ajg.2009.654

97. Choi JW, Lee JM, Kim SJ, Yoon JH, Baek JH, Han JK, et al. Hepatocellular carcinoma: imaging patterns on gadoxetic acid-enhanced MR Images and their value as an imaging biomarker. *Radiology* 2013; **267:** 776-86. doi: 10.1148/radiol.13120775

98. Kim YK, Lee WJ, Park MJ, Kim SH, Rhim H, Choi D. Hypovascular hypointense nodules on hepatobiliary phase gadoxetic acid-enhanced MR images in patients with cirrhosis: potential of DW imaging in predicting progression to hypervascular HCC. *Radiology* 2012; **265:** 104-14. doi: 10.1148/radiol.12112649

99. Hyodo T, Murakami T, Imai Y, Okada M, Hori M, Kagawa Y, et al. Hypovascular nodules in patients with chronic liver disease: risk factors for development of hypervascular hepatocellular carcinoma. *Radiology* 2013; **266:** 480-90. doi: 10.1148/radiol.12112677

100. Kumada T, Toyoda H, Tada T, Sone Y, Fujimori M, Ogawa S, et al. Evolution of hypointense hepatocellular nodules observed only in the hepatobiliary phase of gadoxetate disodium-enhanced MRI. *AJR Am J Roentgenol* 2011; **197:** 58-63. doi: 10.2214/AJR.10.5390

101. Yoon JH, Lee JM, Yang HK, Lee KB, Jang JJ, Han JK, et al. Non-hypervascular hypointense nodules ≥1 cm on the hepatobiliary phase of gadoxetic acid-enhanced magnetic resonance imaging in cirrhotic livers. *Dig Dis* 2014; **32:** 678-89. doi: 10.1159/000368000

102. Motosugi U, Ichikawa T, Sano K, Motosugi U, Ichikawa T, Sano K, et al. Outcome of hypovascular hepatic nodules revealing no gadoxetic acid uptake in patients with chronic liver disease. *J Magn Reson Imaging* 2011; **34:** 88-94. doi: 10.1002/jmri.22630

103. Efremidis SC, Hytiroglou P, Matsui O. Enhancement patterns and signal-intensity characteristics of small hepatocellular carcinoma in cirrhosis: pathologic basis and diagnostic challenges. *Eur Radiol* 2007; **17:** 2969-82. doi: 10.1007/s00330-007-0705-z

104. Yu MH, Kim JH, Yoon JH, Kim HC, Chung JW, Han JK, et al. Small (≤1-cm) hepatocellular carcinoma: diagnostic performance and imaging features at gadoxetic acid-enhanced MR imaging. *Radiology* 2014; **271:** 748-60. doi: 10.1148/radiol.14131996

105. Jeong YY, Mitchell DG, Kamishima T. Small (<20 mm) enhancing hepatic nodules seen on arterial phase MR imaging of the cirrhotic liver: clinical implications. *AJR Am J Roentgenol* 2002; **178:** 1327-34. doi: 10.2214/ajr.178.6.1781327

106. Holland AE, Hecht EM, Hahn WY, Holland AE, Hecht EM, Hahn WY, et al. Importance of small (< or = 20-mm) enhancing lesions seen only during the hepatic arterial phase at MR imaging of the cirrhotic liver: evaluation and comparison with whole explanted liver. *Radiology* 2005; **237:** 938-44. doi: 10.1148/radiol.2373041364

107. Hussain HK, Syed I, Nghiem HV, Johnson TD, Carlos RC, Weadock WJ, et al. T2-weighted MR imaging in the assessment of cirrhotic liver. *Radiology* 2004; **230:** 637-44. doi: 10.1148/radiol.2303020921

108. Kim JE, Kim SH, Lee SJ, Rhim H. Hypervascular hepatocellular carcinoma 1 cm or smaller in patients with chronic liver disease: characterization with gadoxetic acid-enhanced MRI that includes diffusion-weighted imaging. *AJR Am J Roentgenol* 2011; **196:** W758-65. doi: 10.2214/AJR.10.4394

109. Semelka RC, Brown ED, Ascher SM, Patt RH, Bagley AS, Li W, et al. Hepatic hemangiomas: a multi-institutional study of appearance on T2-weighted and serial gadolinium-enhanced gradient-echo MR images. *Radiology* 1994; **192:** 401-6. doi: 10.1148/radiology.192.2.8029404

110. Kitao A, Zen Y, Matsui O, Kitao A, Zen Y, Matsui O, et al. Hepatocellular carcinoma: signal intensity at gadoxetic acid-enhanced MR Imaging--correlation with molecular transporters and histopathologic features. *Radiology* 2010; **256:** 817-26. doi: 10.1148/radiol.10092214

111. Leonhardt M, Keiser M, Oswald S, Kühn J, Jia J, Grube M, et al. Hepatic uptake of the magnetic resonance imaging contrast agent Gd-EOB-DTPA: role of human organic anion transporters. *Drug Metab Dispos* 2010; **38:** 1024-8. doi: 10.1124/dmd.110.032862

112. Asayama Y, Tajima T, Nishie A, Ishigami K, Kakihara D, Nakayama T, et al. Uptake of Gd-EOB-DTPA by hepatocellular carcinoma: radiologic-pathologic correlation with special reference to bile production. *Eur J Radiol* 2011; **80:** e243-8. doi: 10.1016/j.ejrad.2010.10.032

113. Grazioli L, Morana G, Caudana R, Benetti A, Portolani N, Talamini G, et al. Hepatocellular carcinoma: correlation between gadobenate dimeglumine-enhanced MRI and pathologic findings. *Invest Radiol* 2000; **35:** 25-34. doi: 10.1097/00004424-200001000-00003]

114. Tsuda N, Kato N, Murayama C, Narazaki M, Yokawa T. Potential for differential diagnosis with gadolinium-ethoxybenzyl-diethylenetriamine pentaacetic acid-enhanced magnetic resonance imaging in experimental hepatic tumors. *Invest Radiol* 2004; **39:** 80-8. doi: 10.1097/01.rli.0000105331.11373.c0

115. Vavricka SR, Jung D, Fried M, Grützner U, Meier PJ, Kullak-Ublick GA. The human organic anion transporting polypeptide 8 (SLCO1B3) gene is transcriptionally repressed by hepatocyte nuclear factor 3 beta in hepatocellular carcinoma. *J Hep*atol 2004; **40:** 212-8. doi: 10.1016/j.jhep.2003.10.008

116. Tsuboyama T, Onishi H, Kim T, Akita H, Hori M, Tatsumi M, et al. Hepatocellular carcinoma: hepatocyte-selective enhancement at gadoxetic acid-enhanced MR imaging-correlation with expression of sinusoidal and canalicular transporters and bile accumulation. *Radiology* 2010; **255:** 824-33. doi: 10.1148/radiol.10091557

117. Kondo Y, Nakajima T. Pseudoglandular hepatocellular carcinoma. A morphogenetic study. *Cancer* 1987; **60:** 1032-7. doi: 10.1002/1097-0142(19870901)60:5<1032::aid-cncr2820600518>3.0.co;2-k

118. Kim JY, Kim MJ, Kim KA, Jeong HT, Park YN. Hyperintense HCC on hepatobiliary phase images of gadoxetic acid-enhanced MRI: correlation with clinical and pathological features. *Eur J Radiol* 2012; **81:** 3877-82. doi: 10.1016/j.ejrad.2012.07.021

119. Yoneda N, Matsui O, Kitao A, Kita R, Kozaka K, Koda W, et al. Hypervascular hepatocellular carcinomas showing hyperintensity on hepatobiliary phase of gadoxetic acid-enhanced magnetic resonance imaging: a possible subtype with mature hepatocyte nature. *Jpn J Radiol* 2013; **31:** 480-90. doi: 10.1007/s11604-013-0224-6

120. Kitao A, Matsui O, Yoneda N, Kita R, Kozaka K, Kobayashi S, et al. Differentiation between hepatocellular carcinoma showing hyperintensity on the hepatobiliary phase of gadoxetic acid-enhanced MRI and focal nodular hyperplasia by CT and MRI. *AJR Am J Roentgenol* 2018; **211:** 347-57. doi: 10.2214/AJR.17.19341

121. Vilgrain V, Lewin M, Vons C, Denys A, Valla D, Flejou JF, et al. Hepatic nodules in Budd–Chiari syndrome: imaging features. *Radiology* 1999; **210:** 443-50. doi: 10.1148/radiology.210.2.r99fe13443

122. Renzulli M, Lucidi V, Mosconi C, Quarneti C, Giampalma E, Golfieri R. Large regenerative nodules in a patient with Budd–Chiari syndrome after TIPS positioning while on the liver transplantation list diagnosed by Gd-EOB-DTPA MRI. *Hepatobiliary Pancreat Dis Int* 2011; **10:** 439-42. doi: 10.1016/s1499-3872(11)60075-1

*review*

# Surgical treatment and fertility perservation in endometrial cancer

Nina Kovacevic[1,2,3]

[1] Department of Gynaecological Oncology, Institute of Oncology Ljubljana, Ljubljana, Slovenia
[2] Faculty of Medicine, University of Ljubljana, Ljubljana, Slovenia
[3] Faculty of Health Care Angela Boškin, Jesenice, Slovenia

Radiol Oncol 2021; 55(2): 144-149.

Received 24 November 2020
Accepted 18 January 2021

Correspondence to: Assist. Nina Kovačević M.D., Ph.D., Department of Gynaecological Oncology, Institute of Oncology Ljubljana, Zaloška cesta 2, SI-1000 Ljubljana, Slovenia. Phone: + 386 41 277 602; E-mail: nkovacevic@onko-i.si .

Disclosure: No potential conflicts of interest were disclosed.

**Background.** Endometrial cancer (EC) represents a high health burden in Slovenia and worldwide. The incidence is increasing due to lifestyle and behavioural risk factors such as obesity, smoking, oestrogen exposure and aging of the population. In many cases, endometrial cancer is diagnosed at an early stage due to obvious signs and symptoms. The standard treatment is surgery with or without adjuvant therapy, depending on the stage of the disease and the risk of recurrence. However, treatment modalities have changed in the last decades, considerably in the extent of lymphadenectomy.

**Conclusions.** The gold standard of treatment for is surgery, which may be the only treatment modality in the early stages of low-grade tumours. In recent years, a minimally invasive approach with sentinel node biopsy (SNB) has been proposed. A conservative approach with hormonal treatment is used if fertility preservation is desired. If EC is in advance stage, high-risk histology, or high grade, radiotherapy, chemotherapy, or a combination of both is recommended.

Key words: endometrial cancer; uterus, treatment; minimally invasive surgery; laparoscopy

## Introduction

Endometrial cancer (EC) is the most common gynaecological cancer in Slovenia and worldwide. Due to the rapid onset of symptoms and good diagnostic possibilities, the majority of cases are diagnosed at an early stage of the disease, which provides good treatment prospects and high overall survival rate.[1]

EC is the fifth most common cancer among women in Slovenia. The average number of new cases per year in 2013–2017 was 305 (29.5/100,000 women) and 61 women died (5.9/100,000 women). EC in 90% of cases occurs in women over the age of 50. The median age at diagnosis is 63 years.[2] Approximately 4% of patients diagnosed with EC are under 40 years of age and wish to preserve their fertility.[3]

In most cases, EC is diagnosed at the early stages of the disease (80% in FIGO stage I ), with a five-year overall survival rate of over 95%. However, if the disease is locally advanced or distant metastases are present, the five-year overall survival rate is 68% for locally advanced disease and 17% for distant metastases.[4] In early stage of the disease, surgery alone is the gold standard of treatment. In advanced stage of EC, adjuvant therapy is often suggested, but is not standardized. Adjuvant therapy may include chemotherapy, radiotherapy, or a combination of both.[5] In this article we give an overview of the surgical treatment for EC.

## Classification

EC, which accounts for about 98% of cancers of the uterine body, can be divided into two groups according to clinical and pathological characteristics.

EC type I generally has a favorable prognosis. Most tumors in this group are endometrioid carcinomas, but mucinous carcinomas are also included in this group. Type I carcinomas are the result of long-term exposure to estrogen without progesterone. They arise from endometrial hyperplasia or endometrial intraepithelial neoplasia (EIN). In most cases they are well differentiated and are usually detected at an early stage of the disease. Most risk factors are related to estrogen exposure. Risk factors include obesity, hormone replacement therapy, polycystic ovary syndrome, early onset of menarche and late menopause. The most important risk factor is obesity, which increases the relative risk by 2.54.[6] Women who are unable to conceive or have never given birth are also at higher risk.[7] The use of combined oral contraceptives reduces the incidence of EC.[8]

EC type II are aggressive tumours with a worse prognosis. This group includes serous, clear cell, neuroendocrine, mixed-cell, undifferentiated and dedifferentiated endometrial carcinomas and carcinosarcoma. Type II carcinomas are not related to the action of oestrogen. They occur in the atrophic endometrium and are by definition highly malignant or high-grade tumors.[7,9]

All tumours must be histologically verified. Endometrioid carcinomas, which account for 75% of EC, are classified by nuclear grade and architectural pattern.[10] If the tumour has less than 5% of the solid growth pattern, the tumour is classified as grade 1. If 6–50% of solid growth patterns are present, the tumour is classified as grade 2 and grade 3 if it accounts for more than 50% of solid growth patterns.

Mucinous adenocarcinomas have a mucinous appearance in more than 50% of the tumour. They usually have a favourable prognosis. Serous carcinomas have a papillary architecture with atypical mitosis and nucleolus. Clear cell adenocarcinomas have the worst prognosis and different histological patterns, from papillary, glandular to tubulocystic and diffuse. Mixed cell carcinomas combine two or more pure types. In undifferentiated carcinomas there is no differentiation.[11]

## Genetic predisposition

EC may also occur in association with various hereditary syndromes or inherited genetic disorders. 2–3% of EC occur in women with Lynch / Hereditary Non-Polyposis Colorectal Cancer syndrome.[12] EC is caused by germline mutations in mismatch repair (MMR) genes, namely MLH1, MLH2, MSH6, and PMS2. People with Lynch syndrome have a 10–80% risk of developing colorectal cancer by age 70 and a 15–60% risk of developing endometrial cancer by age 70.[13] Lynch syndrome carriers are diagnosed with EC at an early age (60% between the ages of 44 and 62).[14] Screening colonoscopy every 1 to 2 years for women with Lynch syndrome is part of the recommendations. The importance of screening endometrial biopsy every 1–2 years after the age of 30–35 years still needs to be proven but is recommended by National Comprehensive Cancer Network (NCCN Guidelines Genetic/Familial High Risk Assessment: Colorectal, Version 1.2020, Lynch syndrome).[15] Prophylactic hysterectomy with bilateral salpingo-oophorectomy is recommended in women who have completed childbearing.[4,16] Cowden syndrome is another, much rarer hereditary cause of EC. A germline mutation in the tumour suppressor PTEN gene is present.[17]

## Surgical treatment

The diagnosis of EC must be made before surgery. It can be made by pipelle aspiration, by dilatation of the cervix and curettage or by hysteroscopy with biopsy of the endometrium. Today, hysteroscopy is the most commonly used procedure. There is some evidence of an increased risk of intraperitoneal spread of malignant cells into the abdominal cavity. The reason for this could be the use of distension fluid.[18–20]

The standard treatment for EC is surgery, where minimally invasive surgery has become increasingly prevalent in recent years.[21] Randomised trials comparing laparoscopy and laparotomy for surgical staging of EC reported no difference in detection of overall disease at advanced stages, equal or fewer intra- and postoperative complications with laparoscopic approach and shorter hospital stays.[22,23]

The standard approach for the treatment of early stages EC (FIGO stages IA–IIA) is surgical, with removal of the uterus, ovaries, fallopian tubes and with or without sentinel node biopsy (SNB). The approach can be by laparotomy or minimally invasive by laparoscopy or robotic-assisted laparoscopy. Studies have shown that obese patients and patients with comorbidities also benefit from laparoscopic approach.[24,25]

Young premenopausal patients under 40 years of age usually have early stage disease and low-grade tumours.[26] Artificially induced menopause and its

consequences should be avoided. Therefore, ovarian preservation should be considered in selected cases. Retrospective studies and meta-analysis have shown no effect on overall survival if the ovaries are left *in situ* in selected cases at early stages EC. However, synchronous malignant ovarian tumors must be excluded.[27,28]

Lymphadenectomy has its role in staging of EC. However, there is still no consensus on the therapeutic value, indications and extent of the procedure (pelvic, para-aortic to the inferior mesenteric artery or para-aortic to the left renal vein). The sentinel lymph node is the first lymph node in the lymphatic basin into which the lymph of the primary tumour drains. Histologic examination of the sentinel lymph node is representative of all other lymph nodes in the area, and a histologically negative sentinel lymph node signifies the absence of metastases in other non-sentinel lymph nodes. Indocyanine green (ICG) solution is applied to the cervix, which then fluoresces in infrared light so that the lymphatic pathway can be followed until it enters the sentinel lymph nodes.[29] ICG solution is injected superficially into the cervix at 2 or 4 points (at 3, 6, 9 and 12 o'clock), 1-3 mm below the mucosa. Optionally, the solution can be injected deeper, 1–2 cm into the cervical stroma. This allows excellent redistribution of ICG solution around the uterine vessels and lymphatic basin of the parameterium and broad ligament. SNB is performed in the early stage EC, with no suspicious lymph nodes and/or extrauterine spread on imaging.[30]

SNB is an intermediate step between the omission of radical lymphadenectomy and the renunciation of lymphadenectomy. In 2017, FIRES multicentre prospective study showed that the use of the SNB procedure can safely replace lymphadenectomy in the early stage EC.[31]

While SNB can be falsely negative and fails to detect metastases in 3% of cases, the procedure has the potential to expose fewer patients to the morbidity of a complete lymphadenectomy.[31]

The risk rate for regional lymph node seeding in the group of patients with low and intermediate risk EC is approximately 1.4%.[32,33] The risk that would justify a pelvic lymphadenectomy should reach at least 3%, so in most cases routine pelvic lymphadenectomy is not recommended in this group of patients.[4]

Part of the surgical treatment of high- risk EC is also a complete pelvic and para-aortic lymphadenectomy with the upper border to the left renal vein.[4] In two retrospective studies, it was observed that the overall survival of patients with the removal of more than 10–12 pelvic lymph nodes was longer.[34,35] It is important to remember that in 7–8% of cases para-aortic lymph nodes may also be positive even if the pelvic lymph nodes are negative.[36,37] Therefore, removal of both pelvic and para-aortic lymph nodes is recommended in high-risk EC.[4,36]

In non-endometrioid and other high- risk histologic types, omentectomy is also performed as part of the staging procedure. Studies have shown longer progression-free survival and overall survival in patients in whom complete or optimal cytoreduction has been achieved.[38]

## Radiotherapy for inoperable endometrial cancer

In 3–9% of patients, surgery is not an option due to medical comorbidities, advanced age, or patient refusal of surgery. Non-surgical treatment, such as radiotherapy, is available as an alternative for this group of patients. It can be used in early or advanced stage EC.[39] Treatment includes brachytherapy alone or in combination with external- beam radiotherapy (EBRT).[4]

Patients with low grade and stage I EC can be treated with brachytherapy alone. Recurrence usually occurs in vaginal vault, which supports the idea of omitting EBRT. EBRT is part of the treatment regimen for patients with indications for lymphadenectomy (tumor grade II and III and high-risk histology). Patients with stage II-IV disease, regardless of grade, should receive a combination of EBRT and brachytherapy. Overall survival rate ranges from 70% to 80% among inoperable population.[39]

## Adjuvant treatment

### Risk groups for the use of adjuvant therapy

The classification system for patients with EC divides patients into six groups, namely low-, intermediate-, high-intrmediate-, high risk, advanced and metastatic. The system is based on surgical and clinicopathologic prognostic factors and indicates the prognosis, the disease recurrence rate and determines the indications for further adjuvant treatment.[4] Lymph node metastases are the most important prognostic factor causing increased risk of relapse and a higher mortality rate.[40,41]

Low risk EC are considered, endometriod cancers, stage I, grade 1 and 2 with less than 50% myo-

metrial invasion and no limfovascular invasion. The risk of locoregional recurrence is less than 3% in this group, and therefore adjuvant treatment not recommended.[4,42]

Intermediate risk EC are considered endometrioid cancers, stage I, grade 1 and 2, with 50% or more myometrial invasion and no limfovascular invasion. Adjuvant brachytherapy is recommended to decrease the vaginal recurrence rate. No adjuvant therapy is an option in patients younger than 60 years.[4]

High-intermediate risk EC are stage I, grade 3 endometrioid carcinomas with less than 50% myometrial invasion, with positive or negative limfovascular invasion. This group also includes stage I, grade 1 and 2 endometrioid carcinomas with positive limfovascular invasion, regardless of the depth of myometrial invasion.[4] Without adjuvant treatment, the 5-year recurrence rate in this group is up to 25%.[43]

High risk EC are stage I endometrioid carcinomas, grade 3 with 50% or more myometrial invasion, all stage II and III carcinomas with no residual disease after primary cyoreduction, and all other non-endometrioid histologies.[4] In this group, adjuvant radiotherapy of the whole pelvis is standard. In stage IIIC2 (involvement of paraaortic lymph nodes with or without positive pelvic lymph nodes) extended field radiotherapy should be considered. The 5-year overall survival rate is only 20-60% due to the higher recurrence rate and higher rate of distant metastases.[44]

Radiotherapy is most commonly used as adjuvant therapy for intermediate- to high-risk carcinomas.[45] Chemotherapy is used as postoperative treatment for high-risk stage I and II disease, stage III and IV disease or as primary treatment for unresectable advanced, metastatic, or recurrent disease.[5] The combination of carboplatin and paclitaxel is considered first- line chemotherapy. The purpose of chemotherapy is to prevent the occurrence of distant metastases, and the purpose of concomitant chemotherapy and radiation is to reduce the likelihood of local recurrence.[5,12,46]

## Preservation of fertility

EC is rather rare in younger patients, usually with a lower stage and grade, and therefore with a favorable prognosis and a higher 5-year survival rate.[47,48] Approximately 4% of patients with EC are under 40 years of age at the time of diagnosis and have a desire to preserve their fertility.[47] They are still at reproductive age and are postponing motherhood. After careful consideration and counselling, selected patients can be treated conservatively with oral progestin, preserving the uterus and ovaries. This treatment is only possible in women with endometrioid type EC, grade 1, in whom the tumour is confined to the endometrium without evidence of myometrial invasion or spread of disease outside the uterus. Selected patients must have a strong desire for fertility preservation and an age of less than 40 years.[47,49] Patients should be clearly informed that this is not a standard treatment approach. Strong and diffuse immunohistochemical expression of progesterone receptors on endometrial specimens is a reliable predictor of remission, but 50% of patients with negative progesterone receptors also achieve remission.[50] The most important predictive factor for outcome is tumour stage. There is no optimal method to determine the stage of the disease before conservative treatment. Clinical staging of EC remains a challenge. The gold standard for staging remains surgery.[51] Histologic type and grade of tumour should be confirmed by fractional abrasion or hysteroscopy. Magnetic resonance imaging of the abdomen should be performed to more accurately determine the depth of invasion into the myometrium and the possible extrauterine extent of the disease. If the evaluation is still inconclusive, exploratory laparoscopy with peritoneal lavage, SNB, and ovarian biopsy should be considered. There is still a 5–30% chance that the tumour is higher grade or more widespread than indicated by the tests.[51,52]

Medroxyprogesterone acetate and megestrol acetate are the most commonly used oral progestin for conservative treatment of EC. Cyclic (14 days every month) or continuous different dosing regimens are used.[4] In the study published by Kallogianidis and Agorastos, the overall response rate to oral progestin was 73% and the relapse rate was 36%.[48] Levonorgestrel-releasing intrauterine device is an alternative to oral progestin for the conservative treatment of EC. The study published by Pal *et al*. showed similar recurrence and relapse rates to oral progestin.[53] Patient response to treatment should be assessed every 3–6 months with cervical dilatation and curettage. If EC recurrence occurs after initial response, hysterectomy should be suggested.[4]

Total hysterectomy with bilateral tubectomy is also recommended after childbearing has been terminated, even if complete response to conservative treatment has been achieved, as risk factors often persist after treatment has ended.[49]

## Follow-up

After completion of primary treatment, women undergo long-term follow-up. The aim of routine follow-up is to detect recurrence and spread of the disease before clinical symptoms appear. Early detection of recurrence allows better treatment modalities to be offered with higher survival rates. Most recurrences occur in the first two years after primary treatment. EC metastases are often found in the vaginal vault, suburethral, pelvis, upper abdomen, and lungs. Regular follow-up appointments also allow the gynaecological oncologist to assess the physical and psychological consequences of treatment.[54]

## Conclusions

Due to the high incidence of EC, it must be taken into account that primary prevention is important, especially the reduction of oestrogen exposure. Considered use of hormone replacement therapy has halted the growing trend of EC in recent years. The gold standard of EC treatment is surgery, which may be the only treatment modality for early stage, low- grade tumours. In recent years, a minimally invasive approach with SNB has been introduced. In high grade EC, high-risk hystologies or advanced stage EC adjuvant treatment is recommended. Radiotherapy, chemotherapy or a combination of both is applicable.

When EC affects younger women, hereditary syndromes must be considered. A conservative approach with hormonal treatment is used if fertility preservation is desired.

Regular follow-up by an experienced gynaecological oncologist is crucial for early detection of EC recurrence

## References


1. Šegedin B, Merlo S, Smrkolj Š, Bebar S, Blatnik A, Cerar O, et al. [*Recommendations in management of endometrial cancer*]. [Slovenian]. Institute of Oncology Ljubljana: Radiotherapy and Oncology Society: Ljubljana; 2018.
2. *Cancer in Slovenia 2017*. Ljubljana: Institute of Oncology Ljubljana, Epidemiology and Cancer Registry, Slovenian Cancer Registry; 2020.
3. Corzo C, Barrientos Santillan N, Westin SN, Ramirez PT. Updates on conservative management of endometrial cancer. *J Minim Invasive Gynecol* 2018; **25:** 308-13. doi: 10.1016/j.jmig.2017.07.022
4. Colombo N, Creutzberg C, Amant F, Bosse T, González-Martín A, Ledermann J, *et al.* ESMO-ESGO-ESTRO consensus conference on endometrial cancer: diagnosis, treatment and follow-up. *Ann Oncol* 2016; **27:** 16-41. doi: 10.1093/annonc/mdv484
5. Neri M, Peiretti M, Melis GB, Piras B, Vallerino V, Paoletti AM, et al. Systemic therapy for the treatment of endometrial cancer. *Expert Opin Pharmacother* 2019; **20:** 2019-32. doi: 10.1080/14656566.2019.1654996
6. Zhang Y, Liu H, Yang S, Zhang J, Qian L, Chen X. Overweight, Obesity and endometrial cancer risk: results from a systematic review and meta-analysis. *Int J Biol Markers* 2014; **29:** e21-9. doi: 10.5301/jbm.5000047
7. Malik TY, Chishti U, Aziz AB, Sheikh I. Comparison of risk factors and survival of type 1 and type II endometrial cancers. *Pak J Med Sci* 2016; **32:** 886-90. doi: 10.12669/pjms.324.9265
8. Hannaford PC, Iversen L, Macfarlane TV, Elliott AM, Angus V, Lee AJ. Mortality among contraceptive pill users: cohort evidence from Royal College of General Practitioners' Oral Contraception Study. *BMJ* 2010; **340:** c927. doi: 10.1136/bmj.c927
9. Setiawan VW, Yang HP, Pike MC, McCann SE, Yu H, Xiang Y-B, et al. Type I and II endometrial cancers: have they different risk factors? *J Clin Oncol* 2013; **31:** 2607-18. doi: 10.1200/JCO.2012.48.2596
10. Kurman RJ, Carcangiu ML, Herrington CS, Young RH, editors. *WHO classification of tumours of female reproductive organs*. 4th edition. Lyon: International Agency for Research on Cancer, World Health Organization; 2014.
11. Arko D, Kozar N, Rmuš M, Takač I. The reliability of preoperative determination of tumour grade in endometrial cancer. *Zdrav Vest* 2018; **87:** 167-75. doi: 10.6016/ZdravVestn.2495
12. Brooks RA, Fleming GF, Lastra RR, Lee NK, Moroney JW, Son CH, et al. Current recommendations and recent progress in endometrial cancer. *CA Cancer J Clin* 2019; **69:** 258-79. doi: 10.3322/caac.21561
13. Hampel H. Genetic counseling and cascade genetic testing in Lynch syndrome. *Fam Cancer* 2016; **15:** 423-7. doi: 10.1007/s10689-016-9893-5
14. Hinchcliff EM, Bednar EM, Lu KH, Rauh-Hain JA. Disparities in gynecologic cancer genetics evaluation. *Gynecol Oncol* 2019; **153:** 184-91. doi: 10.1016/j.ygyno.2019.01.024
15. National Comprehensive Cancer Network. Genetic/familial high-risk assessment: colorectal: Version 1.2020 - July 21, 2020. [cited 2021 Jan 11]. Available at: https://www.nccn.org/professionals/physician_gls/pdf/genetics_colon.pdf
16. Daniels MS, Lu KH. Genetic predisposition in gynecologic cancers. *Semin Oncol* 2016; **43:** 543-7. doi: 10.1053/j.seminoncol.2016.08.005
17. Farooq A, Walker LJ, Bowling J, Audisio RA. Cowden syndrome. *Cancer Treat Rev* 2010; **36:** 577-83. doi: 10.1016/j.ctrv.2010.04.002
18. Dovnik A, Crnobrnja B, Zegura B, Takac I, Pakiz M. Incidence of positive peritoneal cytology in patients with endometrial carcinoma after hysteroscopy vs. dilatation and curettage. *Radiol Oncol* 2016; **51:** 88-93. doi: 10.1515/raon-2016-0035
19. Chen J, Clark LH, Kong WM, Yan Z, Han C, Zhao H, et al. Does hysteroscopy worsen prognosis in women with type II endometrial carcinoma? *PLoS One* 2017; **12:** e0174226. doi: 10.1371/journal.pone.0174226
20. Biewenga P, de Blok S, Birnie E. Does diagnostic hysteroscopy in patients with stage I endometrial carcinoma cause positive peritoneal washings? *Gynecol Oncol* 2004; **93:** 194-8. doi: 10.1515/raon-2016-0035
21. Falcone F, Balbi G, Di Martino L, Grauso F, Salzillo ME, Messalli EM. Surgical management of early endometrial cancer: an update and proposal of a therapeutic algorithm. *Med Sci Monit* 2014; **20:** 1298-313. doi: 10.12659/MSM.890478
22. Walker JL, Piedmonte MR, Spirtos NM, Eisenkop SM, Schlaerth JB, Mannel RS, et al. Recurrence and survival after random assignment to laparoscopy versus laparotomy for comprehensive surgical staging of uterine cancer: Gynecologic Oncology Group LAP2 Study. *J Clin Oncol* 2012; **30:** 695-700. doi: 10.1200/JCO.2011.38.8645
23. Zullo F, Falbo A, Palomba S. Safety of laparoscopy vs laparotomy in the surgical staging of endometrial cancer: a systematic review and metaanalysis of randomized controlled trials. *Am J Obstet Gynecol* 2012; **207:** 94-100. doi: 10.1016/j.ajog.2012.01.010
24. Rabinovich A. Minimally invasive surgery for endometrial cancer. *Curr Opin Obstet Gynecol* 2015; **27:** 302-7. doi: 10.1097/GCO.0000000000000187

25. Bourgin C, Lambaudie E, Houvenaeghel G, Foucher F, Levêque J, Lavoué V. Impact of age on surgical staging and approaches (laparotomy, laparoscopy and robotic surgery) in endometrial cancer management. *Eur J Surg Oncol* 2017; **43:** 703-9. doi: 10.1016/j.ejso.2016.10.022

26. Biler A, Solmaz U, Erkilinc S, Gokcu M, Bagci M, Temel O, et al. Analysis of endometrial carcinoma in young women at a high-volume cancer center. *Int J Surg* 2017; **44:** 185-90. doi: 10.1016/j.ijsu.2017.06.083

27. Sun C, Chen G, Yang Z, Jiang J, Yang X, Li N, et al. Safety of ovarian preservation in young patients with early-stage endometrial cancer: a retrospective study and meta-analysis. *Fertil Steril* 2013; **100:** 782-7. doi: 10.1016/j.fertnstert.2013.05.032

28. Gu H, Li J, Gu Y, Tu H, Zhou Y, Liu J. Survival impact of ovarian preservation on women with early-stage endometrial cancer: a systematic review and meta-analysis. *Int J Gynecol Cancer* 2017; **27:** 77-84. doi: 10.1097/IGC.0000000000000857

29. Bodurtha Smith AJ, Fader AN, Tanner EJ. Sentinel lymph node assessment in endometrial cancer: a systematic review and meta-analysis. *Am J Obstet Gynecol* 2017; **216:** 459-76.e10. doi: 10.1016/j.ajog.2016.11.1033

30. Bedyńska M, Szewczyk G, Klepacka T, Sachadel K, Maciejewski T, Szukiewicz D, et al. Sentinel lymph node mapping using indocyanine green in patients with uterine and cervical neoplasms: restrictions of the method. *Arch Gynecol Obstet* 2019; **299:** 1373-84. doi: 10.1007/s00404-019-05063-6

31. Rossi EC, Kowalski LD, Scalici J, Cantrell L, Schuler K, Hanna RK, et al. A comparison of sentinel lymph node biopsy to lymphadenectomy for endometrial cancer staging (FIRES trial) **:** a multicentre, prospective, cohort study. *Lancet Oncol* 2017; **18:** 384-92. doi: 10.1016/S1470-2045(17)30068-2

32. Dowdy SC, Borah BJ, Bakkum-Gamez JN, Weaver AL, McGree ME, Haas LR, et al. Prospective assessment of survival, morbidity, and cost associated with lymphadenectomy in low-risk endometrial cancer. *Gynecol Oncol* 2012; **127:** 5-10. doi: 10.1016/j.ygyno.2012.06.035

33. Vargas R, Rauh-Hain JA, Clemmer J, Clark RM, Goodman A, Growdon WB, et al. Tumor size, depth of invasion, and histologic grade as prognostic factors of lymph node involvement in endometrial cancer: a SEER analysis. *Gynecol Oncol* 2014; **133:** 216-20. doi: 10.1016/j.ygyno.2014.02.011

34. Lutman CV, Havrilesky LJ, Cragun JM, Secord AA, Calingaert B, Berchuck A, et al. Pelvic lymph node count is an important prognostic variable for FIGO stage I and II endometrial carcinoma with high-risk histology. *Gynecol Oncol* 2006; **102:** 92-7. doi: 10.1097/01.ogx.0000238643.54754.6a

35. Abu-Rustum NR, Iasonos A, Zhou Q, Oke E, Soslow RA, Alektiar KM, et al. Is there a therapeutic impact to regional lymphadenectomy in the surgical treatment of endometrial carcinoma? *Am J Obstet Gynecol* 2008; **198:** 457.e1-5; discussion 457.e5-6. doi: 10.1016/j.ajog.2008.01.010

36. Mariani A, Dowdy SC, Cliby WA, Gostout BS, Jones MB, Wilson TO, et al. Prospective assessment of lymphatic dissemination in endometrial cancer: a paradigm shift in surgical staging. *Gynecol Oncol* 2008; **109:** 11-8. doi: 10.1016/j.ygyno.2008.01.023

37. AlHilli MM, Mariani A. The role of para-aortic lymphadenectomy in endometrial cancer. *Int J Clin Oncol* 2013; **18:** 193-9. doi: 10.1007/s10147-013-0528-7

38. Shih KK, Yun E, Gardner GJ, Barakat RR, Chi DS, Leitao MM. Surgical cytoreduction in stage IV endometrioid endometrial carcinoma. *Gynecol Oncol* 2011; **122:** 608-11. doi: 10.1016/j.ygyno.2011.05.020

39. van der Steen-Banasik E, Christiaens M, Shash E, Coens C, Casado A, Herrera FG, et al. Systemic review: radiation therapy alone in medical non-operable endometrial carcinoma. *Eur J Cancer* 2016; **65:** 172-81. doi: 10.1016/j.ejca.2016.07.005

40. Uccella S, Falcone F, Greggi S, Fanfani F, De Iaco P, Corrado G, et al. Survival in clinical stage I endometrial cancer with single vs. multiple positive pelvic nodes: results of a multi-institutional Italian study. *J Gynecol Oncol* 2018; **29:** e100. doi: 10.3802/jgo.2018.29.e100

41. Muallem MZ, Sehouli J, Richter R, Babayeva A, Gasimli K, Parashkevova A. Pre-operative serum CA125, peritoneal cancer index and intra-operative mapping score as predictors of surgical results in primary epithelial ovarian cancer. *Int J Gynecol Cancer* 2020; **30:** 62-6. doi: 10.1136/ijgc-2019-000778

42. Lin YJ, Hu YW, Twu NF, Liu YM. The role of adjuvant radiotherapy in stage I endometrial cancer: a single-institution outcome. *Taiwan J Obstet Gynecol* 2019; **58:** 604-9. doi: 10.1016/j.tjog.2019.07.005

43. Morrow CP, Bundy BN, Kurman RJ, Creasman WT, Heller P, Homesley HD, et al. Relationship between surgical-pathological risk factors and outcome in clinical stage I and II carcinoma of the endometrium: a Gynecologic Oncology Group study. *Gynecol Oncol* 1991; **40:** 55-65. doi: 10.1016/0090-8258(91)90086-k

44. Creasman W, Odicino F, Maisonneuve P, Quinn M, Beller U, Benedet J, et al. Carcinoma of the corpus uteri. *Int J Gynaecol Obstet* 2006; **95(Suppl 1):** S105-43. doi: 10.1016/S0020-7292(06)60031-3

45. Rovirosa Á, Cortés KS, Ascaso C, Glickman A, Valdés S, Herreros A, et al. Are endometrial cancer radiotherapy results age related? *Clin Transl Oncol* 2018; **20:** 1416-21. doi: 10.1007/s12094-018-1872-x

46. Bestvina CM, Fleming GF. Chemotherapy for endometrial cancer in adjuvant and advanced disease settings. *Oncologist* 2016; **21:** 1250-9. doi: 10.1634/theoncologist.2016-0062

47. Gressel GM, Parkash V, Pal L. Management options and fertility-preserving therapy for premenopausal endometrial hyperplasia and early-stage endometrial cancer. *Int J Gynaecol Obstet* 2015; **131:** 234-9. doi: 10.1016/j.ijgo.2015.06.031

48. Kalogiannidis I, Agorastos T. Conservative management of young patients with endometrial highly-differentiated adenocarcinoma. *J Obstet Gynaecol* 2011; **31:** 13-7. doi: 10.3109/01443615.2010.532249

49. Carneiro MM, Lamaita RM, Ferreira MCF, Silva-Filho AL. Fertility-preservation in endometrial cancer: is it safe? Review of the literature. *JBRA Assist Reprod* 2016; **20:** 232-9. doi: 10.5935/1518-0557.20160045

50. Eskander RN, Randall LM, Berman ML, Tewari KS, Disaia PJ, Bristow RE. Fertility preserving options in patients with gynecologic malignancies. *Am J Obstet Gynecol* 2011; **205:** 103-10. doi: 10.1016/j.ajog.2011.01.025

51. Bogani G, Dowdy SC, Cliby WA, Ghezzi F, Rossetti D, Frigerio L, et al. Management of endometrial cancer: issues and controversies. *Eur J Gynaecol Oncol* 2016; **37:** 6-12. PMID: 27048101

52. Zivanovic O, Carter J, Kauff ND, Barakat RR. A review of the challenges faced in the conservative treatment of young women with endometrial carcinoma and risk of ovarian cancer. *Gynecol Oncol* 2009; **115:** 504-9. doi: 10.1016/j.ygyno.2009.08.011

53. Pal N, Broaddus RR, Urbauer DL, Balakrishnan N, Milbourne A, Schmeler KM, et al. Treatment of low-risk endometrial cancer and complex atypical hyperplasia with the levonorgestrel-releasing intrauterine device: *Obstet Gynecol* 2018; **131:** 109-16. doi: 10.1097/AOG.0000000000002390

54. Aslam RW, Pye KL, Rai TK, Hall B, Timmis LJ, Yeo ST, et al. Follow-up strategies for women with endometrial cancer after primary treatment. *Cochrane Db Syst Rev* 2016. doi: 10.1002/14651858.CD012386

*research article*

# Relationships between apparent diffusion coefficient (ADC) histogram analysis parameters and PD-L 1-expression in head and neck squamous cell carcinomas: a preliminary study

Hans-Jonas Meyer[1], Anne Kathrin Höhn[2], Alexey Surov[3]

[1] Department of Diagnostic and Interventional Radiology, University of Leipzig, Leipzig, Germany
[2] Department of Pathology, University of Leipzig, Leipzig, Germany
[3] Department of Diagnostic and Interventional Radiology, University of Magdeburg, Germany

Radiol Oncol 2021; 55(2): 150-157.

Received 22 October 2020
Accepted 13 December 2020

Correspondence to: Hans-Jonas Meyer M.D., Department of Diagnostic and Interventional Radiology, University of Leipzig, Germany. E-mail: hans-jonas.meyer@medizin.uni-leipzig.de

Disclosure: No potential conflicts of interest were disclosed. All authors contributed equally to this work

**Background.** Immunotherapy has become a cornerstone of the modern cancer treatment. It might be crucial to predict its expression non-invasively by imaging. The present study used diffusion-weighted imaging (DWI) quantified by whole lesion apparent diffusion coefficient (ADC) values to elucidate possible associations with programmed cell death ligand 1(PD-L1) expression in head and neck squamous cell cancer (HNSCC).

**Patients and methods.** Overall, 29 patients with primary HNSCC of different localizations were involved in the study. DWI was obtained by using a sequence with b-values of 0 and 800 s/mm$^2$ on a 3 T MRI. ADC values were evaluated with a whole lesion measurement and a histogram approach. PD-L1 expression was estimated on bioptic samples before any form of treatment using 3 scores, tumor positive score (TPS), immune cell score (ICS), and combined positive score (CPS).

**Results.** An inverse correlation between skewness derived from ADC values and ICS was identified (r = -0.38, p = 0.04). $ADC_{max}$ tended to correlate with ICS (r = -0.35, p = 0.06). Other ADC parameters did not show any association with the calculated scores.

**Conclusions.** There is a weak association between skewness derived from ADC values and PD-L1 expression in HNSCC, which might not be strong enough to predict PD-L1 expression in clinical routine. Presumably, ADC values are more influenced by complex histopathology compartments, comprising cellular and extracellular aspects of tumors than only of a single subset of tumor associated cells.

Key words: head and neck squamous cell cancer; apparent diffusion coefficient; diffusion weighted imaging; programmed cell death ligand 1

## Introduction

Head and neck squamous cell carcinoma (HNSCC) is one of the most frequent malignancies.[1] Modern functional imaging modalities, comprising diffusion-weighted imaging (DWI) and Dynamic-contrast enhanced MRI provide further insight into tumor microstructure.[2] With these approaches, several diagnostic and prediction aspects were made possible, including the prediction of several histological features in tumors, treatment success and new prognostic.[2-5]

DWI assesses random-water motion in tissues, namely Brownian molecular movement and can be quantified by apparent diffusion coefficient (ADC).[3,5] This water movement is hindered predominantly by cellularity and thus it is a well-known fact that ADC values are inversely correlated with cell count with yet different results across several tumor entities.[5] However, ADC values are not only associated with cellularity, but also with other histopathologic features, such as proliferation potential, neoangiogenesis, tumor invading lymphocytes or extracellular matrix. This was also shown for HNSCC.[6-9]

Recently, various studies elucidated further associations of ADC values and tumor characteristics in oncology. ADC values aid in diagnostic purposes, as benign tumors have significantly higher ADC values than malignant tumors. This was also reported for head and neck lesions.[10-12] Another important aspect is treatment prediction. A higher pretreatment ADC value and, therefore, presumably a tumor with a lower cell density and a less malignant tumor biology, is an independent favorable prognostic factor to chemotherapy and radiochemotherapy.[13-15] Moreover, ADC values are independently associated with overall prognosis.[13-15]

There is a growing interest in targeting immune modulatory checkpoints, especially the programmed cell death protein 1 (PD-1) around oncology.[16] It is a transmembrane protein that is frequently expressed on the surface of T-lymphocytes.

**TABLE 1.** Overview of the included patients

| Localization | n (%) |
|---|---|
| Tonsil | 7 (24.1) |
| Tongue | 7 (24.1) |
| Hypopharynx | 6 (20.7) |
| Oropharynx | 5 (17.2) |
| Larynx | 4 (13.9) |
| **Grading** | |
| Moderate (G2) | 12 (37.5) |
| Poor (G3) | 17 (62.5) |
| **Stage** | |
| T2 | 6 (20.7) |
| T3 | 10 (34.5) |
| T4 | 13 (44.8) |
| **Nodal status** | |
| Nodal positive | 25 (86.2) |
| Nodal negative | 4 (13.8) |

Programmed cell death ligand 1 (PD-L1) is a transmembrane protein, which is physiologically expressed at low levels in several cells, such as vascular, endothelial and immune cells. Interestingly, it can be highly expressed in neoplastic cells.[16] The binding of PD-L1 to PD-1 forms an immunological situation that can impair the proliferation and the function of the immune cells against the tumor. That is why high expression of PD-L1 enables cancer cells to escape from immunologic response.[16]

Immunotherapy was stated as a new paradigm shift in HNSCC treatment.[17] Moreover PD-L1 expression on immunohistochemical specimen was shown to predict progression free survival in in advanced HNSCC stages and can predict metastases.[18-20]

However, it is unclear, whether ADC values derived from MRI are associated with the amount of PD-L1 stained tumor cells and the associated PD-L1 stained immune cells and not only with the whole tumor cellularity of the lesion, which might not be as clinically relevant as to predict several subtypes of cells.

Therefore, the present study sought to elucidate possible associations between ADC values derived from MRI and the amount of PD-L1 stained tumor parts including tumor cells and immune cells within the tumor.

## Patients and methods

This study is a retrospective analysis of a prospectively acquired patient sample of consecutive HNSCC patients undergoing MRI evaluation for staging purposes. It was approved by the institutional review board (Ethic committee of the University of Leipzig, study codes 180-2007, 201-10-12072010, and 341-15-05102015) and every patient gave their written consent.

### Patients

Overall, 29 patients with primary HNSCC of different localizations were involved in the study. There were 8 (27.6%) women and 21 (72.4%) men with a mean age of 55.2 ± 10.8 years, range 33 - 77 years. The patients received no specific treatment before the MRI.

Table 1 gives an overview of the included patients. In 12 patients (37.5%) moderately differentiated tumors (G2), and in 17 cases (62.5%) poorly differentiated carcinomas (G3) were diagnosed. The identified tumors were staged as T2 in 6 pa-

tients (20.7%), T3 in 10 patients (34.5%), and as T4 in 13 cases (44.8%). Most patients ($n$ = 25, 86.2%) had nodal metastases.

### DWI

DWI was obtained by using an axial EPI (echo planar imaging) sequence with b-values of 0 and 800 s/mm$^2$ (TR/TE: 8620/73 ms, slice thickness 4 mm, and voxel size 3.2 × 2.6 × 4.0 mm) on a 3T MRI scanner (Siemens Biograph mMR; Siemens Healthcare, Erlangen, Germany) within a routinely acquired MRI protocol. ADC maps were automatically generated by the implemented software. DWI data was processed with a custom-made Matlab-based application (The Mathworks, Natick, MA, USA). On the ADC maps a volume of interest was manually drawn at tumor boundary in accordance to the T1-weighted contrast enhancing tumor areas using all slices, as performed before.[8,9] All measures were performed by one experienced author (AS, 16 years of general radiological experience and 6 years of experience on the field of head and neck radiology) blinded to the histopathology results. The following histogram parameters were calculated: mean, maximum, minimum, median, mode, 10$^{th}$, 25$^{th}$, 75$^{th}$ and 90$^{th}$ percentile as well as kurtosis, skewness and entropy.

### PD-L1 expression analysis

The histopathology analysis was performed by an experienced board-certified pathologist blinded to the imaging results. PD-L1 expression was retrospectively evaluated by using an immunohistochemistry (IHC) assay, a routinely used version of PD-L1 (SP142) IHC assay (Roche Diagnostics, 68305 Mannheim, Germany). The staining protocol used in this study was as described in the instructions for the approved commercial assay. The assay was used to determine PD-L1 expression on tumor samples derived from clinical pretherapeutic bioptic specimen of the primary tumor. The biopsy was performed before the MRI within a short time interval of a few days. Three scoring methods were used to assess the immunohistochemical expression. Firstly, only the amount of positive tumor cells were scored, tumor proportion score (TPS). Of note, membrane as well as cytoplasmatic staining was assessed as positive. Secondly, the immune related cells comprising macrophages and lymphocytes were assessed, immune cell score (ICS). Finally, a combined positive score (CPS) of both was calculated. For all scores, the amount of positive cells was calculated in relation to tumor cells multiplied by 100. All calculations were made on 20-fold magnification.

### Statistical analysis

Statistical analysis was performed using performed using GraphPad Prism 5 (GraphPad Software, La Jolla, CA, USA). Collected data were evaluated by means of descriptive statistics. Mean values were stated with standard deviation in all instances. Spearman's correlation coefficient (r) was used to analyze associations between investigated parameters. A two-sided Mann-Whitney-Test was used to test between groups. P-values < 0.05 were taken to indicate statistical significance.

## Results

Table 2 summarizes the investigated ADC histogram parameters.

For the PD-L1 expression of the TPSa mean value of 3.1 ± 14.8 was identified. Overall, 23 tumors (79.3% of all patients) showed no expression.

Furthermore, for the PD-L1 expression of the CPS a mean value of 4.7 ± 14.0 was identified and 13 tumors (45.0%) showed no expression.

Finally, for the PD-L1 expression of the ICS a mean value of 2.5 ± 3.8 was identified. 13 patients (45.0%) showed no expression.

**TABLE 2.** Overview of the investigated apparent diffusion coefficient (ADC) histogram parameters

| Parameter | Mean ± standard deviation, x10$^{-3}$ mm$^2$/s | Range, x10$^{-3}$ mm$^2$/s |
|---|---|---|
| Mean | 1.14 ± 0.22 | 0.78-1.68 |
| Min | 0.70 ± 0.25 | 0.17-1.24 |
| Max | 1.78 ± 0.32 | 1.35-2.39 |
| P10 | 0.90 ± 0.21 | 0.54-1.41 |
| P25 | 1.0 ± 0.21 | 0.64-1.50 |
| P75 | 1.27 ± 0.24 | 0.87-1.82 |
| P90 | 1.41 ± 0.26 | 0.94-2.03 |
| Median | 1.12 ± 0.22 | 0.76-1.64 |
| Mode | 0.97 ± 0.28 | 0.78-1.55 |
| Kurtosis | 3.74 ± 1.40 | 2.23-7.93 |
| Skewness | 0.49 ± 0.49 | -0.54-1.49 |
| Entropy | 2.44 ± 0.49 | 1.67-3.75 |

P = percentile

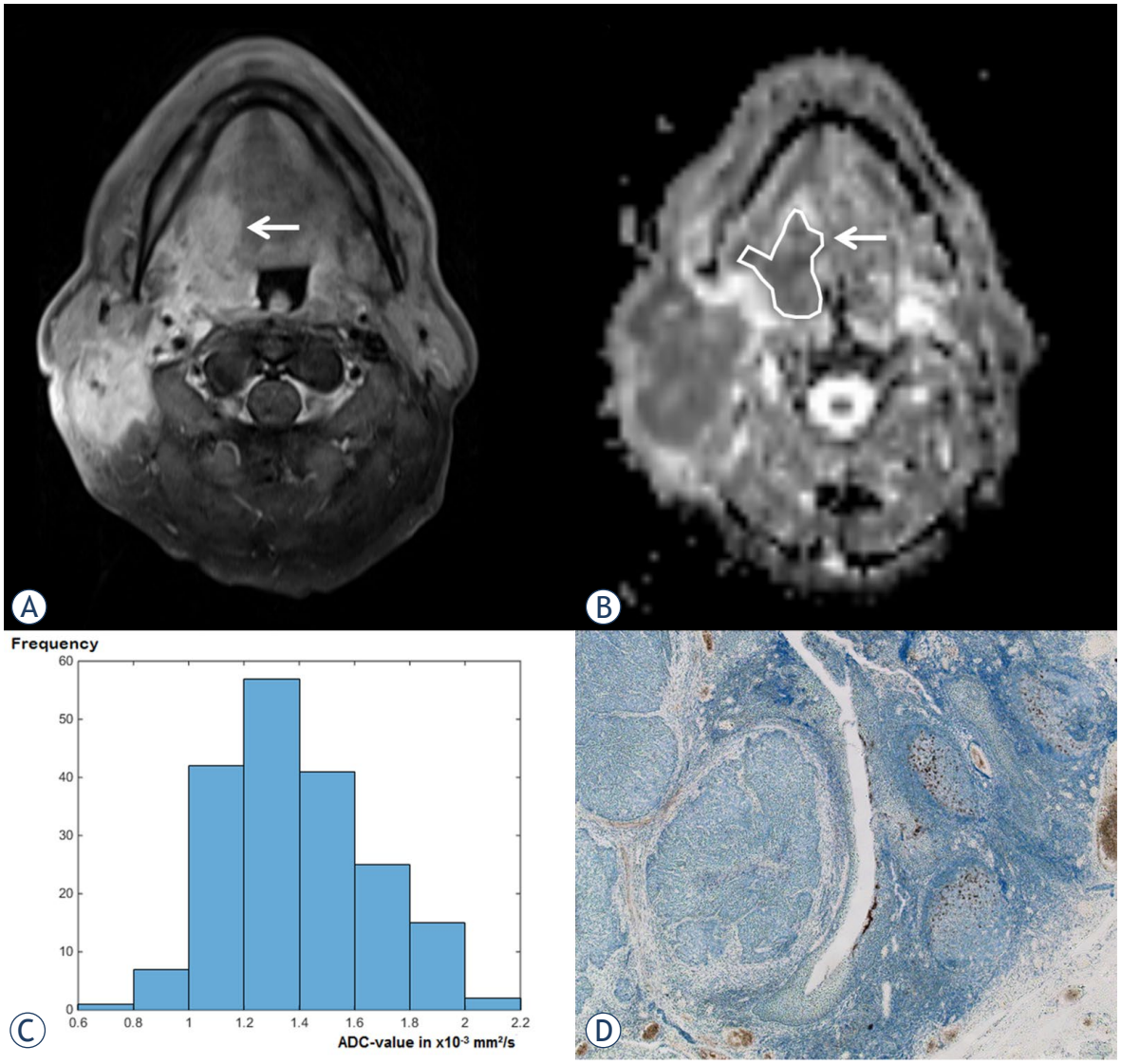


**FIGURE 1.** Representative case with a negative programmed cell death ligand 1 (PD-L1) score. **(A)** Postcontrast T1-weighted image shows a large enhancing tumor of the right tongue base (arrow). A large lymph node metastasis on the right side can also be appreciated. **(B)** Apparent diffusion coefficient (ADC) map of the same slide. Both lesions show a marked hypointensity consistent with a diffusion restriction. The tumor (arrow) is surrounded with a region of interest, which is drawn on every tumor showing slide within the margins of the tumor in accordance to the corresponding T1-weighted images. **(C)** The resulting ADC histogram of the tumor. The histogram analysis parameters (× $10^{-3}$ $mm^2/s$) are as follows: ADCmin = 0.79, ADCmean = 1.38, ADCmax = 2.05, P10 = 1.05, P25 = 1.19, P75 = 1.53, P90 = 1.78, median = 1.35,mode = 1.27, kurtosis = 2.61, skewness = 0.41 and entropy = 2.44. **(D)** The corresponding PD-L1 stained specimen. No staining can be appreciated resulting in a value of 0 in all calculated scores.

There was a moderate correlation between TPS and CPS (r = 0.57, p = 0.0015) and ICS (r = 0.57, p = 0.016). There was a strong correlation between ICS and CPS (r = 0.95, p < 0.001).

Regarding associations between ADC histogram parameters and PD-L1-expression scores, there was only one weak correlation identified between skewness and ICS (r = -0.38, p = 0.04). $ADC_{max}$ tended to correlate with ICS (r = -0.35, p = 0.06). For TPS, the best association was identified withADCp25 (r= -0.36, p = 0.052).

In discrimination analysis there were no significant differences between TPS negative and positive tumors in regard of ADC histogram parameters.

In tumors with high expression of ICS (5–15 points) skewness was significantly lower than in lesions without ICS expression, 0.09 ± 0.26 *vs*. 0.56 ± 0.51 (p = 0.025), respectively. Other parameters did not differ significantly.

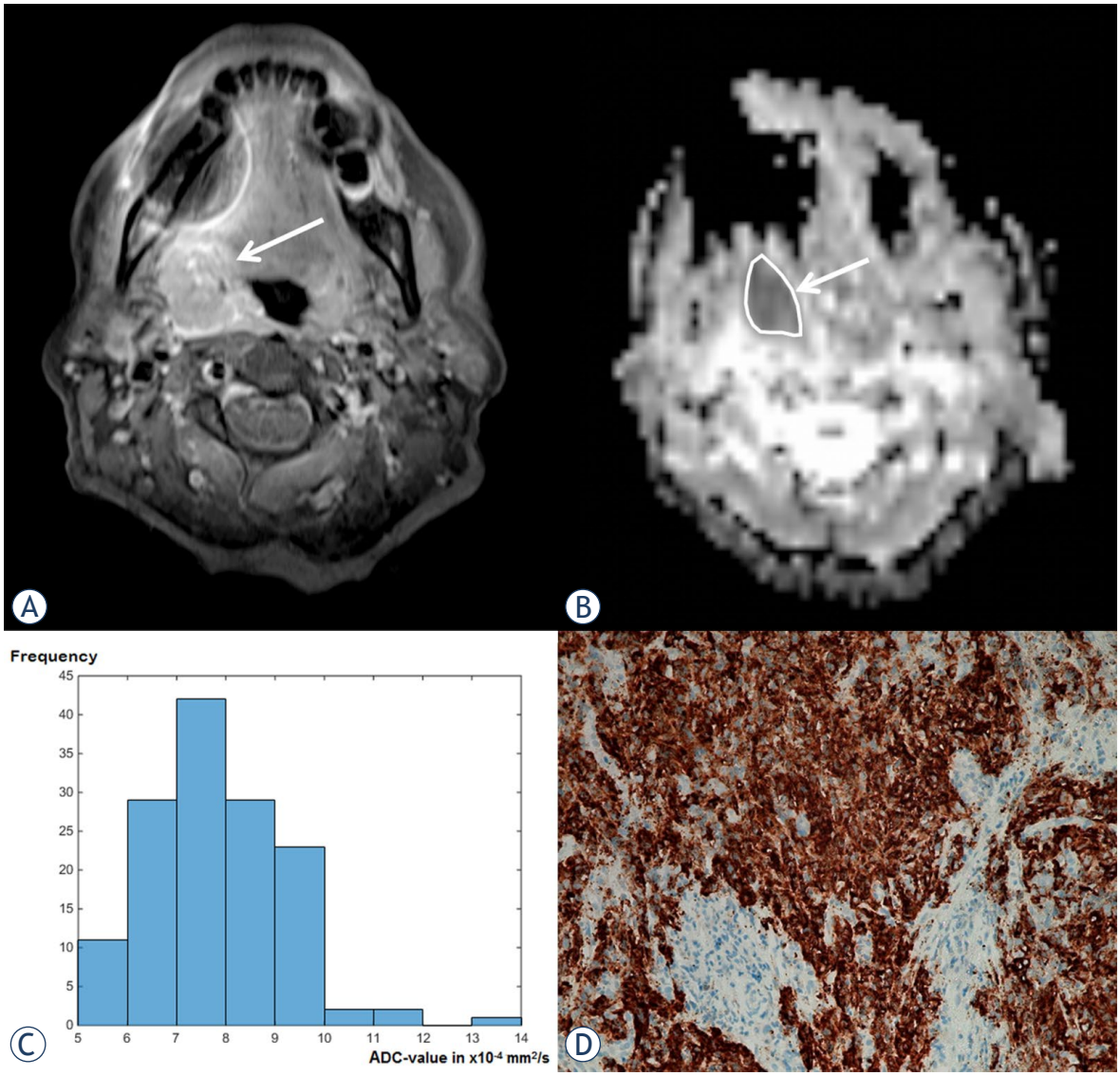


**FIGURE 2.** Representative case with a positive programmed cell death ligand 1 (PD-L1) score. **(A)** On the postcontrast T1-weighted image a large enhancing tumor of the side within the right palatine tonsil (arrow). Susceptibility artifacts due to dental material can also be appreciated. **(B)** Apparent diffusion coefficient (ADC) map on the corresponding slide. A marked hypointensity can be seen consistent with a diffusion restriction. **(C)** The resulting ADC histogram of the tumor. The histogram analysis parameters ($\times 10^{-3}$ mm²/s) are as follows: ADCmin = 0.51, ADCmean = 0.78, ADCmax = 1.36, P10 = 0.63, P25 = 0.69, P75 = 0.87, P90 = 0.94, median = 0.76, mode = 0.69, kurtosis = 4.57, skewness = 0.72, and entropy = 2.41. **(D)** The corresponding PD-L1 stained specimen. A weak staining of PD-L1 for tumor cells and associating immune cells can be appreciated. The resulting score values are 5 for the combined positive score and 3 for the immune cell score.

## Discussion

This study sought to elucidate associations between DWI and PD-L1-expression in HNSCC. As shown, a moderate association between skewness derived from ADC values and the immune cell score was identified.

There is increasing body of evidence that different ADC values are capable to reflect tumor microstructure.[3-5] Thus, results pooled out of many tumor entities suggests that there is an overall moderate inverse correlation between ADC values and tumor cellularity.[5]

Beyond that, there are several studies, which emphasized the fact that ADC values can also predict several biological features of tumors, such as neoangiogenesis and proliferation potential.[4,6-8] Regarding proliferation potential, an overall mod-

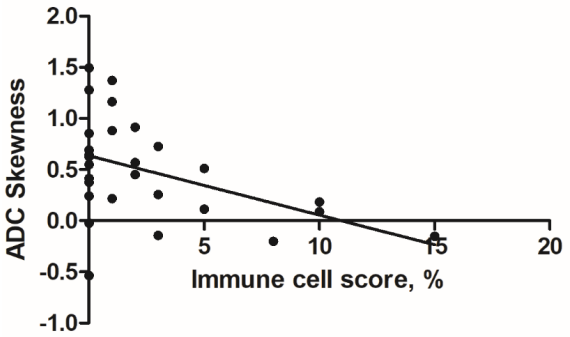


**FIGURE 3.** Correlation analysis between skewness derived from apparent diffusion coefficient (ADC) and the immune cell score (ICS). The resulting Spearman's correlation coefficient is r = -0.38, p = 0.04.

erate inverse correlation was identified between ADC values and Ki 67 index pooled for various tumors[21] indicating that ADC can predict the amount of proliferating cells in tissue.

Regarding HNSCC, the relationship between ADC values and Ki 67 index was also identified (r = -0.61).[4] In another study it was reported that ADC values were associated with CD3 positive stained cells (r = -0.568, p = 0.009), which is a measurement of the influx of T-cells within the tumor.[7] Therefore, it can be assumed that ADC values cannot only reflect the whole cell density within the tumor but are sensitive to smaller specific tumor cell fractions. Interestingly, skewness was only associated with the amount of positive PD-L1-stained immune cells. Taken together with the results that ADC values were associated with the amount of tumor invading T-cells within the tumor, there might be a possibility to reflect and predict tumor microenvironment in HNSCC.

The parameter skewness represents the asymmetry of the distribution within the histogram in regard of the ADC values.[22] In short, tumors which lean to the left have consecutively lower ADC values and thus a higher malignancy, whereas tumors, which lean to the right have higher ADC values tumors and thus lower malignancy.[22] Regarding HNSCC, skewness was significantly higher in patients with HPV-mediated oropharyngeal cancer.[23] Interestingly, there is an association between positive human papilloma patients and PD-L1 expression.[18] This might explain why skewness derived from ADC values is related to both histopathological features of HNSCC.

In a recent excellent investigation, a direct correlation between PET-MRI and immunohistochemical analysis was performed based upon postoperative MRI scans with direct pathology coregistration.[24] Furthermore, ADC correlated well with the apoptotic marker p53, Ki67, and with the apoptotic biomarker Bcl-2. Interestingly, ADC correlated also with expression of PD-L1.[24]

Also, ADC related parameters significantly correlated with the proportion of tumor stroma.[25]

In short, there is preliminary data to elucidate the possibility for imaging modalities to predict histopathology features for better patient guidance. More studies are definitely needed for better understanding of these complex interactions.

Recently, there is extensive interest about PD-1- and PD-L1-inhibitors as a form of immunotherapy in oncology.[16,17] In melanoma patients, PD-1 and PD-L1 inhibitors showed the first very promising results. The effectiveness of this immunotherapy was shortly after also shown for non-small lung cancer and other tumor entities.[17]

Regarding HNSCC, there were several trials establishing the effectiveness of this novel treatment in the recurrent setting.[26-28] In these trials, PD-L1 status was defined as negative or positive with at least 1% of positive staining, well comparable with the approach in the present study.

In one study the probability of response was not significantly different between PD-L1 negative and positive patients, when only tumor cells were calculated but only when immune cells were also included into the analysis.[28] Correspondingly to our results, skewness was only significantly associated with the scoring system regarding immune cells, reflecting these small, yet not negligible differences in PD-L1 staining scores. As shown in our results, there are significant differences between the scores, which needs to be considered. The immune cell score only measures the tumor associated PD-L1 cells and not the expression of the cancer cells themselves.

Moreover, it is well known that HNSCC is a highly heterogeneous tumor with different biological behavior comprising different localizations andHPV-mediated oropharyngeal cancer.[17]

Beyond that, even intratumoral heterogeneity was described as very important in HNSCC, which the amount of heterogeneity differing between primary localization.[29] This might be important for biopsy sampling, as the tumor might significantly show different PD-L1 expression in several biopsy sites. This is, moreover, of special interest, as PD-L1 expression in head and neck cancer is localized at the tumor borders in HPV-positive cancers.[30] Presumably, only imaging with a quantitative analysis approach can display this tumor

heterogeneity completely during clinical routine. There might also be the opportunity for ADC histogram parameters to indicate treatment changes of the tumors during PD-L1 treatment.

To date, only one other study investigated possible associations between ADC values and PD-L1 expression in other tumors in oncology.[31] In this study, there was a reported statistical difference between PD-L1 positive compared to negative tumors in regard of ADCmax in rectal cancers.[31] Correspondingly, there was a statistical trend in the present study for ADCmax to correlate with the ICS, but it did not reach statistical significance, presumably due to small sample size. More studies are needed to investigate, whether ADCmax might be a promising biomarker to predict PD-L1 expression in oncologic imaging.

To overcome this limitation, further studies are needed with a multiparametric approach including MRI, CT and PET data guided with artificial intelligence. Presumably, non-invasive prediction of histopathology by imaging can be translated into clinical routine employing this approach.

There are several limitations of the present study to address. First, it is a retrospective analysis performed on a prospectively recruited patient sample. However, the imaging and pathology analyses were performed independently to each other to reduce possible bias. Second, the imaging analysis was performed as a whole tumor measurement, whereas the PD-L1analysis was performed on bioptic specimens with possible spatial incongruencies. Yet, this approach represents daily clinical practice for which no whole lesion pathology-radiology correlation is possible. Third, the ADC measurement was performed by one reader with possible accompanied reader-bias. However, it is reported that ADC values have a good to excellent interreader variability in HNSCC, which might reduce this limitation. Fourth, because of the exploratory study design we did not correct for multiple tests, which has an impact on the presented results. Fifth, the biopsy was taken from the primary tumor before the MRI. This might cause biopsy-related artifacts of the tumor, such as hematoma or local inflammation, which can have an impact on the ADC values.

In conclusion, here is a weak association between skewness derived from ADC values and PD-L1 expression in HNSCC, which might not be strong enough to predict PD-L1 expression in clinical routine. Presumably, ADC values are more influenced by complex histopathology compartments, comprising cellular and extracellular aspects of tumors than only of a single subset of tumor associated cells.

## References


1. McDermott JD, Bowles DW. Epidemiology of head and neck squamous cell carcinomas: impact on staging and prevention strategies. *Curr Treat Options Oncol* 2019; **20:** 43. doi: 10.1007/s11864-019-0650-5
2. Widmann G, Henninger B, Kremser C, Jaschke W. MRI sequences in head & neck radiology - state of the art. *Rofo* 2017; **189:** 413-22. doi: 10.1055/s-0043-103280
3. Padhani AR, Liu G, Koh DM, Chenevert TL, Thoeny HC, Takahara T, et al. Diffusion-weighted magnetic resonance imaging as a cancer biomarker: consensus and recommendations. *Neoplasia* 2009; **11:** 102-25. doi: 10.1593/neo.81328
4. Surov A, Meyer HJ, Wienke A. Can imaging parameters provide information regarding histopathology in head and neck squamous cell carcinoma? A meta-analysis. *Transl Oncol* 2018; **11:** 498-503. doi: 10.1016/j.tranon.2018.02.004
5. Surov A, Meyer HJ, Wienke A. Correlation between apparent diffusion coefficient (ADC) and cellularity is different in several tumors: a meta-analysis. *Oncotarget* 2017; **8:** 59492-9. doi: 10.18632/oncotarget.17752
6. Hauge A, Wegner CS, Gaustad JV, Simonsen TG, Andersen LMK, Rofstad EK. Diffusion-weighted MRI-derived ADC values reflect collagen I content in PDX models of uterine cervical cancer. *Oncotarget* 2017; **8:** 105682-91. doi: 10.18632/oncotarget.22388
7. Swartz JE, Driessen JP, van Kempen PMW, de Bree R, Janssen LM, Pameijer FA, et al. Influence of tumor and microenvironment characteristics on diffusion-weighted imaging in oropharyngeal carcinoma: a pilot study. *Oral Oncol* 2018; **77:** 9-15. doi: 10.1016/j.oraloncology.2017.12.001
8. Meyer HJ, Leifels L, Hamerla G, Höhn AK, Surov A. ADC-histogram analysis in head and neck squamous cell carcinoma. Associations with different histopathological features including expression of EGFR, VEGF, HIF-1α, Her 2 and p53. A preliminary study. *Magn Reson Imaging* 2018; **54:** 214-7. doi: 10.1016/j.mri.2018.07.013
9. Surov A. Meyer HJ, Winter K, Richter C, Hoehn AK. Histogram analysis parameters of apparent diffusion coefficient reflect tumor cellularity and proliferation activity in head and neck squamous cell carcinoma. *Oncotarget* 2018; **9:** 23599-607. doi: 10.18632/oncotarget.25284
10. Driessen JP, van Kempen PM, van der Heijden GJ, Philippens ME, Pameijer FA, Stegeman I, et al. Diffusion-weighted imaging in head and neck squamous cell carcinomas: a systematic review. *Head Neck* 2015; **37:** 440-8. doi: 10.1002/hed.23575
11. Koontz NA, Wiggins RH 3rd. Differentiation of benign and malignant head and neck lesions with diffusion tensor imaging and DWI. *AJR Am J Roentgenol* 2017; **208:** 1110-5. doi: 10.2214/AJR.16.16486
12. Surov A. Meyer HJ, Wienke A. Apparent diffusion coefficient for distinguishing between malignant and benign lesions in the head and neck region: a systematic review and meta-analysis. *Front Oncol* 2020; **9:** 1362. doi: 10.3389/fonc.2019.01362
13. King AD, Chow KK, Yu KH, Mo FK, Yeung DK, Yuan J, et al. Head and neck squamous cell carcinoma: diagnostic performance of diffusion-weighted MR imaging for the prediction of treatment response. *Radiology* 2013; **266:** 531-8. doi: 10.1148/radiol.12120167
14. Law BK, King AD, Bhatia KS, Ahuja AT, Kam MK, Ma BB, et al. Diffusion-weighted imaging of nasopharyngeal carcinoma: can pretreatment DWI predict local failure based on long-term outcome? *AJNR Am J Neuroradiol* 2016; **37:** 1706-12. doi: 10.3174/ajnr.A4792.
15. Matoba M, Tuji H, Shimode Y, Toyoda I, Kuginuki Y, Miwa K, et al. Fractional change in apparent diffusion coefficient as an imaging biomarker for predicting treatment response in head and neck cancer treated with chemoradiotherapy. *AJNR Am J Neuroradiol* 2014; **35:** 379-85. doi: 10.3174/ajnr.A3706
16. Schneider S, Kadletz L, Wiebringhaus R, Kenner L, Selzer E, Füreder T, et al. PD-1 and PD-L1 expression in HNSCC primary cancer and related lymph node metastasis - impact on clinical outcome. *Histopathology* 2018; **73:** 573-84. doi: 10.1111/his.13646

17. Leemans CR, Snijders PJF, Brakenhoff RH. The molecular landscape of head and neck cancer. *Nat Rev Cancer* 2018; **18:** 269-82. doi: 10.1038/nrc.2018.11

18. Tang H, Zhou X, Ye Y, Zhou Y, Wu C, Xu Y. The different role of PD-L1 in head and neck squamous cell carcinomas: a meta-analysis. *Pathol Res Pract* 2020; **216:** 152768. doi: 10.1016/j.prp.2019.152768

19. Yang WF, Wong MCM, Thomson PJ, Li KY, Su YX. The prognostic role of PD-L1 expression for survival in head and neck squamous cell carcinoma: a systematic review and meta-analysis. *Oral Oncol* 2018; **86:** 81-90. doi: 10.1016/j.oraloncology.2018.09.016

20. Lin YM, Sung WW, Hsieh MJ,Tsai SC, Lai HW, Yang SM, et al. High PD-L1 expression correlates with metastasis and poor prognosis in oral squamous cell carcinoma. *PLoS One* 2015; **10:** e0142656. doi: 10.1371/journal.pone.0142656.

21. Surov A, Meyer HJ, Wienke A. Associations between apparent diffusion coefficient (ADC) and KI 67 in different tumors: a meta-analysis. Part 1: $ADC_{mean.}$ *Oncotarget* 2017; **8:** 75434-44. doi: 10.18632/oncotarget.20406

22. Just N. Improving tumour heterogeneity MRI assessment with histograms. *Br J Cancer* 2014; **111:** 2205-13. doi: 10.1038/bjc.2014.512

23. de Perrot T, Lenoir V, Domingo Ayllón M, Dulguerov N, Pusztaszeri M, Becker M. Apparent diffusion coefficient histograms of human papillomavirus-positive and human papillomavirus-negative head and neck squamous cell carcinoma: assessment of tumor heterogeneity and comparison with histopathology. *AJNR Am J Neuroradiol* 2017; **38:** 2153-60. doi: 10.3174/ajnr.A5370.

24. Rasmussen JH, Olin A, Lelkaitis G, Hansen AE, Andersen FL, Johannesen HH, et al. Does multiparametric imaging with $^{18}$F-FDG-PET/MRI capture spatial variation in immunohistochemical cancer biomarkers in head and neck squamous cell carcinoma? *Br J Cancer* 2020; **123:** 46-53. doi: 10.1038/s41416-020-0876-9

25. Choi JW, Lee D, Hyun SH, Han M, Kim JH, Lee SJ. Intratumoural heterogeneity measured using FDG PET and MRI is associated with tumour-stroma ratio and clinical outcome in head and neck squamous cell carcinoma. *Clin Radiol* 2017; **72:** 482-9. doi: 10.1016/j.crad.2017.01.019

26. Chow LQM, Haddad R, Gupta S, Mahipal A, Mehra R, Tahara M, et al. Antitumor activity of pembrolizumab in biomarker-unselected patients with recurrent and/or metastatic head and neck squamous cell carcinoma: results from the phase Ib KEYNOTE-012 expansion cohort. *J Clin Oncol* 2016; **34:** 3838-45. doi: 10.1200/JCO.2016.68.1478.

27. Ferris RL, Blumenschein G Jr, Fayette J, Guigay J, Colevas AD, Licitra L, et al. Nivolumab for recurrent squamous-cell carcinoma of the head and neck. *N Engl J Med* 2016; **375:** 1856-67. doi: 10.1056/NEJMoa1602252

28. Seiwert TY, Burtness B, Mehra R, Weiss J, Berger R, Eder JP, et al. Safety and clinical activity of pembrolizumab for treatment of recurrent or metastatic squamous cell carcinoma of the head and neck (KEYNOTE-012): an open-label, multicentre, phase 1b trial. *Lancet Oncol* 2016; **17:** 956-65. doi: 10.1016/S1470-2045(16)30066-3

29. Ledgerwood LG, Kumar D, Eterovic AK, Wick J, Chen K, Zhao H, et al. The degree of intratumor mutational heterogeneity varies by primary tumor sub-site. *Oncotarget* 2016; **7:** 27185-98. doi: 10.18632/oncotarget.8448.

30. Lyford-Pike S, Peng S, Young GD, Taube JM, Westra WH, Akpeng B, et al. Evidence for a role of the PD-1: PD-L1 pathway in immune resistance of human papillomavirus -associated head and neck squamous cell carcinoma. *Cancer Res* 2013; **73:** 1733-41. doi: 10.1158/0008-5472.CAN-12-2384.

31. Meyer HJ, Höhn A, Surov A. Histogram analysis of ADC in rectal cancer: associations with different histopathological findings including expression of EGFR, Hif1-alpha, VEGF, p53, PD1, and KI 67. A preliminary study. *Oncotarget* 2018; **9:** 18510-7. doi: 10.18632/oncotarget.24905

*research article*

# Configuration of soft-tissue sarcoma on MRI correlates with grade of malignancy

Sam Sedaghat[1,2], Mona Salehi Ravesh[1], Maya Sedaghat[1,2], Marcus Both[1], Olav Jansen[1]

[1] Department for Radiology and Neuroradiology, University Hospital Schleswig-Holstein, Campus Kiel, Germany
[2] Institute of Diagnostic and Interventional Radiology and Nuclear Medicine, University Hospital Bergmannsheil, Bochum, Germany

Radiol Oncol 2021; 55(2): 158-163.

Received 11 November 2020
Accepted 14 December 2020

Correspondence to: Sam Sedaghat, M.D., Department for Radiology and Neuroradiology, University Hospital Schleswig-Holstein Campus Kiel, Arnold-Heller-Str. 3, 24105 Kiel, Germany. E-mail: samsedaghat1@gmail.com

Disclosure: No potential conflicts of interest were disclosed.

**Background.** The aim of the study was to assess whether the configuration of primary soft-tissue sarcoma (STS) on MRI correlates with the grade of malignancy.

**Patients and methods.** 71 patients with histologically proven STS were included. Primary STS were examined for configuration, borders, and volume on MRI. The tumors were divided into high-grade (G3), intermediate-grade (G2) and low-grade (G1) STS according to the grading system of the French Federation of Cancer Centers Sarcoma Group (FNCLCC).

**Results.** 30 high-grade, 22 intermediate-grade and 19 low-grade primary STS lesions were identified. High- and intermediate-grade (G3/2) STS significantly most often appeared as polycyclic/multilobulated tumors ($p < 0.001$ and $p = 0.002$, respectively). Low-grade (G1) STS mainly showed an ovoid/nodular or streaky configuration ($p = 0.008$), and well-defined borders. The appearance of high-, intermediate- and low-grade STS with an ovoid/nodular configuration were mainly the same on MRI. All streaky G3/2 sarcoma and 17 of 20 patients with polycyclic/multilobulated G3 sarcoma showed infiltrative borders. High-grade streaky and polycyclic/multilobulated STS are larger in volume, compared to intermediate- and low-grade STS.

**Conclusions.** Configuration of STS on MRI can indicate the grade of malignancy. Higher-grade (G2/3) STS most often show a polycyclic/multilobulated configuration, while low-grade STS are mainly ovoid/nodular or streaky. Infiltrative behavior might suggest higher-grade STS in streaky and polycyclic/multilobulated STS.

Key words: soft-tissue sarcoma; MRI; configuration; FNCLCC; malignancy; prediction

## Introduction

Soft-tissue sarcomas (STS) comprise a heterogeneous group of malignancies, accounting for only about 1% of all cancers.[1] More than 50 histologic subtypes of STS have been identified, with pleomorphic sarcoma, liposarcoma, leiomyosarcoma, synovial sarcoma, and malignant peripheral nerve sheath tumors being the most common.[2,3] STS mostly originate in the extremities but can occur at any site in the body.[3] Different risk factors for the development of STS have been reported, for example, radiation therapy and radiation-induced sarcoma.[4,5] While sonography is still sometimes used for screening of STS[6], MRI has become the most important imaging modality these days for pre- and post-operative evaluation of STS, as it can evaluate tumoral characteristics and extent of disease very well.[3,7-9] The two most common systems for grading STS are those of the French Federation of Cancer Centers Sarcoma Group (FNCLCC) and the National Cancer Institute in the U.S. Of the two, the FNCLCC system is superior in predicting distant metastasis and tumor mortality.[2,10] According to this system, STS are divided into three grades of malignancy: G1 (low-grade), G2 (intermediate-grade), and G3 (high-grade). Knowledge of the STS grade is very relevant because it influences the

therapy options and helps determine which treatment should be implemented.[11,12] Furthermore, the STS grade is reported to be a valuable predictor of STS recurrence and of the benefit of adjuvant chemotherapy.[13] A relatively new morphological aspect on MRI is to characterize STS by their configurations.[14,15] Therefore, the purpose of this study was to determine whether the grade of malignancy can be predicted by the configuration of primary STS on MRI and whether low-, intermediate and high-grade STS can be distinguished by tumor configuration on MRI.

## Patients and methods

### Patients

Altogether 163 patients with STS were identified in whom pre- and/or post-therapeutic imaging had been performed between 2008 and 2020. Patients with other examination than MRI were excluded (n = 21), as were patients with lack of pre-therapeutic MRI (n = 42) and patients with lipo-, angio- and retroperitoneal sarcomas (n = 29). Finally, 71 primary STS were included in this study. Information on the histological subtypes of STS were deliberately not included in our study in order to prevent any assessments of the degree of malignancy by knowing the subtype. However, histological STS grades were derived from all available pathological reports and all included STS were classified by their grade of malignancy. Consecutively, primary STS were divided into three groups according to the FNCLCC grading system: G1 (low-grade), G2 (intermediate) and G3 (high-grade). G3 and G2 sarcoma were both regarded as higher-grade tumors. Nevertheless, the two grades were examined separately.

### Imaging

The configuration of the tumors was divided into polycyclic/multilobulated, fascicular, ovoid/nodular, streaky, and fusiform. Furthermore, the tumors were examined for contrast enhancement (homogeneous or heterogeneous), borders (infiltrative or well-defined), and volume on MRI. The volume was measured from length, width, and height.

For imaging, a 1.5-Tesla MRI system (MAGNETOM Symphony, Siemens Healthineers) was employed. The MRI protocol included the following sequences: axial T2-weighted (TE: 64–114ms, TR: 3010–5840ms, FOV: 22–44 $cm^2$), axial T1-weighted (TE: 10–14 ms, TR: 587–868 ms, FOV: 22–44 $cm^2$), axial proton density-weighted (PDw) (TE: 26–36ms, TR: 2740–4610ms, FOV: 22–40 $cm^2$), coronal Turbo-Inversion Recovery Magnitude (TIRM) (TE: 68–77ms, TR: 4410–6980 ms, FOV: 37–45 $cm^2$), axial (10–12 ms, TR: 645–865ms, FOV: 22–44 $cm^2$), coronal (TE: 10 13ms, TR: 533–1440ms, FOV: 37–45 cm2), and sagittal (TE: 10–13ms, TR: 577–866ms, FOV: 22–37 $cm^2$) T1-weighted after administering a contrast agent intravenously. Additionally, in some recent examinations diffusion-weighted-images (DWI) were available.

Two musculoskeletal radiologists, with a minimum of five years of experience in diagnosing sarcoma reviewed each MRI, with findings reached by consensus.

**TABLE 1.** Overview of configuration of high-grade (G3), intermediate-grade (G2) and low-grade (G1) soft-tissue sarcomas (STS). Additional information on tumor infiltration (infiltrative or well-defined), contrast enhancement (homogeneous or heterogeneous), and volume in "$cm^3$" is shown

| Configuration of STS | G3 (number, contrast enhancement, infiltration) | Volume G3 ($cm^3$) | G2 (number, contrast enhancement, infiltration) | Volume G2 ($cm^3$) | G1 (number, contrast enhancement, infiltration) | Volume G1 ($cm^3$) |
|---|---|---|---|---|---|---|
| Polycyclic/ multilobulated | **20* 19 heterogeneous 17 infiltrative** | Median: 765.9**** (Min. 15.6, Max. 4572.5, SD: 1176.5) | **13** 11 heterogeneous 7 well-defined** | Median: 114.8 (Min. 6, Max. 334, SD: 94.6) | 3 all homogeneous all well-defined | Median: 198.1 (Min. 15.8, Max. 447.2, SD: 223.3) |
| Fascicular | 1 | | - | | 2 | - |
| Ovoid/nodular | **4 all homogeneous 3 well-defined** | Median: 9 (Min. 3.3, Max. 20.3, SD: 9.8) | **5 all homogeneous all well-defined** | Median: 26.5 (Min. 2.6, Max. 41.4, SD: 17.7) | **8*** all homogeneous all well-defined** | Median: 11.2 (Min. 1.6, Max. 25.4, SD: 7.7) |
| Streaky | **4 all homogeneous all infiltrative** | Median: 49.4 (Min. 5.6, Max. 130.9, SD: 70.7) | **2 all homogeneous all infiltrative** | Median 7.9 (Min. 7.1, Max. 8.6, SD: 1.1) | **5*** all homogeneous 4 well-defined** | Median: 4.4 (Min. 2.6, Max. 6.5, SD: 1.4) |
| Fusiform | 1 | - | 2 | | 1 | - |
| **Total** | **30** | | **22** | | **19** | |

p-values are marked with "*"; †soft tissue sarcoma; *p<0.001, **p=0.002, ***p=0.008, ****p=0.051

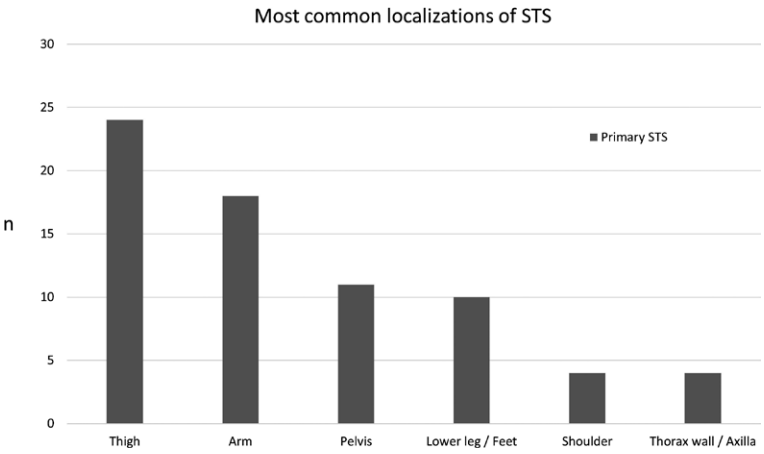


**FIGURE 1.** Overview of most common localizations of primary soft-tissue sarcoma (STS), shown as number of cases "n".

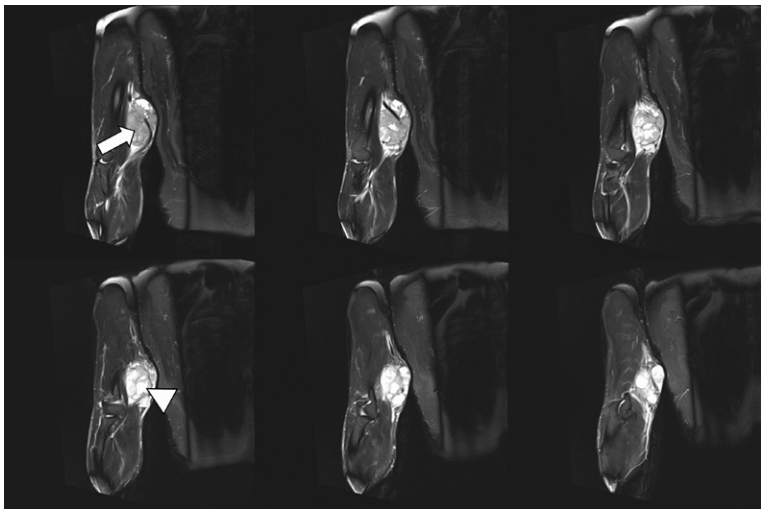

**FIGURE 2.** 1.5-T MRI of the arm (proton density [PD] fat saturation [FS]: 6 consecutive slices of 3 mm) of a 54-year-old patient. The higher-grade polycyclic/multilobulated sarcoma in the upper arms shows solid (white arrow) and cystic (white arrowhead) components.

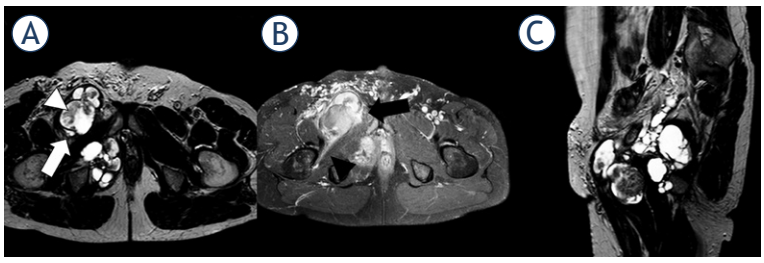


**FIGURE 3.** 1.5-T MRI of the pelvis **(A)** proton density [PD] axial, **(B)** contrast-enhanced T1 fat saturation [FS] axial, **(C)** PD sagittal) of a 49-year-old patient. The higher-grade polycyclic/multilobulated sarcoma in the right pelvis (white arrow) shows heterogeneous contrast enhancement (black arrow), infiltrative behavior (black arrowhead), and solid components within cystic tissue (white arrowhead).

### Statistical data

Data are given as median values with range (minimum to maximum) or mean and standard deviation (SD). Parametric and nonparametric tests to compare group values ($\chi$2-test, Mann-Whitney U-test, ANOVA) were performed as indicated. Statistical significance for all tests was set at a level of $p < 0.05$. Statistical analysis was done using the IBM-SPSS version 22.0 software package (IBM, Armonk, NY, USA).

### Ethics approval

The study was conducted in accordance with and was approved by the responsible IRB/Ethics Committee.

## Results

Patient's mean age was 55.7 years (SD: 18.2, Min.: 10, Max.: 88). In all, 71 primary STS were included, and 30 high-grade, 22 intermediate-grade and 19 low-grade primary STS lesions were identified (Table 1). Primary STS significantly most often occurred in the extremities ($p < 0.001$), while the thigh represented the predominant localization of STS (Figure 1). Most of the high-grade (G3) and intermediate-grade (G2) primary STS showed a polycyclic/multilobulated configuration ($p < 0.001$ and $p = 0.002$, respectively; Table 1; Figure 2 and 3), while low-grade primary STS (G1) were mostly ovoid/nodular (Figure 4 and 5) or streaky (Figure 6; $p = 0.008$). G3 polycyclic/multilobulated STS were significantly more often infiltrative, compared to G2 polycyclic/multilobulated STS ($p = 0.014$). For ovoid/nodular primary STS, no significant difference was observed between high-, intermediate and low-grade STS regarding contrast enhancement and borders. Streaky G3 and G2 sarcoma were all infiltrative, while streaky G1 sarcoma mostly showed well-defined borders. High-grade streaky and polycyclic/multilobulated STS are larger (not significant) in volume, compared to intermediate- and low-grade STS.

## Discussion

In this study we wanted to assess whether low-, intermediate and high-grade STS can be distinguished by tumor configuration on MRI and whether one or the other configuration might

already suggest the grade of malignancy. STS comprise a group of rare malignancies of the soft tissue that may occur anywhere in the body[1] but mainly develop in the extremities and especially in adults.[16,17] In our study the most prominent site of primary STS is the extremities, where STS mainly occurred in the thigh, followed by the arm. The FNCLCC uses a scoring system to grade STS. Accordingly, this scoring system includes information on tumor differentiation, mitotic count, and tumor necrosis and then classifies STS into three grades: G1 (low-grade), G2 (intermediate) and G3 (high-grade).[18,19] As the distinction between G2 and G3 STS is not always clear in the routine clinical setting, both sarcoma grades are often considered as "higher-grade". The grade of STS is a highly valuable parameter for assessing therapy. In patients with higher-grade STS, neoadjuvant chemotherapy is often considered, while it is not administered for low-grade STS.[20] In contrast, surgery alone is often selected as the first therapeutic option in low-grade STS.[18,21] As a standard diagnostic procedure, needle biopsy is performed before initiating treatment.[22] However, percutaneous biopsy sometimes misses the grade of STS, which in turn can be represent a missed opportunity for neoadjuvant chemotherapy or radiation therapy.[18] This shows the importance of imaging in the diagnostic workup and for STS grading, especially by using MRI.[23]

MRI represents a valuable imaging modality in pre- and postoperative screening of STS, the advantages of which lie in the absence of ionizing radiation and its relatively high contrast resolution compared to PET-CT or CT.[18] Only few previous studies have investigated the issue of distinguishing between low-, intermediate- and high-grade STS by tumor characteristics on MRI. However, there have been reports of a correlation between tumor margins or contrast enhancement with the STS grade, for example.[24] In the literature, MRI signal characteristics of low- and high-grade STS were also examined; however, they lacked specific descriptions of the imaging and signal characteristics of most STS.[25,26] Additionally, MRI signal characteristics of STS are often misleading.[27] Therefore, we did not focus on the signal characteristics of STS in this study. Notably, no previous investigations have focused on the configuration of low- and higher-grade STS on MRI for grading STS. Our data suggest that by focusing on the configuration of STS it is possible to distinguish between G1 and G2/3 STS, especially when they show a polycyclic configuration. It becomes more difficult with other configurations, such as ovoid/nodular or streaky.

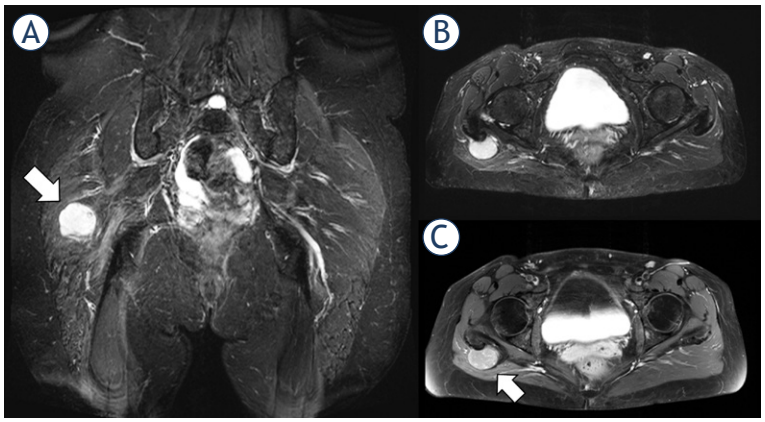


**FIGURE 4.** 1.5-T MRI of the pelvis **(A)** proton density [PD] fat saturation [FS]: coronal, **(B)** PD FS axial, **(C)** contrast-enhanced T1 FS axial) of a 51-year-old patient. The low-grade sarcoma in the right gluteal region (white arrow) shows an ovoid/nodular configuration and well-defined borders.

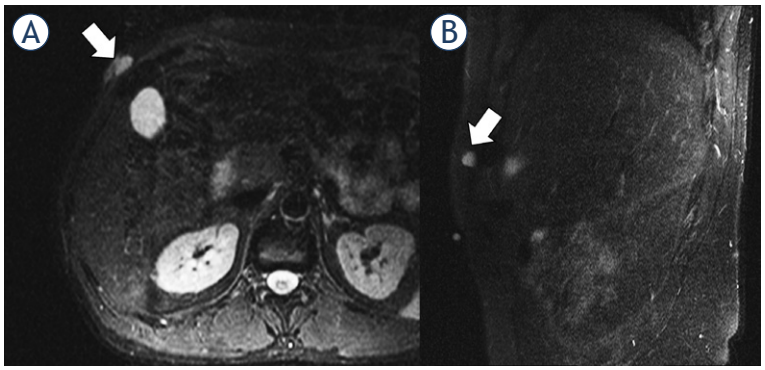


**FIGURE 5.** 1.5-T MRI of the abdomen **(A)** contrast-enhanced T1 axial, **(B)** contrast-enhanced T1 sagittal) of a 41-year-old patient. The low-grade sarcoma in the right abdominal wall (white arrow) presents with a ovoid/nodular configuration.

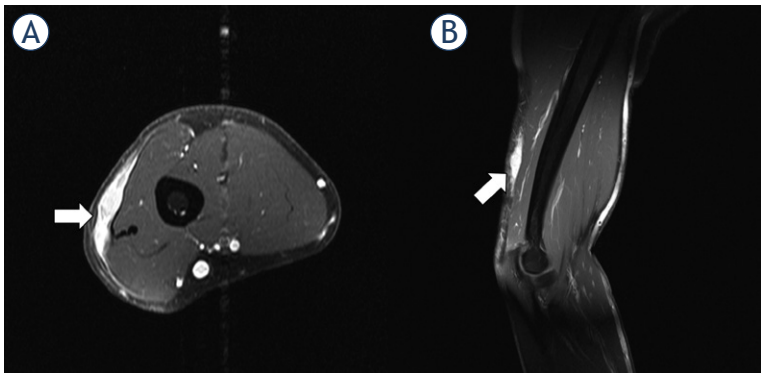


**FIGURE 6.** 1.5-T MRI of the upper arm **(A)** contrast-enhanced T1 axial, **(B)** contrast-enhanced T1 sagittal) of a 48-year-old patient. The higher-grade sarcoma in the subcutaneous tissue (white arrow) has a streaky configuration and shows slight infiltration of the surrounding subcutaneous tissue.

Primary STS with an ovoid/nodular configuration usually shows the same appearance in low-, intermediate and high-grade STS.

Previous authors mainly associated higher-grade STS to an infiltration of the tumor-surrounding tissue. Our findings show that higher-grade STS may show well-defined borders as well, especially in ovoid/nodular STS.[20,28] In the case of streaky STS, infiltration of the surrounding tissue can be used as a characteristic for differentiating between G3/2 and G1 STS, as all higher-grade STS show infiltrative borders, while the borders of low-grade STS are mostly well-defined. Furthermore, our data shows that in polycyclic/multilobulated STS the proportion of infiltrative sarcomas increases with the grade of malignancy (G1 to G3). While in G1 polycyclic/multilobulated STS all tumors are well-defined, G3 sarcomas with the same configuration are mainly infiltrative.

For the evaluation of STS, contrast material is routinely administered.[24] In our study contrast-enhanced MRI was performed in all patients as well. As radiologists have been aiming to restrict the use of contrast media for some time, especially due to reported adverse events after gadolinium-based contrast agent administration[29], the question arises as to whether a contrast medium is needed for the diagnosis of STS. As mentioned, it is possible to distinguish between higher- and low-grade STS on MRI, especially when they show a polycyclic/multilobulated configuration. In these cases, the use of a contrast agent is questionable and this issue should be investigated in further studies.

Contrary to previous data, the size of STS cannot determine the grade of STS, as in our study no significant differences in the volumes of higher- and low-grade STS were found, even if polycyclic/multilobulated G3 STS show a not significant larger volume, compared to G2/1 sarcoma.[30,31]

We cannot guarantee that a polycyclic/multilobulated configuration will always verify a higher-grade STS, but we were able to show that the configuration of STS can give an indication of STS grade, which ultimately leads to more targeted diagnostic tests and earlier therapy. Our study has some limitations. The main limitations are the retrospective design and the single-center approach. As STS is a rare tumor, the inclusion of almost similar numbers of patients in a prospective study would take a long time. In addition, the benefit would be disproportionate to the additional time that would be spent. A multicenter study approach could improve this study, as the comparison of non-polycyclic/-multilobulated STS configurations could be better investigated. Therefore, further studies on this topic should be multicenter in design. Another limitation of this study is the lack of diffusion weighted images (DWI), which were only available in a few and mainly recent examinations.

## Conclusions

Configuration of STS on MRI can indicate the grade of malignancy, as higher-grade (G2/3) STS significantly most often show a polycyclic/multilobulated configuration, while low-grade STS (G1) are mainly ovoid/nodular or streaky. Furthermore, infiltrative behavior might suggest higher-grade STS in streaky and polycyclic/multilobulated STS. For ovoid/nodular configurations, high-, intermediate and low-grade STS cannot be distinguished on MRI.

## References


1. Clark MA, Fisher C, Judson I, Thomas JM. Soft-tissue sarcomas in adults. *N Engl J Med* 2005; **353:** 701-11. doi: 10.1056/NEJMra041866
2. Demetri GD, Antonia S, Benjamin RS, Bui MM, Casper ES, Conrad EU, et al. Soft tissue sarcoma. *J Natl Compr Canc Netw* 2010; **8:** 630-74. doi: 10.6004/jnccn.2010.0049
3. Cormier JN, Pollock RE. Soft tissue sarcomas. *CA Cancer J Clin* 2004; **54:** 94-109. doi: 10.3322/canjclin.54.2.94
4. Patel SR. Radiation-induced sarcoma. *Curr Treat Options Oncol* 2000; **1:** 258-61. doi: 10.1007/s11864-000-0037-6
5. Brady MS, Gaynor JJ, Brennan MF. Radiation-associated sarcoma of bone and soft tissue. *Arch Surg* 1992; **127:** 1379-85. doi: 10.1001/archsurg.1992.01420120013002
6. Arya S, Nagarkatti DG, Dudhat SB, Nadkarni KS, Joshi MS, Shinde SR. Soft tissue sarcomas: ultrasonographic evaluation of local recurrences. *Clin Radiol* 2000; **55:** 193-7. doi: 10.1053/crad.1999.0343
7. Patel DB, Matcuk Jr GR. Imaging of soft tissue sarcomas. *Chin Clin Oncol* 2018; **7:** 35. doi: 10.21037/cco.2018.07.06
8. Ilaslan H, Schils J, Nageotte W, Lietman SA, Sundaram M. Clinical presentation and imaging of bone and soft-tissue sarcomas. *Cleve Clin J Med* 2010; **77(Suppl 1):** S2-7. doi: 10.3949/ccjm.77.s1.01
9. Wu JS, Hochman MG. Soft-tissue tumors and tumorlike lesions: a systematic imaging approach. *Radiology* 2009; **253:** 297-316. doi: 10.1148/radiol.2532081199
10. Guillou L, Coindre J-M, Bonichon F, Nguyen BB, Terrier P, Collin F, et al. Comparative study of the National Cancer Institute and French Federation of Cancer Centers Sarcoma Group grading systems in a population of 410 adult patients with soft tissue sarcoma. *J Clin Oncol* 1997; **15:** 350-62. doi: 10.1200/JCO.1997.15.1.350
11. Verweij J, Baker LH. Future treatment of soft tissue sarcomas will be driven by histological subtype and molecular abberations. *Eur J Cancer* 2010; **46:** 863-8. doi: 10.1016/j.ejca.2010.01.016
12. Grimer R, Judson I, Peake D, Seddon B. Guidelines for the management of soft tissue sarcomas. *Sarcoma* 2010; **2010:** 506182. doi: 10.1155/2010/506182
13. Italiano A, Le Cesne A, Mendiboure J, Blay JY, Piperno-Neumann S, Chevreau C, et al. Prognostic factors and impact of adjuvant treatments on local and metastatic relapse of soft-tissue sarcoma patients in the competing risks setting. *Cancer* 2014; **120:** 3361-9. doi: 10.1002/cncr.28885

14. Sedaghat S, Schmitz F, Sedaghat M, Nicolas V. Appearance of recurrent dermatofibrosarcoma protuberans in postoperative MRI follow-up. *J Plast Reconstr Aesthet Surg* 2020; **73:** 1960-65. doi: 10.1016/j.bjps.2020.08.089

15. Sedaghat S, Schmitz F, Krieger A, Sedaghat M, Reichardt B. Appearance of recurrent adult fibrosarcoma of the soft tissue and loco-regional post-treatment changes on MRI follow-up. *Eur J Plast Surg* 2020. doi: 10.1007/s00238-020-01669-1

16. Brennan MF, Alektiar KM, Maki RG. Sarcomas of the soft tissue and bone. Section 1: Soft tissue sarcoma. In: Devita VT, Hellman S, Rosenberg SA, editors. Cancer: principles and practice of oncology, 6th edition. Philadelphia: Lippincott, Williams & Wilkins. p. 1841-91.

17. Weiss SW, Goldblum JR, Folpe AL. Enzinger and Weiss's soft tissue tumors. 5th edition. Philadelphia PA: Elsevier Health Sciences; 2007.

18. Wang X, Jacobs MA, Fayad L. Therapeutic response in musculoskeletal soft tissue sarcomas: evaluation by MRI. *NMR Biomed* 2011; **24:** 750-63. doi: 10.1002/nbm.1731

19. Coindre J-M. Grading of soft tissue sarcomas: review and update. *Arch Pathol Lab Med* 2006; **130:** 1448-53. doi: 10.1043/1543-2165(2006)130[1448:GOSTSR]2.0.CO;2

20. Zhao F, Ahlawat S, Farahani SJ, Weber KL, Montgomery EA, Carrino JA, Fayad LM. Can MR imaging be used to predict tumor grade in soft-tissue sarcoma? *Radiology* 2014; **272:** 192-201. doi: 10.1148/radiol.14131871

21. Lietman SA. Soft-tissue sarcomas: overview of management, with a focus on surgical treatment considerations. *Cleve Clin J Med* 2010; **77:** S13. doi: 10.3949/ccjm.77.s1.03

22. Welker JA, Henshaw RM, Jelinek J, Shmookler BM, Malawer MM. The percutaneous needle biopsy is safe and recommended in the diagnosis of musculoskeletal masses: outcomes analysis of 155 patients at a sarcoma referral center. *Cancer* 2000; **89:** 2677-86. doi: 10.1002/1097-0142(20001215)89:12<2677::aid-cncr22>3.0.co;2-l

23. Yang J, Frassica FJ, Fayad L, Clark DP, Weber KL. Analysis of nondiagnostic results after image-guided needle biopsies of musculoskeletal lesions. *Clin Orthop Relat Res* 2010; **468:** 3103-11. doi: 10.1007/s11999-010-1337-1

24. Engellau J, Bendahl P-O, Persson A, Domanski HA, Åkerman M, Gustafson P, et al. Improved prognostication in soft tissue sarcoma: independent information from vascular invasion, necrosis, growth pattern, and immunostaining using whole-tumor sections and tissue microarrays. *Hum Pathol* 2005; **36:** 994-1002. doi: 10.1016/j.humpath.2005.07.008

25. Brisse HJ, Orbach D, Klijanienko J. Soft tissue tumours: imaging strategy. *Pediatr Radiol* 2010; **40:** 1019-28. doi: 10.1007/s00247-010-1592-z

26. Liang C, Mao H, Tan J, Ji Y, Sun F, Dou W, et al. Synovial sarcoma: Magnetic resonance and computed tomography imaging features and differential diagnostic considerations. *Oncol Lett* 2015; **9:** 661-6. doi: 10.3892/ol.2014.2774

27. am de Schepper, Beuckeleer L de, Vandevenne J, Somville J. Magnetic resonance imaging of soft tissue tumors. *European radiology* 2000; **10:** 213-23. doi: 10.1007/s003300050037

28. Liu Q-Y, Li H-G, Chen J-Y, Liang B-L. Correlation of MRI features to histopathologic grade of soft tissue sarcoma. *Chin J Cancer* 2008; **27:** 856-60.

29. McDonald JS, Hunt CH, Kolbe AB, Schmitz JJ, Hartman RP, Maddox DE, et al. Acute adverse events following gadolinium-based contrast agent administration: a single-center retrospective study of 281 945 injections. *Radiology* 2019; **292:** 620-7. doi: 10.1148/radiol.2019182834

30. Am De S, Ramon FA, Degryse HR. Statistical analysis of MRI parameters predicting malignancy in 141 soft tissue masses. *Rofo* 1992; **156:** 587-91. doi: 10.1055/s-2008-1032948

31. Tung GA, Davis LM. The role of magnetic resonance imaging in the evaluation of the soft tissue mass. *Crit Rev Diagn Imaging* 1993; **34:** 239.

*research article*

# TIPS *vs.* endoscopic treatment for prevention of recurrent variceal bleeding: a long-term follow-up of 126 patients

Spela Korsic[1,2], Borut Stabuc[2,3], Pavel Skok[4,5], Peter Popovic[1,2]

[1] Clinical Institute of Radiology, University Medical Centre Ljubljana, Ljubljana, Slovenia
[2] Faculty of Medicine, University of Ljubljana, Ljubljana, Slovenia
[3] Department of Gastroenterology and Hepatology, University Medical Centre Ljubljana, Ljubljana, Slovenia
[4] Department of Gastroenterology, University Medical Centre Maribor, Maribor, Slovenia
[5] Faculty of Medicine, University of Maribor, Maribor, Slovenia

Radiol Oncol 2021; 55(2): 164-171.

Received 10 December 2020
Accepted 7 January 2021

Correspondence to: Assoc. Prof. Peter Popovič, M.D., Ph.D., Clinical Institute of Radiology, University Medical Centre Ljubljana, Zaloška cesta 7, SI-1000 Ljubljana, Slovenia. E-mail: peter.popovic@kclj.si

Disclosure: No potential conflicts of interest were disclosed.

**Background.** Recurrent bleeding from gastroesophageal varices is the most common life-threatening complication of portal hypertension. According to guidelines, transjugular intrahepatic portosystemic shunt (TIPS) should not be used as a first-line treatment and should be limited to those bleedings which are refractory to pharmacologic and endoscopic treatment (ET). To our knowledge, long-term studies evaluating the role of elective TIPS in comparison to ET in patients with recurrent variceal bleeding episodes are rare.

**Patients and methods.** This study was designed as a retrospective single-institution analysis of 70 patients treated with TIPS and 56 with ET. Patients were followed-up from inclusion in the study until death, liver transplantation, the last follow-up observation or until the end of our study.

**Results.** Recurrent variceal bleeding was significantly more frequent in ET group compared to patients TIPS group (66.1% *vs.* 21.4%, $p < 0.001$; $\chi 2$-test). The incidence of death secondary to recurrent bleeding was higher in the ET group (28.6% *vs.* 10%). Cumulative survival after 1 year, 2 years and 5 years in TIPS group compared to ET group was 85% *vs.* 83%, 73% *vs.* 67% and 41% *vs.* 35%, respectively. The main cause of death in patients with cumulative survival more than 2 years was liver failure. Median observation time was 47 months (range; 2–194 months) in the TIPS group and 40 months (range; 1–168 months) in the ET group.

**Conclusions.** In present study TIPS was more effective in the prevention of recurrent variceal bleeding and had lower mortality due to recurrent variceal bleeding compared to ET.

Key words: transjugular intrahepatic portosystemic shunt; endoscopic treatment; portal hypertension; esophageal and gastric varices; recurrent variceal bleeding; survival

## Introduction

Gastroesophageal variceal bleeding (GEVB) is a severe complication of portal hypertension. In cirrhotic patients with a history of variceal bleeding, the incidence of GEVB within 1 year is 60%, while the mortality from each rebleeding episode is nearly 20%.[1] In terms of prevention of recurrent bleeding, current guidelines recommend management of patients with the history of variceal bleeding. The first-line treatment for preventing recurrent variceal bleeding is pharmacologic treatment with non-selective β-adrenergic blockers (NSBB), or a combination of isosorbide mononitrate (ISMN) and nadolol combined with endoscopic treatment (ET), *i.e.* variceal sclerotherapy and/or variceal ligation.[2,3] In

frequently recurring bleeding episodes, in patients unresponsive to pharmacological and endoscopic treatment, transjugular intrahepatic portosystemic shunt (TIPS) or surgical procedures (*i.e.* portocaval or splenorenal shunt) are the treatments of choice. TIPS is recommended as a "rescue-urgent" treatment if primary haemostasis cannot be obtained with endoscopic and pharmacological treatment, or if uncontrollable early rebleeding occurs within 48 hours.[4-6] TIPS is used as an elective procedure after the second or third (and/or more) recurrent bleeding episode from varices (especially if repeated over short periods of time) in hemodynamically and clinically stable patients with optimally regulated risk factors for the complication of the procedure (*i.e.* improvement of coagulation factors, elimination or reduction of ascites, regulation of cardiac and renal function, and clinically significant improvement in hepatic encephalopathy). In most of the randomized studies, patients were included in the study 24 to 96 hours from the last bleeding.[7-11] Studies which could evaluate the role of elective TIPS in comparison to combined ET and NSBB treatment in patients with recurrent variceal bleeding episodes are rare.[8,12,13] According to literature, there are even fewer studies which analysed the long-term effect of TIPS *vs.* ET, 30 months being the longest observation period in terms of survival.[14] The purpose of our study was therefore to compare elective TIPS with combined ET and NSBB treatment in terms of their long-term efficacy in preventing recurrent GEVB in patients with portal hypertension.

## Patients and methods

This retrospective study included 126 patients with liver cirrhosis and recurrent GEVB episodes originating from ruptured esophageal and gastric varices. The inclusion criteria were: (1) at least three gastroesophageal variceal bleedings or two recurrent episodes of bleeding within a less than a month period; (2) < 1 month since the previous bleeding episode; (3) Child-Pugh score < 13; (4) technically successful TIPS procedure; (5) 18 < age < 75; (6) patient's written informed consent. Exclusion criteria were: (1) patients who did not meet inclusion criteria; (2) chronic occlusion of portal vein; (3) hepatocellular carcinoma (HCC) or/and other types of cancer (with the exceptions of non-melanoma skin cancer and *in situ* cervical cancer); (4) acute hepatitis.

Patients who were treated with elective TIPS were included in the study from the time of the procedure, *i.e.* on average 35 days after the last variceal bleeding episode. Those patients were hemodynamically and otherwise (in terms of disease) stable. ET patients were included in the study after the last variceal bleeding, that is after successful pharmacological and endoscopic eradication, *i.e.* on average 30 days after the last bleeding episode. All patients were followed-up with clinical evaluations, serum laboratory tests, and Doppler ultrasound before hospital discharge, in the outpatient clinic at 3 months after TIPS and every 6 months thereafter. Portal venography was performed only as an introduction to a re-intervention in patients with suspected or impaired shunt malfunction. Patients were followed-up from inclusion in the study until death, liver transplantation, the last follow-up observation or until the end of our study.

Primary endpoint of our study was rebleeding rate. Bleeding-related mortality and survival were considered as secondary endpoints.

The study took place at the Institute of Radiology and Department of Gastroenterology of University Medical Centre Ljubljana, and at the Department of Gastroenterology of University Medical Centre Maribor.

The study was approved by the National Medical Ethics Committee of the Republic of Slovenia (Number 94/11/11) and was in agreement with the Declaration of Helsinki.

### TIPS procedure

TIPS was placed using a technique described in available literature, the procedure took place in the interventional radiology suite.[12,15] Prior to elective TIPS, patients were hemodynamically and systemically stable. After indirect portography between the portal and hepatic veins, shunt tracts were lined with wallstent endoprosthesis (Wallstent, Schneider, Switzerland) or polytetrafluoroethylene-covered stents (GoreÒViatorrÒ; United States). Portal and central venous pressures were measured before and after stenting. Patients were cared for in a semi-intensive care unit for 24 h after the procedure.

### Endoscopic treatment

In patients with recurrent variceal bleeding, endoscopic sclerosation (EST) *via* paravariceal and intravariceal injection of 1% polydocanol (Resinag, Zug, Switzerland) was performed first, after that EST was repeated or endoscopic ligation (EVL)

**TABLE 1.** Baseline demographic, clinical and biochemical characteristics of the 126 patients

| | TIPS | ET | P |
|---|---|---|---|
| | n = 70 | n = 56 | value |
| Sex | | | |
| Male | 45 (64.3%) | 35 (62.5%) | |
| Female | 25 (35.7%) | 22 (37.5%) | 0.836 |
| Age | 53.56 ± 11.15 | 57,57 ± 11,69 | 0.052 |
| Etiology | | | |
| Alcohol | 49 (70%) | 30 (67.9%) | |
| Non-alcohol | 21 (30%) | 18 (32.1%) | 0.796 |
| Child A | 15 (21.4%) | 8 (14.3%) | |
| Child B | 41 (58.6%) | 31 (55.4%) | |
| Child C | 14 (20.0%) | 17 (30.4%) | 0.319 |
| Child-Pugh score | 7.9 ± 1.7 | 8.5 ± 1.7 | 0.051 |
| Variceal grade | | | |
| I–II | 11 (15.8%) | 6 (10.7%) | |
| III–IV | 59 (84.2%) | 50 (89.3%) | 0.519 |
| Type of varices | | | |
| Esophageal | 36 (51.4%) | 32 (57.1%) | |
| Gastroesophageal | 34 (48.6%) | 24 (42.9%) | 0.573 |
| Site of bleeding | | | |
| Esophagus | 46 (65.7%) | 41 (73.2%) | |
| Gastric | 7 (10.0%) | 6 (10.7%) | |
| Gastroesophageal | 17 (24.3%) | 9 (16.1%) | 0.526 |
| No. of variceal bleeds | 3.46 ± 1,15 | 3.36 ± 1,06 | 0.651 |
| Leukocytes ($10^9$/L) | 5.09 ± 1.87 | 6.31 ± 3.03 | 0.034 |
| Platelets ($10^9$/L) | 109.07 ± 47.82 | 101.96 ± 52.10 | 0.309 |
| PT (s) | 0.64 ± 0.14 | 0.57 ± 0.14 | 0.003[a] |
| Bilirubin (mmol/L) | 40.90 ± 34.98 | 50.91 ± 50.77 | 0.125 |
| Albumin (mmol/L) | 30.78 ± 6.30 | 29.44 ± 5.25 | 0.256 |
| Urea (mmol/L) | 5.81 ± 3.02 | 8.33 ± 4.69 | 0.001[b] |
| Creatinine (mmol/L) | 78.93 ± 20.46 | 105.91 ± 117.1 | 0.226 |
| Ammonia (mmol/L) | 48.37 ± 23.66 | 60.94 ± 43.79 | 0.234 |
| gGT (mkat/L) | 1.21 ± 1.21 | 1.64 ± 1.49 | 0.070 |
| ALT (mkat/L) | 0.51 ± 0.46 | 0.74 ± 1.83 | 0.409 |
| AST (mkat/L) | 0.75 ± 0.65 | 1.11 ± 2.18 | 0.330 |
| Ascites | | | |
| No ascites | 31(44.3%) | 20 (35.7%) | |
| Ascites decrease | 18 (25.7%) | 13 (25.0%) | |
| Ascites increase | 21 (30.0%) | 22 (39.3%) | 0.507 |
| HE prior to proc. | | | |
| No HE | 51 (72.9%) | 39 (69.6%) | |
| CS, no H | 17 (24.2%) | 11 (19.6%) | |
| CS + H | / | 3 (5.4%) | |
| CHE | 2 (2.9%) | 3 (5.4%) | 0.295 |

[a]$P < 0.05$ *vs.* control group; [b]$P < 0.001$ *vs.* control group

ALT = alanine aminotransferase; AST = aspartate aminotransferase; CHE = chronic hepatic encephalopathy; CS = clinical signs; ET = endoscopic treatment; gGT = gamma-glutamyl transferase; H = hospitalization; HE = hepatic encephalopathy; PT = prothrombin time; TIPS = transjugular intrahepatic portosystemic shunt

was performed until scarring of the varices was achieved. Histoacryl adhesive (B Braun Medical, Melsungen, Switzerland), used in the same proportion as polydocanol, was injected directly into the varices. Patients received antibiotic prophylaxis prior to and after ET, and octreotide (1.2 mg/24 h for 3–5 days) after the procedure. Until the varices were eradicated, subsequent ET was undertaken at 3–4 weeks intervals on an outpatient basis. After variceal obliteration, surveillance endoscopy was performed at 6 months and then annually to identify patients in whom varices had recurred. Repeat ET was performed whenever residual or recurrent varices were identified during surveillance endoscopy. All patients in the ET group received oral propranolol twice a day, starting at 40 mg/day and increasing to a maximum of 120 mg/day, according to the target reduction of pulse rate.

### Statistical analysis

Collected data were coded, tabulated and analysed by the biomedical statistician using SPSS statistical software, version 19.0 for Windows. The results are presented in graphical, tabular and numerical form as mean + SD. Demographic data, laboratory values and other numerical data were analysed using descriptive statistics methods. To compare the two methods of treatment, t-test, $\chi$2-test and Mann-Whitney test were used. Data for prognostic factors of recurrent bleeding was analysed using multivariate logistic regression method. Cox proportional hazards regression model was used for the evaluation of prognostic factors of time to rebleeding. $P < 0.05$ was considered as statistically significant.

## Results

### Demographic, clinical and biochemical characteristics of the patients, prior inclusion in the study

Demographic, clinical and biochemical characteristics of the patients are shown in Table 1, as is aetiology of their liver disease. In the ET group of patients, leukocytes and urea values were significantly higher (P = 0.034 and P = 0.001, respectively; Mann-Whitney test) in comparison to those in TIPS group. Moreover, prothrombin time was significantly lower in ET group of patients (P = 0.003; Mann-Whitney test). There were no other statistically significant differences between the two groups.

### Follow-up observations

The median observation time was 47 months (range 3–194 months) in the TIPS group and 40 months

(range 2–168 months) in the ET group. The observation time for the survivours in the TIPS group (n = 20) was 57.65 months (median 38 months) and 42.65 months (median 32 months) in the ET group (n = 20).

## TIPS procedure

In 68 patients, the procedure was performed in general anaesthesia, and in two patients in the local anaesthesia. Wallstent (diameter 8–10 mm) was used in 48 patients and Viatorr-type endoprosthesis, 8–10 mm in diameter, 6–8 cm in length, in 22 patients. TIPS was dilated to 8 mm of diameter reaching the hemodynamic target of a portosystemic pressure gradient (PSG). In 9 patients, not reaching the hemodynamic target, the stent was dilated to 10 mm of diameter. After reaching a sufficient pressure reduction, which in our study was, on average, 35.9% lower than the baseline, the procedure was completed, and the manual haemostasis was made after removal of the vascular device from the jugular vein. The mean portal pressure prior to procedure was 29.32 ± 5.93 mmHg (range 20–45 mmHg) and 18.67 ± 4–22 mmHg (range 8–30 mmHg) after the procedure.

## Hepatic encephalopathy

Prior the study, 25.7% of patients in the TIPS group and 30.4% in the ET group had hepatic encephalopathy (HE). The difference between the groups was not statistically significant (P = 0.563; $\chi$2-test). At the end of the study, 42.8% of patients had hepatic encephalopathy in the TIPS group and 35.6% in the ET group. The difference between the groups was not statistically significant (P = 0.542; $\chi$2-test; p = 0.058; Wilcoxon test). In the TIPS group, 7.1% of patients with chronic hepatic encephalopathy and 8.9% in the ET group were present. The difference between groups was not statistically significant (P = 0.584; $\chi$2-test). 21.4% of patients treated with TIPS and 12.5% of patients treated with ET experienced new or worsening of pre-existing hepatic encephalopathy. The difference between the groups was not statistically significant (P = 0.150; $\chi$2-test). Only 14.3% of patients in the TIPS group and 11.1% of patients in the ET group had to be hospitalized due to HE.

## Liver transplantation

10 patients (14.3%) in the TIPS group and three patients (5.4%) in the ET group had liver transplantation. Statistically significant differences in the number of liver transplantations were not observed (P = 0.102; $\chi$2-test).

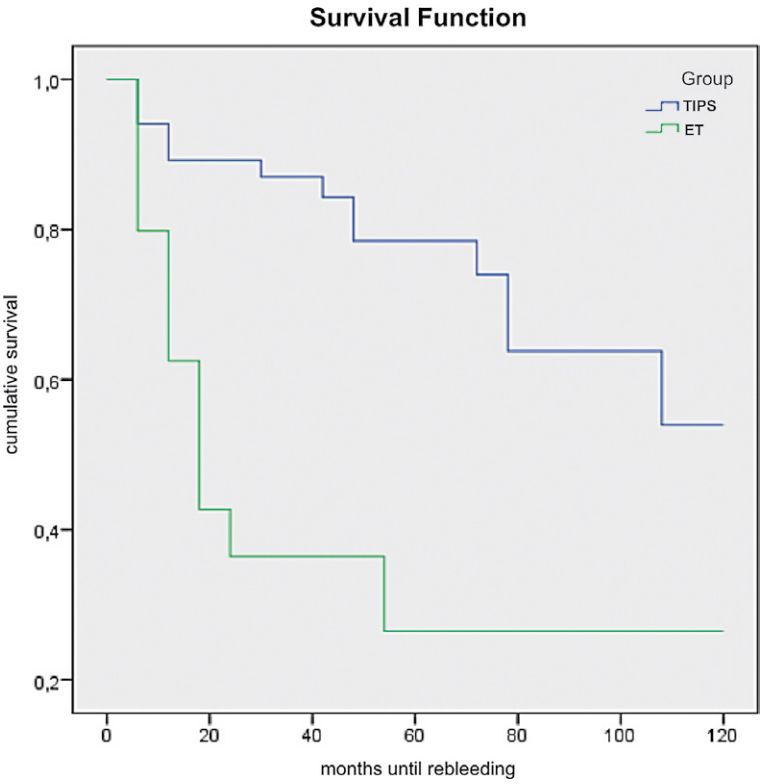


**FIGURE 1.** Proportion of patients without recurrent bleedings in the two groups.

ET = Endoscopic treatment; TIPS = Transjugular intrahepatic portosystemic shunt

## Recurrent bleeding

In the TIPS group, 15 (21.4%) patients developed recurrent bleeding episode from gastroesophageal varices; 1 patient had two episodes of bleeding. 33.3% of patients had recurrent bleeding within the first year and 46.6% within the first two years. In the ET group, 37 (66.1%) patients developed recurrent bleeding episode from gastroesophageal varices; 20 patients had several recurrent bleedings. 56.7% of patients had recurrent bleeding within the first year and 83.7% within the first two years. There were 63 recurrent bleeding episodes in the ET group. The difference in the number of patients with recurrent bleeding episodes was statistically significant (P = 0.001; $\chi$2-test). Most frequently, *i.e.* 11 of the 15 cases (73.3%), the recurrent bleeding in the TIPS group occurred due to shunt malfunction. In 3 TIPS patients, liver failure was the cause of the recurrent bleeding, and progression of HCC in 1 patient. In all those 4 patients, shunt malfunc-

**TABLE 2.** Predictive factors of recurrent bleeding in the two groups

| | P | OR | 95% CI for OR | |
|---|---|---|---|---|
| | value | | Lower | Upper |
| Treatment | 0.000[a] | 7.088 | 3.039 | 16.529 |
| Age > 60 years | 0.074 | 2.216 | 0.927 | 5.299 |
| Aetiology of liver cirrhosis | 0.382 | 0.656 | 0.255 | 1.688 |
| Child A | 0.716 | | | |
| Child B | 0.684 | 1.279 | 0.391 | 4.190 |
| Child C | 0.818 | 0.848 | 0.209 | 3.442 |
| Site of bleeding: *E* | 0.251 | | | |
| Site of bleeding: *G* | 0.097 | 3.089 | 0.815 | 11.712 |
| Site of bleeding: *E* + G | 0.857 | 1.103 | 0.381 | 3.190 |
| HE prior to procedure | 0.747 | 0.932 | 0.607 | 1.430 |

[a]P < 0.001

CI = confidence interval; ; E = esophagus; ET = endoscopic treatment; G = stomach; HE = hepatic encephalopathy; OR = odds ratio; TIPS = transjugular intrahepatic portosystemic shunt

**TABLE 3.** Cause of death of 86 patients in the two groups

| | TIPS | | ET | |
|---|---|---|---|---|
| | N = 50 | | N = 36 | |
| | N | % | N | % |
| Variceal bleeding | 7 | 10.0 | 16 | 28.6 |
| Liver failure | 22 | 31.4 | 12 | 21.4 |
| Sepsis | 1 | 1.4 | 0 | 0.0 |
| Pneumonia | 3 | 4.3 | 2 | 3.6 |
| Tumor progression | 6 | 8.6 | 1 | 1.8 |
| Accidental | 2 | 2.9 | 0 | 0.0 |
| Cardiovascular disease | 3 | 4.3 | 3 | 5.4 |
| Unknown | 6 | 8.6 | 2 | 3.6 |

ET = endoscopic treatment; TIPS = transjugular intrahepatic portosystemic shunt

tion was excluded using ultrasound. 11 patients with recurrent variceal bleeding due to shunt malfunction underwent esophagogastroduodenoscopy (EGDS), which confirmed esophageal variceal bleeding in 8 patients and gastric variceal bleeding in 3 patients. 6 of 11 shunt malfunctions were successfully repaired with an additional procedure, 5 of 11 patients died before the additional procedure.

The proportion of patients without recurrent bleedings after 6 months, 1 year, 2 years and 5 years in the TIPS group compared to the ET group was 89% *vs.* 63%; 89% *vs.* 43% ; 87% *vs.* 36% and 78% *vs.* 26% (Figure 1).

### Predictive factors of recurrent bleeding

Prognostic value of predictive factors of recurrent variceal bleeding was analysed using multivariate logistic regression method. Cathegorized variables, such as site ob bleeding and Child-Pugh classification for prognosis of chronic liver disease, were divided into three cathegories. Our study showed that only ET was a significant independent predictor of recurrent bleeding (P = 0.001). The odds ratio for recurrent bleeding in the ET group versus TIPS group was 7 (95% confidence interval [CI]; 3.0–16.5).

### Mortality due to recurrent bleeding

During our observation time, 50 (71.4%) patients died of various causes in the TIPS group and 36 (64.3%) in the ET group (Table 3). There were no statistically significant differences between the two groups (P = 0.392; $\chi$2-test). Mean survival time of the patients treated with TIPS was 64.38 ± 8.6 months and 50.4 ± 9.6 months of the patients who were treated with ET. The median survival time of patients in the TIPS group was 50.0 ± 5.2 months and 32.0 ± 7.4 months in the ET group. The leading cause of death in the group of patients treated with TIPS was liver failure (31.4% of the patients), and recurrent bleeding in the group of patients treated with ET (28.6% of the patients) (Table 3). The difference in the causes of recurrent bleeding between the two groups was statistically significant (P = 0.086; $\chi$2-test).

7 patients (10%) in the TIPS group died due to recurrent variceal bleeding; in 5 of those patients, recurrent bleeding was caused by shunt malfunction. Of those 5 patients, 2 patients died within 1 year; in total, 4 patients died within first 2 years. In the ET group, 8 (38.1%) of 21 patients with recurrent bleeding died within 1 year, and 16 (51.6%) of 31 patients within the first two years. Cumulative survival after 1 year, 2 years and 5 years in the TIPS group compared to the ET group was 85% *vs.* 83%, 73% *vs.* 67% and 41% *vs.* 35% (Figure 2).

## Discussion

Following the current guidelines for preventing recurrent gastroesophageal variceal bleeding, TIPS should not be used as a first-line treatment and should be limited to those bleedings, which are refractory to pharmacologic and endoscopic treatment.[3,4] This recommendation is mainly be-

cause the rate of hepatic encephalopathy is significantly higher in patients undergoing TIPS than in those receiving ET and NSBBs. Moreover, according to meta-analysis, deaths due to all causes do not differ between the two groups of patients.[11,16] Consequently, use of TIPS treatment has been limited worldwide in the last decade. However, in the present study, elective TIPS was found to be more effective than ET in terms of prevention of recurrent GEVB and was associated with a similar rate of encephalopathy, and with a similar survival rate which accords with the results of recently published studies.[5,15-18] These results were also in line with a meta-analysis that included mostly studies from 2000–2010.[19] So far, most evidence for the use of TIPS for secondary prevention of GEVB comes from randomized studies published between 1995 and 2002 with patient's follow-up period, on average 20 months (ranged from 15 to 37 months).[7-11] In twelve studies, patients were included in the study 24 hours to 96 hours from the last bleeding and only in one study two weeks after the last bleeding.[8] A meta-analysis of studies showed a small number of recurrent bleeding in the TIPS group (19%, range 9–40% *vs.* 44.4%, range 21–61% in the ET group). In these studies, they basically did not distinguish urgent TIPS from elective TIPS.

Studies which could evaluate the role of elective TIPS in comparison to ET in patients with recurrent variceal bleeding episodes are rare.[12] There is even fewer studies which could analyse the long-term effect of TIPS *vs.* ET.[13,14]

In our study, there was less recurrent bleeding episodes in the TIPS group of patients in comparison to the ET group of patients (21.4% *vs.* 66.1%, respectively), which accords with the results of previous comparable studies.[17-20] Most of the patients in our study had recurrent bleeding episode within the first two years (46.6% in the TIPS group *vs.* 83.7% in the ET group). Moreover, a total number of recurrent bleeding episodes (which required endoscopic intervention and hospitalization) was lower in the TIPS group; the difference between the two groups was statistically significant. Multivariate analysis identified ET as the only significant independent predictor of recurrent bleeding. The main advantage of TIPS procedure compared to ET seems to be due to the direct and controlled reduction of hepatic venous pressure gradient (HVPG) during procedure below the threshold value for variceal rupture and bleeding (*i.e.* < 12 mmHg) or ≥ 20% reduction of baseline HVPG value.[20,21] By reducing HVPG, we not only improve the rate of variceal rebleeding, but also reduce other complications of PH, such as ascites, and improve liver and kidney function. In our study, the mean reduction of HVPG was 35.9%. This correlates to previous studies, which showed that reducing HVPG > 20% below baseline value contributes to lower risk for recurrent bleeding, spontaneous bacterial peritonitis, ascites and death.[21] Reducing of HVPG is therefore crucial for higher quality and longer survival of patients with liver cirrhosis. There are also fewer recurrent bleeding episodes in patients who are treated with surgical portosystemic shunts, which correlates with our asumption of direct impact of reduced HVPG on the course of disease.[22] The recurrent bleeding in the TIPS group occurred most frequently due to shunt malfunction, and in more than half of patients, shunt malfunctions were successfully repaired with an additional balloon dilatation and stent or stent graft insertion. In the majority of patients, shunt malfunction was determined by Doppler ultrasound before the appearance of clinical signs. Fewer reintervention and rebleeding episodes were reported for studies where patients, as in the present study, had regular ultrasound monitoring.[23]

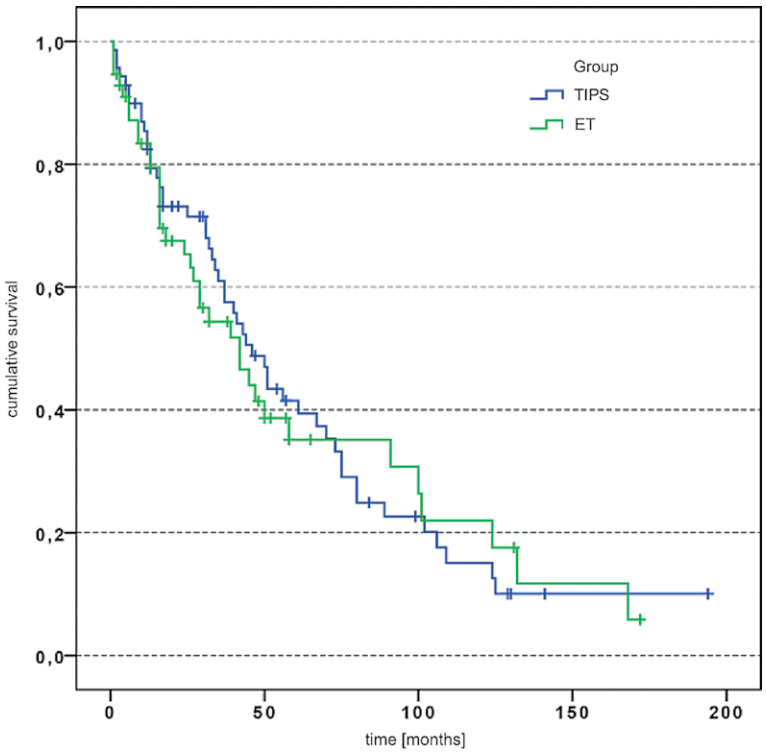


**FIGURE 2.** Survival curves for the two groups.

Kaplan-Meier curve. ET = Endoscopic treatment; TIPS = transjugular intrahepatic portosystemic shunt; N (TIPS) = 70; N (ET) = 56

Because rebleeding is associated with increased risk of mortality, preventing variceal rebleeding may be a substitute outcome of survival.[24-26] Based on our study, recurrent bleeding episode seems to be the leading cause of death in the ET group of patients and liver failure in the TIPS group of patients; differences were statistically significant (Table 3). Despite statistically significant lower mortality rate due to recurrent variceal bleeding episode in the TIPS group of patients, it did not result in improved long-term survival between the two groups. The TIPS group of patients had better 2-year survival rates, but the difference was not statistically significant. We assumed that other factors than rebleeding may have contributed to the observed mortality in both groups. Liver failure was the leading cause of death in patients who survived more than 2 years, which suggests that preserved liver function is the main predicting factor of long-term survival in patients with liver cirrhosis and portal hypertension, whereas occurrence of recurrent variceal bleeding only has a minor effect (5–10% based on our study).[17]

The incidence of hepatic encephalopathy before joining the study was the same in both groups and is comparable to literature.[14,27,28] Causes of the same frequency of HE are the most likely comparable clinical characteristics of patients prior to being included in the study: hemodynamically stable and under-conditions, patients with similar liver cirrhosis, the same number of patients with Child B and Child C hepatic impairment, and similar age of patients. Compared to previous studies, the incidence of HE in the TIPS group is lower in our study and slightly higher than in the ET control group, but the difference is not statistically significant, which accords with the results of comparable studies.[27,28]

Our study has limitations which have to be mentioned. First, the most important is its retrospective nature, so the analysis is subject to potential patient selection bias. Our data recording was limited to the available medical records and documentation, so we cannot exclude some degree of underreporting due to inherent limitations of non-standardized clinical documentations outside of clinical studies. Second, because the primary endpoint is variceal rebleeding, the power calculation is primarily based on a difference in the rate of variceal rebleeding between both groups. Thus, the data regarding mortality should not be overemphasized. Third, this study is being conducted in a single tertiary centre with the TIPS technique experience. Accordingly, our findings might not be promptly generalized to other centres with less experience. Fourth, treatment of GEVB has improved over the past few decades in all fields of medicine, including the treatment of complications of liver cirrhosis and portal hypertension, EVL and the use of endoprosthesis in the TIPS group in later years as compared to earlier years, when EST and stent were commonly used. Despite these limitations, there was a large number of patients enrolled in this study, and they were followed for a long time period. Acorrding to available international literature, our study was the longest in terms of observation time of both, TIPS and ET, groups of patients (median observation time 47 months for the TIPS group and 40 months for the ET group).

In conclusion, TIPS compared to ET in combination with NSBB was more effective in the prevention of recurrent gastroesophageal variceal bleeding, had significantly lower mortality due to recurrent variceal bleeding, but did not result in long-term survival benefit. The incidence of hepatic encephalopathy was similar in both groups. Liver failure was the leading cause of death in patients surviving more than 2 years, which suggests that preserved liver function is the main predicting factor of long-term survival, whereas occurrence of recurrent variceal bleeding only has a minor effect.

## References


1 Garcia-Tsao G, Sanyal AJ, Grace ND, Carey W. Prevention and management of gastroesophageal varices and variceal hemorrhage in cirrhosis. *Hepatology* 2007; **46:** 922-38. doi: 10.1002/hep.21907

2 Bandali MF, Mirakhur A, Lee EW, Ferris MC, Sadler DJ, Gray RR, et al. Portal hypertension: imaging of portosystemic collateral pathways and associated image-guided therapy. *World J Gastroenterol* 2017; **23:** 1735-46. doi: 10.3748/wjg.v23.i10.1735

3 Garcia-Tsao G, Abraldes JG, Berzigotti A, Bosch J. Portal hypertensive bleeding in cirrhosis: risk stratification, diagnosis, and management: 2016 practice guidance by the American Association for the study of liver diseases. *Hepatology* 2017; **65:** 310-35. doi: 10.1002/hep.28906

4 Boyer TD, Haskal ZJ. AASLD practice guidelines: the role of transjugular intrahepatic portosystemic shunt (TIPS) in the management of portal hypertension: update 2009. *Hepatology* 2010; **51:** 306. doi: 10.1002/hep.23383

5 Bucsics T, Schoder M, Diermayr M, Feldner-Busztin M, Goeschl N, Bauer D, et al. Transjugular intrahepatic portosystemic shunts (TIPS) for the prevention of variceal re-bleeding – a two decades experience. *PLoS One* 2018; **13:** e0189414. doi: 10.1371/journal.pone.0189414

6 Dariushnia SR, Haskal ZJ, Midia M, Martin LG, Walker TG, Kalva SP, et al. Quality improvement guidelines for transjugular intrahepatic portosystemic shunts. *J Vasc Interv Radiol* 2016; **27:** 1-7. doi: 10.1016/j.jvir.2015.09.018

7 Rössle M, Deibert P, Haag K, Ochs A, Olschewski M, Siegerstetter V, et al. Randomised trial of transjugular-intrahepatic-portosystemic shunt versus endoscopy plus propranolol for prevention of variceal rebleeding. *Lancet* 1997; **349:** 1043-9. doi: 10.1016/s0140-6736(96)08189-5

8 Merli M, Salerno F, Riggio O, de Franchis R, Fiaccadori F, Meddi P, et al. Transjugular intrahepatic portosystemic shunt versus endoscopic sclerotherapy for the prevention of variceal bleeding in cirrhosis: a randomized multicenter trial. *Hepatology* 1998; **27:** 48-53. doi: 10.1002/hep.510270109

9 Jalan R, Forrest EH, Stanley AJ, Redhead DN, Forbes J, Dillon JF, et al. A randomized trial comparing transjugular intrahepatic portosystemic stent-shunt with variceal band ligation in the prevention of rebleeding from esophageal varices. *Hepatology* 1997; **26:** 1115-22. doi: 10.1002/hep.510260505

10 Narahara Y, Kanazawa H, Kawamata H, Tada N, Saitoh H, Matsuzaka S, et al. A randomized clinical trial comparing transjugular intrahepatic portosystemic shunt with endoscopic sclerotherapy in the long-term management of patients with cirrhosis after recent variceal hemorrhage. *Hepatol Res* 2001; **21:** 189-98. doi: 10.1016/S1386-6346(01)00104-8

11 Zheng M, Chen Y, Bai J, Zeng Q, You J, Jin R, et al. Transjugular intrahepatic portosystemic shunt versus endoscopic therapy in the secondary prophylaxis of variceal rebleeding in cirrhotic patients. *J Clin Gastroenterol* 2008; **42:** 507-16. doi: 10.1097/MCG.0b013e31815576e6

12 Popovic P, Stabuc B, Skok P, Surlan M. Transjugular intrahepatic portosystemic shunt versus endoscopic sclerotherapy in the elective treatment of recurrent variceal bleeding. *J Int Med Res* 2010; **38:** 1121-33. doi: 10.1177/147323001003800341

13 Holster IL, Tjwa ETTL, Moelker A, Wils A, Hansen BE, Vermeijden JR, et al. Covered transjugular intrahepatic portosystemic shunt versus endoscopic therapy + β-blocker for prevention of variceal rebleeding. *Hepatology* 2016; **63:** 581-9. doi: 10.1002/hep.28318

14 Lv Y, Qi X, He C, Wang Z, Yin Z, Niu J, et al. Covered TIPS versus endoscopic band ligation plus propranolol for the prevention of variceal rebleeding in cirrhotic patients with portal vein thrombosis: a randomised controlled trial. *Gut* 2018; **67:** 2156-68. doi: 10.1136/gutjnl-2017-314634

15 Xue H, Zhang M, Pang JX, Yan F, Li YC, Lv LS, et al. Transjugular intrahepatic portosystemic shunt vs endoscopic therapy in preventing variceal rebleeding. *World J Gastroenterol* 2012; **18:** 7341-7. doi: 10.3748/wjg.v18.i48.7341

16 Bai M, Qi XS, Yang ZP, Wu KC, Fan DM, Han GH. EVS vs TIPS shunt for gastric variceal bleeding in patients with cirrhosis: a meta-analysis. *World J Gastrointest Pharmacol Ther* 2014; **5:** 97-104. doi: 10.4292/wjgpt.v5.i2.97

17 Zhang F, Zhuge Y, Zou X, Zhang M, Peng C, Li Z, et al. Different scoring systems in predicting survival in Chinese patients with liver cirrhosis undergoing transjugular intrahepatic portosystemic shunt. *Eur J Gastroenterol Hepatol* 2014; **26:** 853-60. doi: 10.1097/MEG.0000000000000134

18 Kim HK, Kim YJ, Chung WJ, Kim SS, Shim JJ, Choi MS, et al. Clinical outcomes of transjugular intrahepatic portosystemic shunt for portal hypertension: Korean multicenter real-practice data. *Clin Mol Hepatol* 2014; **20:** 18-27. doi: 10.3350/cmh.2014.20.1.18

19 Lin LL, Du S-M, Fu Y, Gu HY, Wang L, Jian ZY, et al. Combination therapy versus pharmacotherapy, endoscopic variceal ligation, or the transjugular intrahepatic portosystemic shunt alone in the secondary prevention of esophageal variceal bleeding: a meta-analysis of randomized controlled trials. *Oncotarget* 2017; **8:** 57399-408. doi: 10.18632/oncotarget.18143

20 Sauerbruch T, Mengel M, Dollinger M, Zipprich A, Rössle M, Panther E, et al. Prevention of rebleeding from esophageal varices in patients with cirrhosis receiving small-diameter stents versus hemodynamically controlled medical therapy. *Gastroenterology* 2015; **149:** 660-8. doi: 10.1053/j.gastro.2015.05.011

21 Addley J, Tham TC, Cash WJ. Use of portal pressure studies in the management of variceal haemorrhage. *World J Gastrointest Endosc* 2012; **4:** 281. doi: 10.4253/wjge.v4.i7.281

22 Clark W, Hernandez J, McKeon B, Villadolid D, Al-Saadi S, Mullinax J, et al. Surgical shunting versus transjugular intrahepatic portasystemic shunting for bleeding varices resulting from portal hypertension and cirrhosis: a meta-analysis. *Am Surg* 2010; **76:** 857-64. PMID: 20726417

23 Pereira K, Baker R, Salsamendi J, Doshi M, Kably I, Bhatia S. An approach to endovascular and percutaneous management of transjugular intrahepatic portosystemic shunt (TIPS) dysfunction: a pictorial essay and clinical practice algorithm. *Cardiovasc Intervent Radiol* 2016; **39:** 639-51. doi: 10.1007/s00270-015-1247-4

24 Garcia-Pagán JC, Di Pascoli M, Caca K, Laleman W, Bureau C, Appenrodt B, et al. Use of early-TIPS for high-risk variceal bleeding: results of a post-RCT surveillance study. *J Hepatol* 2013; **58:** 45-50. doi: 10.1016/j.jhep.2012.08.020

25 Qi X, Guo X, Fan D. A Trend toward the improvement of survival after TIPS by the use of covered stents: a meta-analysis of two randomized controlled trials. *Cardiovasc Intervent Radiol* 2015; **38:** 1363-4. doi: 10.1007/s00270-014-0996-9

26 Heinzow HS, Lenz P, Köhler M, Reinecke F, Ullerich H, Domschke W, et al. Clinical outcome and predictors of survival after TIPS insertion in patients with liver cirrhosis. *World J Gastroenterol* 2012; **18:** 5211-8. doi: 10.3748/wjg.v18.i37.5211

27 García-Pagán JC, Caca K, Bureau C, Laleman W, Appenrodt B, Luca A, et al. Early use of TIPS in patients with cirrhosis and variceal bleeding. *N Engl J Med* 2010; **362:** 2370-9. doi: 10.1056/NEJMoa0910102

28 Pereira K, Carrion AF, Salsamendi J, Doshi M, Baker R, Kably I. Endovascular management of refractory hepatic encephalopathy complication of transjugular intrahepatic portosystemic shunt (TIPS): comprehensive review and clinical practice algorithm. *Cardiovasc Intervent Radiol* 2016; **39:** 170-82. doi: 10.1007/s00270-015-1197-x

*research article*

# Analysis of emergency head computed tomography in critically ill oncological patients

Cristian Pristavu[1], Adrian Martin[1], Anca Irina Ristescu[1,2], Emilia Patrascanu[1,2], Laura Gavril[1,2], Olguta Lungu[1,2], Madalin Manole[1], Daniel Rusu[1], Ioana Grigoras[1,2]

[1] Anesthesia and Intensive Care Department, Regional Institute of Oncology, Iasi, Romania

[2] Anesthesia and Intensive Care Department, School of Medicine, "Grigore T. Popa" University of Medicine and Pharmacy, Iasi, Romania

Radiol Oncol 2021; 55(2): 172-178.

Received 14 December 2020
Accepted 21 February 2021

Correspondence to: Anca Irina Ristescu, M.D., Anesthesia and Intensive Care Department, Regional Institute of Oncology, General Henri Mathias Berthelot 2-4, Iasi 700483, Romania. E-mail: iristescu@yahoo.com anca.ristescu@umfiasi.ro

Disclosure: No potential conflicts of interest were disclosed.

**Background.** Critically ill cancer patients have an increased risk of developing acute neurological signs. The study objective was to evaluate the use and the usefulness of emergency head computed tomography (EHCT) in this category of patients.

**Patients and methods.** This retrospective, single-centre, cohort study included patients with EHCT performed during Intensive Care Unit (ICU) admission for a period of three years. Indications, imagistic findings, type of malignancy, and outcome were evaluated to identify diagnostic yield and correlations between abnormal findings on positive scans, malignancy type, and mortality rate.

**Results.** Sixty-four EHCTs were performed in 54 critically ill cancer patients, with 32 scans (50%) showing previously unknown lesions and considered to be positive. The most frequent abnormal findings were ischemic (15 EHCTs, 47%) and haemorrhagic (13 EHCTs, 40%) lesions. Thirty-eight EHCTs (59%) were indicated for altered mental status, with a positivity rate of 50%. Eighteen EHCTs (48%) were performed in hematological malignancy patients: 9 (50%) of which were positive with 8/9 (89%) displaying hemorrhagic lesions. Twenty EHCTs were performed in solid tumour patients, 10 (50%) of which were positive, with 9/10 (90%) displaying ischemic lesions. Out of 54 patients, 30 (55%) died during ICU stay. The mortality rate was higher in patients with hematological malignancies and positive EHCT (78% *vs*. 58%).

**Conclusions.** Diagnostic yield of EHCT in critically ill cancer patients is much higher than in other categories of ICU patients. We support the systematic use of EHCT in critically ill, mainly hemato-oncological patients with nonspecific neurological dysfunction, as it may lead to early identification of intracranial complications.

Key words: emergency head CT; altered mental status; cancer; critically ill; neurological complications

## Introduction

Acute neurological dysfunction is common in patients admitted to the Intensive Care Unit (ICU) with a wide spectrum of neurological findings including depressed consciousness, delirium, seizures and focal neurological signs.[1] Underlying etiologies include, but are not limited to, stroke (due to hemodynamic instability and coagulation abnormalities), use of sedative drugs, systemic inflammatory response and metabolic and endocrine disturbances.[2]

Emergency head computed tomography (EHCT) is often performed in critically ill patients to investigate neurologic signs and symptoms, such as focal neurologic deficits and seizure activity. The utility of imaging for patients who develop nonspecific altered mental status (AMS) is unclear.[3] AMS is a broad term, and can imply either change in consciousness (supratentorial function) or in

arousal (executed by the brainstem). Underlying etiologies include both systemic and central nervous system processes, the latter encompassing both organic and functional causes. The complex differential diagnosis can make AMS a potentially vexing clinical problem.[4]

Obviously, EHCT can provide important information for patient management, but in critically ill patients there are risks associated with transport and examination.[3] In addition, the financial expenses of possible unnecessary testing should also be taken into consideration.[5] Therefore, an EHCT request in an ICU patient should be carefully assessed, in order to decide if the potential benefits outweigh the risks.

Studies on head CTs use and appropriateness in critically ill medical and surgical patients were previously conducted, to assess the usefulness of clinical variables in selecting patients to be scanned[2,6,7] or to provide estimates of the frequency of acute changes on head CTs and therefore, their diagnostic yield.[3,8-10]

Critically ill oncological patients have an increased risk of developing acute neurological dysfunction due to several reasons. Sepsis is the most frequent cause of ICU admission in oncological patients; therefore, septic encephalopathy is common. Multiple organ dysfunction increases the risk for metabolic neurological dysfunction related to renal, hepatic or electrolytic disturbances. Thrombocytopenia and coagulation abnormalities predispose to intracranial bleeding. Central nervous system metastasis/infiltration by malignant cells may be present. The differential diagnosis of putative processes is challenging in these complex circumstances.

Therefore, the primary aim of this study was to evaluate EHCT diagnostic yield in a cohort of oncological patients treated in a mixed, non-neurosurgical ICU. Furthermore, we evaluated the distribution of positive EHCT according to the type of malignancy (hematological or solid tumour) and the relationship between positive EHCT and clinical indications. Finally, we evaluated the patients' outcomes related to their EHCT results.

## Patients and methods

### Study design

The study was performed in the Regional Institute of Oncology, Iasi, Romania, a 300-bed teaching hospital providing all types of antineoplastic treatment (surgery, chemo-, radio-, hormone- and immunotherapy). Neurosurgery is not performed in our institution; thus, the cohort of oncological patients did not include neurosurgical patients, who have specific indications for EHCT.

This retrospective, single-centre, cohort study included all patients admitted to our 11-beds ICU for a period of 3 years, with at least one EHCT performed during ICU admission, as indicated by the intensivist/neurologist. The medical charts of the included patients were reviewed. The scanned patients were identified using the Radiology and Imaging Department records. Data were extracted from electronic medical records, CT reports, CT scan request forms and ICU charts. We extracted demographic information, comorbidities, risk factors for stroke, hospital/ICU admission/discharge data, ICU admission diagnosis, type of malignancy (hematological or solid tumour), clinical indication for EHCT, contrast or non-contrast agent EHCT, platelet count and coagulation profile, and outcome.

### Indications for EHCT

We assessed the indications for EHCT using the CT request forms and relevant physician notes in the ICU charts. Head CT exclusion criteria included indications related to craniofacial cancers (diagnostic or follow-up CT); head trauma during hospitalisation (e.g., falling from the same level during a syncopal state); missing information about the clinical indication; and missing CT report. One head CT was also excluded due to a massive lung bleeding, so the scan could not be completed.

Indications of EHCT were recorded as: (1) AMS, (2) focal neurologic deficit (FND), (3) seizure activity, or (4) other. AMS was defined as an alteration in consciousness or cognition documented in the charts as assessed by clinical examination. FND was identified by screening patients' medical charts for key phrases within the documentation of neurologic examinations performed by ICU physicians or neurology consultants. These key phrases indicative for neurologic abnormalities: new cranial nerve deficit, motor or sensory unilateral limb deficit or reflex abnormalities. Seizure activity was also identified during the review of charts. Other CT scan indications included persistent headache, re-evaluation after a previous scan, or post-anoxic encephalopathy. For patients who had more than one indication for EHCT, all were recorded in our database. Also, multiple scans for the same patient during the ICU stay were introduced in the database alongside the recorded clinical indications.

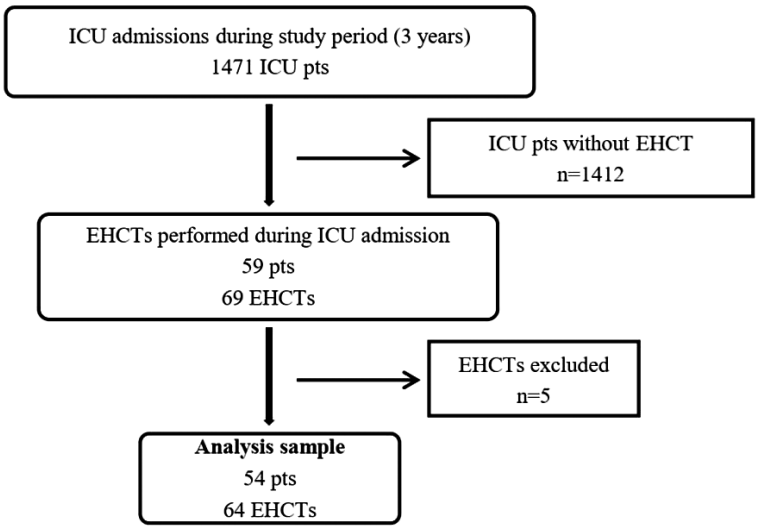


**FIGURE 1.** Study flowchart.

### Interpretation of head CTs

All the EHCTs were interpreted by radiologists from the Radiology and Imaging Department. The CT reports were retrospectively scored as positive or negative by the study team. A positive EHCT was defined as one that found any previously unknown intracranial abnormality that could correlate with the clinical indication. All hemorrhagic lesions (intracerebral, subarachnoid, and intraventricular hemorrhage) were counted as „intracranial hemorrhagic lesions". Also, concomitant lesions on the same CT scan were counted, so abnormal findings consequently outnumbered positive EHCTs.

### Statistical analysis

Data were analyzed using MedCalc Statistical Software version 19.1.7 (MedCalc Software Ltd, Ostend, Belgium; https://www.medcalc.org; 2020). Variables distribution assumptions were tested for normality using histograms and the Shapiro-Wilk test. Comparisons between normally distributed continuous variables were performed using Student's t-test. Comparisons between non-normally distributed continuous variables were performed using the Mann-Whitney U-test. Comparisons between categorical variables were performed using the Chi-squared test or Fisher's exact test.

Categorical variables were presented as number (n) and percentage (%). Continuous variables were presented as mean and standard deviation (SD) if normally distributed, or as median and interquartile range (IQR) if non-normally distributed.

### Ethical issues

The study was approved by the Research Ethics Committee of the Regional Institute of Oncology Iasi. Being a retrospective study, an informed consent waiver was issued.

## Results

### Study group

A total of 1471 patients from three hospital departments, namely: Oncological Surgery, Oncology, and Hematology, were admitted to ICU during the study period. These patients were mostly men (55%), with a mean age of 63.0 ± 12.5 years, and 522/1471 (35.5%) had hematological malignancies. The median ICU length of stay (LOS) was 6.5 (3–9) days, 400 patients (27.2%) died during their ICU hospitalization.

In the study period 69 head CT scans were performed for 59 ICU patients, representing 4% of ICU-admitted patients. Five head CTs performed for five patients were excluded for reasons mentioned above. At the end, the analysis sample included 64 EHCTs for 54 ICU patients (Figure 1). Intravenous contrast agent was used in 39 (57%) EHCTs in 34 (63%) patients, according to clinical indications and patient comorbidities (e.g., renal failure).

The EHCT patients had similar characteristics in terms of gender, age, and malignancy type distribution to the whole group of ICU-admitted patients. The median ICU LOS of EHCT patients was higher than the general median ICU LOS (10.5 *vs*. 6.5 days). The ICU mortality of EHCT patients was twice the general ICU mortality (55% *vs*. 27.2%), (Table 1).

### Indications for EHCT

Out of 64 EHCTs, 18 (28%) had more than one clinical indication. Thirty-eight scans (59%) were indicated for AMS, 21 (32%) for FND and 7 (11%) for seizure. As expected, the proportion of positive EHCTs indicated for FND (13/21, 62%) and for seizure (5/7, 71%) was higher than the proportion of positive EHCTs indicated for AMS (19/38, 50%). The number of positive EHCTs indicated for other reasons was significantly lower (3/16, 18%), (Table 2).

### Positive EHCT

In the group with positive EHCT, 24 (44%) out of 54 patients had previously unknown lesions (Table 1). When analyzing positive EHCTs, 32 (50%) scans out of 64, showed previously unknown lesions (Table 2).

### Abnormal findings on positive EHCT

When analyzing the positive EHCTs, the abnormal findings were: ischemic lesions, intracranial hemorrhagic lesions, cerebral oedema, brain metastases, leukemic infiltration, arteriovenous brain malformation, solid tumours, and hydrocephalus (Table 2). Abnormal findings with the highest frequencies were ischemic and hemorrhagic lesions. Their distributions were further analyzed according to EHCT indications (Table 3).

Because AMS was the most frequent nonspecific indication for scanning, we analyzed abnormal findings on EHCT performed for this indication. Out of 38 scans indicated for AMS, 18 (48%) were performed in hematological patients: 9 (50%) of which were positive, with 8/9 (89%) hemorrhagic and 2/9 (21%) ischemic lesions. In 18 patients with solid tumours, 20 EHCTs were performed for AMS, and 10 (50%) of which were positive 9/10 (90%) were ischemic and 2/10 (20%) displayed hemorrhagic lesions.

### Outcome

Out of 54 patients, 30 (55%) died during ICU hospitalization. The mortality was similar in patients with positive (58%) *vs.* negative (53%) EHCT, but higher in patients with hematological malignancies and positive EHCT *vs.* negative EHCT (7/9, 78% respectively 7/12, 58%), (Table 4).

Twenty-two out of 30 patients (73%) with EHCT indicated for AMS died in the ICU. The mortality of haematological patients with AMS was higher for positive (6/7, 85%) than negative (6/9, 67%) EHCTs, (Table 5).

## Discussions

Our study showed a high rate of newly diagnosed intracranial processes by EHCT in a cohort of non-neurosurgical oncological patients admitted to ICU for non-neurological reasons. Exclusion of neurosurgical patients is worth mentioning, because this class of patients demands more scans for diagnosis and follow-up, usually with a higher probability of positive findings.

The main indications for EHCTs in our study were FND/seizure. Analyzing the newly diagnosed

**TABLE 1.** Characteristics of EHCT patients

| Variables | Overall (*n* = 54) | (+) EHCT (*n* = 24) | (-) EHCT (*n* = 30) | *p* value |
|---|---|---|---|---|
| Age | 61 (12.7) | 62 (13.2) | 60 (12.4) | 0.74 |
| Gender | | | | |
| Male | 28 (51.9) | 16 (67.7) | 12 (40.0) | 0.05 |
| Female | 26 (48.1) | 8 (33.3) | 18 (60.0) | |
| Malignancy type | | | | |
| Solid tumour | 33 (61.1) | 15 (62.5) | 18 (60.0) | 0.85 |
| Haematological malignancy | 21 (38.9) | 9 (37.5) | 12 (40.0) | |
| Outcome | | | | |
| ICU LOS | 10.5 (6–14) | 8.5 (4–11) | 12.5 (7–15) | 0.03 |
| Hospital LOS | 18 (12–30) | 15.5 (10–26) | 20.0 (14–34) | 0.10 |
| ICU mortality | 30 (55.6) | 14 (58.3) | 16 (53.3) | 0.71 |

Variables are presented as number (%), mean (standard deviation [SD]) or median (interquartile range [IQR]).

EHCT = emergency head computed tomography; ICU = Intensive Care Unit; LOS = length of stay; *n* = number

**TABLE 2.** Characteristics of ECHTs

| Variables | EHCT (*n* = 64) | (+) EHCT (*n* = 32) | (-) EHCT (*n* = 32) | *p* value |
|---|---|---|---|---|
| **Indications** | | | | |
| Altered mental status | 38 (59.4) | 19 (59.4) | 19 (59.4) | 1.00 |
| Focal neurological deficits | 21 (32.8) | 13 (40.6) | 8 (25.0) | 0.27 |
| Seizures | 7 (10.9) | 5 (15.6) | 2 (6.2) | 0.26 |
| Other | 16 (25.0) | 3 (9.4) | 13 (40.6) | < 0.01 |
| **Results** | | | | |
| Ischemic stroke | 15 (23.4) | 15 (46.9) | | |
| Haemorrhagic lesions | 13 (20.3) | 13 (40.6) | | |
| Cerebral oedema | 10 (15.6) | 10 (31.2) | | |
| Brain metastases | 5 (7.8) | 5 (15.6) | | |
| CNS infiltrates | 1 (1.6) | 1 (3.1) | | |
| Arterio-venous malformation | 2 (3.1) | 2 (6.2) | | |
| Hydrocephalus | 1 (1.6) | 1 (3.1) | | |
| Primary brain tumour | 2 (3.1) | 2 (6.2) | | |

Variables are presented as number (%).

EHCT = emergency head computed tomography; n = number

**TABLE 3.** Distribution of ischemic and haemorrhagic lesions according to EHCTs indications

| Indications for EHCT | (+) EHCT (*n* = 32) | Ischemic stroke (*n* = 15) | Haemorrhagic lesions (*n* = 13) | *p* value |
|---|---|---|---|---|
| Altered mental status | 19 (59.4) | 11 (28.9) | 10 (26.3) | 0.80 |
| Focal neurological deficits | 13 (40.6) | 5 (23.8) | 6 (28.6) | 0.73 |
| Seizures | 5 (15.6) | 1 (14.3) | 1 (14.3) | - |
| Other | 3 (9.4) | 1 (6.2) | 0 (0.0) | - |

Variables are presented as number (%).

EHCT = emergency head computed tomography; n = number

**TABLE 4.** Mortality in patients with positive and negative EHCTs

| Patients | Total | Solid tumours | Haematological tumours |
|---|---|---|---|
| EHCT+, all | 24 | 15 | 9 |
| EHCT+, dead (%) | 14 (58) | 7 (46) | 7 (78) |
| EHCT-, all | 30 | 18 | 12 |
| EHCT-, dead (%) | 16 (53) | 9 (50) | 7 (58) |

EHCT = emergency head computed tomography

**TABLE 5.** Mortality in patients with positive and negative EHCTs indicated for AMS

| Patients with AMS | Total | Solid tumours | Haematological |
|---|---|---|---|
| AMS & EHCT+, all | 13 | 6 | 7 |
| AMS & EHCT+, dead (%) | 10 (76) | 4 (67) | 6 (85) |
| AMS & EHCT-, all | 17 | 8 | 9 |
| AMS & EHCT-, dead (%) | 12(70) | 6 (75) | 6 (67) |

AMS = altered mental status; EHCT = emergency head computed tomography

intracranial processes, we found a higher rate of hemorrhagic lesions in hematological patients and ischemic lesions in solid tumour patients. All patients were undergoing antineoplastic treatment at the time of ICU admission, i.e.: chemotherapy for hematological patients and chemotherapy, radiotherapy, or surgery for patients with solid tumours. Along with other recognized risk factors specific for critical illness (e.g., septic encephalopathy, residual sedation, immobilization, comorbidities), antineoplastic treatment adds to risk factors for neurological complications. Hematologic malignancies and chemotherapy usually lead to thrombocytopenia and coagulation disorders, predisposing to intracranial bleeding. On the other hand, inflammation associated with antineoplastic treatments in solid tumours significantly increases ischemic risk in patients who already have a procoagulant status. These features explain the distribution pattern of abnormal radiologic findings among patients and seem to be related to their outcomes.

ICU physicians are often faced with the dilemma of selecting the most appropriate diagnostic test for their patients. CT is widely used in critically ill patients due to its availability, accessibility, no need for compatible devices, and shorter duration, and is indicated for many clinical reasons in a wide range of suspected pathology.[10] Cerebral magnetic resonance imaging (MRI) is a superior diagnostic tool for critically ill patients with neurological disturbances. Compared with CT, MRI has an increased diagnostic sensitivity for acute stroke, neoplasms, infections and encephalopathy due to hypoxia, sepsis, uremia, hyperammonemia, glucose and sodium abnormalities.[12] Comparing CT and MRI performed in critically ill patients during the same ICU admission, the MRI diagnostic yield was better by 33%, but changed the CT based working diagnosis for only 4.4% of patients.[11] In addition, MRI has numerous safety challenges in ICU patients, the particular one being the need for MRI-compatible monitoring and life-support equipment. Considering the risk-benefit ratio, MRI indications in critically ill patients should probably include request for additional assessment of CT findings and evaluation of patient with persistent neurologic symptoms despite a normal/equivocal CT.

The associated risks and costs of every investigation must be weighed against the failure of a correct diagnosis. Moreover, in oncological patients, it is difficult to keep a good balance between under- and over-imaging, mainly in the case of non-specific clinical signs. Our results support the need for systematic EHCT in the subgroup of critically ill hemato-oncological patients with AMS.

In our study, we recorded very low scanning rates when compared to published data (4% *vs.* 10.7–33%).[2,3,7,9,12] There are several explanations for this seemingly under-investigation. In contrast to other published studies, we analyzed only EHCTs indicated during ICU stay in oncological patients admitted with non-neurological diagnosis. Namely, we analyzed only EHCTs that were indicated for new neurological signs developed during ICU admission. The high risks associated with transport and CT examination in unstable oncological pa-

tients should be weighed against the benefits in terms of prognosis and therapeutic options.

Complications involving the central nervous system are frequently encountered in critically ill patients. In the literature, when present, they nearly double the risk of ICU mortality (55% *vs*. 28.5% in patients without neurological complications).[13] Similarly, in our study, the outcomes of patients with EHCTs were worse than of patients without brain scans, thus, without neurological impairment.

We found that half of the EHCTs were positive, which was higher than reported by other published retrospective studies (8%–37%).[2,3,7-10] This difference can be explained by the above mentioned study design specificities.

Beyond the number of positive EHCTs, it is worth analyzing their distribution according to clinical indication. The occurrence of FND or seizures is an undisputable EHCT indication. Whether new AMS requires EHCT is debatable. In critically ill patients, AMS is a frequent condition and could indicate an acute intracranial process, but much more commonly is the consequence of systemic conditions (e.g., medications and their interactions, metabolic impairments, sepsis, renal, hepatic, or electrolytic disturbances). Therefore, AMS is probably becoming an important topic in research: two recent studies[8,10] included only patients with AMS, while another two[3,7] found AMS to be the clinical indication in 70% and 88% of cases (though with a lower rate of positive CTs, in 7.5% and 22.8% cases, respectively). Critically ill oncological patients have certain particularities, with sepsis being the most common cause of ICU admission; this increases both the probability of septic encephalopathy and the risk of acute intracranial processes. Hemato-oncology patients are often admitted with severe neutropenia and thrombocytopenia and represent a specific subgroup due to their extremely high risk of septic, hemorrhagic and/or ischemic complications. Brain metastases or leukemic infiltration, which are associated with cerebral oedema, may also be present. These conditions make it difficult to assess the risks and benefits correctly in critically ill haemato-oncological patients. Our data revealed a higher probability of abnormal findings on scans performed for AMS in oncological ICU patients, suggesting that physicians should have a low threshold indicating EHCT for this group.

In the present study, the two main changes identified using CT were acute ischemic and hemorrhagic lesions. While the prevalence of ischemic stroke was comparable with literature data (25–62%)[10,12], the prevalence of hemorrhagic lesions was close to the highest percentage reported (40%).[10,12] Limited published data in critically ill cancer patients indicate that approximately 18%, who underwent brain CT for acute neurologic symptoms and signs, had intracranial hemorrhage.[13]

EHCT and positive EHCT indicated for AMS show similar distribution between hematological and solid tumours. For positive EHCT, the type of newly occurred intracranial processes varies greatly between hematological (mainly hemorrhagic lesions) and solid tumour patients (mainly ischemic lesions). This distribution pattern could be explained by the risk factors mentioned above.

In EHCT studied patients, we recorded a doubled mortality rate compared with the general mortality in ICU patients. However, the mortality rate in positive and negative EHCT patients was similar. In hematological patients, the difference in mortality was recorded between positive and negative EHCT, with higher values for those with AMS as the clinical indication. The mortality of our patients with intracranial hemorrhage was in line with that reported in other studies on critically ill cancer patients (78%)[14] and in hospitalized non-oncological patients (81%).[15,16]

Several limitations of our study should be highlighted. Being a retrospective study, all data were collected from patients' files, which could have led to missed or incomplete information. The cohort size might be considered another limitation, as our study group was smaller than others.[2,3,6,7,9] While the cited studies were conducted on medical, surgical, or mixed ICU patients with or without previous neurological pathology, we included only critically ill oncological patients with new neurological signs occurring during ICU admission. Also, only a fraction of the EHCT performed in our patients were contrast-enhanced due to various contraindications.

## Conclusions

In oncological critically ill patients, the diagnostic yield of EHCT is much higher than in other categories of ICU patients. AMS, a clinical sign usually produced by multiple causes, should be a red flag announcing the presence of a new intracranial pathologic process in this specific group of patients. The results of our study support the systematic use of EHCT examination for emerging AMS, as it may identify intracranial complications early, particularly bleeding in hemato-oncological patients.

## Author contributions

*Conceptualization:* Cristian Pristavu, Irina Ristescu, Madalin Manole, Ioana Grigoras. *Data curation:* Cristian Pristavu, Adrian Martin. *Formal analysis:* Cristian Pristavu, Madalin Manole. *Investigation:* Cristian Pristavu. *Methodology:* Cristian Pristavu, Adrian Martin, Irina Ristescu, Emilia Patrascanu, Laura Gavril, Olguta Lungu, Madalin Manole, Ioana Grigoras. *Resources:* Cristian Pristavu. *Software:* Daniel Rusu, Cristian Pristavu. *Supervision:* Ioana Grigoras. *Writing – original draft:* Cristian Pristavu. *Writing-review & editing:* Cristian Pristavu, Adrian Martin, Irina Ristescu, Emilia Patrascanu, Laura Gavril, Olguta Lungu, Madalin Manole, Daniel Rusu, Ioana Grigoras.

## References


1. Stevens RD, Nyquist PA. Coma, delirium, and cognitive dysfunction in critical illness. *Crit Care Clin* 2006; **22:** 787-804. doi: 10.1016/j.ccc.2006.11.006
2. Salerno D, Marik PE, Daskalakis C, Kolm P, Leone F. The role of head computer tomographic scans on the management of MICU patients with neurological dysfunction. *J Intensive Care Med* 2009; **24:** 372-5. doi: 10.1177/0885066609344940
3. Khan S, Guerra C, Khandji A, Bauer RM, Claassen J, Wunsch H. Frequency of acute changes found on head computed tomographies in critically ill patients: a retrospective cohort study. *J Crit Care* 2014; **29:** 884.e7-12. doi: 10.1016/j.jcrc.2014.05.001
4. Uzelac A. Imaging of altered mental status. *Radiol Clin North Am* 2020; **58:** 187-97. doi: 10.1016/j.rcl.2019.08.002
5. Cassel CK, Guest JA. Choosing wisely: helping physicians and patients make smart decisions about their care. *JAMA* 2012; **307:** 1801-2. doi: 10.1001/jama.2012.476
6. Rafanan AL, Kakulavar P, Perl J, Andrefsky JC, Nelson DR, Arroliga AC. Head computed tomography in medical intensive care unit patients: clinical indications. *Crit Care Med* 2000; **28:** 1306-9. doi: 10.1097/00003246-200005000-00008
7. Mehta A, Khirfan G, Shah P, Wiles S, Moghekar A, Narechania S, et al. Scanning the confusion away: The diagnostic utility of head computer tomography (CT) in the evaluation of altered mental status in a non-neurological medical ICU of a tertiary care center. *Chest* 2016; **150:** 289A. doi: 10.1016/j.chest.2016.08.302
8. Finkelmeier F, Walter S, Peiffer KH, Cremer A, Tal A, Vogl T, et al. Diagnostic yield and outcomes of computed tomography of the head in critically ill nontrauma patients. *J Intensive Care Med* 2019; **34:** 955-66. doi: 10.1177/0885066617720901
9. Chokshi FH, Sadigh G, Carpenter W, Kang J, Duszak R, Khosa F. Altered mental status in ICU patients: diagnostic yield of noncontrast head CT for abnormal and communicable findings. *Crit Care Med* 2016; **44:** e1180–5. doi: 10.1097/CCM.0000000000002005
10. Gadde JA, Weinberg BD, Mullins ME. Neuroimaging of patients in the intensive care unit: Pearls and pitfalls. *Radiol Clin North Am* 2020; **58:** 167-85. doi: 10.1016/j.rcl.2019.08.003
11. Algethamy HM, Alzawahmah M, Young GB, Mirsattari SM. Added value of MRI over CT of the brain in intensive care unit patients. *Can J Neurol Sci* 2015; **42:** 324-32. doi: 10.1017/cjn.2015.52
12. Hijazi Z, Lange P, Watson R, Maier AB. The use of cerebral imaging for investigating delirium aetiology. *Eur J Intern Med* 2018; **52:** 35-9. doi: 10.1016/j.ejim.2018.01.024
13. Rubinos C, Ruland S. Neurologic complications in the intensive care unit. *Curr Neurol Neurosci Rep* 2016; **16:** 57. doi: 10.1007/s11910-016-0651-8
14. Ryu JA, Lee D, Yang JH, Chung CR, Park CM, Suh GY, et al. Spontaneous intracranial haemorrhage in critically ill patients with malignancies. *Support Care Cancer* 2016; **24:** 2971-8. doi: 10.1007/s00520- 016-3094-5
15. Loggini A, Del Brutto VJ, El Ammar F, Bulwa ZB, Saleh Velez F, McKoy C, et al. Intracranial hemorrhage in hospitalized patients: an infrequently studied condition with high mortality. *Neurocrit Care* 2020; **33:** 725-31. doi: 10.1007/s12028-020-00946-y
16. Owattanapanich W, Auewarakul CU. Intracranial hemorrhage in patients with hematologic disorders: prevalence and predictive factors. *J Med Assoc Thai* 2016; **99:** 15-24. PMID: 27455820

*research article*

# The role of polymorphisms in glutathione-related genes in asbestos-related diseases

Alenka Franko[1,2], Katja Goricar[3], Metoda Dodic Fikfak[1,2], Viljem Kovac[2,4], Vita Dolzan[3]

[1] Clinical Institute of Occupational Medicine, University Medical Centre Ljubljana, Ljubljana, Slovenia
[2] Faculty of Medicine, University of Ljubljana, Ljubljana, Slovenia
[3] Pharmacogenetics Laboratory, Institute of Biochemistry and Molecular Genetics, Faculty of Medicine, University of Ljubljana, Ljubljana, Slovenia
[4] Institute of Oncology Ljubljana, Ljubljana, Slovenia

Radiol Oncol 2021; 55(2): 179-186.

Received 9 November 2020
Accepted 2 December 2020

Correspondence to: Prof. Vita Dolžan, M.D., Ph.D., Pharmacogenetics Laboratory, Institute of Biochemistry and Molecular Genetics, Faculty of Medicine, University of Ljubljana, Vrazov trg 2, SI-1000 Ljubljana, Slovenia; Phone +386 1 543 76 70; GSM: +386 51 625 455; Fax: + 386 1 543 76 41; E-mail: vita.dolzan@mf.uni-lj.si

Disclosure: No potential conflicts of interest were disclosed.

**Background.** The study investigated the influence of *GCLC, GCLM, GSTM1, GSTT1* and *GSTP1* polymorphisms, as well as the influence of interactions between polymorphism and interactions between polymorphisms and asbestos exposure, on the risk of developing pleural plaques, asbestosis and malignant mesothelioma (MM).

**Subjects and methods.** The cross sectional study included 940 asbestos-exposed subjects, among them 390 subjects with pleural plaques, 147 subjects with asbestosis, 225 subjects with MM and 178 subjects with no asbestos-related disease. *GCLC* rs17883901, *GCLM* rs41303970, *GSTM1* null, *GSTT1* null, *GSTP1* rs1695 and *GSTP1* rs1138272 genotypes were determined using PCR based methods. In statistical analysis, logistic regression was used.

**Results.** *GSTT1* null genotype was associated with the decreased risk for pleural plaques (OR = 0.63; 95% CI = 0.40–0.98; p = 0.026) and asbestosis (OR = 0.51; 95% CI = 0.28–0.93; p = 0.028), but not for MM. A positive association was found between *GSTP1* rs1695 AG + GG *vs*. AA genotypes for MM when compared to pleural plaques (OR = 1.39; 95% CI = 1.00–1.94; p = 0.049). The interactions between different polymorphisms showed no significant influence on the risk of investigated asbestos-related diseases. The interaction between *GSTT1* null polymorphism and asbestos exposure decreased the MM risk (OR = 0.17; 95% CI = 0.03–0.85; p = 0.031).

**Conclusions.** Our findings suggest that *GSTT1* null genotype may be associated with a decreased risk for pleural plaques and asbestosis, may modify the association between asbestos exposure and MM and may consequently act protectively on MM risk. This study also revealed a protective effect of the interaction between *GSTP1* rs1695 polymorphism and asbestos exposure on MM risk.

Key words: polymorphisms; glutathione-related genes; asbestos; asbestosis; pleural plaques; malignant mesothelioma

## Introduction

Asbestos exposure, which still represents an important health problem worldwide, is known to be associated with the development of asbestos-related diseases, including benign pleural diseases (e.g. pleural plaques), asbestosis, lung cancer, malignant mesothelioma (MM) and other types of cancer.[1,2] The pathogenesis of asbestos-related diseases is complicated and not entirely elucidated. Nevertheless, numerous studies have suggested that in addition to a direct mechanical injury, asbestos may stimulate the production of reactive oxygen and nitric species (ROS and RNS) that were shown to have an important role in the pathogenesis of these diseases. ROS and RNS may cause

asbestos-related lung injury, DNA strand breaks in mesothelial cells and may increase the risk for developing malignancy.[3-5]

To detoxify ROS and consequently prevent the adverse effects of oxidative stress, the human organism possesses antioxidant defence systems. Glutathione (GSH), a tripeptide composed from glutamic acid, cysteine and glycine, is an abundant cellular antioxidant which has a major role in the protection against oxidative injury in cells. It serves as a substrate of many antioxidative enzymes.[6,7] The antioxidant capacity of the glutathione system depends on enzymes involved in its biosynthesis, such as glutamate cysteine ligase (GCL), also known as gamma glutamylcysteine synthetase, as well as on detoxification enzymes, such as glutathione S-transferases (GSTs).[6,8-10]

GCL is the rate limiting enzyme of the GSH synthesis and it is suggested to be the major factor that determines GSH level in healthy subjects. The enzyme consists of two subunits: a heavy catalytic subunit (GCLC) and a light modifier subunit (GCLM).[6,10] High GSH concentration levels found in many tumors have been associated with the increased GCL activity.[11,12]

GSTs are phase II detoxifying enzymes involved in the inactivation of the electrophiles produced by ROS and RNS by catalyzing the conjugation of electrophilic compounds with reduced glutathione.[8,9] In mammals, seven classes of cytosolic GST isoenzymes have been recognized: Alpha, Mu, Pi, Sigma, Theta, Omega and Zeta.[13] The crucial GST enzyme in the human lung, which belongs to the Pi class, is GSTP1.[14,15] Two other important polymorphic GSTs are GSTM1 (Mu class) and GSTT1 (Theta class).[15,16]

Genes coding for GSH related enzymes are polymorphic. Among the most commonly investigated promoter polymorphisms of the *GCLC* and *GCLM* genes are *GCLC* rs17883901 (c.-129C>T) and *GCLM* rs41303970 (c.-590 C>T).[17-20] Some studies indicated that polymorphisms in *GCLC* and *GCLM* genes are associated with low levels of reduced GSH *in vitro*, which may explain susceptibility to certain diseases related to oxidative stress.[17,18] The *GCLC* rs17883901 polymorphism has been suggested to suppress the *GCLC* gene induction response to oxidants and it has been implicated in coronary endothelial dysfunction and myocardial infarction.[17] *GCLC* rs17883901 has also been proposed to modulate the renal disease risk in type 1 diabetes patients.[21] The presence of *GCLC* rs17883901 T allele and *GCLM* rs41303970 T allele has also been associated with an increased risk of ischemic heart disease.[19] However, according to the available literature the association between *GCLC* and *GCLM* polymorphisms and asbestos-related diseases has not been studied so far.

Regarding *GSTM1* and *GSTT1* genes, the most common polymorphism is due to homozygous deletion of these genes (null genotype), which results in the lack of the GSTM1 and GSTT1 enzyme activity.[22,23] In the *GSTP1* gene, two common single nucleotide polymorphisms (SNPs) have been described that lead to amino acid substitution and consequently reduced enzyme conjugating activity: *GSTP1* rs1138272 (p.Ala114Val) and *GSTP1* rs1138272 (p.Ala114Val).[22] Hirvonen *et al*. reported an increased risk for developing MM for individuals with *GSTM1* null genotype.[24] Similarly, Landi *et al*. found an increased risk for MM in subject with *GSTM1* null allele, while no effect was observed for *GSTP1* and *GSTT1* polymorphisms.[25] In the study of Kukkonen *et al*., *GSTT1* null genotype increased the risk for asbestos-related severe fibrotic changes and *GSTM*1 null genotype was associated with the greatest thickness of the pleural plaques.[26] Our former study showed that asbestosis was associated with *GSTT1* null genotype, but not with *GSTM1* null genotype.[27] Furthermore, we have reported the influence of *GSTP1* rs1695 on the asbestosis risk, while no association was found between *GSTP1* rs1138272 and asbestosis risk.[28]

The present study aimed to investigate the influence of *GCLC, GCLM, GSTM1, GSTT1* and *GSTP1* polymorphisms on the risk for developing pleural plaques, asbestosis and MM. In addition, we also investigated the influence of gene-gene interactions and interactions between glutathione-related polymorphisms and asbestos exposure on the risk for developing these diseases.

## Subjects and methods

### Study population

The cross sectional study included all together 940 asbestos-exposed subjects, among them 390 subjects with pleural plaques, 147 subjects with asbestosis, 225 subjects with MM and 178 subjects with no asbestos-related disease. Subjects with pleural plaques, asbestosis and MM were considered as cases, and those with no asbestos-related disease as controls.

Additionally, comparison was made between subjects with MM and subjects with pleural plaques.

Subjects with pleural plaques, asbestosis and subjects with no asbestos-related disease were presented at the State Board for the Recognition of Occupational Asbestos Diseases in the period from 1 January 1998 to 31 December 2007 and were all occupationally exposed to asbestos. The information on all the subjects included was revised in 2018 to verify the latest diagnoses of asbestos-related diseases. Subjects with MM were recruited at the Institute of Oncology Ljubljana, where they were treated in the period between 1 February 2004 and 31 December 2018. The study was approved by the Slovenian Ethics Committee for Research in Medicine and was carried out according to the Declaration of Helsinki.

### Clinical diagnosis

The diagnosis of pleural plaques, asbestosis or "no asbestos-related disease" was verified by two groups of experts of the State Board for the Recognition of Occupational Asbestos Diseases, each group consisting of a specialist of occupational medicine, a pulmonologist, and a radiologist. Subjects with pleural MM were diagnosed by ultrasound-guided biopsy or thoracoscopy and those with peritoneal MM by laparoscopy. The diagnosis of MM was proved histopathologically by a pathologist experienced in diagnosing this malignant disease.

### Smoking and asbestos exposure

Data on smoking were collected during an interview based on a standardized questionnaire. The number of pack-years of smoking was calculated from the duration of smoking and the number of cigarettes smoked per day.

Data on cumulative asbestos exposure in fibres/cm$^3$-years were available for the subjects with pleural plaques, asbestosis, "no asbestos-related disease" and for 28 patients with MM. Based on the data on cumulative asbestos exposure, the asbestos exposures in these subjects were divided into three groups: low (< 11 fibres/cm$^3$-years), medium (11–20 fibres/cm$^3$-years) and high (> 20 fibres/cm$^3$-years) asbestos exposure. For the subjects with MM who lacked the data on cumulative asbestos exposure, asbestos exposures were assessed based on the precise work history and comparison with exposures of the group of subjects with known cumulative asbestos exposure. Accordingly, their asbestos exposures were divided into three groups with presumed low, medium or high asbestos exposure.

### DNA extraction and genotyping

Genomic DNA was extracted from peripheral blood samples using Qiagen FlexiGene Kit (Qiagen, Hilden, Germany) according to the manufacturer's instructions.

*GSTP1* rs1695, *GSTP1* rs1138272, *GCLC* rs17883901, and *GCLM* rs41303970 genotypes were determined using competitive allele-specific polymerase chain reaction (KASP) assays (LGC Genomics, UK) following the manufacturer's instructions. Homozygous *GSTM1* and *GSTT1* gene deletions (null genotype) were determined using multiplex PCR in a single reaction as previously described with *HBB* gene serving as a positive control.[29]

### Statistical methods

Standard descriptive statistics was used to describe central tendency and variability of investigated variables. Chi-square test and Kruskal-Wallis test were used to compare categorical and continuous variables among different groups, respectively. Deviation from Hardy-Weinberg equilibrium (HWE) was also evaluated using chi-square test. Dominant and additive genetic models were used in the analysis. To compare genotype frequencies among groups, univariable and multivariable logistic regression models were used and odds ratios (ORs) with 95% confidence intervals (CIs) were calculated. Characteristics used for adjustment in multivariable analysis were selected using stepwise forward-conditional logistic regression. The possible interactions between genotypes as well as between genetic polymorphisms, and between genetic polymorphisms and asbestos exposure were tested by logistic regression models using dummy variables.

Statistical analysis was carried out with IBM SPSS Statistics version 21.0 (IBM Corporation, Armonk, NY, USA). All statistical tests were two-sided and the level of significance was set at 0.05.

## Results

The characteristics of the groups of subjects with pleural plaques, asbestosis, MM and subjects without asbestos-related disease are presented in Table 1. A statistically significant difference between the groups was observed for the age ($p < 0.001$), pack-years of smoking ($p = 0.024$) and asbestos exposure ($p < 0.001$). The mean age was the highest for subjects with MM (65 ± 10.7 years), followed by subjects with asbestosis (58.7 ± 9.1 years).

**TABLE 1.** Characteristics of subjects without asbestos-related disease, subjects with pleural plaques, asbestosis or malignant mesothelioma

| Characteristic | | No disease (N = 178) | Pleural plaques (N = 390) | Asbestosis (N = 147) | Malignant mesothelioma (N = 225) | P |
|---|---|---|---|---|---|---|
| Gender | Male, N (%) | 119 (66.9) | 277 (71.0) | 110 (74.8) | 164 (72.9) | 0.407 Chi-square = 2.905, df = 3 |
| | Female, N (%) | 59 (33.1) | 113 (29.0) | 37 (25.2) | 61 (27.1) | |
| Age (years) | Mean ± SD | 57.6 ± 9.5 | 55.8 ± 9.5 | 58.7 ± 9.1 | 65.0 ± 10.7 | < 0.001 Test-statistic = 115.390 |
| | Median (25%–75%) | 56.6 (49.6–65.1) | 55.0 (48.8–62.7) | 59.1 (51.4–65.3) | 66 (58–73) | |
| | Min–max | 38.2–79.9 | 34.4–85.8 | 37.2–79.2 | 19–95 | |
| Smoking | No, N (%) | 95 (53.4) | 193 (49.5) | 72 (49.0) | 117 (53.7) [7] | 1.614 Chi-square = 0.656, df = 3 |
| | Yes, N (%) | 83 (46.6) | 197 (50.5) | 75 (51.0) | 101 (46.3) | |
| Pack-years of smoking (smokers only) | Mean ± SD | 21.0 ± 15.8 [4] | 18.1 ± 15.6 [22] | 24.4 ± 18.6 [2] | 23.2 ± 17.2 [14] | 0.024 Test-statistic = 9.474 |
| | Median (25%–75%) | 20 (9–30) | 15 (5–28) | 22.8 (10–32.7) | 20 (8–35) | |
| | Min–max | 0.1–65.3 | 0.05–96.6 | 0.15–90 | 1–69 | |
| Asbestos exposure | Low, N (%) | 138 (77.5) | 277 (72.3) [7] | 75 (51.7) [2] | 34 (45.9) [151] | < 0.001 Chi-square = 53.864, df = 6 |
| | Middle, N (%) | 13 (7.3) | 38 (9.9) | 28 (19.3) | 23 (31.1) | |
| | High, N (%) | 27 (15.2) | 68 (17.8) | 42 (29.0) | 17 (23.0) | |

Number of missing data is presented in [] brackets. P-values were calculated using chi-square test for categorical or Kruskal-Wallis test for continuous variables. SD = standard deviation

The mean values of pack-years of smoking were the highest in subjects with asbestosis (24.4 ± 18.6) and in subjects with MM (23.2 ± 17.2). Regarding asbestos exposure, the percent of subjects with low asbestos exposure was the highest for the group of subject with no asbestos-related disease (77.5%), followed by the group of subjects with pleural plaques (72.3%) (Table 1).

The genotype frequencies for all studied genetic polymorphisms are shown in Table 2. Genotype frequencies for all investigated SNPs were concordant with HWE.

**TABLE 2.** Genotype frequencies in all subjects, subjects without asbestos-related disease, subjects with pleural plaques, asbestosis and malignant mesothelioma

| Polymorphism | Genotype | All subjects (N = 940) | No disease (N = 178) | Pleural plaques (N = 416) | Asbestosis (N = 160) | Malignant mesothelioma (N = 154) |
|---|---|---|---|---|---|---|
| *GCLC* rs17883901 c.-129C>T | CC | 772 (82.1) | 149 (83.7) | 310 (79.5) | 124 (84.4) | 189 (84) |
| | CT | 162 (17.2) | 29 (16.3) | 78 (20) | 23 (15.6) | 32 (14.2) |
| | TT | 6 (0.6) | 0 (0) | 2 (0.5) | 0 (0) | 4 (1.8) |
| *GCLM* rs41303970 c.-590C>T | CC | 581 (61.8) | 114 (64) | 233 (59.7) | 87 (59.2) | 147 (65.3) |
| | CT | 306 (32.6) | 54 (30.3) | 135 (34.6) | 51 (34.7) | 66 (29.3) |
| | TT | 53 (5.6) | 10 (5.6) | 22 (5.6) | 9 (6.1) | 12 (5.3) |
| *GSTM1* Gene deletion | present | 384 (40.9) | 74 (41.6) | 159 (40.8) | 64 (43.5) | 87 (38.7) |
| | null genotype | 556 (59.1) | 104 (58.4) | 231 (59.2) | 83 (56.5) | 138 (61.3) |
| *GSTT1* Gene deletion | present | 782 (83.2) | 138 (77.5) | 330 (84.6) | 128 (87.1) | 186 (82.7) |
| | null genotype | 158 (16.8) | 40 (22.5) | 60 (15.4) | 19 (12.9) | 39 (17.3) |
| *GSTP1* rs1695 p.Ile105Val | AA | 454 (78.3) | 78 (43.8) | 202 (51.8) | 76 (51.7) | 98 (43.6) |
| | AG | 394 (41.9) | 81 (45.5) | 155 (39.7) | 55 (37.4) | 103 (45.8) |
| | GG | 92 (9.8) | 19 (10.7) | 33 (8.5) | 16 (10.9) | 24 (10.7) |
| *GSTP1* rs1138272 p.Ala114Val | CC | 785 (83.5) | 141 (79.2) | 334 (85.6) | 121 (82.3) | 189 (84) |
| | CT | 146 (15.5) | 34 (19.1) | 54 (13.8) | 23 (15.6) | 35 (15.6) |
| | TT | 9 (1.0) | 3 (1.7) | 2 (0.5) | 3 (2) | 1 (0.4) |

**TABLE 3.** The association between different asbestos-related diseases and genotypes in univariate analysis

| Polymorphism | Genotype | Asbestos-related disease vs. no disease | | Pleural plaques vs. no disease | | Asbestosis vs. no disease | | MM vs. no disease | | MM vs. plaques | |
|---|---|---|---|---|---|---|---|---|---|---|---|
| | | OR (95% CI) | P | OR (95% CI) | P | OR (95% CI) | P | OR (95% CI) | P | OR (95% CI) | P |
| *GCLC* rs17883901 | CC | Reference | | Reference | | Reference | | Reference | | Reference | |
| | CT+TT | 1.15 (0.74–1.78) | 0.541 | 1.33 (0.83–2.12) | 0.237 | 0.95 (0.52–1.73) | 0.874 | 0.98 (0.57–1.67) | 0.937 | 0.74 (0.48–1.14) | 0.169 |
| *GCLM* rs41303970 | CC | Reference | | Reference | | Reference | | Reference | | Reference | |
| | CT | 1.14 (0.80–1.63) | 0.476 | 1.22 (0.83–1.80) | 0.308 | 1.24 (0.77–1.99) | 0.378 | 0.95 (0.61–1.46) | 0.809 | 0.77 (0.54–1.11) | 0.164 |
| | TT | 1.05 (0.51–2.15) | 0.895 | 1.08 (0.49–2.35) | 0.853 | 1.18 (0.46–3.03) | 0.732 | 0.93 (0.39–2.23) | 0.872 | 0.86 (0.42–1.80) | 0.697 |
| | CT+TT | 1.13 (0.80–1.58) | 0.495 | 1.20 (0.83–1.73) | 0.330 | 1.23 (0.78–1.93) | 0.369 | 0.95 (0.63–1.43) | 0.788 | 0.79 (0.56–1.11) | 0.170 |
| *GSTM1* | present | Reference | | Reference | | Reference | | Reference | | Reference | |
| | null genotype | 1.04 (0.74–1.44) | 0.828 | 1.03 (0.72–1.48) | 0.857 | 0.92 (0.59–1.44) | 0.721 | 1.13 (0.76–1.69) | 0.554 | 1.09 (0.78–1.53) | 0.608 |
| *GSTT1* | present | Reference | | Reference | | Reference | | Reference | | Reference | |
| | null genotype | 0.63 (0.42–0.95) | **0.026** | 0.63 (0.40–0.98) | **0.041** | 0.51 (0.28–0.93) | **0.028** | 0.72 (0.44–1.18) | 0.198 | 1.15 (0.74–1.79) | 0.527 |
| *GSTP1* rs1695 | AA | Reference | | Reference | | Reference | | Reference | | Reference | |
| | AG | 0.80 (0.57–1.13) | 0.209 | 0.74 (0.51–1.07) | 0.114 | 0.70 (0.44–1.11) | 0.129 | 1.01 (0.67–1.53) | 0.955 | 1.37 (0.97–1.94) | 0.075 |
| | GG | 0.80 (0.45–1.40) | 0.428 | 0.67 (0.36–1.25) | 0.208 | 0.86 (0.41–1.80) | 0.698 | 1.01 (0.51–1.97) | 0.988 | 1.50 (0.84–2.67) | 0.170 |
| | AG+GG | 0.80 (0.58–1.11) | 0.185 | 0.73 (0.51–1.04) | 0.078 | 0.73 (0.47–1.13) | 0.157 | 1.01 (0.68–1.5) | 0.958 | 1.39 (1.00–1.94) | **0.049** |
| *GSTP1* rs1138272 | CC | Reference | | Reference | | Reference | | Reference | | Reference | |
| | CT+TT | 0.70 (0.46–1.05) | 0.087 | 0.64 (0.40–1.01) | 0.056 | 0.82 (0.47–1.43) | 0.482 | 0.73 (0.44–1.21) | 0.216 | 1.14 (0.72–1.79) | 0.583 |

Statistically significant results are printed in bold. MM = malignant mesothelioma

In univariate logistic regression analysis, no association was found between *GCLC* rs17883901 and *GCLM* rs41303970 genetic polymorphisms and asbestos-related diseases.

*GSTT1* null genotype was associated with the decreased risk for asbestos-related diseases when analysed together (OR = 0.63; 95% CI = 0.42–0.95; p = 0.026). When analysing the risk for each disease separately, *GSTT1* null genotype was associated with the decreased risk for pleural plaques (OR = 0.63; 95% CI = 0.40–0.98; p = 0.026) and asbestosis (OR = 0.51; 95% CI = 0.28–0.93; p = 0.028), but not for MM. No association was found between *GSTM1* null genotype and asbestos-related diseases. Regarding *GSTP1* polymorphisms, a positive association was found between *GSTP1* rs1695 AG + GG *vs*. AA genotypes for MM only when compared to pleural plaques (OR = 1.39; 95% CI = 1.00–1.94; p = 0.049) (Table 3).

Regarding age, no association was found between age and pleural plaques (OR = 0.98; 95% CI = 0.96–1.00; p = 0.032). A slight association was observed between age and MM (OR = 1.07; 95% CI = 1.05–1.10; p < 0.001), as well as between age and MM when compared to pleural plaques (OR = 1.10; 95% CI = 1.08–1.12; p < 0.001).

The analysis of association between asbestos exposure and asbestos-related diseases revealed a positive association between high and medium *vs*. low asbestos exposure and all asbestos-related diseases (OR = 1.93; 95 % CI = 1.31–2.85; p = 0.001), between high and medium *vs*. low asbestos exposure and asbestosis (OR = 3.22; 95% CI = 1.99–5.20; p < 0.001), and between high and medium *vs*. low asbestos exposure and MM (OR = 4.06; 95% CI = 2.28–7.23; p < 0.001). When analysing the association between high and medium *vs*. low asbestos exposure and MM compared to pleural plaques, the OR was 3.07 (95 % CI = 1.85–5.12; p < 0.001).

In multivariate logistic regression analysis, the risk of *GSTT1* null genotype for all asbestos-related diseases together (OR = 0.62; 95% CI = 0.41–0.94; p = 0.025) and separately for asbestosis (OR = 0.51; 95% CI = 0.27–0.95; p = 0.033) did not change considerably after adjustment for asbestos exposure. Similarly, the risk of *GSTT1* null genotype for pleural plaques remained practically unchanged after adjustment for age (OR = 0.63; 95% CI = 0.40–0.99; p = 0.046). On the contrary, the risk of *GSTP1* rs1695 AG + GG *vs*. AA genotypes for MM compared to pleural plaques increased slightly (OR = 1.97; 95% CI = 1.14–3.39; p = 0.015)

**TABLE 4.** The association between different asbestos-related diseases and genotypes in multivariate analysis

| Polymorphism | Genotype | Asbestos-related disease vs. no disease | | Pleural plaques vs. no disease | | Asbestosis vs. no disease | | MM vs. no disease | | MM vs. plaques | |
|---|---|---|---|---|---|---|---|---|---|---|---|
| | | OR (95% CI) | P | OR (95% CI) | P | OR (95% CI) | P | OR (95% CI) | P | OR (95% CI) | P |
| *GCLC* rs17883901 | CC | Reference | | Reference | | Reference | | Reference | | Reference | |
| | CT+TT | 1.18 (0.75–1.86) | 0.466 | 1.33 (0.83–2.12) | 0.240 | 0.96 (0.52–1.78) | 0.893 | 0.66 (0.28–1.57) | 0.344 | 0.57 (0.26–1.23) | 0.154 |
| *GCLM* rs41303970 | CC | Reference | | Reference | | Reference | | Reference | | Reference | |
| | CT | 1.16 (0.8–1.68) | 0.431 | 1.22 (0.82–1.79) | 0.323 | 1.10 (0.67–1.81) | 0.695 | 0.98 (0.51–1.87) | 0.945 | 0.76 (0.43–1.36) | 0.360 |
| | TT | 1.16 (0.55–2.42) | 0.696 | 1.06 (0.48–2.32) | 0.883 | 1.37 (0.52–3.63) | 0.524 | 1.13 (0.33–3.84) | 0.844 | 1.05 (0.35–3.09) | 0.934 |
| | CT+TT | 1.16 (0.82–1.64) | 0.406 | 1.19 (0.82–1.72) | 0.351 | 1.14 (0.72–1.83) | 0.576 | 1.00 (0.55–1.84) | 0.994 | 0.80 (0.47–1.38) | 0.429 |
| *GSTM1* | present | Reference | | Reference | | Reference | | Reference | | Reference | |
| | null genotype | 1.04 (0.74–1.46) | 0.837 | 1.06 (0.74–1.53) | 0.738 | 0.84 (0.53–1.34) | 0.464 | 1.09 (0.60–1.98) | 0.774 | 1.09 (0.63–1.87) | 0.756 |
| *GSTT1* | present | Reference | | Reference | | Reference | | Reference | | Reference | |
| | null genotype | 0.62 (0.41–0.94) | **0.025** | 0.63 (0.4–0.99) | **0.046** | 0.51 (0.27–0.95) | **0.033** | 1.00 (0.48–2.08) | 0.996 | 1.28 (0.65–2.53) | 0.479 |
| *GSTP1* rs1695 | AA | Reference | | Reference | | Reference | | Reference | | Reference | |
| | AG | 0.78 (0.54–1.11) | 0.162 | 0.74 (0.51–1.07) | 0.113 | 0.65 (0.40–1.06) | 0.087 | 1.23 (0.66–2.32) | 0.513 | 1.86 (1.04–3.30) | **0.036** |
| | GG | 0.8 (0.45–1.43) | 0.461 | 0.67 (0.36–1.24) | 0.203 | 0.96 (0.45–2.06) | 0.920 | 1.65 (0.65–4.16) | 0.288 | 2.40 (1.04–5.54) | **0.039** |
| | AG+GG | 0.78 (0.56–1.1) | 0.153 | 0.72 (0.51–1.04) | 0.077 | 0.71 (0.45–1.12) | 0.140 | 1.31 (0.72–2.39) | 0.370 | 1.97 (1.14–3.39) | **0.015** |
| *GSTP1* rs1138272 | CC | Reference | | Reference | | Reference | | Reference | | Reference | |
| | CT+TT | 0.68 (0.44–1.04) | 0.078 | 0.64 (0.4–1.02) | 0.059 | 0.84 (0.47–1.51) | 0.565 | 0.73 (0.34–1.60) | 0.433 | 1.02 (0.49–2.13) | 0.965 |

MM = malignant mesothelioma. Statistically significant results are printed in bold.

Adjustments made: Asbestos-related disease *vs.* no disease, Asbestosis *vs.* no disease: adjusted for asbestos exposure; Pleural plaques *vs.* no disease: adjusted for age; MM *vs.* no disease, MM *vs.* plaques: adjusted for asbestos exposure, age

after adjustment for asbestos exposure and age (Table 4).

In further logistic regression analysis, the interactions between polymorphisms showed no significant influence on the risk for developing asbestos-related diseases (data not shown).

Testing the influence of interactions between asbestos high and medium *vs*. low exposure and genetic polymorphisms on the risk of asbestos-related diseases, the interaction between asbestos exposure and *GSTT1* null polymorphism decreased the risk for developing MM (OR = 0.17; 95% CI = 0.03-0.85; p = 0.031). Similarly, the interaction between asbestos exposure and *GSTT1* null polymorphism (OR = 0.11; 95% CI = 0.02–0.49; p = 0.004) and the interaction between asbestos exposure and *GSTP1* rs1695 polymorphism (OR = 0.14; 95% CI = 0.03–0.65; p = 0.012) decreased the risk of MM when compared to pleural plaques.

## Discussion

The present study investigated the influence of genetic polymorphisms in GSH related genes, the interactions between these polymorphism, and interactions between polymorphisms and asbestos exposure on the risk of asbestos-related diseases.

The present study revealed a protective effect of *GSTT1* null genotype on the risk of all studied asbestos-related diseases together and particularly on the risk of pleural plaques and asbestosis. The explanation of these findings could be that in some instances GSTT1 may catalyse toxification and not detoxification reaction, leading to even more reactive conjugate.[15] This observation is in agreement with the results of our previous study, in which *GSTT1* null genotype also decreased the asbestosis risk.[27] On the other hand, in the present study *GSTM1* null genotype showed no effect on the risk of asbestos-related diseases, which is also consistent with the results of our previous study.[27] Similar findings were observed by Jakobsson *et al*., who reported no association between GSTM1 deficiency and parenchymal and pleural abnormalities among the workers exposed to asbestos[30], and also by Hirvonen *et al*., who revealed no increased risk for the asbestos-related pulmonary disorders in subjects with homozygous deletion of *GSTM1* gene.[16] Contrary to the results of our study,

Kukkonen *et al*. reported that *GSTT1* null genotype increased the risk of asbestosis and *GSTM*1 null genotype was related to the greatest thickness of the pleural plaques.[26] Although Landi *et al*. observed an increased risk for MM in subjects bearing *GSTM1* null allele[25], in our current study, no association was found between either *GSTM1* null genotype or *GSTT1* null genotype and MM risk.

The results of our study showed that *GSTP1* rs1695 AG + GG *vs*. AA genotypes increased the MM risk, while *GSTP1* rs1138272 polymorphism did not affect the risk of this malignoma. On the contrary, *GSTP1* polymorphisms did not influence the MM risk in the study by Landi *et al*.[25]

Our study revealed no influence of *GCLC* rs17883901 and *GCLM* rs41303970 on the risk for asbestos-related diseases. Our results suggest that these two polymorphisms are not related to the susceptibility to asbestos-related diseases. To our knowledge, no other studies investigated the role of polymorphic genes involved in GSH synthesis in asbestos-related diseases.

Our study confirmed the impact of high and medium *vs*. low asbestos exposure on the risk for asbestosis and MM, which is consistent with the findings of previous studies.[31-34] However, our results also showed that nearly 46% of subjects with MM, 52% of subjects with asbestosis and 72% subjects with pleural plaques had low asbestos exposure. This suggests that asbestos-related diseases can also develop when asbestos exposures are low, which was indicated especially for MM.[35,36]

In this study, the interactions between investigated GSH related gene polymorphisms did not influence the risk for developing asbestos-related diseases. On the other hand, we observed that the interaction between *GSTT1* null polymorphism and asbestos exposure decreased the risk for developing MM, although there was no independent association between *GSTT1* null and MM when compared to controls with no asbestos-related disease. In other words, *GSTT1* null genotype modified the association between high and medium *vs*. low asbestos exposure and MM and acted protectively on the risk of this malignant disease.

Another interesting finding of this study showed that the interaction between *GSTP1* rs1695 AG + GG *vs*. AA genotypes and asbestos exposure decreased the risk of MM when compared to pleural plaques, despite the fact that in univariate analysis both *GSTP1* polymorphism and asbestos exposure were associated with an increased risk of MM. The relation between benign pleural plaques and the risk of MM has not been clearly proved so far. Although pleural plaques may be the endpoint and the development of pleural plaques may be an entirely independent process from the development of MM[37], it is likely that there is a relation between pleural plaques and MM.[38] The present study suggests a modifying and protective effect of *GSTP1* rs1695 genotypes on the association between asbestos exposure and MM risk when compared to pleural plaques.

Considering the potential limitations of the study, the data on asbestos exposure were not available for all subjects, especially not for patients with MM. Consequently, the analyses of the interactions between genetic polymorphisms and asbestos exposure could be performed only for the subgroup of MM patients.

On the other hand, the study also brings novel findings and has some important strengths. Firstly, according to our knowledge, this is the first study to investigate the association between *GCLC* rs17883901 and *GCLM* rs41303970 genetic polymorphisms and asbestos-related diseases. Secondly, it included relatively large numbers of subjects with different asbestos-related diseases from genetically homogenous population and investigated functional genetic polymorphisms in different GSH related genes.

In conclusion, our findings suggest that among genetic polymorphisms in GSH related genes, *GSTT1* null polymorphism may be associated with the risk for developing pleural plaques and asbestosis and may also modify the association between asbestos exposure and MM and therefore act protectively on the risk for this malignoma. This study also revealed a modifying and protective effect of *GSTP1* rs1695 polymorphism on the association between asbestos exposure and MM risk when pleural plaques were considered as controls.

## Acknowledgements and funding

The authors would like to thank Savica Soldat, Urška Slapšak, Ana Cirnski and Maj Bavec for their help with genotyping analyses. This work was financially supported by the Slovenian Research Agency (ARRS Grants Nos. P1-0170, L3-8203 and L3-2622).

## References

1. Stayner L, Welch LS, Lemen R. The worldwide pandemic of asbestos-related diseases. *Annu Rev Public Health* 2013; **34:** 205-16. doi: 10.1146/annurev-publhealth-031811-124704

2. Vainio H. Epidemics of asbestos-related diseases - something old, something new. *Scand J Work Environ Health* 2015; **41:** 1-4. doi: 10.5271/sjweh.3471

3. Kamp DW, Graceffa P, Pryor WA, Weitzman SA. The role of free radicals in asbestos-induced diseases. *Free Radic Biol Med* 1992; **12:** 293-315. doi: 10.1016/0891-5849(92)90117-y

4. Kinnula VL. Oxidant and antioxidant mechanisms of lung disease caused by asbestos fibres. *Eur Respir J* 1999; **14:** 706-16. doi: 10.1034/j.1399-3003.1999.14c35.x

5. Solbes E, Harper RW. Biological responses to asbestos inhalation and pathogenesis of asbestos-related benign and malignant disease. *J Investig Med* 2018; **66:** 721-7. doi: 10.1136/jim-2017-000628

6. Nichenametla SN, Muscat JE, Liao JG, Lazarus P, Richie JP, Jr. A functional trinucleotide repeat polymorphism in the 5'-untranslated region of the glutathione biosynthetic gene GCLC is associated with increased risk for lung and aerodigestive tract cancers. *Mol Carcinog* 2013; **52:** 791-9. doi: 10.1002/mc.21923

7. Zhang H, Liu H, Zhou L, Yuen J, Forman HJ. Temporal changes in glutathione biosynthesis during the lipopolysaccharide-induced inflammatory response of THP-1 macrophages. *Free Radic Biol Med* 2017; **113:** 304-10. doi: 10.1016/j.freeradbiomed.2017.10.010

8. Ketterer B. A bird's eye view of the glutathione transferase field. *Chem Biol Interact* 2001; **138:** 27-42. doi: 10.1016/s0009-2797(01)00277-0

9. Strange RC, Spiteri MA, Ramachandran S, Fryer AA. Glutathione-S-transferase family of enzymes. *Mutat Res* 2001; **482:** 21-6. doi: 10.1016/s0027-5107(01)00206-8

10. Chen Y, Shertzer HG, Schneider SN, Nebert DW, Dalton TP. Glutamate cysteine ligase catalysis: dependence on ATP and modifier subunit for regulation of tissue glutathione levels. *J Biol Chem* 2005; **280:** 33766-74. doi: 10.1074/jbc.M504604200

11. Traverso N, Ricciarelli R, Nitti M, Marengo B, Furfaro AL, Pronzato MA, et al. Role of glutathione in cancer progression and chemoresistance. *Oxid Med Cell Longev* 2013; **2013:** 972913. doi: 10.1155/2013/972913

12. Zmorzynski S, Swiderska-Kolacz G, Koczkodaj D, Filip AA. Significance of polymorphisms and expression of enzyme-encoding genes related to glutathione in hematopoietic cancers and solid tumors. *Biomed Res Int* 2015; **2015:** 853573. doi: 10.1155/2015/853573

13. Flanagan JU, Smythe ML. Sigma-class glutathione transferases. *Drug Metab Rev* 2011; **43:** 194-214. doi: 10.3109/03602532.2011.560157

14. Tan XL, Moslehi R, Han W, Spivack SD. Haplotype-tagging single nucleotide polymorphisms in the GSTP1 gene promoter and susceptibility to lung cancer. *Cancer Detect Prev* 2009; **32:** 403-15. doi: 10.1016/j.cdp.2009.02.004

15. Hayes JD, Strange RC. Glutathione S-transferase polymorphisms and their biological consequences. *Pharmacology* 2000; **61:** 154-66. doi: 10.1159/000028396

16. Hirvonen A, Saarikoski ST, Linnainmaa K, Koskinen K, Husgafvel-Pursiainen K, Mattson K, et al. Glutathione S-transferase and N-acetyltransferase genotypes and asbestos-associated pulmonary disorders. *J Natl Cancer Inst* 1996; **88:** 1853-6. doi: 10.1093/jnci/88.24.1853

17. Koide S, Kugiyama K, Sugiyama S, Nakamura S, Fukushima H, Honda O, et al. Association of polymorphism in glutamate-cysteine ligase catalytic subunit gene with coronary vasomotor dysfunction and myocardial infarction. *J Am Coll Cardiol* 2003; **41:** 539-45. doi: 10.1016/s0735-1097(02)02866-8

18. Yuniastuti A, Susanti R, Mustikaningtyas D. Polymorphism of glutamate-cysteine ligase subunit catalytic (GCLC) gene in pulmonary tuberculosis patients. *Pak J Biol Sci* 2017; **20:** 397-402. doi: 10.3923/pjbs.2017.397.402

19. Skvortsova L, Perfelyeva A, Khussainova E, Mansharipova A, Forman HJ, Djansugurova L. Association of GCLM -588C/T and GCLC -129T/C promoter polymorphisms of genes coding the subunits of glutamate cysteine ligase with ischemic heart disease development in Kazakhstan population. *Dis Markers* 2017; **2017:** 4209257. doi: 10.1155/2017/4209257

20. Li J, Yin F, Lin Y, Gao M, Wang L, Liu S, et al. Genetic susceptibility analysis of GCLC rs17883901 polymorphism to preeclampsia in Chinese Han women. *Gynecol Endocrinol* 2020; **36:** 781-5. doi: 10.1080/09513590.2020.1725970

21. Vieira SM, Monteiro MB, Marques T, Luna AM, Fortes MA, Nery M, et al. Association of genetic variants in the promoter region of genes encoding p22phox (CYBA) and glutamate cysteine ligase catalytic subunit (GCLC) and renal disease in patients with type 1 diabetes mellitus. *BMC Med Genet* 2011; **12:** 129. doi: 10.1186/1471-2350-12-129

22. Hayes JD, Flanagan JU, Jowsey IR. Glutathione transferases. *Annu Rev Pharmacol Toxicol* 2005; **45:** 51-88. doi: 10.1146/annurev.pharmtox.45.120403.095857

23. Ali-Osman F, Akande O, Antoun G, Mao JX, Buolamwini J. Molecular cloning, characterization, and expression in Escherichia coli of full-length cDNAs of three human glutathione S-transferase Pi gene variants. Evidence for differential catalytic activity of the encoded proteins. *J Biol Chem* 1997; **272:** 10004-12. doi: 10.1074/jbc.272.15.10004

24. Hirvonen A, Pelin K, Tammilehto L, Karjalainen A, Mattson K, Linnainmaa K. Inherited GSTM1 and NAT2 defects as concurrent risk modifiers in asbestos-related human malignant mesothelioma. *Cancer Res* 1995; **55:** 2981-3. PMID: 7606714

25. Landi S, Gemignani F, Neri M, Barale R, Bonassi S, Bottari F, et al. Polymorphisms of glutathione-S-transferase M1 and manganese superoxide dismutase are associated with the risk of malignant pleural mesothelioma. *Int J Cancer* 2007; **120:** 2739-43. doi: 10.1002/ijc.22590

26. Kukkonen MK, Hamalainen S, Kaleva S, Vehmas T, Huuskonen MS, Oksa P, et al. Genetic susceptibility to asbestos-related fibrotic pleuropulmonary changes. *Eur Respir J* 2011; **38:** 672-8. doi: 10.1183/09031936.00049810

27. Franko A, Dodic-Fikfak M, Arneric N, Dolzan V. Glutathione S-transferases GSTM1 and GSTT1 polymorphisms and asbestosis. *J Occup Environ Med* 2007; **49:** 667-71. doi: 10.1097/JOM.0b013e318065b855

28. Franko A, Dolzan V, Arneric N, Dodic-Fikfak M. The influence of genetic polymorphisms of GSTP1 on the development of asbestosis. *J Occup Environ Med* 2008; **50:** 7-12. doi: 10.1097/JOM.0b013e31815cbab5

29. Chen CL, Liu Q, Relling MV. Simultaneous characterization of glutathione S-transferase M1 and T1 polymorphisms by polymerase chain reaction in American whites and blacks. *Pharmacogenetics* 1996; **6:** 187-91. doi: 10.1097/00008571-199604000-00005

30. Jakobsson K, Rannug A, Alexandrie AK, Rylander L, Albin M, Hagmar L. Genetic polymorphism for glutathione-S-transferase mu in asbestos cement workers. *Occup Environ Med* 1994; **51:** 812-6. doi: 10.1136/oem.51.12.812

31. Jamrozik E, de Klerk N, Musk AW. Asbestos-related disease. *Intern Med J* 2011; **41:** 372-80. doi: 10.1111/j.1445-5994.2011.02451.x

32. Frank AL, Joshi TK. The global spread of asbestos. *Ann Glob Health* 2014; **80:** 257-62. doi: 10.1016/j.aogh.2014.09.016

33. Lacourt A, Lévêque E, Guichard E, Gilg Soit Ilg A, Sylvestre MP, Leffondré K. Dose-time-response association between occupational asbestos exposure and pleural mesothelioma. *Occup Environ Med* 2017; **74:** 691-7. doi: 10.1136/oemed-2016-104133

34. Ulvestad B, Kjærheim K, Martinsen JI, Damberg G, Wannag A, Mowe G, et al. Cancer incidence among workers in the asbestos-cement producing industry in Norway. *Scand J Work Environ Health* 2002; **28:** 411-7. doi: 10.5271/sjweh.693

35. Nishimura Y, Kumagai-Takei N, Matsuzaki H, Lee S, Maeda M, Kishimoto T, et al. Functional alteration of natural killer cells and cytotoxic T lymphocytes upon asbestos exposure and in malignant mesothelioma patients. *Biomed Res Int* 2015; **2015:** 238431. doi: 10.1155/2015/238431

36. Rosner D, Markowitz G, Chowkwanyun M. "Nondetected": the politics of measurement of asbestos in talc, 1971-1976. *Am J Public Health* 2019; **109:** 969-74. doi: 10.2105/ajph.2019.305085

37. Pairon JC, Laurent F, Rinaldo M, Clin B, Andujar P, Ameille J, et al. Pleural plaques and the risk of pleural mesothelioma. *J Natl Cancer Inst* 2013; **105:** 293-301. doi: 10.1093/jnci/djs513

38. Maxim LD, Niebo R, Utell MJ. Are pleural plaques an appropriate endpoint for risk analyses? *Inhal Toxicol* 2015; **27:** 321-34. doi: 10.3109/08958378.2015.1051640

*research article*

# Long term results of follow-up after HPV self-sampling with devices Qvintip and HerSwab in women non-attending cervical screening programme

Teodora Bokan[1], Urska Ivanus[2,3], Tine Jerman[2], Iztok Takac[4,5], Darja Arko[4,5]

[1] Mistelbach-Gänserndorf Regional Hospital, Mistelbach Austria
[2] Institute of Oncology Ljubljana, Ljubljana, Slovenia
[3] Faculty of Medicine, University of Ljubljana, Ljubljana Slovenia
[4] University Medical Centre Maribor, Maribor, Slovenia
[5] Faculty of Medicine, University of Maribor, Maribor, Slovenia

Radiol Oncol 2021; 55(2): 187-195.

Received 1 October 2020
Accepted 9 December 2020

Correspondence to: Assoc. prof. Darja Arko, M.D., Ph.D., Division of Gynaecology and Perinatology, University Medical Centre Maribor, Ljubljanska 5, 2000 Maribor. E-mail: darja.arko@ukc-mb.si

Disclosure: No potential conflicts of interest were disclosed.

**Background.** We are presenting the results of the Slovenian human papillomaviruses (HPV) self-sampling pilot study in colposcopy population of National Cervical Cancer Screening Programme ZORA for the first time. One-year and four-year follow-up results are presented for two different self-sampling devices.

**Participants and methods.** A total of 209 women were enrolled in the study at colposcopy clinic. Prior to the gynaecological examination, all women performed self-collected vaginal swab at the clinic; 111 using Qvintip and 98 using HerSwab self-sampling device. After self-sampling, two cervical smears were taken by a clinician; first for conventional cytology and second for HPV test. After that, all women underwent colposcopy and a cervical biopsy if needed. We compared sensitivity, specificity, and predictive values of cytology (at the cut-off atypical squamous cells of undetermined significance or more [ASC-US+]) and HPV test (on self- and clinician-taken samples) for the detection of cervical intraepithelial neoplasia grade 2 or more (CIN2+) after one and four years of follow-up. Hybrid Capture 2 (HC2) assay was used for all HPV testing.

**Results.** The mean age of 209 women was 37.6 years and HPV positivity rate 67.0% (140/209), 36.9 years and 70.3% (78/111) in the Qvintip group and 38.4 years and 63.3% (62/98) in the HerSwab group, respectively. Overall, percent agreement between self and clinician-taken samples was 81.8% (kappa 0.534) in the Qvintip and 77.1% (kappa 0.456) in the HerSwab group. In the Qvintip group, the longitudinal sensitivity, specificity, positive and negative predictive values were 71.8%, 75.0%, 83.6%, 60.0% for cytology; 83.1%, 51.3%, 75.6% and 62.5% for HPV test of self-taken samples and 94.4%, 57.5%, 79.8% and 85.2% for HPV test on clinician-taken samples. In the HerSwab group, the corresponding results were 71.7%, 46.7%, 61.3%, 58.3% for cytology; 75.0%, 47.7%, 62.9% and 61.8% for HPV test on self-taken samples and 94.3%, 44.4%, 66.7% and 87.0% for clinician-taken samples, respectively.

**Conclusions.** The results confirm that HPV self-sampling is not as accurate as clinician sampling when HC2 is used. All HPV tests showed a higher sensitivity in detecting CIN2+ compared to cytology. Due to non-inferior longitudinal sensitivity of HPV self-sampling compared to cytology, HPV self-sampling might be an option for non-attenders to the National Cancer Screening Programme.

Key words: HPV self-sampling; cytology; high-grade intraepithelial lesion

## Introduction

Since the introduction of the cervical cancer screening based on cell samples for cervical cytology (Pap smear) the incidence and mortality of cervical cancer has decreased dramatically.[1,2] In Slovenia, the highest peak of the cervical cancer incidence was registered in 1962 when age-standardised incidence rate (world) was 27.5/100,000. Due to the opportunistic screening the incidence was decreasing till the end of the eighties and a second peak was observed in 1997.[3] Organised cervical screening national program ZORA (NP ZORA) was implemented in 2003 with conventional cytology at a three-years interval in women aged 20-64. A three-year coverage of the target population with a screening test is just above 70%.[4] The lowest incidence of cervical cancer in Slovenia was registered in 2017 when 85 new cases were diagnosed and the age-standardised incidence rate (world) was 4.9/100,000.[5]

Despite good results of NP ZORA, there are still subgroups of women who do not attend for screening. In Slovenia, the coverage of the target population with screening test is decreasing with women's age. It is below the targeted 70% in women 50 years or more. The lowest rate is in women aged 60-64 years with only 57%.[4]

In countries with organised screening programmes, the majority of new cases are diagnosed in women who were never screened or are underscreened. These women are often diagnosed at advanced stages. Nonattendance for screening is one of the most important risk factors for developing cervical cancer. Studies exploring screening non-attendance suggest a wide range of barriers, including fear of pain, embarrassment, shame, low perceived risk, absence of symptoms, lack of physicians, inconvenient clinic hours, forgetting an appointment, cultural barriers, low socioeconomic status, indirect costs, and worry about the result.[6,7]

The discovery that human papillomaviruses (HPV) are aetiologically linked with cervical cancer has led to efforts to apply this knowledge to improve cervical cancer screening. Over the last two decades, HPV testing has become a part of clinical guidelines for cervical cancer screening, triage and follow-up after treatment in several countries.[8]

One of the advantages of HPV testing is the possibility for women to perform self-sampling. Systematic reviews and meta-analysis published in recent years have shown that self-sampling for HPV testing may increase a population uptake of cervical cancer screening, especially when HPV self-sampling kits were mailed directly to women.[9,10] HPV self-sampling is a process where a woman uses a kit to collect a vaginal sample, which is then sent for analysis by a laboratory, while sample taken by gynaecologist is obtained from the cervix. The difference between both methods has raised concerns about whether vaginal self-sampling is comparable to cervical clinician-sampling in detecting HPV. In the updated meta-analysis by Arbyn *et al*. in 2018, HPV assays based on polymerase chain reaction were as sensitive on self-samples as on clinical samples; however, the specificity to exclude cervical intraepithelial neoplasia grade 2 or more (CIN 2+) was 2% or 4% lower on self-samples than on clinical samples.[11] HPV assays based on signal amplification were less sensitive on self-samples.[11]

For the first time, we are presenting the results of the Slovenian HPV self-sampling pilot study in colposcopy population that was conducted one year prior the large-scale randomised trial of HPV self-sampling.[12] One and four-year sensitivity, specificity, positive, and negative predictive values for CIN2+, test agreement and CIN 2+ detection rates in women enrolled in the study were analysed. Results are stratified by the sampling modality (self, clinician), test (cytology, HPV), and self-sampling device (Qvintip, HerSwab).

## Participants and methods

Women were consecutively enrolled in the study at the colposcopy clinic at the University Medical Centre Maribor and General Hospital Celje during 2014–2016 and followed by the central National Cervical Cancer Screening Registry until the end of 2019. Women with pathologic Pap test, age 20–64 years, referred for a colposcopy according to National guidelines for the management of women with pathological cervical results[13], were invited to participate in prospective observational study and all included women signed informed consent. Exclusion criteria were acute kolpitis or cervicitis and pregnancy. All women performed a self-collected vaginal swab for HPV testing at the clinic prior to the gynaecological examination. After self-sampling, the gynaecologist collected two cervical smears, first for conventional cytology and second for a HPV test. After that, all women underwent colposcopy and in case of abnormal colposcopy cervical biopsy was performed. Women were managed according to the colposcopy and biopsy results and the National guidelines for the

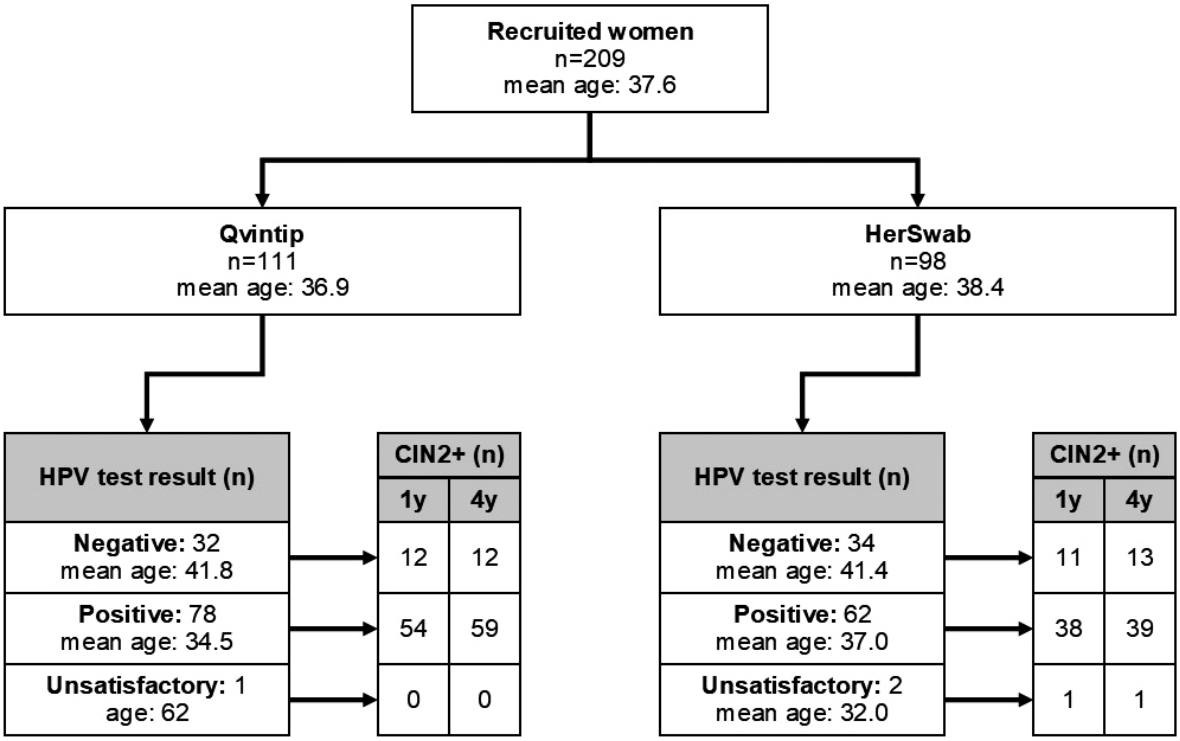


**FIGURE 1.** Flow chart of women enrolled in the study with results of human papillomaviruses (HPV) self-sampling and histological cervical intraepithelial neoplasia grade 2 or more (CIN2+) results after one and four-year follow-up.

management of women with pathological cervical results.[13] There were two self-sampling devices used in the study: Qvintip (Aprovix AB, Uppsala Sweden) and HerSwab (Eve Medical, Toronto, Canada); however, each woman used only one self-sampling device. Hybrid Capture 2 (HC2, Qiagen, Hilden, Germany) assay was used for all HPV testing. Cytological and histological evaluations were performed by certified pathologists in laboratories as part of a regular Cervical Cancer Screening Programme. In the event of having more than one histopathological result, the pathological change of the highest grade was included in the analysis. Each cytology slide was evaluated twice: at the institution performing gynaecological examination and at Institute of Oncology Ljubljana.

## Statistical analysis

The Mann-Whitney U Test was used to compare whether there is a difference in age and the Chi-squared test to compare proportions of positive results and CIN2+ among tester groups. Test performance for CIN 2+ was evaluated with a 4-year longitudinal sensitivity, specificity, negative predictive value (NPV), and positive predictive value (PPV). Confidence intervals (CI) for performance measures were calculated with the bootstrap method. Relative performance was calculated as a ratio of performance measures of HPV test on a self-sample *vs*. HPV test on a sample taken by a gynaecologist and cytology. All women in the Qvintip group had a histological follow up of at least 4 years, while two women without CIN2+ event in the HerSwab group had a histological follow up of 3 years, and 9 and 11 months, respectively. They both had negative cytology and HPV test and they were included in analysis as negative for CIN2+. All women included in the study were followed-up after 4 years according to national guidelines by personal gynaecologists who are providers of National cancer screening programme. Cumulative incidence was calculated using the Kaplan-Meier method. The duration of histological follow up was at least 5 years for all women in the Qvintip group and more than 50% of women in the HerSwab group. Women were censored at the end of histological follow up or death. One woman without CIN2+ event from the HerSwab group was censored due to death after follow up time of just below two years and two women were censored three and one month before the four years mark due to end of histological follow up. The data were obtained from the National cervical screening program registry. Agreement

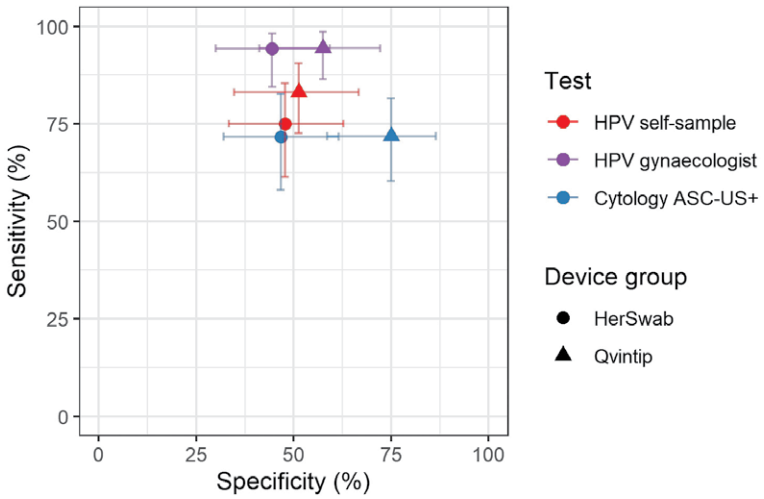


**FIGURE 2.** Sensitivity and specificity for cervical intraepithelial neoplasia grade 2 or more (CIN2+) by test (cytology, human papillomaviruses [HPV]), testing modality (self, clinician) and self-sampling device (Qvintip, HerSwab) after four years of follow-up following enrolment.

ASC-US+ = atypical squamous cells of undetermined significance or more

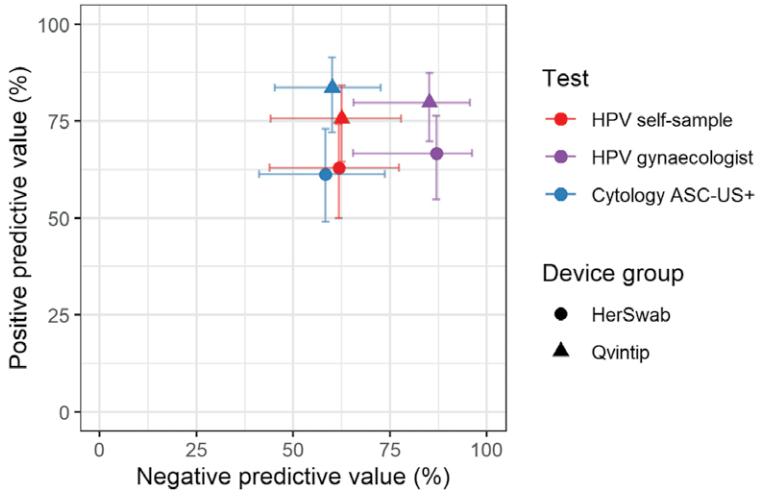


**FIGURE 3.** Positive predictive value and negative predictive value for cervical intraepithelial neoplasia grade 2 or more (CIN2+) by test (cytology, human papillomaviruses [HPV]), testing modality (self, clinician) and self-sampling device (Qvintip, HerSwab).

ASC-US+ = atypical squamous cells of undetermined significance or more

was evaluated with overall percent agreement (OPA) and Cohen's kappa. Atypical squamous cells of undetermined significance or more (ASC-US+) was considered a positive result for cytology. Cytology results in the test performance analysis are provided by the Institute of Oncology. Women with negative colposcopy and no histology were considered negative for CIN2+. Unsatisfactory self-samples were excluded from analyses of agreement, test performance, and cumulative incidence. All analyses were conducted in R v3.6.3[14] using the significance level $\alpha = 0.050$.

The study was coordinated by the Institute of Oncology Ljubljana. It was conducted in compliance with the Helsinki Declaration and was approved by the National Medical Ethics Committee at the Slovenian Ministry of Health (consents Nos. 155/03/13 and 136/04/14). All women gave their written informed consent prior to study inclusion.

## Results

### Characteristics of the enrolled women

A total of 209 women were enrolled in the study, of them 111 to the Qvintip and 98 to the HerSwab group (Figure 1). The mean age of the enrolled women was 37.6 years; 140 women were tested positive with a HPV self-sampling test (67.0%), 66 negative (31.6%) and in three women, the self-taken sample was technically inadequate (1.4%). One year after the enrolment, CIN2+ was diagnosed in 116 women (55.5%) and four years after the enrolment in 124 (59.3%) women.

Women in the Qvintip group were on average younger than women in the HerSwab group (mean age 36.9 *vs.* 38.4 years, p = 0.221), had a higher probability for a positive result of HPV self-sampling (70.3% *vs.* 63.3%, p = 0.283) and CIN2+ diagnosis after one (59.4% *vs.* 51.0%) and four years of follow up (64.0% *vs.* 54.1%, p = 0.146) (Figure 1).

### Accuracy of HPV self-sampling

Four-year longitudinal sensitivity and specificity of HPV self-sampling for CIN2+ were 83.1% and 51.3%, respectively, in the Qvintip and 75.0% and 47.7% in the HerSwab group. Four-years longitudinal NPV and PPV were 62.5% and 75.6% in the Qvintip and 61.8% and 62.9% in the HerSwab group (Figures 2 and 3, Supplementary Table 1).

An increase in the sensitivity and NPV from cytology (blue) and HPV self-sampling (red) toward HPV test on clinician-taken samples (violet) is evident in both device groups (Figures 2 and 3, Supplementary Tables 1 and 2). The sensitivity and NPV of cytology were similar in both device groups, which was also observed for HPV test on clinician-taken samples. In HPV self-sampling, the sensitivity was higher in the Qvintip group compared to the HerSwab group (83.1 *vs.* 75.0); however, NPV was similar (62.5 *vs.* 61.8). Four-

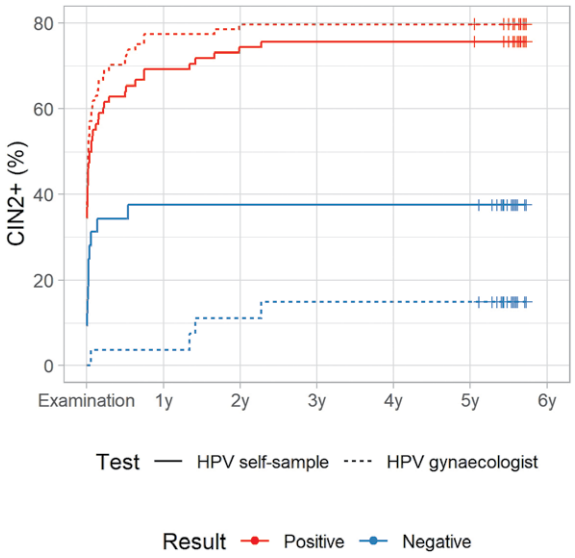


FIGURE 4A. Cumulative incidence of cervical intraepithelial neoplasia grade 2 or more (CIN2+) according to human papillomaviruses (HPV) test result in Qvintip group

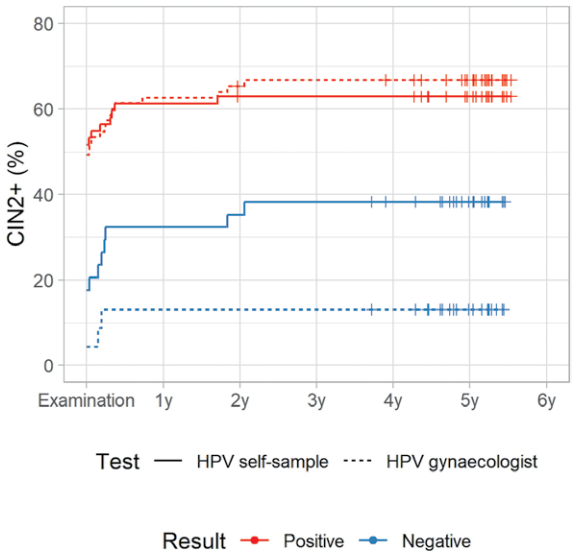


FIGURE 4B. Cumulative incidence of cervical intraepithelial neoplasia grade 2 or more (CIN2+) according to human papillomaviruses (HPV) test result in HerSwab group.

year longitudinal specificity and PPV were higher in the Qvintip group compared to the HerSwab group, regardless the sampling modality and test (Figures 2 and 3, Supplementary Table 1).

Relative performance of HPV self-sampling versus cytology after four-years' follow-up in the HerSwab group with relative sensitivity (1.05), specificity (1.02), PPV (1.03), and NPV (1.01) indicate a similar accuracy of those two testing methods, which is also evident from the close position of red and blue circles in Figures 2 and 3. In the Qvintip group, the relative sensitivity of HPV self-sampling versus cytology (1.16) and relative NPV (1.04) indicates a slightly higher sensitivity with similar NPV, yet a lower specificity (relative 0.68) and PPV (relative 0.90) of self-sampling compared to cytology.

Relative sensitivity, NPV and PPV of HPV self-sampling versus HPV test of clinician-taken samples after four-years' follow-up in the HerSwab group (0.80, 0.71, 0.94) and Qvintip group (0.88, 0.73 and 0.95) indicate lower sensitivity, NPV and PPV of self-sampling compared to HPV test on clinician samples in both device groups. However, relative specificity of HPV self-sampling compared to HPV test on clinician-taken sample indicates a similar specificity in HerSwab (1.07) and a lower one in Qvintip (0.89).

None of the differences between HPV tests on self-collected samples and cytology or HPV test on a sample taken by gynaecologists was statistically significant. The same applies to differences between the two self-sampling devices.

## Cumulative incidence of CIN2+

Figures 4A and 4B show a cumulative incidence of CIN2+ in a five-year follow-up period in the Qvintip and HerSwab group according to the result of HPV self-sampling and HPV test on clinician-taken samples. Most of the CIN2+ cases were detected in the first half of a year after examination at the colposcopy clinic. There were few CIN2+ cases between year two and three and no CIN2+ in years three to five.

For HPV-negative women, the cumulative incidence of CIN2+ after four-years follow up was similar in both device groups; however, it was two-times higher after a negative HPV test on self-samples (37.5%, 95% CI: 18.3–52.2% and 38.2%, 95% CI: 19.5–52.6%) than after a negative HPV test on a clinician-taken sample (14.8%, 95% CI: 0.3–27.2% and 13.0%, 95% CI: 0.0–25.8%). On the other hand, HPV-positive women in the Qvintip group had higher cumulative incidence of CIN2+ after four-years follow up compared to HerSwab group women. However, the difference between HPV self-sampling and a clinician-taken HPV test was small (75.6%, 95% CI: 64.0–83.5% and 62.9%, 95% CI: 48.7–73.2% *vs.* 79.8%, 95% CI: 69.1–86.8% and 66.7%, 95% CI: 54.1–75.9%) (Figures 4A and 4B, Suppl. Table 3).

**TABLE 1.** Concordance of human papillomavirus (HPV) test results (among devices) and cytology (among laboratories)

| | HPV test | | Cytology | |
|---|---|---|---|---|
| | OPA (%) | kappa (95% CI) | OPA[a] (%) | kappa (95% CI) |
| **Qvintip group** | 81.8 | 0.534 (0.349–0.718) | 74.8 | 0.471 (0.3029–0.641) |
| **HerSwab group** | 77.1 | 0.456 (0.2569–0.655) | 74.5 | 0.406 (0.2059–0.607) |
| **Total** | 79.6 | 0.495 (0.3599–0.632) | 74.6 | 0.444 (0.3159–0.574) |

CI = confidence interval; OPA = overall percent agreement

### Agreement of tests

The overall percent agreement (OPA) between HPV test on a self-sample and a sample taken by a gynaecologist was 79.6% (kappa 0.495) and similar in both device groups (Table 1).

## Discussion

This is the first time we are presenting the results of the Slovenian HPV self-sampling pilot study in the colposcopy population within the organised, population-based Slovenian cervical cancer screening programme ZORA. Four-year longitudinal accuracy and cumulative incidence of CIN2+ for HPV testing with samples taken by Qvintip and HerSwab self-sampling devices were analysed and compared to cytology and HPV tests with clinician-taken samples. The prevalence of HPV positive self-sampling results in our group of patients was 67.0%. In colposocpy studies among women with abnormal cervical smears, the reported prevalence of self-collected HPV positive tests ranges between 30 and 77%.[15-21] We found more positive HPV tests in the Qvintip group compared to the HerSwab group (70.3% *vs* 63.3%) probably due to a lower age of women and higher prevalence of CIN2+ in the Qvintip group compared to the HerSwab group.

Our results showed a higher sensitivity to detected CIN2+ in clinician-taken samples comparing to both self-sampling devices after 1 and 4 years. Specificity was higher in clinician-taken samples in the Qvintip group (57.8% *vs.* 45.5% after 1 year and 57.5% *vs*. 51.3% after 4 years) comparing to self-sampling; however, the specificity in the HerSwab group was slightly higher in self-sampling samples compared to clinician-taken samples (48.9% *vs.* 41.7% after 1 year and 47.7% *vs.* 44.4% after 4 years). This finding is consistent with most of reports indicating that HPV self-sampling has a lower sensitivity compared to clinician-taken samples and with of meta-analysis results published in 2014 by Arbyn *et al.*, which included 36 studies and more than 154,500 women. Pooled sensitivity of HPV self-sampling to detect CIN2+ was 76% and specificity 86% while the pooled sensitivity and specificity of HPV testing on self-samples was lower than HPV testing with clinician-taken samples.[22]

In contrary, results of a Netherlands randomised study showed no difference between self-sampling and clinician-taken sampling of CIN2+ sensitivity (self-sampling 92.9%; clinician sampling 96.4%) and specificity (self-sampling 93.9%; clinician sampling 94.2%) of HPV testing.[23]

Arbyn's meta-analysis was updated in 2017 and HPV tests were categorized into polymerase chain reaction (PCR) and signal amplification-based tests. HPV self-sampled assays based on PCR were as sensitive and specific on self-samples as on clinician samples to detect CIN2+. However, self-sampled HPV tests based on signal amplification were not as accurate for the detection of CIN2+.[11]

There was no statistically significant difference between the two testers used in our study regarding accordance to clinician-obtained HPV test. Other authors who compared Qvintip or HerSwab with other self-sampling devices for in their studies also did not find any differences in accordance to clinician-obtained samples.[19,24]

The concordance of self-performed vaginal samples and clinician-performed cervical samples has been the topic of a large number of studies. In our study, the agreement was lower as generally reported in literature, especially in the HerSwab group (OPA 77.1%, kappa 0.456) comparing to the Qvintip group (81.8%, kappa 0.534), although the difference between two testers was not statistically significant. In a 2005 meta-analysis by Ogilvie *et al.*, data from 12 studies were included and kappa values between patients and clinician obtained samples ranged from 0.45-1.00.[25] A systematic review and meta-analysis of 18 studies published in 2007 by Petignat *et al.*, found a concordance between self-sampled and physician-sampled specimens

for detection of HPV DNA in 87.0%, pooled kappa value of 0.66.[26] Most recent studies reported OPA between vaginal self-obtained and cervical clinician-obtained samples for the detection of HPV to be between 91.2 and 96.8%.[19,27-32] The studies using the same self-sampling devices as in our study reported better agreement as well. In a German study, the Qvintip tester showed OPA with clinician collected sample in 89.0% (kappa 0.779), which is better than in our group of patients using the same type of self-sampling device (81.8%).[19] El-Zein *et al*. reported a better agreement for HerSwab device with a kappa value of 0.84 compared to our group of patients (kappa 0.456).[32]

In a CASSIS study, HerSwab was used among others self-sampling devices and showed higher sensitivity (88.6%) and specificity (58.1%) than the one found in our study (77.6% and 48.9% after 1 year; 75.0% and 47.7% after 4 years).[24] Sensitivity (92.4%) with clinician sampling was similar to ours and specificity (58.7%) was similar to that in our Qvintip group. In the same study, PPVs for CIN2+ were 28.0% and 29.7% for HerSwab and clinician taken samples respectively, which is quite lower compared to results in our group using the same self-sampling device (61.3% and 62.3% after 1 year; 62.9% and 66.7% after 4 years).[24] The underlying reason is probably the different prevalence of the diseases. In our study, CIN2+ was diagnosed in 116 women (55.5%) one year after enrolment and four years after enrolment in 124 (59.3%) women. In a CASSIS study of 1217 women, 1076 had complete results for HPV and cytology; 148 (13.8%) had CIN1, 147 (13.7%) had CIN2/3, and 5 (0.5%) had cancer.

Relative sensitivity seems somehow higher in Qvintip compared to HerSwab, HPV self-sampling versus HPV test on clinician-taken samples (83.1/94.4 = 0.88 *vs.* 75.0/94.3 = 0.80) as well as in HPV self-sampling versus cytology (83.1/71.8 = 1.16 *vs.* 75.0/71.7 = 1.05). However, relative specificity seems slightly higher in HerSwab compared to Qvintip, HPV self-sampling versus HPV test on clinician-taken samples (51.3/57.5 = 0.89 *vs.* 47.7/44.4 = 1.07), as well as in HPV self-sampling versus cytology (51.3/75.0 = 0.68 *vs.* 47.7/46.7 = 1.02).

The sensitivity of cytology and HPV test on clinician-taken samples in our colposcopy study were similar between the Qvintip (71.8% and 94.4%) and HerSwab group (71.7% and 94.3%) and higher than in the recent Cochrane database systematic review of comparisons of HC2 results versus conventional cytology (ASC-US+ threshold) in the general population, where the pooled sensitivity of cytology was 62.5% and for HPV test on clinician-taken samples 89.9%.[33]

In a CASSIS study cytology ASC-US+ was 80.2% sensitive and 61.4% specific for CIN2+.[24] The systematic review and meta-analysis in low and middle-income countries included more than 700 cervical cancers from 23 studies and found pooled sensitivity of cytology for cancer 79.4% at a cut-off HSIL+.[34] On the other hand, Greek study authors reported about a very low sensitivity of cytology, 13.6% at cut-off HSIL.[35]

It is known that cervical cytology has limited sensitivity and that results may vary between different pathologists and laboratories and that HPV testing detects more cervical intraepithelial neoplasia than cytology. Therefore, some countries (Netherlands, Great Britain) implemented HPV testing as a primary screening test.[36,37] Randomised clinical trials were conducted in many developed countries to evaluate primary HPV testing for cervical cancer screening in an organized program setting.

However, HPV testing has limitations. One of them is natural history of HPV infection, which is very common in young, sexually active women, but in majority of cases the infection is transient. Therefore, is not reasonable to use HPV testing for cervical screening in young women. Also, in elderly women positive HPV test does not necessarily imply the presence of precancerous cervical lesion. On the other hand, women with negative HPV test, have an extremely low risk of developing cervical cancer.

The European Guidelines do not recommend primary HPV screening before the age of 30 and are in favour of screening starting at the age of 35. Since HPV testing on self-taken samples is less accurate than on clinician-taken samples, self-sampling is recommended only for non-attenders in local settings.[38] As HPV testing has a higher sensitivity than cytology in elderly population[39-41], self-sampling and HPV testing may be a good alternative for non-attenders to cervical screening in this age group.

## Conclusions

Self-sampling for HPV testing was less accurate compared to HPV testing on clinician-taken samples; however, there was no statistically significant difference between two testers used in our study. Conventional cytology was found to have a lower sensitivity for CIN2+ than HPV testing. Our study

included relatively young women with an average age below 40 and we assume that the difference in sensitivity may be even greater in elderly population. The self-sampled HPV test is no less sensitive than cytology and can be safely applied in non-responders to the national ZORA program. However, this kind of screening might also be more suitable for women who used to attend regular gynaecological check-ups.

## Acknowledgment

The authors would like to thank Maja Primic Žakelj, Mojca Florjančič and Mojca Kuster from the NP ZORA coordination centre at the Institute of Oncology Ljubljana for their leading role in the coordination of the study. Special thanks goes to the gynaecologists, nurses and other experts who were involved in the study at all three institutions: Alenka Repše Fokter, Mateja Marčec, Maja Pakiž, Tatjana Kodrič, Andrej Cokan, Sarah Dobnik, Jure Knez, Marica Miklavc, Marcela Živko, Aleksandra Muhič, Uršula Salobir Gajšek, Jakob Koren, Veronika Kloboves Prevodnik and Nataša Nolde. Last but not least, we also thank all the women who participated in the study.

Study was approved for public funding by the Slovenian Research Agency (ARRS) (project number L3-5512). It was financed by ARRS and Ministry of Health of Republic of Slovenia. Materials used in the study were obtained free of charges or with discount from manufacturers. ARRS, Ministry of Health and manufacturers didn`t have any role in the design of the study, study execution, analyses, interpretation of the data, or decision to submit results.

## References

1. Meggiolaro A, Unim B, Semyonov L, Miccoli S, Maffongelli E, La Torre G. The role of Pap test screening against cervical cancer: a systematic review and meta-analysis. *Clin Ter* 2016; **167:** 124-39. doi: 10.7417/CT.2016.1942
2. Jansen EEL, Zielonke N, Gini A, Anttila A, Segnan N, Vokó Z, et al. Effect of organised cervical cancer screening on cervical cancer mortality in Europe: a systematic review. *Eur J Cancer* 2020; **127:** 207-23. doi: 10.1016/j.ejca.2019.12.013
3. Zadnik V, Primic Zakelj M, Lokar K, Jarm K, Ivanus U, Zagar T. Cancer burden in Slovenia with the time trends analysis. *Radiol Oncol* 2017; **51:** 47-55. doi: 10.1515/raon-2017-0008
4. National Cervical Cancer Screening Programme ZORA. DP ZORA: kazalniki. [internet]. [cited 2020 Jan 6]. Available at: https://zora.onko-i.si/publikacije/kazalniki/
5. National Cervical Cancer Screening Programme ZORA. [internet]. [cited 2020 Jan 6]. Available at: https://zora.onko-i.si/
6. Benett KF, Waller J, Chorley AJ, Ferrer RA, Haddrell JB, Marlow LAV. Barriers to cervical screening and interest in self-sampling among women who actively decline screening. *Med Screen* 2018; **25:** 211-7. doi: 10.1177/0969141318767471
7. Logan L, Mcilfatrick S. Exploring women's knowledge, experiences and perceptions of cervical cancer screening in an area of social deprivation. *Eur J Cancer Care* 2011; **20:** 720-7. doi: 10.1111/j.1365-2354.2011.01254.x
8. Arbyn M, Ronco G, Anttila A, Meijer CJLM, Poljak M, Ogilvie G, et al. Evidence regarding human papillomavirus testing in secondary prevention of cervical cancer. *Vaccine* 2012; **30:** 88-99. doi: 10.1016/j.vaccine.2012.06.095
9. Verdoodt F, Jentschke M, Hillemanns P, Racey CS, Snijders PJ, Arbyn M. Reaching women who do not participate in the regular cervical cancer screening programme by offering self-sampling kits: a systematic review and meta-analysis of randomised trials. *Eur J Cancer* 2015; **51:** 2375-85. doi: 10.1016/j.ejca.2015.07.006
10. Yeh PT, Kennedy CE, de Vuyst H, Narasimhan M. Self-sampling for human papillomavirus (HPV) testing: a systematic review and meta-analysis. *BMJ Global Health* 2019; **4:** e001351. doi: 10.1136/bmjgh-2018-001351
11. Arbyn M, Smith SB, Temin S, Sultana F, Castle P; Collaboration on Self-Sampling and HPV Testing. Detecting cervical precancer and reaching underscreened women by using HPV testing on self samples: updated meta-analyses. *BMJ* 2018; **363:** k4823. doi: 10.1136/bmj.k4823
12. Ivanus U, Jerman T, Fokter Repse A, Takac I, Prevodnik VK, Marcec M, et al. Randomised trial of HPV self-sampling among non-attenders in the Slovenian cervical screening programme ZORA: comparing three different screening approaches. *Radiol Oncol* 2018; **52:** 399-412. doi: 10.2478/raon-2018-0036
13. Guidelines for management of women with cervical precancerous lesions. Ursic-Vrscaj M, Rakar S, Možina A, Kobal B, Takač I, Deisinger I, editors. Ljubljana; Institute of Oncology Ljubljana; 2011. [internet]. [cited 2020 Jan 20]. Available at: https://zora.onko-i.si/fileadmin/user_upload/dokumenti/strokovna_priporocila/2011_Smernice_web.pdf
14. R Core Team. R: a language and environment for statistical computing. Vienna: R Foundation for Statistical Computing; 2020. [internet]. [cited 2020 Jan 20]. Available at: http://www.R-project.org/
15. Jentschke M, Soergel P, Hillemanns P. Evaluation of multiplex real time PCR assay for the detection of human papillomavirus infection on self-colleceted cervicovaginal lavage samples. *J Clin Virol* 2013; **193:** 131-4. doi: 10.1016/j.jviromet.2013.05.009
16. Aiko KY, Yoko M, Saito OM, Ryoko A, Yasuyo M, Mikiko AS, et al. Accuracy of self-collected human papillomavirus samples from Japanese women with abnormal cervical cytology. *J Obstet Gynaecol Res* 2017; **43:** 710-7. doi: org/10.1111/jog.13258
17. Nobbenhuis MAE, Helmerhorst TJM, Van den Brule AJC, Rozendaal L, Jaspar LH, Voorhorst FJ, et al. Primary screening for high risk HPV by home obtained cervicovaginal lavage is an alternative screening tool for unscreened women. *J Clin Pathol* 2002; **55:** 435-9. doi: 10.1136/jcp.55.6.435
18. Sellors JW, Lorincz AT, Mahony JB, Mielzynska I, Lytwyn A, Roth P, et al. Comparison of self-collected vaginal. Vulvar and urine samples with physician-collected cervical samples for human papillomavirus testing to detect high-grade squamous intraepithelial lesions. *CMAJ* 2000: **163:** 513-8. PMID: 11006761
19. Jentschke M, Chen K, Arbyn M, Hertel B, Noskowicz M, Soergel P, et al. Direct comparison of two vaginal self-sampling devices for the detection of human papillomavirus infections. *J Clin Virol* 2016; **82:** 46-50. doi: 10.1016/j.jcv.2016.06.016
20. Darlin L, Bergfeldt C. Forslund O, Hénic E, Dillner J, Kannisto P. Vaginal self-sampling without preservative for human papillomavirus testing shows good sensitivity. *J Clin Virol* 2013; **56:** 52-6. doi: 10.1016/j.jcv.2012.09.002
21. Seo SS, Song YS, Kim JW, Park NH, Kang SB, Lee HP. Good correlation oh HPV DNA test between self-collected vaginal and clinician-collected cervical samples by the oligonucleotide microarray. *Gynecol Oncol* 2006; **102:** 67-73. doi: 10.1016/j.ygyno.2005.11.030
22. Arbyn M, Verdoodt F, Snijeders PJF, Verhoef VMJ, Suonio E, Dillner L, et al. Accuracy of human papillomavirus testing on self-collected versus clinician-collected samples: a meta-analysis. *Lancet Oncol* 2014; **15:** 172-83. doi: 10.1016/S1470-2045(13)70570-9

23. Polman NJ, Ebisch RMF, Heideman DAM, Melchers WJG, Bekkers DAM, Molijn AC, et al. Performance of human papillomavirus testing on self-collected versus clinician-collected samples for the detection of cervical intraepithelial neoplasia of grade 2 or worse: a randomised, paired screen-positive, non-inferiority trial. *Lancet Oncol* 2019; **20:** 229-38. doi: 10.1016/S1470-2045(18)30763-0

24. El-Zein M, Bouten S, Louvanto K, Gilbert L, Gotlieb W, Hemnings R, et al. Validation of a new HPV self-sampling device for cervical cancer screening: the cervical and self-sample in screening (CASSIS) study. *Gynecol Oncol* 2018; **149:** 491-7. doi: 10.1016/j.ygyno.2018.04.004

25. Ogilvie GS, Patrick DM, Schulzer M, Sellors JW, Petric M, Chambers K, et al. Diagnostic accuracy of self-collected vaginal specimens for human papillomavirus compared to clinician collected human papillomavirus specimens: a meta-analysis. *Sex Transm Infect* 2005; **8:** 207-12. doi: 10.1136/sti.2004.011858

26. Petignat P, Faltin DL, Bruchim I, Tramèr MR, Franco EL, Coutlée F. Are self-collected samples comparable to physician-collected cervical specimens for human papillomavirus DNA testing? A systematic review and meta-analysis. *Gynecol Oncol* 2007; **105:** 530-5. doi: 10.1016/j.ygyno.2007.01.023

27. Boggan JC, Walmer DK, Henderson G, Chakhtoura N, McCarthy SH, Beauvais HJ, et al. Vaginal self-sampling for human papillomavirus infection as a primary cervical cancer screening tool in a Haitian population. *Sex Transm Dis* 2015; **42:** 655-9. doi: 10.1097/OLQ.0000000000000345

28. Leinonen MK, Schee K, Jonassen CM, Lie AK, Nystrand CF, Rangberg A, et al. Safety and acceptability of human papillomavirus testing of self-collected specimens: a methodologic study of the impact of collection devices and HPV assays on sensitivity for cervical cancer and high-grade lesions. *J Clin Virol* 2017; **9:** 22-30. doi: 10.1016/j.jcv.2017.12.008

29. Toliman P, Badman SG, Gabuzzi J, Silim S, Forereme L, Kumbia A, et al. Field evaluation of Xpert HPV point-of-care test for detection of human papillomavirus infection by use of self-collected vaginal and clinician-collected cervical specimens. J *Clin Microbiol* 2016; **54:** 1734-7. doi: 10.1128/JCM.00529-16

30. Obiri-Yeboah D, Adu-Sarkodie Y, Djigma F, Hayfron-Benjamin A, Abdul L, Simpore J, et al. Self-collected vaginal sampling for the detection of genital human papillomavirus (HPV) using careHPV among Ghanaian women. *BMC Womens Health* 2017; **17:** 86. doi: 10.1186/s12905-017-0448-1

31. Ketelaars PJW, Bosgraaf RP, Siebers AG, Massuger LFAG, van der Linden JC, Wauters CAP, et al. High-risk human papillomavirus detection in self-sampling compared to physician-taken smear in a responder population of the Dutch cervical screening: results of the VERA study. *Prev Med* 2017; **101:** 96-101. doi: 10.1016/j.ypmed.2017.05.021

32. El-Zein M, Bouten S, Louvanto K, Gilbert L, Gotlieb WH, Hemmings R, et al. Predictive value of HPV testing in self-collected and clinician-collected samples compared with cytology in detecting high-grade cervical lesions. *Cancer Epidemiol Biomark Prev* 2019; **28:** 1134-40. doi: 10.1158/1055-9965.EPI-18-1338

33. Koliopoulos G, Nyaga VN, Santesso N, Bryant A, Martin-Hirsch PP, Mustafa RA, et al. Cytology versus HPV testing for cervical cancer screening in the general population. *Cochrane Database Syst Rev* 2017; **8:** CD008587. doi: 10.1002/14651858.CD008587.pub2

34. Castanov A, Landy R, Michalopoulos D, Bhudia R, Leaver H, Qiao YL, et al. Systematic review and meta-analysis of individual patient data to assess the sensitivity of cervical cytology for diagnosis of cervical cancer in low- and middle-income countries. *J Glob Oncol* 2017; **3:** 524-38. doi: 10.1200/JGO.2016.008011

35. Pesic A, Krings A, Hempel M, Preyer R, Chatzistamatius K, Agorastos T, et al. CIN2+ detection of the HPV DNA Array genotyping assay in comparison with the Cobas 4800 HPV test and cytology. *Virol J* 2019; **16:** 92. doi: 10.1186/s12985-019-1197-6

36. Polman NJ, Snijders PJF, Kenter GG, Berkhof J, Meijer CJLM. HPV-based cervical screening: rationale, expectations and future perspectives of the new Dutch screening programme. *Prev Med* 2019; **119:** 108-17. doi: /10.1016/j.ypmed.2018.12.021

37. Rebolj M, Rimmer J, Denton K, Tidy J, Mathev C, Ellis K, et al. Primary cervical screening with high risk human papillomavirus testing: observational study. *BMJ* 2019; **364:** 240. doi: https://doi.org/10.1136/bmj.l240

38. von Karsa L, Arbyn M, De Vuyst H, Dillner J, Dillner L, Franchesci S, et al. European guidelines for quality assurance in cervical cancer screening. Summary of the supplements on HPV screening and vaccination. *Papillomavirus Res* 2015; **1:** 22-31. doi: /10.1016/j.pvr.2015.06.006

39. Ronco G, Giorgi-Rossi P, Carozzi F, Confortini M, Dalla Palma P, Del Mistro A, et al. New Technologies for Cervical Cancer screening (NTCC) Working Group. Efficacy of human papillomavirus testing for the detection of invasive cervical cancers and cervical intraepithelial neoplasia: a randomised controlled trial. *Lancet Oncol* 2010; **11:** 249-57. doi: 10.1016/S1470-2045(09)70360-2

40. Hermansson RS, Olovsson M, Hoxell E, Lindström AK. HPV prevalence and HPV-related dysplasia in elderly women. *PLoS One* 2018; **13:** e0189300. doi: 10.1371/journal.pone.0189300

41. Lindström AK, Hermansson RS, Gustavsson I, Hedlund Lindberg J, Gyllensten U, Olovsson M. Cervical dysplasia in elderly women performing repeated self-sampling for HPV testing. *PLoS One* 2018; **13:** e0207714. doi: 10.1371/journal.pone.0207714

*research article*

# The performance of the Xpert Bladder Cancer Monitor Test and voided urinary cytology in the follow-up of urinary bladder tumors

Tomaz Smrkolj[1,2], Urska Cegovnik Primozic[3], Teja Fabjan[3], Sasa Sterpin[3], Josko Osredkar[3,4]

[1] Department of Urology, Ljubljana University Medical Centre, Ljubljana, Slovenia
[2] Department of Surgery, Faculty of Medicine, University of Ljubljana, Ljubljana, Slovenia
[3] Clinical Institute of Clinical Chemistry and Biochemistry, Ljubljana University Medical Centre, Ljubljana, Slovenia
[4] Faculty of Pharmacy, University of Ljubljana, Ljubljana, Slovenia

Radiol Oncol 2021; 55(2): 196-202.

Received 22 September 2020
Accepted 3 November 2020

Correspondence to: Prof. Joško Osredkar, Ph.D., Clinical Institute of Clinical Chemistry and Biochemistry, Ljubljana University Medical Centre, SI-1000 Ljubljana, Slovenia. E-mail: josko.osredkar@kclj.si

Disclosure: The Xpert® Urine Transport Reagent kits and Xpert® Bladder Cancer Cartridges were provided free of charge by Biomedis M.B. d.o.o., Jurančičeva ul. 11, Maribor, Slovenia. The costs of the application of the present study at The National Medical Ethics Committee of the Republic of Slovenia were covered by Biomedis M.B. d.o.o., Jurančičeva ul. 11, Maribor, Slovenia. No other conflicts of interest are declared.

**Background.** Cystoscopy in complement with urinary cytology represents the gold standard for the follow-up of patients with urinary bladder tumours. Xpert Bladder Cancer Monitor Test (XBC) is a novel mRNA-based urine test for bladder cancer surveillance. The aim of the study was to evaluate the performance of the XBC and voided urinary cytology (VUC) in the follow-up of bladder tumours.

**Patients and methods.** The XBC was performed on stabilized voided urine and VUC was performed on urine samples. The results were compared to cystoscopic findings and histopathological results after transurethral resection of the bladder lesion.

**Results.** For the prediction of malignant histopathological result sensitivity, the specificity and negative predictive value were 76.9%, 97.5% and 93.0% for the XBC and 38.4%, 97.5% and 83.3%, respectively for VUC. For the prediction of suspicious or positive cystoscopic finding sensitivity, the specificity and negative predictive value were 75.0%, 95.2%, and 93.0% respectively for the XBC and 41.7%, 97.6%, and 85.4% for VUC. The sensitivities for papilary urothelial neoplasms of low malignant potential (PUNLMP), low- and high-grade tumours were 0.0%, 66.7% and 100.0% for the XBC and 0.0%, 66.7% and 42.9%, respectively for VUC.

**Conclusions.** The XBC showed significantly higher overall sensitivity and negative predictive value than VUC and could be used to increase the recommended follow-up cystoscopy time intervals. Complementing the XBC and voided urinary cytology does not improve performance in comparison to the XBC alone.

Key words: cystoscopy; Xpert BC Monitor Test; urinary bladder neoplasm; voided urinary cytology

## Introduction

Bladder cancer is the ninth most common cancer worldwide. The estimated age-standardized incidence rate of bladder cancer in Europe in 2012 was 17.7 per 100,000 in men and 3.5 per 100,000 in women.[1] Ninety percent of bladder tumours are urothelial carcinomas of which 80% are classified as a superficial disease at presentation[2], while the rest invade the muscularis propria of the detrusor.

The gold standard for diagnosing and following up bladder tumours is cystoscopy complemented with voided urinary cytology (VUC), and computer tomography urography (CTU), to exclude urothelial carcinoma of the upper urinary tract.[3] Cystoscopy is an invasive and painful procedure with potential short- and long-term complications.

VUC on the other hand is noninvasive, detects urothelial carcinoma in both lower and upper urinary tracts, but its sensitivity for detecting well-differentiated bladder tumours is as low as 16% in contrast to 84% for high-grade tumours[4], therefore VUC cannot replace cystoscopy. The overall sensitivity of CTU for diagnosing bladder cancer is also insufficient to obviate cystoscopy.[5]

In the past two decades, numerous urinary markers for the detection of bladder tumours have been devised, but despite numerous studies, none of these markers have been accepted for diagnosis or follow-up in routine practice or clinical guidelines.[3] Nuclear matrix protein 22 (NMP22), the bladder tumour antigen stat (BTA) test, BTA TRAK test, Immuno Cyt, and fibroblast growth factor receptor 3 (FGFR 3) are FDA approved and commercially available, while many other biomarkers are still being evaluated.[6]

Xpert BC Monitor Test (XBC) is a novel mRNA-based urine test for bladder cancer surveillance, which measures five target mRNAs encoding the following proteins: tyrosine-protein kinase ABL1, corticotropin-releasing hormone (CRH), insulin growth factor 2 (IGF2), uroplakin 1B (UPK1B), and annexin A10 (ANXA10). Except UPK1B, which is a structural protein found in urothelial cells, these proteins play multiple roles during carcinogenesis and are implicated in cell proliferation, division, differentiation, growth, adhesion and signalling. Overall sensitivity (84%) and negative predictive value (93%) of the XBC were reported to be significantly superior to VUC by Pichler *et al*., who published the first study on the XBC in 2017.[7] Since the XBC is noninvasive and requires little additional time and labour for processing of samples in an outpatient setting, it might represent a promising candidate for routine urinary test in follow-up of urinary bladder tumours.

The aims of our study were to compare the performance of XBC and VUC and to determine whether the clinical performance of the XBC is high enough to reduce the need for cystoscopy in follow-ups of urinary bladder tumours.

## Patients and methods

### Patients

The study was approved by The National Medical Ethics Committee of the Republic of Slovenia (0120-566/2018/5) and informed consent was obtained from each participant.

The exclusion criteria were a history of urinary stone disease, ongoing urinary tract infection, suspicion of upper urinary tract tumour, a presence or history of foreign bodies (stent, nephrostomy tube), an invasive procedure on the urinary tract in the past 2 weeks (3 months in case of transurethral resection (TUR) procedure), intravesical chemotherapy or immunotherapy in the past 3 months and prior systemic chemotherapy or radiotherapy of the pelvis.

A total of 54 patients previously diagnosed with bladder tumours were prospectively enrolled in our study from January 2019 to October 2019.

### Detection methods

A single voided urinary specimen was collected before conventional white light cystoscopy during a follow-up visit. The frequency of follow-up cystoscopies was based on the European association of urology (EAU) guidelines.[8] The urine specimen was divided to provide samples for the XBC (4.5ml) and voided urinary cytology (minimally 50 ml). Voided urinary cytology was analysed in the cytopathological laboratory of the Institute of Pathology, Faculty of Medicine, Ljubljana, Slovenia, and reported according to the Paris classification system.[9] The results were classified as negative, suspicious, or positive. In the analysis, suspicious results and cellular atypia were included in the positive group for the comparison of detection performance.

In addition to urine cytology, we also analysed urine samples with the Xpert BC Monitor test (Cepheid, Sunnyvale, CA, USA), which measured the levels of five target mRNAs (ABL1, CRH, IGF2, UPK1B, ANXA10) using reverse transcriptase polymerase chain reaction (RT-PCR) according to the manufacturer's protocol. 4.5 ml of collected urine was transferred to the prepared transport medium within 1 hour after collection and thus stabilized. The sample thus prepared is stable for up to 7 days at temperatures between 2°C and 28°C. The urine thus prepared was transferred to a reagent cartridge in the laboratory, which contained all the reagents needed for RT-PCR analysis. Automated processing included filter capture on cells, lysis of cells by sonication, addition of nucleic acid to dry RT-PCR reagents, transfer to a reaction chamber, RT-PCR multiplexing, and detection. Sample adequacy monitoring (ABL1) ensures that the sample contains human cells and human RNA. An ABL1 signal was required for a valid test result. The internal control detects pattern-related inhibition of

RT-PCR. Control by probe verification (measurement of the fluorescence signal from the probes) is performed prior to sample analysis to monitor bead rehydration, cartridge filling in the cartridge, probe integrity, and toner stability. The Xpert BC Monitor test gives results as "positive" and "negative" based on the results of a linear discriminant analysis (LDA) algorithm that uses the results of the cycle threshold (Ct) of five mRNAs: ABL1, CRH, IGF2, UPK1B and ANXA10 (LDA total calculation). The measurement result is valid if the total LDA value is in the range of -20 to 20. The interpretation of the result is as follows: A "positive" result is obtained if the total LDA is equal to or exceeds the limit value; and ABL1 Ct and total LDA are within the valid range. Not all mRNA targets need be detected for a "positive" test result. A "negative" result is achieved if the LDA Total is below the limit value; and ABL1 Ct is within the valid range. The total LDA of the manufacturer is 0.50 and was determined on the basis of statistical analysis of a large number of samples.[7,10]

The histopathological report on the transurethral resection of a bladder lesion was done by the histopathological laboratory of the Institute of Pathology, Faculty of Medicine, Ljubljana, Slovenia. The tumour stage was reported according to the TNM classification of malignant tumours, 8th edition, 2017[11], and the tumour grade was classified according to the 2016 WHO classification.[12] The stage and grade from the histopathological report were used in the analysis of results.

### Statistical analysis

Data was analysed using the SPSS software (Statistical Package for the Social Sciences, version 22.0, IBM Corp., Armonk, NY, USA). After testing for normal distribution using the Shapiro Wilk normality test for the variables, differences in the LDA total were compared using the Mann-Whitney U test for benign and malignant histology groups, negative and positive cistoscopy groups, and negative and positive cytology groups. The optimal cut-off value of the LDA total was determined using the Youden index method, after which the receiver operating characteristic (ROC) curve was calculated to determine the performance of the Xpert BC Monitor test. The diagnostic value of the XBC and VUC was tested by determining the sensitivity (number of true positive tests / sum of number of true positive and false negative tests), specificity (number of true negative tests / sum of true negative and false positive tests) and positive (PPV - number of true positive tests / sum of true positive and false positive tests) and negative (NPV- number of true negative tests / sum of true negative and false negative tests) predictive value. A $p$ value less than 0.05 was considered statistically significant.

## Results

The XBC and VUC were performed in 54 patients scheduled for check-up using conventional white light urethrocystoscopy. Indications for transurethral resection after check-up urethrocystoscopy were: visible recidivant tumour in 12 patients, atypia in VUC in 1 patient, and a missed recidivant tumour that was only discovered during the subsequent check-up urethrocystoscopy. A histology report on the transurethral resection of the bladder lesion was obtained in 12 patients, whereas 2 patients only had electrocoagulation performed on clearly visible malignant recidivant tumours and these two are counted as malignant in further analysis. Out of the 12 histology reports, 11 were malignant and 1 was benign. Patients who had not undergone transurethral resection after the check-up urethrocystoscopy are counted as negative/benign in the histology analysis.

The median LDA totals were 0.2474 (0.1331-0.3617) and 0.8102 (0.4367-1.1836) in the negative and positive cystoscopy groups respectively (Mann-Whitney U = 73.00, $p < 0.000$). The median LDA totals were 0.2486 (0.1286–0.3685) and 0.9869 (0.8872–1.0866) in the negative and positive cytology groups respectively (Mann-Whitney U = 12.00, $p < 0.000$). The Median LDA totals were 0.2467 (0.1357–0.3578) and 0.9273 (0.5904–1.2642) in the negative/benign and malignant histology groups respectively (Mann-Whitney U = 63.00, $p < 0.000$).

Area under the curve in the receiver operating characteristic (ROC) curve for the XBC in predicting cystoscopic finding was 0.855 with a 95% confidence interval between 0.722 and 0.998 (n = 54) (Figure 1).

The area under the curve in the receiver operating characteristic (ROC) curve for the XBC in predicting histology result was 0.882 with a 95% confidence interval between 0.759 and 1.000 (n = 54) (Figure 2).

From the ROC curve for the prediction of cystoscopic findings and histology results, the optimal cut-off value of 0.4923 for the LDA total was determined using the Youden method.

For the prediction of positive cystoscopic findings, the sensitivity and specificity were 75.0% and

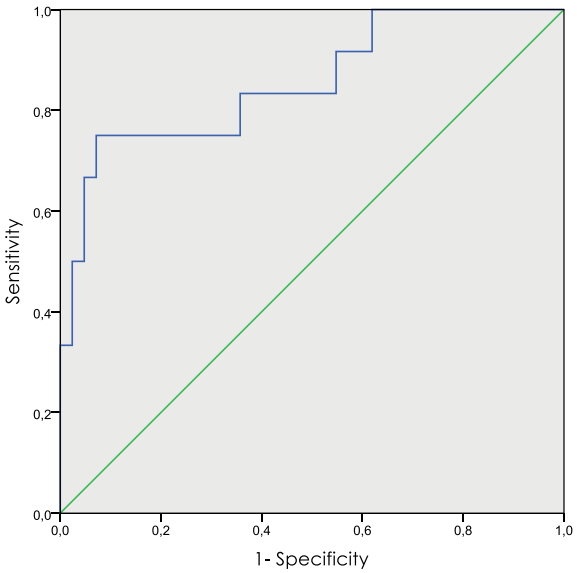


FIGURE 1. ROC curve for predicting cystoscopic finding.

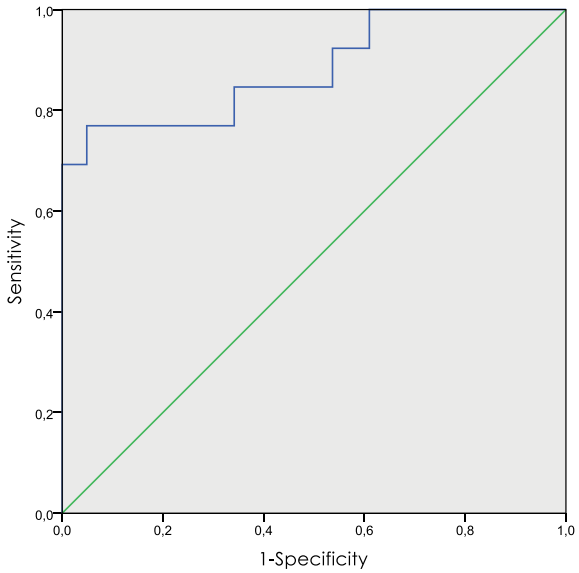


FIGURE 2. ROC curve for histology prediction.

95.2% respectively for the XBC (at optimal 0.4923 cut-off value) and 41.7% and 97.6% for VUC. For the prediction of malignant histological results, the sensitivity and specificity were 76.9% and 97.5% respectively for the XBC (at optimal 0.4923 cut-off value) and 38.4% and 97.5% for VUC. Combining the results of the XBC and VUC did not improve the detection of bladder tumours since VUC did not identify any additional patient that was not already positive in the XBC (Tables 2 and 3).

Stratification for grade sensitivities of the XBC were 0.0%, 66.7%, and 100% for papilary urothelial neoplasms of low malignant potential (PUNLMP), low-grade, and high-grade tumours respectively, while the sensitivities of VUC were 0.0%, 66.7%, and 42.9% for the same grade categories respectively. Stratification for stage sensitivities of the XBC were 100%, 80.0%, 100%, and 100% for carcinoma in situ (CIS), Ta, T1 and T2 tumours, respectively, while the sensitivities of VUC were 50.0%, 40.0%, 50.0% and 100% for the same stage categories respectively. (Table 4).

## Discussion

In our study, we have evaluated two voided urinary tests: the XBC and VUC in the follow-ups of urinary bladder tumours. Despite the availability of noninvasive urinary tests, cystoscopy complemented with VUC is still the gold standard for the follow-up of urinary bladder tumours.[3] Urinary cytology has low sensitivity for low-grade tumours, which are the most numerous and represent two-thirds of primarily diagnosed bladder tumours.[13] Consequently, the Paris system for reporting urinary cytology was introduced in 2015, instructing cytopathologists to emphasize that a negative result is only valid for high-grade tumours and "suspicious for high grade urothelial carcinoma" and "atypia" categories are still present in this new classification and are reported based on cell characteristics and numbers.[14] Low grade urothelial neoplasia (LGUN) should only be reported if strict criteria are satisfied, but a suggestion of LGUN can

TABLE 1. Summary of the patients' demographics and test results numbers

| Gender | Number of patients | Mean age, years ± SD |
|---|---|---|
| All | 54 (100.0%) | 70.5 ± 8.8 |
| Male | 42 (77.8%) | 70.5 ± 8.7 |
| Female | 12 (22.2%) | 70.5 ± 9.6 |
| **Noninvasive test / standard invasive diagnostic procedure** | **Number of patients with TP / FN / TN / FP noninvasive test result** | |
| XBC / cystocopy (LDATC 0.4923)<br>XBC / cystocopy (LDATC 0.5) | 9 / 3 / 40 / 2<br>8 / 4 / 40 / 2 | |
| VUC / cystoscopy | 5 / 7 / 41 / 1 | |
| XBC / histology (LDATC 0.4923)<br>XBC / histology (LDATC 0.5) | 10 / 3 / 40 / 1<br>9 / 4 / 40 / 1 | |
| VUC / histology | 5 / 8 / 40 / 1 | |

FN = false negative; FP = false positive; LDATC = linear discriminant analysis total cut-off; SD = standard deviation; TN = true negative; TP = true positive; VUC = voided urinary cytology; XBC = Xpert BC Monitor Test

**TABLE 2.** Specificity, sensitivity and positive and negative predictive value of noninvasive urinary tests for the prediction of positive cystoscopic findings

| Test | Sensitivity | Specificity | PPV | NPV |
|---|---|---|---|---|
| XBC, LDATC 0.4923 | 75.0% | 95.2% | 81,8% | 93.0% |
| XBC, LDATC 0.5 | 66.7% | 95.2% | 80.0% | 90.9% |
| VUC | 41.7% | 97.6% | 83.3% | 85.4% |
| XBC, LDATC 0.4923 + VUC | 75.0% | 95.2% | 81,8% | 93.0% |

LDATC = linear discriminant analysis total cut-off; NPV = negative predictive value; PPV = positive predictive value; VUC = voided urinary cytology; XBC = Xpert BC Monitor Test

**TABLE 3.** Specificity, sensitivity and positive and negative predictive value of noninvasive urinary tests for the prediction of positive histological results

| Test | Sensitivity | Specificity | PPV | NPV |
|---|---|---|---|---|
| XBC, LDATC 0.4923 | 76.9% | 97.5% | 90,9% | 93.0% |
| XBC, LDATC 0.5 | 69.2% | 97.5% | 90.0% | 90.9% |
| VUC | 38.4% | 97.5% | 83.3% | 83.3% |
| XBC, LDATC 0.4923 + VUC | 76.9% | 97.5% | 90,9% | 93.0% |

LDATC = linear discriminant analysis total cut-off; NPV = negative predictive value; PPV = positive predictive value; VUC = voided urinary cytology; XBC = Xpert BC Monitor Test

be made including recommendation to repeat VUC or perform other diagnostic procedures. The cytological result is affected by the presence of several benign urinary tract conditions and is also dependent on the subjective judgment of the cytopathologist.[15]

Depending on the calculated risk of recurrence and progression, 6 to 15 cystoscopy procedures should be performed in the follow-up after the TUR of superficial bladder tumours within 5 years[3], which represents invasive instrumentation and a risk for complications for patients, as well as healthcare and economic burden.

Replacing cystoscopy with a noninvasive, simple, low-cost urine-based test with sufficient performance could modify these follow-up schedules. Such a noninvasive test should have high sensitivity to detect small recurrent high-grade tumours and avoid the growth and progression to a muscle-infiltrative disease, which considerably aggravates the patient's prognosis and quality of life.[16]

The expression levels of the markers combined in linear discriminate analysis (LDA) are used to classify samples as negative or positive using a linear model.[10] While the LDA total value primarily serves as a criterion for a positive result of the XBC at the cut-off value suggested by the manufacturer (0.5), we used the ROC curve and Youden method to optimize the cut-off value to 0.4923, which improved the sensitivity of XBC for the prediction of positive cystoscopic findings from 66.7% to 75.0%. Considering the LDA total value rather than reporting the results of the XBC as negative/positive could also be used in longitudinal studies as was shown by Hurle *et al*., who monitored the LDA total in the active surveillance of patients with non-muscle-invasive bladder cancer in the Bladder Cancer Italian Active Surveillance project (BIAS) and reported that an increasing LDA total in a patient is connected to progressing bladder tumours and could be used to initiate follow-up cystoscopy instead of enforcing firm scheduling protocols. They also proposed that in this setting, the LDA total cut-off would be 0.4.[17]

Our data shows that sensitivities of the XBC for predicting positive or suspicious cystoscopic results is considerably higher than for VUC (75.0% *vs*. 41.2% respectively), and also NPV is improved in comparison to VUC (93.0% *vs*. 85.4% respectively). The results are comparable to the results of the studies of Van Valenberg *et al*. and Pichler *et al*. (74 % and 84% for sensitivity and 93% and 93% for NPV respectively).[7,18] In contrast, the study performed by Elia *et al*. reported an overall sensitivity of only 46.2% for the XBC, though the vast majority (87%) of the detected bladder tumours in that study were low-grade.[19] In our study, none of the patients with negative XBC had a positive VUC, therefore complementing the results of the XBC

**TABLE 4.** Sensitivity of the XBC and voided urinary cytology stratified by tumour stage and grade. Number of cases detected by noninvasive test against number of cases detected by hystology analysis is shown in the parenthsis

| Test / Stage | CIS | Ta | T1 | T2 | Grade | PUNLMP | low grade | high grade |
|---|---|---|---|---|---|---|---|---|
| XBC, LDATC 0.4923 | 100% (2/2) | 80.0% (4/5) | 100% (2/2) | 100% (1/1) | | 0.0% (0/1) | 66.7% (2/3) | 100.0% (7/7) |
| VUC | 50.0% (1/2) | 40.0% (2/5) | 50.0% (1/2) | 100% (1/1) | | 0.0% (0/1) | 66.7% (2/3) | 42.9% (3/7) |

LDATC = linear discriminant analysis total cut-off; PUNLMP = papillary urinary neoplasm of low malignant potential; VUC = voided urinary cytology; XBC = Xpert BC Monitor Test

with VUC did not increase sensitivity, specificity, NPV, or PPV, which was also observed in the study by Pichler *et al*.[7]

Until more studies on the XBC have been conducted, the range of sensitivities and NPVs cannot be estimated, though our data and already published studies[7,18] show that the performance of the XBC is at least comparable to previously studied bladder cancer biomarkers for which studies have reported wide variability in performance. A recent review of bladder cancer biomarkers summarized data from several studies listing the sensitivities of NMP22 in the range of 24% to 81%, of BTA STAT 40% to 72%, of ImmunoCyt 50% to 85%, and of UroVysion 13 to 100%. Probably due to the variability in performance, the authors of this review conclude that current commercially available urinary biomarker-based tests are not sufficiently validated to be widely used in clinical practice.[20]

Cystoscopy was negative in two of our patients, who were positive in the XBC. One of them had an atypical VUC and a high-grade T1 tumour was confirmed with transurethral resection biopsy (TURB), while in another patient with negative VUC, a tumour was identified at a follow-up cystoscopy after 3 months and a high-grade T1 tumour was confirmed. Both cases suggest that even though cystoscopy is the gold standard for the follow-up of bladder tumours, it should be complemented with a noninvasive urinary test.

The high discrimination power of the XBC between malignant and benign histology groups is a consequence of the highly significant difference between the median LDA total in both groups (0.2486 for benign and 0.9869 for malignant group respectively). Overall sensitivity and NPV for the prediction of a malignant histological result of the XBC (76.9% and 93.0%) greatly outperforms the sensitivity and NPV of VUC (38.4% and 83.3)

Stratification for the tumour grade sensitivity of the XBC was comparable to VUC for PUNLMP (0%) and low-grade tumours (66.7%), though the sensitivity of VUC for high-grade tumours was only 42.6%, while no high-grade tumour was missed by the XBC. Improved performance was also reported by Pichler *et al*.[7], who showed considerably higher sensitivity for low-grade tumours (77% *vs*. 3%) and high-grade tumour +s (100% *vs*. 25%) for the XBC and VUC respectively. However, the study published by Elia *et al*. showed significantly lower sensitivity for low-grade (42%) and high-grade tumours (85.7%).[19] When tumours are stratified by grade, the sensitivity in our study is comparable to the study of Van Velenberg *et al*.[18] in categories T1 and T2 (100%) and to the study of Pichler *et al*.[7] in categories CIS (100%) and Ta (80%).

Since high-grade bladder tumours have a stage progression risk of 23% in five years compared to only 4% in low-grade tumours[21], the XBC could emerge as a noninvasive test to guide the follow-up schedule for the cystoscopic surveillance of a bladder tumour, as was already proposed by Hurle *et al*.[17] Small, Ta low-grade papillary recurrence, which the XBC could miss, does not present an immediate danger to the patient and early detection is not essential for successful therapy,[3,22] while for T1 and T2 high-grade tumours or CIS, the XBC is very likely to be positive.

Even though XBC has high sensitivity and NPV for high grade tumours, the rate of adoption of this and other noninvasive molecular tests to routine clinical practice will also depend on financial resources of the healthcare system. Molecular tests typically cost three to five times the price of VUC (XBC 250 EUR and VUC 40 EUR in Slovenia) and are more expensive than single rigid or even flexible cystoscopic procedure in countries, where fees of healthcare professionals are low to moderate.

The main limitation of the present study is the low number of included patients (54) and therefore the low number of patients with recurrent tumours identified at follow-up (14 patients or 25.9%), which is a consequence of the low recurrence rate and study design. A similar proportion of new recurrence tumours (30.7% ) was also observed in a larger study by Pichler *et al*.[7], while the largest published study only reported a 17.9% recurrence rate.[18] Furthermore, only 1 patient in the negative histology group had a TUR done, while all the others were counted as negative on the basis of the negative cystoscopic result, possibly missing a small hidden lesion or a lesion in the upper urinary tract.

## Conclusions

The XBC showed significantly higher overall sensitivity and negative predictive value than VUC. Its ability to detect intermediate and high-risk superficial tumour recurrences could modify follow-up cystoscopy schedules by increasing the recommended time intervals in patients with a negative XBC. Complementing the XBC and voided urinary cytology does not improve the performance in comparison to the XBC alone.

## Acknowledgments

The authors wish to thank Biomedis M.B. d.o.o., Jurančičeva ul. 11, Maribor, Slovenia for kindly providing The Xpert® Urine Transport Reagent kits and Xpert® Bladder Cancer Cartridges, and for covering the costs of application of the present study at The National Medical Ethics Committee of the Republic of Slovenia.

## References

1. Antoni S, Ferlay J, Soerjomataram I, Znaor A, Jemal A, Bray F. Bladder cancer incidence and mortality: A Global Overview and Recent Trends. *Eur Urol* 2017; **71:** 96-108. doi: 10.1016/j.eururo.2016.06.010
2. Mariappan P, Fineron P, O'Donnell M, Gailer RM, Watson DJ, Smith G, et al. Combining two grading systems: the clinical validity and inter-observer variability of the 1973 and 2004 WHO bladder cancer classification systems assessed in a UK cohort with 15 years of prospective follow-up. *World J Urol* 2020; [Ahead of print]. doi: 10.1007/s00345-020-03180-5
3. Babjuk M, Burger M, Compérat E, Gontero P, Mostafid AH, Palou J, et al. EAU Guidelines on non-muscle-invasive bladder cancer (TaT1 and CIS) 2020. *European Association of Urology Guidelines 2020 Edition*. Presented at the EAU Annual Congress Amsterdam 2020. Arnhem, The Netherlands: European Association of Urology Guidelines Office; 2020.
4. Yafi FA, Brimo F, Steinberg J, Aprikian AG, Tanguay S, Kassouf W. Prospective analysis of sensitivity and specificity of urinary cytology and other urinary biomarkers for bladder cancer. *Urol Oncol* 2015; **33:** 66.e25-31. doi: 10.1016/j.urolonc.2014.06.008
5. Trinh TW, Glazer DI, Sadow CA, Sahni VA, Geller NL, Silverman SG. Bladder cancer diagnosis with CT urography: test characteristics and reasons for false-positive and false-negative results. *Abdom Radiol* 2018; **43:** 663-71. doi: 10.1007/s00261-017-1249-6
6. Kim J, Kim WT, Kim WJ. Advances in urinary biomarker discovery in urological research. *Investig Clin Urol* 2020; **61:** S8-22. doi: 10.4111/icu.2020.61.S1.S8.
7. Pichler R, Fritz J, Tulchiner G, Klinglmair G, Soleiman A, Horninger W, et al. Increased accuracy of a novel mRNA-based urine test for bladder cancer surveillance. *BJU Int* 2018; **121:** 29-37. doi: 10.1111/bju.14019
8. Babjuk M, Bohle A, Burger M, Capoun O, Cohen D, Comperat EM, et al. EAU Guidelines on non-muscle-invasive urothelial carcinoma of the bladder: update 2016. *Eur Urol* 2017; **71:** 447-61. doi: 10.1016/j.eururo.2016.05.041
9. Barkan GA, Wojcik EM, Nayar R, Savic-Prince S, Quek ML, Kurtycz DF, et al. The Paris System for reporting urinary cytology: the quest to develop a standardized terminology. *Adv Anat Pathol* 2016; **23**: 193-201. doi: 10.1097/PAP.0000000000000118
10. Wallace E, Higuchi R, Satya M, McCann L, Sin MLY, Bridge JA, et al. Development of a 90-minute integrated noninvasive urinary assay for bladder cancer detection. *J Urol* 2018; **199:** 655-62. doi: 10.1016/j.juro.2017.09.141
11. Brierley J, Gospodarowicz MK, Wittekind C. *TNM classification of malignant tumours.* Eighth edition. Chichester, West Sussex, UK; Hoboken, NY: John Wiley & Sons, Inc.; 2017.
12. Moch H, Reuter VE, Humphrey PA, Ulbright TM. *WHO classification of tumours of the urinary system and male genital organs.* International Agency for Research on Cancer; 2016.
13. Hentschel AE, van Rhijn BWG, Brundl J, Comperat EM, Plass K, Rodriguez O, et al. Papillary urothelial neoplasm of low malignant potential (PUN-LMP): still a meaningful histo-pathological grade category for Ta, noninvasive bladder tumors in 2019? *Urol Oncol* 2020; **38:** 440-8. doi: 10.1016/j.urolonc.2019.10.002
14. *The Paris System for reporting urinary cytology***.** Rosenthal DL**,** Wojcik EM, Kurtycz DFI, editors. New York, NY: Springer Science and Business Media; 2015.
15. Raitanen MP, Aine R, Rintala E, Kallio J, Rajala P, Juusela H, et al. Differences between local and review urinary cytology in diagnosis of bladder cancer. An interobserver multicenter analysis. *Eur Urol* 2002; **41:** 284-9. doi: 10.1016/s0302-2838(02)00006-4
16. Stenzl A, Cowan NC, De Santis M, Jakse G, Kuczyk MA, Merseburger AS, et al. The updated EAU guidelines on muscle-invasive and metastatic bladder cancer. *Eur Urol* 2009; **55:** 815-25. doi: 10.1016/j.eururo.2009.01.002
17. Hurle R, Casale P, Saita A, Colombo P, Elefante GM, Lughezzani G, et al. Clinical performance of Xpert Bladder Cancer (BC) Monitor, a mRNA-based urine test, in active surveillance (AS) patients with recurrent non-muscle-invasive bladder cancer (NMIBC): results from the Bladder Cancer Italian Active Surveillance (BIAS) project. *World J Urol* 2020; **38:** 2215-20. doi: 10.1007/s00345-019-03002-3
18. Valenberg F, Hiar AM, Wallace E, Bridge JA, Mayne DJ, Beqaj S, et al. Prospective validation of an mRNA-based urine test for surveillance of patients with bladder cancer. *Eur Urol* 2019; **75:** 853-60. doi: 10.1016/j.eururo.2018.11.055
19. Elia DC, Pycha A, Folchini DM, Mian C, Hanspeter E, Schwienbacher C, et al. Diagnostic predictive value of Xpert Bladder Cancer Monitor in the follow-up of patients affected by non-muscle invasive bladder cancer. *J Clin Pathol* 2019; **72:** 140-4. doi: 10.1136/jclinpath-2018-205393
20. Soria F, Droller MJ, Lotan Y, Gontero P, D'Andrea D, Gust KM, et al. An up-to-date catalog of available urinary biomarkers for the surveillance of non-muscle invasive bladder cancer. *World J Urol* 2018; **36:** 1981-95. doi: 10.1007/s00345-018-2380-x
21. Holmang S, Andius P, Hedelin H, Wester K, Busch C, Johansson SL. Stage progression in Ta papillary urothelial tumors: relationship to grade, immunohistochemical expression of tumor markers, mitotic frequency and DNA ploidy. *J Urol* 2001; **165:** 1124-8. PMID: 11257652
22. Gofrit ON, Pode D, Lazar A, Katz R, Shapiro A. Watchful waiting policy in recurrent Ta G1 bladder tumors. *Eur Urol* 2006; **49:** 303-6. doi: 10.1016/j.eururo.2005.12.029

*research article*

# Prognostic factors in postoperative radiotherapy for prostate cancer - tertiary center experience

Marcin Miszczyk[1], Wojciech Majewski[2], Konrad Stawiski[3], Konrad Rasławski[1], Paweł Rajwa[4], Iwona Jabłońska[1], Łukasz Magrowski[1], Oliwia Masri[1], Andrzej Paradysz[4], Leszek Miszczyk[2]

[1] 3rd Radiotherapy and Chemotherapy Department, Maria Sklodowska-Curie National Research Institute of Oncology, Gliwice, Poland

[2] Radiotherapy Department, Maria Sklodowska-Curie National Research Institute of Oncology, Gliwice, Poland

[3] Department of Biostatistics and Translational Medicine, Medical University of Łodź, Łódź, Poland

[4] Department of Urology, Medical University of Silesia, Zabrze, Poland

Radiol Oncol 2021; 55(2): 203-211.

Received 20 November 2020
Accepted 6 February 2021

Correspondence to: Marcin Miszczyk, 3rd Radiotherapy and Chemotherapy Department, Maria Sklodowska-Curie National Research Institute of Oncology, ul. Wybrzeże Armii Krajowej 15, 44-102, Gliwice, Poland. E-mail: marcinmmiszczyk@gmail.com

Disclosure: No potential conflicts of interest were disclosed.

**Background.** The aim of the study was to analyse the prognostic factors in postoperative prostate cancer irradiation and develop a nomogram for disease-free survival (DFS).

**Patients and methods.** This retrospective study included 236 consecutive prostate cancer patients who had radical prostatectomy followed by radiotherapy (RT) at a single tertiary institution between 2009 and 2014. The main outcome was DFS analysed through uni- and multivariable analysis, Kaplan-Meier curves, log-rank testing, recursive partitioning analysis, and nomogram development.

**Results.** The median follow up was 62.3 (interquartile range [IQR] 38.1–79) months. The independent clinical factors associated with increased risk of recurrence or progression in the multivariate analysis (MVA) were prostate-specific antigen (PSA) level before RT, pT3 characteristic, and local failure as salvage indication. The value of PSA nadir had a significant impact on the risk of biochemical failure. Biochemical control and DFS were significantly different depending on treatment indication ($p < 0.0001$). The recursive partitioning analysis highlighted the importance of the PSA level before RT, Gleason Grade Group, PSA nadir, and local failure as a treatment indication. Finally, the nomogram for DFS was developed and is available online at https://apps.konsta.com.pl/app/prostate-salvage-dfs/.

**Conclusions.** The Pre-RT PSA level, pT3 characteristic and local failure as salvage indication are pivotal prognostic factors associated with increased risk of recurrence or progression. The Gleason grade group of 4–5 and PSA nadir value allow for further risk stratification. The treatment outcomes in postoperative prostate cancer irradiation are significantly different depending on treatment indication. An online nomogram comprising of both pre-treatment and current data was developed allowing for visualization of changes in prognosis depending on clinical data.

Key words: prostate cancer; prognostic factors; postoperative radiotherapy; nomogram; disease-free survival

## Introduction

The incidence of prostate cancer (PCa) has been steadily rising over the last decades. For example, The Polish National Cancer Registry has recorded a 28-fold increase in newly diagnosed Prostate Cancer patients, from 582 in 1963, through 2273 in 1990, up to 16253 newly diagnosed PCa patients in the year 2017.[1,2] The change is directly associated with broad implementation of prostate-specific antigen (PSA) testing and aging society, but from a clinician's point of view, it means ever more patients to take care of. Despite changing patterns of PCa management, radical prostatectomy (RP) remains

one of the pivotal treatment modalities in localized prostate cancer management, and so remains the necessity for management of post-prostatectomy treatment failures which occur in approximately 1/4th of the patients, including up to 1/2nd of those presenting high and very high risk group features.[3]

Historically, the necessity for further treatment was most commonly met by adjuvant radiotherapy (aRT), whose rationale was based on three large randomized clinical trials – SWOG S8794[4], EORTC 22911[5], and ARO 96–02/AUO AP 09/95.[6] Although consistent in conclusions, these studies compared aRT with an outdated concept of salvage radiotherapy (sRT). The salvage treatment in the wait-and-see groups was initiated significantly later than currently accepted standards, at the median PSA of 1.0 and 1.7 μg/ml for SWOG and EORTC studies respectively. Shortly after, authors started publishing reports on the superiority of early sRT initiation, which was later discussed along with the results of the ARO/AUO trial. Currently, the adverse association between PSA level prior to sRT and treatment results is well documented[7], and the introduction of salvage treatment even prior to reaching the criteria for biochemical recurrence (*i.e.* > 0.4 ng/ml as in European Association of Urology [EAU] guidelines[8]) is encouraged.

The shift of the paradigm came with the recent results of TROG 08.03/ANZUP RAVES[9], RADICALS-RT[10], and GETUG-AFU 17[11], three large multicentre prospective randomized clinical trials comparing aRT with sRT initiated at very low levels of PSA, prior to the usual threshold of > 0.4 ng/ml for biochemical recurrence (BCR). The results were in favor of early sRT, and indicated that routine use of aRT leads to overtreatment of PCa patients. Although the studies were met with critique, the consistent results of the planned systemic review and meta-analysis published by the ARTISTIC collaboration[12] suggest that for now, at least until data on long-term outcomes is available, sRT should be offered to all patients that are able and willing to adhere to the early sRT routine.

In this article, we present data from a large one-institutional set of consecutive PCa patients treated during the transitional period between aRT and sRT, and a thorough analysis of the prognostic factors.

## Patients and methods

The retrospective observational cohort study included a group of 236 consecutive prostate cancer patients at median age of 63.6 years (min. 40, max. 82), who underwent RP between 1993 and 2013, and were later irradiated with aRT or sRT at single tertiary high-volume institution between 2009 and 2014 to the prostatic bed (as defined by the local protocol, similar to TROG 0803 RAVES trial[13]) with a median dose of 70 Gy (62–76 Gy) in 2 Gy fractions 5 times a week, using IGRT in all cases. Pelvic lymph node irradiation was performed in 26% of the patients using a standard dose of 44 Gy in 22 fractions. The androgen deprivation therapy (ADT) was administered in 37.6% of the patients prior to RT. Approximately 25.8% of the patients were receiving ADT at 4 months, 21.2% at 14 months, 18.2% at 26 months, 14.8% at 38 months and 11.4% at 50 months after treatment respectively. The ADT was administered at primary doctors' discretion. The follow up (FU) was collected retrospectively, based on our institutional database. In patients with FU < 36 months a phone call was attempted twice to obtain information regarding current PSA, ADT uptake, late side effects of RT, and permission to access the patients' medical history wherever further control visits took place. Data regarding overall survival (OS) was obtained from the Polish National Cancer Registry.

The study group was divided into four subgroups depending on the treatment indication including positive surgical margins (R1) and ≥ pT3 characteristic (pT3) for aRT, and BCR and local failure (LF) for sRT. In the case of dual treatment indications (*i.e.* R1 + pT3 or BCR + LF) patients were assigned to pT3 and LF groups respectively. In few cases where patients qualified for aRT due to pT3 characteristic have had barely detectable PSA level (> 0.2 ng/ml) in a post-qualification repeated PSA test immediately before RT, such patients were still regarded as part of the aRT group. The measured endpoints for the study were OS, disease-free survival (DFS), and biochemical control (BC). The OS, DFS and BC were calculated from the last day of RT to the day of death for OS, clinical recurrence defined as the locoregional failure, distant metastasis or both for DFS, and biochemical recurrence defined as PSA > 0.2 ng/ml for BC. Remaining cases were censored using the date of last observation with appropriate data to exclude the occurrence of the respective endpoint.

### Univariable analysis & recursive partitioning analysis

The univariate analysis was performed by fitting the proportional subdistribution hazards regres-

**TABLE 1.** Description of the study group

| | Whole group | aRT | | sRT | |
|---|---|---|---|---|---|
| Number of cases | 236 | 113 | | 123 | |
| Age* | 63.6 (59.8-68.4) | 62.3 (58.8-65.9) | | 65.2 (60.5-70.2) | |
| Time from surgery to RT (months)* | 6 (3.3-25.8) | 3.6 (2.9-4.8) | | 24.1 (7.3-48.3) | |
| Indication | n/a | R1[1] 56 | pT3[2] 57 | BCR[3] 69 | LF[4] 54 |
| Positive surgical margins | 61.5% | 100% | 77.2% | 39.1% | 27.8% |
| Max PSA pre-op* (ng/ml) | 9.16 (6.81-14.6) | 8.24 (6.33-11.78) | 9.37 (7.19-14.79) | 10.67 (7.3-17) | 8.8 (6.6-13.3) |
| Max PSA post-op*[5] (ng/ml) | 0.27 (0.04-1.13) | 0.035 (<0.008-0.071) | 0.027 (<0.008-0.104) | 0.72 (0.38-1.92) | 1.19 (0.45 – 2.89) |
| PSA before RT* (ng/ml) | 0.2 (0.023-0.78) | 0.015 (<0.008-0.055) | 0.017 (<0.008-0.077) | 0.56 (0.29-1.07) | 1.05 (0.35-2.38) |
| **Gleason Grade Group (post-op):** | | | | | |
| 1 | 42.2% | 47.3% | 26.3% | 39.7% | 57.7% |
| 2 | 33.6% | 38.2% | 40.4% | 32.3% | 23.1% |
| 3 | 13.4% | 9.1% | 15.8% | 16.2% | 11.5% |
| 4 | 5.6% | 1.8% | 7% | 7.4% | 5.8% |
| 5 | 5.2% | 3.6% | 10.5% | 4.4% | 1.9% |
| **TNM (post-op):** | | | | | |
| pT2a-c | 61.6% | 100% | 0% | 63.6% | 84.3% |
| pT3a | 17.5% | 0% | 50.9% | 12.1% | 7.8% |
| pT3b | 21% | 0% | 49.1% | 24.2% | 7.8% |
| pN1 | 5.8% | 1.8% | 16.4% | 1.5% | 4% |
| ADT prior to RT | 37.6% | 16.4% | 43.9% | 42.6% | 46.3% |
| RT dose^ | 70 / 71.5 | 70 / 70.3 | 70 / 70.2 | 70 / 71.4 | 76 / 74.4 |
| Lymph node irradiation | 25.8% | 15% | 47.8% | 12.7% | 23.1% |

* = median (interquartile range); ^ = median/mean Gy; ADT = androgen deprivation therapy; BCR[3] = biochemical recurrence; LF[4] = local failure; pT3[2] = pT3a or pT3b; R1[1] = R1 resection; RT = radiotherapy; [1-4] = in case of multiple indications only one is indicated. The assumed priority is: LF>BCR>pT3>R1

sion model, thus including the competing risk of death from other causes. Subdistribution hazard ratios (HR) were provided with their 95% confidence intervals (95% CI). To maintain consistency and generalizability, every univariate model was adjusted to the time length between surgery and radiation treatment (as a covariate). All factors tested in univariate analysis were included in the multivariate analysis which was also adjusted to the time between surgery and RT.

As an addition to multivariate analysis, to find the subgroups of different survival risks and select the most important clinical features, recursive partitioning for censored responses was performed. This utilized the development of a survival tree for DFS based on adjusted log-rank statistics (ctree algorithm).

## Nomogram development

To develop the predictive model utilizing the current PSA and ADT status cause-specific Cox proportional hazards regression model with time-varying covariates was developed. The current PSA value was simplified to a binary variable based on the definition of post-RP BCR.[14] Internal validation of the model and, thus, assessment of overfitting was performed using the bootstrap method with 1000 repetitions. The model performance was assessed using Harrell's C-index, with a value of 1.0 indicating perfect model concordance. The developed model was visualized using a nomogram and was implemented in the online calculator. The whole analysis was done using R programming language.

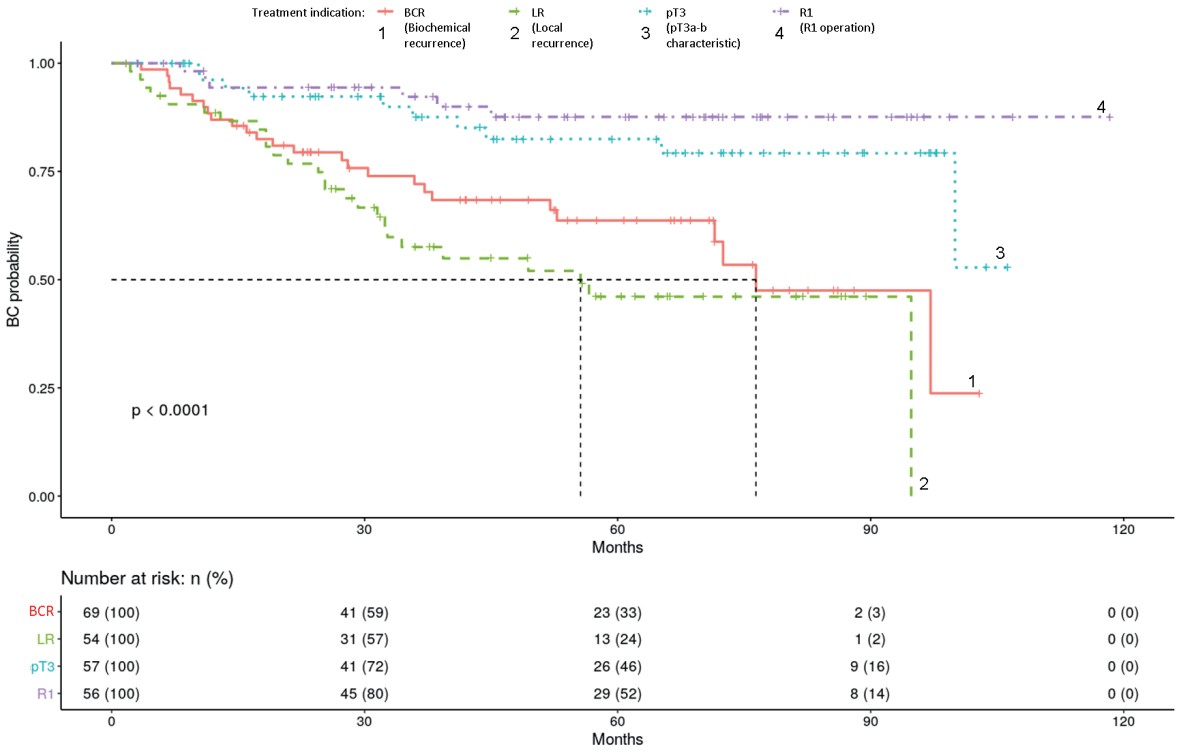


**FIGURE 1.** Biochemical control depending on treatment indication.

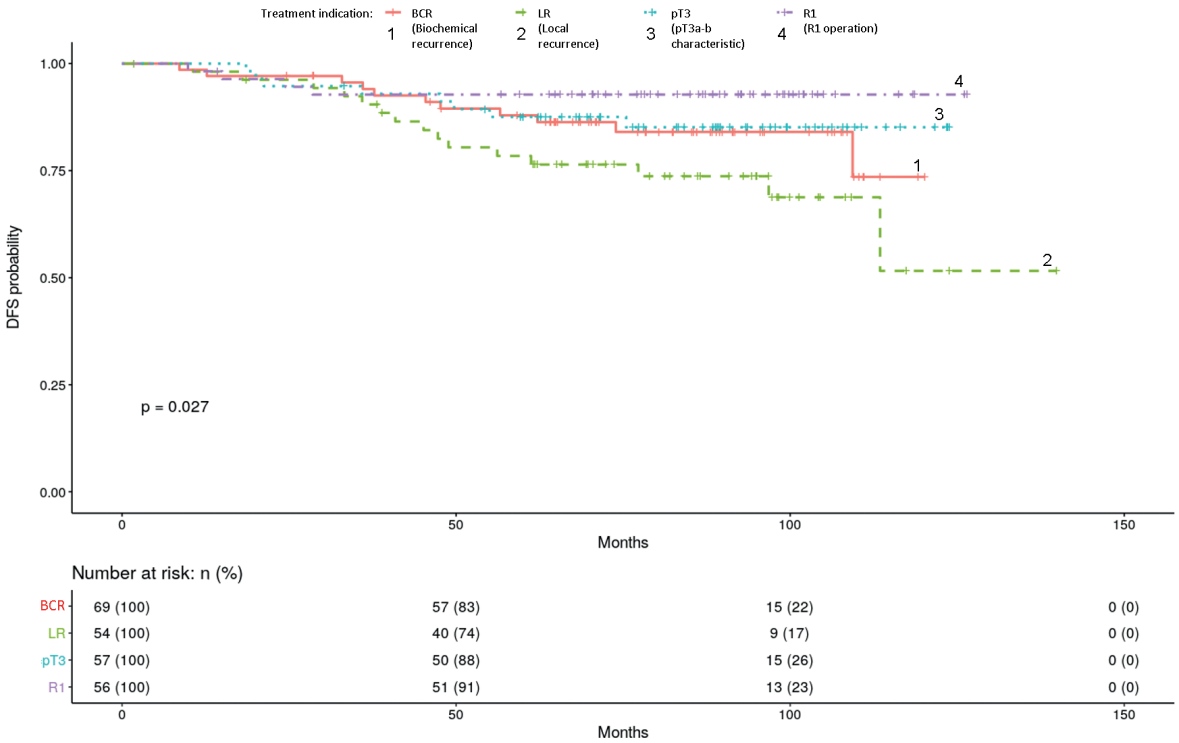


**FIGURE 2.** Disease-free survival (DFS) depending on treatment indication.

**TABLE 2.** Univariate and multivariate analysis

| | Univariate analysis | | | | Multivariate analysis | | | |
|---|---|---|---|---|---|---|---|---|
| | DFS | | BC | | DFS | | BC | |
| Covariate: | HR (95% CI) | p-value | HR (95% CI) | p-value | HR (95% CI) | p-value | HR (95% CI) | p-value |
| Age | 0.99 (0.94, 1.04) | 0.59 | 1.03 (0.99, 1.08) | 0.14 | 0.97 (0.92, 1.02) | 0.19 | 1.02 (0.98, 1.07) | 0.34 |
| max PSA prior to operation | 1.03 (0.97, 1.08) | 0.35 | 1.03 (1, 1.07) | 0.078 | 1.04 (0.97, 1.11) | 0.25 | 1.05 (1.02, 1.08) | **0.001** |
| max PSA post operation | 1 (0.96, 1.05) | 0.91 | 1.04 (1.02, 1.05) | **<.001** | 0.53 (0.28, 1.01) | 0.052 | 1 (0.99, 1.02) | 0.65 |
| PSA before radiotherapy | 1.24 (1.12, 1.37) | **<.001** | 1.26 (1.17, 1.35) | **<.001** | 2.17 (1.04, 4.55) | **0.04** | 1.19 (1.03, 1.38) | **0.017** |
| ADT prior to RT | 1.42 (0.74, 2.74) | 0.29 | 1.06 (0.64, 1.75) | 0.82 | 1.39 (0.69, 2.77) | 0.35 | 0.82 (0.5, 1.35) | 0.43 |
| pT3a-b vs. pT2a-c | 2.57 (1.29, 5.1) | **0.007** | 1.35 (0.83, 2.19) | 0.23 | 4.29 (1.8, 10.25) | **0.001** | 1.89 (1.02, 3.5) | **0.044** |
| pN0 vs pN1 | 0.58 (0.16, 2.13) | 0.42 | 0.94 (0.3, 2.99) | 0.92 | 0.82 (0.31, 2.19) | 0.69 | 0.98 (0.56, 1.72) | 0.95 |
| aRT indication - R1 | 0.6 (0.27, 1.31) | 0.2 | 0.36 (0.2, 0.64) | **<.001** | 0.81 (0.19, 3.52) | 0.78 | 0.21 (0.09, 0.52) | **0.001** |
| aRT indication - pT3a-b | 1.45 (0.69, 3.04) | 0.33 | 0.86 (0.48, 1.55) | 0.62 | 0.72 (0.18, 2.89) | 0.64 | 1.04 (0.43, 2.53) | 0.93 |
| sRT indication - biochemical failure | 1.31 (0.64, 2.68) | 0.46 | 2.02 (1.17, 3.49) | **0.011** | 1.95 (0.41, 9.27) | 0.4 | 1.12 (0.52, 2.41) | 0.77 |
| sRT indication - local failure | 2.03 (1.06, 3.89) | **0.033** | 2.36 (1.45, 3.84) | **0.001** | 2.39 (1.11, 5.15) | **0.026** | 1.48 (0.77, 2.83) | 0.24 |
| R1 operation (regardless of RT indication) | 1.2 (0.61, 2.35) | 0.59 | 0.82 (0.5, 1.32) | 0.41 | 1.52 (0.59, 3.92) | 0.38 | 2.17 (1.23, 3.84) | **0.007** |
| PSA nadir (per 1ng/ml) | 1.34 (1.2, 1.5) | **<.001** | 1.29 (1.19, 1.39) | **<.001** | 1.16 (0.93, 1.46) | 0.19 | 1.37 (1.28, 1.46) | **<.001** |
| Gleason Grade Group | 1.4 (1.09, 1.8) | **0.009** | 1.15 (0.96, 1.38) | 0.12 | 1.28 (0.95, 1.73) | 0.1 | 1.13 (0.93, 1.38) | 0.23 |

ADT = androgen deprivation therapy; aRT = adjuvant RT; RT = radiotherapy; sRT = salvage RT

## Results

The median age of the patients at the onset of RT was 63.6 years (interquartile range [IQR] 59.8–68.4), median FU was 62.3 months (IQR 38.1–79) and 10.2% of the patients were found to be deceased at the time of data collection. The 5-year DFS and BC were 86.9% and 70% respectively. A detailed description of the patients' characteristics is presented in Table 1.

The uni- and multivariate (MVA) Cox Regression for the DFS found that among max PSA prior to operation, max PSA post operation and PSA immediately prior to RT, only the last one was a significant covariate and remained an independent adverse factor for the risk of clinical recurrence in the MVA (HR 2.17; 1.04–4.55; p = 0.04). The pT3 characteristic was associated with significantly increased risk of developing clinical recurrence or progression in the MVA (HR 4.29; 1.8–10.25; p = 0.001) as well as local failure as a treatment indication (HR 2.39; 1.11–5.15; p = 0.026). The PSA Nadir and Gleason Grade Group were both associated with an increased risk of DFS failure in the univariate analysis, but were no longer significant in the MVA. The PSA Nadir, however, was associated with significantly increased risk of BCR in the MVA (HR 1.37; 1.28–1.46; p = 0.001) The HR's for the remaining covariates and results for BC can be found in Table 2.

The probability of treatment failure differed between treatment indication. The differences were especially pronounced for BC, and the log-rank testing resulted in a high level of statistical significance (Figure 1). The trend, however, was different for DFS (Figure 2). The difference in Kaplan-Meier curves between aRT due to pT3 characteristic and sRT due to BCR was very well pronounced in terms of BC, but these two curves are similar for DFS.

The recursive partitioning analysis for DFS provided the decision tree presented in Figure 3. Out of all included clinical variables the final algorithm highlighted the importance of PSA before RT, postoperative GG, PSA nadir as well as a local failure as an indication for sRT creating 5 risk groups based on DFS. If the initial PSA level before RT exceeded 2.5 ng/ml, this group was associated with the highest risk of relapse or progression. Postoperative GG was the second most important divider, with the score of GG 3 or lower separating the remaining patients into two further groups. The patients

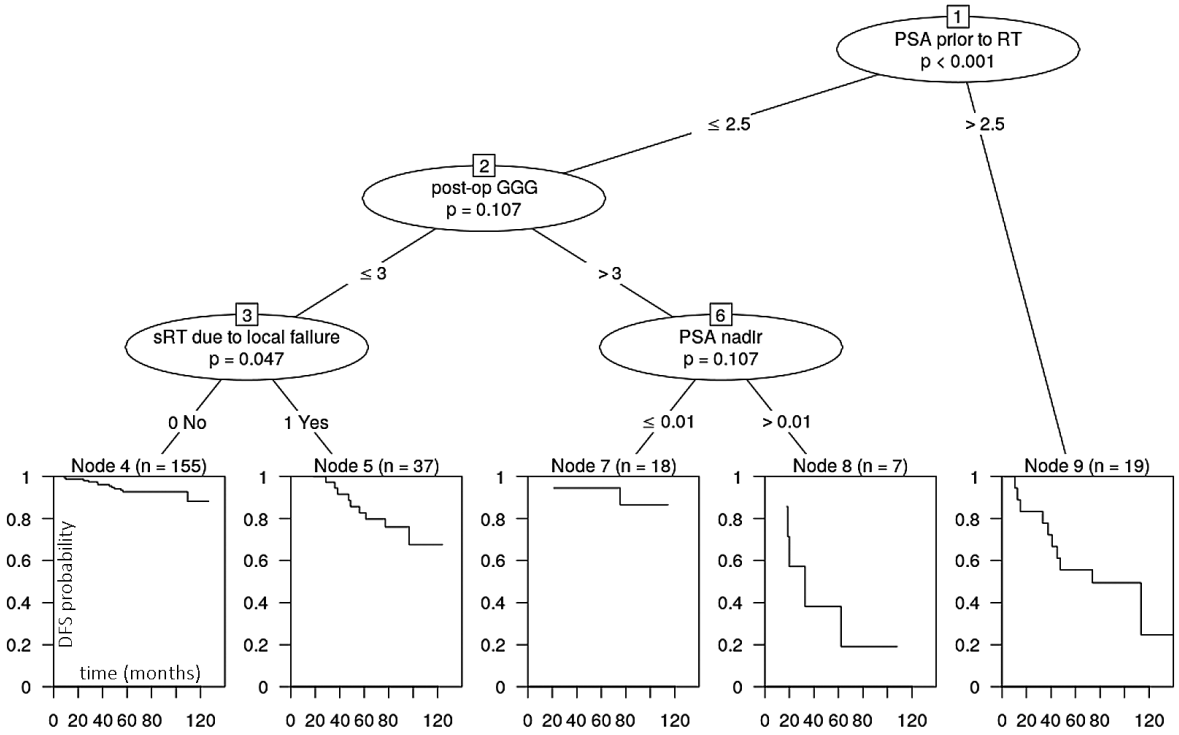


**FIGURE 3.** Recursive partitioning analysis for disease-free survival (DFS).

GGG = Gleason grade group; sRT = salvage RT; RT = radiotherapy

with GG of 4 or 5 were further divided by the value of PSA nadir. If the PSA ever reached values of ≤ 0.01 during Follow Up, the risk of DFS failure was lower. Finally, in patients with GG of 3 or lower, the patients treated with sRT due to LF had a significantly higher risk of relapse or progression.

Finally, the nomogram utilizing time-varying Cox regression model was developed and can be found in Figure 4. The c-index for this model was 0.81 (95%CI: 0.73–0.89) which did not drop (*i.e.* remained 0.81) in a bootstrap-based validation, thus suggesting resilience to overfitting. This model was employed to create an online application, which visualises the impact of changing prognostic factors on the probability of clinical relapse or recurrence. The application is available online at https://apps.konsta.com.pl/app/prostate-salvage-dfs/.

## Discussion

There are many different available nomograms on the subject of prostate cancer treatment, the majority of those addressing the issue of risk stratification after primary radical prostatectomy, but the risk stratification in post-prostatectomy irradiation is significantly more difficult considering the heterogeneity of the patients and the recent changes in treatment recommendations. In this analysis, besides the commonly assessed pre-treatment variables comparable to those provided by the EAU for the post-RP distant metastasis recurrence[15], we included ADT uptake and PSA levels as variables changing over time. Such approach allows for visualisation of changes in patients' prognosis over the course of the follow up, however, on the expense of reduced clinical importance of nomogram for initial risk evaluation.

There is evidence[16] suggesting that distant metastases are a better intermediate clinical endpoint compared to BC. However, the use of distant metastasis as an endpoint in our article was limited due to the median length of FU (approximately 5 years). The BCR on average precedes clinical metastasis by 7 to 8 years[17], and the actual risk of distant metastasis is underestimated. Therefore, we decided to use DFS and BC as surrogate endpoints, the latter universally preceding metastatic progression.[8] Due to limited data, we have also omitted more thorough analysis of the ADT type and duration before RT, as in many cases the precise date of ADT onset was not available. A com-

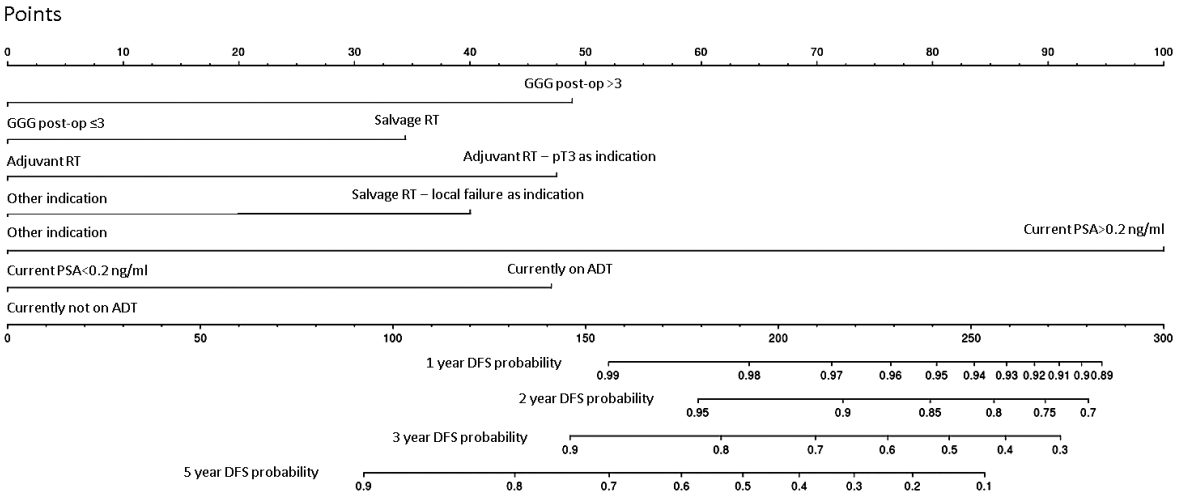


**FIGURE 4.** Nomogram for disease-free survival (DFS).

ADT = androgen deprivation therapy; GGG = Gleason grade group; RT = radiotherapy

mon flaw of retrospective studies on post-RT PCa patients is the lack of differentiation between aRT and sRT subpopulations. For example, a recent analysis by Hwang *et al*. in 2018[18] concluded that aRT reduces BCR and improves metastasis-free survival and OS in high-risk patients. The study was met with criticism regarding omitting patients who were cured by surgery alone. To account for such, we included the treatment indication as a co-factor in the statistical analysis and nomogram. Moreover, such criticism is advised in the interpretation of Kaplan-Meier curves presented in this article (Figure 1–2).

Tendulkar *et al*.[7] published an excellent study which analyses the importance of pre-RT PSA levels and provides a nomogram for risk stratification of BCR and metastases-free survival in patients undergoing sRT. The analysis included a large study group (n = 2460) of node-negative patients with a detectable PSA post-RP. Notably, the nomogram includes one of the independent prognostic factors presented in our article, the pre-RT PSA level, as a continuous variable. Such approach allows for a conceptualization of the importance of early sRT initiation in case of post-RP BCR.

In another study, Dalela *et al*.[19] created a prognostic nomogram including clinical features and Decipher® (GenomeDx Biosciences, Inc., Vancouver, British Columbia) score for the identification of optimal candidates for aRT. Although the clinical importance of such a nomogram is limited in the sRT era, the study highlights the applicability of novel, genomic markers for the patients' risk stratification. Moreover, some authors suggest that a subset of patients presenting multiple and severe adverse prognostic factors, such as pT3b/pT4 feature and high Gleason Score which were also highlighted in this article, could profit from aRT despite the late findings.[10-12,20]

One of the important aspects of changing clinical practice is the introduction of new diagnostic methods. In this study, the majority of the DFS failures were diagnosed through medical imaging performed due to rising PSA (24, 63.2%), which was either fluorodeoxyglucose positron emission tomography (FDG-PET) (10 cases), prostate specific membrane antigen PET (PSMA-PET) (7 cases), bone scintigraphy (3 cases), computer tomography (CT) (2 cases) or magnetic resonance imaging (MRI) (2 cases). In 10 cases (26.3%), at the time of BCR, the localization of the recurrence could not be determined, and clinical recurrence was found later in routine imaging: MRI (5 cases), CT (2 cases), FDG-PET (1 case), PSMA-PET (1 case), or RTG (1 case). Finally, 4 patients had clinical progression diagnosed before BCR, through bone scintigraphy (1 case), CT (1 case), MRI (1 case), or physical examination (1 case). The majority of these diagnostic tools could be replaced with broader usage of PSMA-PET in the future, as it seems to have superior sensitivity and specificity.[21] The EAU guidelines[8] suggest considering PSMA- PET in patients with persistent or recurrent PSA (> 0.2 ng/ml) after RP. However, due to low evidence strength, accessibility, and relatively high cost compared to standard diagnostic methods, the implementation

of routine PET-PSMA imaging is limited. Set aside logistic and economic factors, routine PET-PSMA could reduce the occurrence of treatment failures in the future through early diagnosis of occult distant metastasis and early implementation of modern techniques of localized treatment for oligometastatic disease. For example, despite limited prospective evidence, stereotactic RT has shown potential for long-term disease control in such patients based on our institutional experience.[22,23]

The TROG 08.03/ANZUP RAVES[9], RADICALS-RT[10], and GETUG-AFU 17[11] have recently shown that sRT approach is preferable to aRT for post-RP patients. However, the question remains whether it is possible to reproduce the clinical trial setting in practice. For example, In the RADICALS-RT trial[10], the median PSA value at the onset of sRT was 0.2 ng/ml (0.1–0.3), significantly lower than in our study group - 0.68 ng/ml (IQR 0.31–1.78). Considering that the PSA value before RT is an important prognostic factor[7], which has been shown in our analysis, we can expect that the treatment outcomes of the second group of patients would be significantly worse. According to the pre-sRT PSA nomogram by Tendulkar *et al*.[7], only 12 (9.8%) patients had PSA < 0.2ng/ml before RT, 38 (30.9%) PSA 0.21–0.5ng/ml, 29 (23.5%) PSA 0.51–1 ng/ml, 17 (13.8%) PSA 1.1–2 ng/ml, and finally 25 (20.4%) PSA > 2. In 2 cases (1.6%), the PSA pre-sRT value was missing. Increased frequency of PSA monitoring and early initiation of sRT could improve the treatment outcomes, however, it is often limited by patients' resources and compliance. Therefore, we believe that in patients with limited possibility of close follow-up and significant adverse prognostic factors, offering aRT could reduce the probability of a clinical recurrence.

We acknowledge the limitations and biases of a retrospective study. The study was based on single-institution data and limited follow-up, which could be further improved by the inclusion of other sites and registry-based collection of data, which we will try to accomplish in the future.

## References


1. Kułakowski A, Zatoński W. *Cancer in Poland in 1990.* In: Zatoński W, Tyczyński J, editos. Warsaw: Pracownia Poligraficzna Centrum Onkologii - Instytutu im. Marii Skłodowskiej-Curie; 1990.
2. Didkowska J, Wojciechowska U, Czaderny K, Olasek P, Ciuba A. *Cancer in Poland in 2017*. Warsaw: Pracownia Poligraficzna Centrum Onkologii - Instytutu im. Marii Skłodowskiej-Curie; 2017. [cited 2020 Feb 1]. Available at: http://onkologia.org.pl/wp-content/uploads/Nowotwory_2017.pdf
3. Park SW, Hwang DS, Song WH, Nam JK, Lee HJ, Chung MK. Conditional biochemical recurrence-free survival after radical prostatectomy in patients with high-risk prostate cancer. *Prostate Int* 2020; **8:** 173-7. doi: 10.1016/j.prnil.2020.07.004
4. Thompson IM, Tangen CM, Paradelo J, Lucia MS, Miller G, Troyer D, et al. Adjuvant radiotherapy for pathological T3N0M0 prostate cancer significantly reduces risk of metastases and improves survival: long-term followup of a randomized clinical trial. *J Urol* 2009; **181:** 956-62. doi: 10.1016/j.juro.2008.11.032
5. Bolla M, Van Poppel H, Tombal B, Vekemans K, Da Pozzo L, de Reijke TM, et al. Postoperative radiotherapy after radical prostatectomy for high-risk prostate cancer: long-term results of a randomised controlled trial (EORTC trial 22911). *Lancet* 2012; **380:** 2018-27. doi: 10.1016/S0140-6736(12)61253-7
6. Wiegel T, Bartkowiak D, Bottke D, Bronner C, Steiner U, Siegmann A, et al. Adjuvant radiotherapy versus wait-and-see after radical prostatectomy: 10-year follow-up of the ARO 96-02/AUO AP 09/95 trial. *Eur Urol* 2014; **66:** 243-50. doi: 10.1016/j.eururo.2014.03.011
7. Tendulkar RD, Agrawal S, Gao T, Efstathiou JA, Pisansky TM, Michalski JM, et al. Contemporary update of a multi-institutional predictive nomogram for salvage radiotherapy after radical prostatectomy. *J Clin Oncol* 2016; **34:** 3648-54. doi: 10.1200/JCO.2016.67.9647
8. Mottet N, Conford P, van den Bergh RCN, Briers E, De Santis M, Fantis S, et al. *Prostate Cancer EAU Guidelines.* Presented at the EAU Annual Congress Barcelona 2019. Arnhem, the Netherlands: EAU Guidelines Office; 2019. [cited 2020 Feb 1]. Available at: https://uroweb.org/guideline/prostate-cancer/
9. Kneebone A, Fraser-Browne C, Delprado W, Duchesne G, Fisher R, Frydenberg M, et al. A phase III multi-centre randomised trial comparing adjuvant versus early salvage radiotherapy following a radical prostatectomy: results of the TROG 08.03 and ANZUP "RAVES" trial. *Int J Radiat Oncol* 2019; **105:** S37-8. doi: 10.1016/j.ijrobp.2019.06.456
10. Parker CC, Clarke NW, Cook AD, Kynaston HG, Petersen PM, Catton C, et al. Timing of radiotherapy after radical prostatectomy (RADICALS-RT): a randomised, controlled phase 3 trial. *Lancet* 2020; **396:** 1413-21. doi: 10.1016/S0140-6736(20)31553-1
11. Sargos P, Chabaud S, Latorzeff I, Magné N, Benyoucef A, Supiot S, et al. Adjuvant radiotherapy versus early salvage radiotherapy plus short-term androgen deprivation therapy in men with localised prostate cancer after radical prostatectomy (GETUG-AFU 17): a randomised, phase 3 trial. *Lancet Oncol* 2020; **21:** 1341-52. doi: 10.1016/S1470-2045(20)30454-X
12. Vale CL, Fisher D, Kneebone A, Parker C, Pearse M, Richaud P, et al. Adjuvant or early salvage radiotherapy for the treatment of localised and locally advanced prostate cancer: a prospectively planned systematic review and meta-analysis of aggregate data. *Lancet* 2020; **396:** 1422-31. doi: 10.1016/S0140-6736(20)31952-8
13. *RAVES-Contouring Guidelines Revised July 2011. CTV Delineation*. [cited 2020 Aug 15]. Available at: https://www.trog.com.au/SiteFiles/trogcomau/TROG_0803_-_Guidelines_for_Contouring.pdf
14. Tourinho-Barbosa R, Srougi V, Nunes-Silva I, Baghdadi M, Rembeyo G, Eiffel SS, et al. Biochemical recurrence after radical prostatectomy: what does it mean? *Int Braz J Urol* 2018; **44:** 14-21. doi: 10.1590/S1677-5538.IBJU.2016.0656
15. Van den Broeck T, van den Bergh RCN, Arfi N, Gross T, Moris L, Briers E, et al. Prognostic value of biochemical recurrence following treatment with curative intent for prostate cancer: a systematic review. *Eur Urol* 2019; **75:** 967-87. doi: 10.1016/j.eururo.2018.10.011
16. Xie W, Regan MM, Buyse M, Halabi S, Kantoff PW, Sartor O, et al. Metastasis-free survival is a strong surrogate of overall survival in localized prostate cancer. *J Clin Oncol* 2017; **35:** 3097-104. doi: 10.1200/JCO.2017.73.9987
17. Pound CR, Partin AW, Eisenberger MA, Chan DW, Pearson JD, Walsh PC. Natural history of progression after PSA elevation following radical prostatectomy. *J Am Med Assoc* 1999; **281:** 1591-7. doi: 10.1001/jama.281.17.1591
18. Hwang WL, Tendulkar RD, Niemierko A, Agrawal S, Stephans KL, Spratt DE, et al. Comparison between adjuvant and early-salvage postprostatectomy radiotherapy for prostate cancer with adverse pathological features. *JAMA Oncol* 2018; **4:** e175230. doi: 10.1001/jamaoncol.2017.5230

19. Dalela D, Santiago-Jiménez M, Yousefi K, Karnes RJ, Ross AE, Den RB, et al. Genomic classifier augments the role of pathological features in identifying optimal candidates for adjuvant radiation therapy in patients with prostate cancer: Development and internal validation of a multivariable prognostic model. *J Clin Oncol* 2017; **35:** 1982-90. doi: 10.1200/JCO.2016.69.9918

20. Kneebone A, Fraser-Browne C, Duchesne GM, Fisher R, Frydenberg M, Herschtal A, et al. Adjuvant radiotherapy versus early salvage radiotherapy following radical prostatectomy (TROG 08.03/ANZUP RAVES): a randomised, controlled, phase 3, non-inferiority trial. *Lancet Oncol* 2020; **21:** 1331-40. doi: 10.1016/S1470-2045(20)30456-3

21. Alipour R, Azad A, Hofman MS. Guiding management of therapy in prostate cancer: time to switch from conventional imaging to PSMA PET? *Ther Adv Med Oncol* 2019; **11:** 1758835919876828. doi: 10.1177/1758835919876828

22. Napieralska A, Miszczyk L, Tukiendorf A, Stąpór-Fudzińska M. The results of treatment of prostate cancer bone metastases after CyberKnife radiosurgery. *Ortop Traumatol Rehabil* 2014; **16:** 339-49. doi: 10.5604/15093492.1112535

23. Napieralska A, Miszczyk L, Stąpór-Fudzińska M. CyberKnife stereotactic ablative radiotherapy as an option of treatment for patients with prostate cancer having oligometastatic lymph nodes: single-center study outcome evaluation. *Technol Cancer Res Treat* 2016; **15:** 661-73. doi: 10.1177/1533034615595945

*research article*

# Deep inspiration breath hold reduces the mean heart dose in left breast cancer radiotherapy

Michał Falco[1], Bartłomiej Masojć[1], Agnieszka Macała[2], Magdalena Łukowiak[2], Piotr Woźniak[1], Julian Malicki[3,4]

[1] Radiation Oncology Department, West Pomeranian Oncology Center, Szczecin, Poland
[2] Department of Medical Physics, West Pomeranian Oncology Center, Szczecin, Poland
[3] Department of Electroradiology, University of Medical Sciences, Poznan, Poland
[4] Greater Poland Cancer Centre, Poznan, Poland

Radiol Oncol 2021; 55(2): 212-220.

Received 7 October 2020
Accepted 18 November 2020

Correspondence to: Michał Falco, M.D., Radiation Oncology Department, West Pomeranian Oncology Center, Strzałowska 22, 71-730 Szczecin, Poland. E-mail: mfalco@onkologia.szczecin.pl

Disclosure: No potential conflicts of interest were disclosed.

**Background.** Patients with left breast cancer who undergo radiotherapy have a non-negligible risk of developing radiation-induced cardiovascular disease (CVD). Cardioprotection can be achieved through better treatment planning protocols and through respiratory gating techniques, including deep inspiration breath hold (DIBH). Several dosimetric studies have shown that DIBH reduces the cardiac dose, but clinical data confirming this effect is limited. The aim of the study was to compare the mean heart dose (MHD) in patients with left breast cancer who underwent radiotherapy at our institution as we transitioned from non-gated free-breathing (FB) radiotherapy to gated radiotherapy (FB-GRT), and finally to DIBH.

**Patients and methods.** Retrospective study involving 2022 breast cancer patients who underwent radiotherapy at West Pomeranian Oncology Center in Szczecin from January 1, 2014 through December 31, 2017. We compared the MHD in these patients according to year of treatment and technique.

**Results.** Overall, the MHD for patients with left breast cancer in our cohort was 3.37 Gy. MHD values in the patients treated with DIBH were significantly lower than in patients treated with non-gated FB (2.1 *vs.* 3.48 Gy, $p < 0.0001$) and gated FB (3.28 Gy, $p < 0.0001$). The lowest MHD values over the four-year period were observed in 2017, when nearly 85% of left breast cancer patients were treated with DIBH. The proportion of patients exposed to high (> 4 Gy) MHD values decreased every year, from 40% in 2014 to 7.9% in 2017, while the percentage of patients receiving DIBH increased.

**Conclusions.** Compared to free-breathing techniques (both gated and non-gated), DIBH reduces the mean radiation dose to the heart in patients with left breast cancer. These findings support the use of DIBH in patients with left breast cancer treated with radiotherapy.

Key words: breast cancer; gated radiotherapy; deep inspiration breath hold; free breathing gated radiotherapy; mean heart dose

## Introduction

Most patients with breast cancer, who are treated surgically also undergo postoperative radiotherapy[1,2], which has been shown to improve locoregional control, recurrence rates, and survival.[3-6] However, long-term population-based analyses have found that postoperative radiotherapy is associated with an increased risk of mortality due to radiation-induced cardiovascular disease (CVD).[7-9] In recent years, better radiotherapy treatment planning protocols[6,10,11] and widespread use of respiratory gating techniques – which have been applied in all modern linear accelerators – have improved cardioprotection.[12-16]

Cardioprotection can be achieved through better treatment planning protocols and respiratory gating. When this latter technique is used, the radiation is delivered only during the inspiratory phase, when the heart is at its most distant point from the chest wall, thus reducing the radiation dose to the heart.[8,13-16] In recent years, the deep inspiration breath hold (DIBH) technique has become increasingly common due to the growing body of evidence showing that this approach can reduce the mean heart dose (MHD) by 1–3 Gy compared to conventional techniques.[17] The use of cardioprotective techniques such as DIBH is crucial in patients with left breast cancer, as these patients have a high risk of developing heart disease within 10 years of radiotherapy treatment.[18] Dosimetric studies have shown that DIBH reduces cardiac dose in comparison with free-breathing (FB) without gating. Additional data from population analyses show that MHD decreases over successive years.[19,20]

At our institution, we have modified the radiotherapy treatment protocols over time to reflect technological advances and a better understanding of the importance of cardioprotection. From 2014 to 2017, we gradually transitioned from treating patients with non-gated FB to gated FB, and finally to DIBH. Although some studies have compared FB without gating to DIBH[12-17], the studies analysing whether DIBH reduces the risk of cardiotoxicity in a large, real-world clinical cohort of patients are limited.[19,20] Likewise, clinical data on the influence of DIBH on cardiac complications in these patients is limited.

In this context, the aim of this study was to compare differences in mean heart dose for patients with left breast cancer treated at our institution from 2014 to 2017 during which we transitioned from non-gated free-breathing (FB) radiotherapy to gated radiotherapy, and finally to DIBH.

## Patients and methods

This was a retrospective analysis of all patients (n = 2022) diagnosed and treated for breast cancer at West Pomeranian Oncology Center in Szczecin from January 1, 2014 through December 31, 2017.

Patients' written inform consent about the study was waved because of retrospective clinical data analysis. The study was conducted according the Helsinki Declaration and the European Council Convention on Protection of Human Rights in Bio-Medicine (Oviedo 1997).

Virtually all of patients (99.6%) received postoperative radiotherapy and 1049 (51.9%) were treated for left breast cancer. During the study period, most patients were treated with conventional three-dimensional (3D) radiotherapy (n = 1513, 74.8%) or intensity-modulated radiotherapy (IMRT; n = 69, 3.4%) with free-breathing. A total of 188 patients (9.3%) underwent FB-gated radiotherapy (FB-GRT). Starting in October 2016, all new left breast cancer patients were treated with DIBH. Thus, from that point in time until the study end (2017), the DIBH technique was applied in 252 (12.5%) patients. Gated radiotherapy during FB and DIBH were applied only to left breast cancer patients.

All patients underwent CT-based 3D planning in the therapeutic position. All patients were treated on the same linear accelerator model (Artiste, Siemens Healthcare, Erlangen, Germany). Gated radiotherapy during FB procedures was performed with assistance of a respiratory gating system (AZ-733VI, Anzai Medical Co., Tokyo, Japan), which divides the normal breathing cycle into eight phases, with irradiation administered only during the inhalation phase. Patients who were able to maintain a stable breath cycle received FG-GRT if, in the clinical judgement of the treating radiation oncologist, there was a dosimetric benefit identified by any significant separation of the heart from chest wall (increase of at least 5 mm). DIBH (AlignRT system Vision RT Ltd, London, UK) was used in patients expected to benefit from this approach. Patients unable to hold their breath were not considered eligible for this procedure. The DIBH irradiation technique was used with assistance of a real-time 3D surface tracking system (AlignRT) as described elsewhere.[12,21,22]

Treatment planning followed institutional protocol. CTV contours were drawn according to ESTRO recommendations[23] and heart contours according to Feng *et al*.[24] Regional lymph nodes (ipsilateral axillary and supraclavicular ones) were irradiated in every patients with macrometastases in axillary lymph nodes as internal mammary lymph nodes (upper I–IV) in patients after mastectomy. Five millimetre margin was added to create PTV from CTV. Dose constraints for heart were $V_{20}$ < 10% (less than 10% of the organ covered be dose of 20Gy), $V_{40}$ < 5% for conventional fractionation and $V_{17}$ < 10%, $V_{35}$ < 5% for hypofractionated regimens.

Treatment plans were created with the Prowess Panther system for IMRT (Radiology Oncology Systems, Inc., San Diego, CA, USA) and the Oncentra Masterplan (Nucletron, Veenendaal, The

**TABLE 1.** Patient clinical characteristics by year of treatment

| Variable | | 2014 | 2015 | 2016 | 2017 | p-value |
|---|---|---|---|---|---|---|
| **Side** | Right | 155 | 277 | 278 | 263 | NS |
| | Left | 201 | 284 | 298 | 266 | |
| **BMI** | < 25 | 7 | 12 | 14 | 8 | NS |
| | 25–30 | 67 | 101 | 97 | 77 | |
| | 30–35 | 65 | 102 | 101 | 117 | |
| | > 35 | 62 | 69 | 85 | 63 | |
| **Operation type** | BCS | 137 | 188 | 201 | 182 | NS |
| | Mastectomy | 64 | 92 | 95 | 82 | |
| **Nodal status** | N(-) | 129 | 159 | 180 | 174 | NS |
| | N(+) | 72 | 121 | 116 | 90 | |
| **RNI** | No | 127 | 146 | 156 | 149 | NS |
| | Yes | 74 | 138 | 142 | 117 | |
| **HFX** | No | 165 | 192 | 167 | 80 | < 0.0001 |
| | Yes | 36 | 92 | 131 | 186 | |
| **Gated radiotherapy** | FB | 122 | 197 | 200 | 38 | < 0.0001 |
| | FB-GRT | 42 | 76 | 70 | 0 | |
| | DIBH | 0 | 0 | 24 | 228 | |
| | IMRT | 37 | 11 | 4 | 0 | |

BC = breast conserving surgery; BMI = body mass index; DIBH = deep inspiration breath hold; FB = free breathing; FB-GRT = free breathing gated radiotherapy; HFX = hypofractionation; IMRT = intensity-modulated radiotherapy; Nodal status = lymph node negative *vs.* positive; NS = not significant; RNI = lymph node radiotherapy; Side = indicates right *vs.* left location

Netherlands) for other techniques. All patients treated with FB-GRT or gated radiotherapy during FB and DIBH underwent 3D-RT. IMRT was used in patients with left breast cancer if the 3D conformal plan did not meet the prescribed dose constraints.

The data were obtained from the planning systems, which included the: MHD; the heart volume receiving > 40%, 60%, 80%, 100% of the defined dose ($V_{40\%}$, $V_{60\%}$, $V_{80\%}$, $V_{100\%}$). The MHD value was expressed in Gy and $V_{40\%}$, $V_{60\%}$, $V_{80\%}$, $V_{100\%}$ were the value for the absolute heart volume in cubic centimetres.

The conventional dose scheme was 50 Gy (2 Gy per fraction administered daily from Monday through Friday) to the breast/chest wall, with or without nodal irradiation. A 10–16 Gy boost to the tumor bed was prescribed for patients undergoing breast-conserving surgery (BCS). Hypofractionated schemes were 42.5–45 Gy (2.25–2.5 Gy per fraction) plus a boost of 10 Gy, or 40.05 Gy (2.67 Gy per fraction) without boost. In the subset of patients who underwent BCS, a total of 155 were given a boost dose with either intraoperative radiotherapy (n = 93) as an early boost or brachytherapy (n = 62). The boost dose was not included in the present analysis. We normalized hypofractionated plans to the conventional scheme (50 Gy in 25 fractions) and recalculated them to obtain the corrected MHD ($MHD_{Fx}$).

Patients who received IMRT were not included in the MHD and $MHD_{Fx}$ analyses, as the MHD in IMRT plans is higher than those obtained with 3D conformal radiotherapy, with a different impact on cardiac morbidity.[20,25]

### Statistical analysis

The $\chi^2$ test was used to compare differences among patients treated in different years (2014 *vs.* 2015 *vs.* 2016 *vs.* 2017) and between radiation techniques. The level of statistical significance was set at $p < 0.05$. Student's *t*-test was applied to assess differences between mean values (95% confidence interval, statistical significance was set at $p < 0.05$) of MHD, $MHD_{Fx}$, $V_{40\%}$, $V_{60\%}$, $V_{80\%}$, $V_{100\%}$ over time and among techniques.

## Results

Table 1 shows the clinical characteristics of the left breast cancer patients and treatment parameters according to year of treatment. As that table shows, there were no significant differences in baseline characteristics of the patients (e.g., body mass index, type of surgery, axillary lymph node surgery, nodal irradiation) regardless of the year. Table 1 also shows that the use of IMRT decreased over time as the number of patients undergoing gated therapy increased. Similarly, an increasing proportion of patients received hypofractionated radiotherapy over time.

Overall, MHD values ranged from 0 to 19.44 Gy, with a mean of 2.48 Gy (95% confidence interval [CI], 2.39–2.57). For patients with left breast cancer, the MHD was 3.37 Gy (range, 0.56–19.44 Gy; 95% CI 3.23–3.5) and 1.51 Gy (range 0–17.31; 95% CI 1.43–1.58) for the right side. Overall, the $MHD_{Fx}$ was 2.62 (range, 0–19.44 Gy; 95% CI, 2.53–2.71). For patients with left breast cancer, the $MHD_{Fx}$ was 3.52 (range, 0.66–19.44; 95% CI 3.38–3.65) and 1.62 Gy (range 0–17.31; 95% CI 1.54–1.69).

Table 2 shows the MHD and $MHD_{Fx}$ by year of treatment, indicating that the proportion of patients with left breast cancer exposed to MHD and $MHD_{Fx}$ values > 4 Gy decreased every year – from 40% in 2014 to 7.9% in 2017 – with a statistically sig-

**TABLE 2.** Mean heart dose (MHD) and fractionation-corrected MHD ($MHD_{fx}$) by year of treatment

| | | 2014 | 2015 | 2016 | 2017 | p |
|---|---|---|---|---|---|---|
| **Patients, n** | | 160 | 255 | 294 | 266 | |
| **MHD (Gy)** | < 4 | 98 | 175 | 211 | 248 | < 0.0001 |
| | ≥ 4 | 62 | 80 | 83 | 18 | |
| | Mean (95% CI) | 3.93 (3.53–4.33) | 3.44 (3.19–3.68) | 3.27 (3.07–3.49) | 2.23 (2.1–2.37) | |
| | 2014 vs. 2015: p = 0.027, 2015 vs. 2016: NS, 2016–2017: p < 0.0001 | | | | | |
| **$MHD_{fx}$ (Gy)** | < 4 | 96 | 168 | 205 | 245 | < 0.0001 |
| | ≥ 4 | 64 | 87 | 89 | 21 | |
| | Mean (95% CI) | 4.03 (3.63–4.43) | 3.6 (3.35–3.84) | 3.41 (3.2–3.61) | 2.42 (2.28–2.56) | |
| | 2014 vs. 2015: p = 0.0551, 2015–2016: NS, 2016–2017: p < 0.0001 | | | | | |

NS = not significant

nificant decrease in MHD values from 2014 to 2015 and from 2016 to 2017. Similarly, the maximum MHD values fell every year from 2014 to 2017, from 19.44 Gy to 12.27 Gy to 11.07 and finally to 7.36 Gy in 2017. Figures 1 and 2 show these results graphically, indicating an increase in the proportion and number of patients who received lower MHD ($p < 0.0001$) and $MHD_{Fx}$ ($p < 0.0001$).

Despite the above observation every year MHD and $MHD_{Fx}$ mean values were significantly higher for left-sided breast cancer when compared to right-sided (Table 3). Additionally Table 3 shows, that MHD and $MHD_{Fx}$ improved every year among those either irradiated to lymph nodes or not and in those with body mass index (BMI) either below or above 30. Every year patients with BMI < 30 were exposed to lower MHD and $MHD_{Fx}$ and in 2016 and 2017 regional nodal irradiation (RNI) led to higher MHD and $MHD_{Fx}$ values comparing to no RNI (Table 3).

As Table 4 shows, the mean $V_{40\%}$, $V_{60\%}$, $V_{80\%}$, and $V_{100\%}$ values all decreased year over year, although this decrease was not statistically significant every year (e.g., $V_{100\%}$). Notably, $V_{100\%}$ improved irrespective of the specific gating technique (FB-GRT or DIBH) versus FB, with the best $V_{100\%}$ values observed in patients treated with DIBH. There was a non-significant difference in mean $V_{40\%}$, $V_{60\%}$, $V_{80\%}$ values when comparing gated FB-GRT to non-non-gated FB. For all parameters ($V_{40\%}$, $V_{60\%}$, $V_{80\%}$, $V_{100\%}$) DIBH was significantly better than gated FB-GRT. DIBH was associated with significantly lower mean $V_{60\%}$ and $V_{80\%}$ values compared to FB. The mean $V_{40\%}$ was lower for DIBH than for FB, but not significantly ($p = 0.0529$) (Table 4).

Table 5 shows the comparison according to radiation technique (FB *vs*. FB-GRT *vs*. DIBH). DIBH

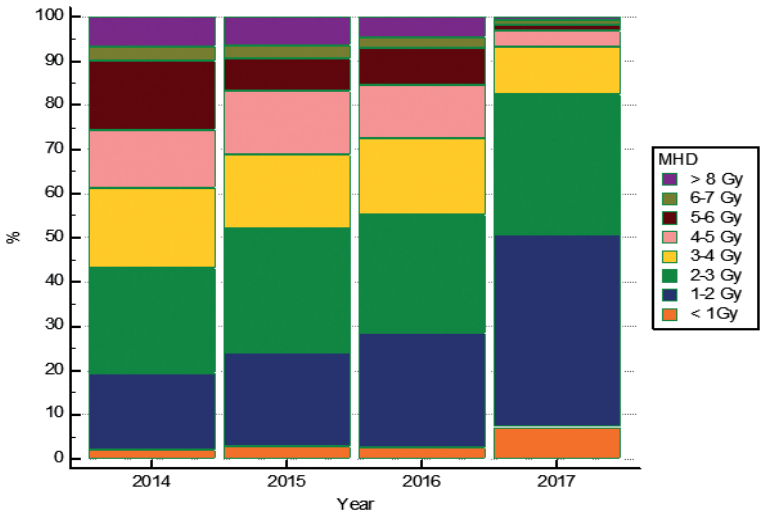


**FIGURE 1.** Mean heart dose (MHD) values by year 2014–2017.

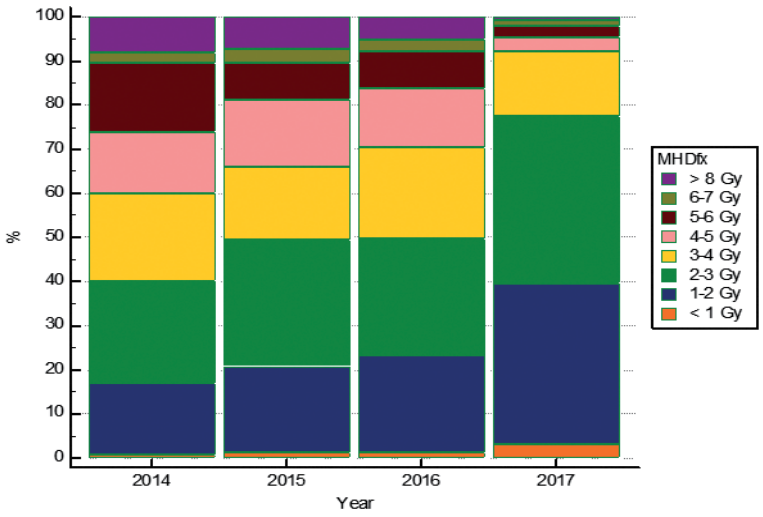


**FIGURE 2.** Fractionation-corrected mean heart dose ($MHD_{fx}$) values by year 2014–2017.

**TABLE 3.** Mean heart dose (MHD) and fractionation-corrected MHD ($MHD_{fx}$) by year of treatment and side, regional nodal irradiation and body mass index

| MHD | | 2014 | 2015 | 2016 | 2017 |
|---|---|---|---|---|---|
| **Side** | Left | 3.93 (3.53–4.33) | 3.44 (3.19–3.68) | 3.27 (3.07–3.49) | 2.23 (2.1–2.37) |
| | Right | 1.55 (1.27–1.83) | 1.54 (1.4–1.67) | 1.37 (1.28–1.46) | 1.47 (1.38–1.56) |
| | p | < 0.0001 | < 0.0001 | < 0.0001 | < 0.0001 |
| **RNI** | No | 3.86 (3.34–4.37) | 3.2 (2.87–3.54) | 2.98 (2.71–3.25) | 1.91 (1.77–2.07) |
| | Yes | 4.03 (3.39–4.67) | 3.68 (3.32–4.03) | 3.56 (3.27–3.91) | 2.64 (2.41–2.86) |
| | p | NS | NS | 0.0038 | < 0.0001 |
| **BMI** | < 30 | 3.23 (2.8–3.65) | 2.53 (2.32–2.82) | 2.66 (2.38–2.94) | 1.92 (1.71–2.14) |
| | ≥ 30 | 4.38 (3.8–4.97) | 4.05 (3.73–4.38) | 3.63 (3.35–3.91) | 2.38 (2.21–2.55) |
| | p | 0.0053 | < 0.0001 | < 0.0001 | 0.002 |
| **$MHD_{fx}$** | | **2014** | **2015** | **2016** | **2017** |
| **Side** | Left | 4.03 (3.63–4.43) | 3.6 (3.35–3.84) | 3.41 (3.2–3.61) | 2.42 (2.28–2.56) |
| | Right | 1.64 (1.36–1.93) | 1.65 (1.51–1.8) | 1.45 (1.36–1.54) | 1.62 (1.52–1.72) |
| | p | 0.0001 | 0.0001 | 0.0001 | 0.0001 |
| **RNI** | No | 3.98 (3.46–4.5) | 3.47 (3.12–3.82) | 3.18 (2.91–3.45) | 2.16 (2–2.32) |
| | Yes | 4.1 (3.44–4.75) | 3.72 (3.36–4.08) | 3.65 (3.33–3.96) | 2.76 (2.53–2.98) |
| | p | NS | NS | 0.0272 | 0.0001 |
| **BMI** | < 30 | 3.29 (2.87–3.71) | 2.7 (2.39–3.01) | 2.79 (2.51–3.07) | 2.12 (1.9–2.34) |
| | ≥ 30 | 4.5 (3.91–5.09) | 4.2 (3.87–4.53) | 3.76 (3.49–4.04) | 2.56 (2.39–2.74) |
| | p | 0.0036 | < 0.0001 | < 0.0001 | 0.0029 |

BMI = body mass index; NS = not significant; RNI = lymph node radiotherapy; Side = indicates right *vs*. left location;

Mean values (95% Confidence Interval in brackets)

was associated with the lowest values (2.1 Gy and 2.31 Gy, respectively), which were significantly lower than those observed for FB-GRT (3.28 Gy, $p < 0.0001$ and 3.45 Gy, $p < 0.0001$, respectively) and non-gated FB (3.58 Gy, $p < 0.0001$ and 3.69 Gy, $p < 0.0001$, respectively). There were no significant differences between the FB and FB-GRT groups. Note that fewer patients were exposed to high (> 4 Gy) MHD and $MHD_{Fx}$ values when gated irradiation was used, particularly in the DIBH group in which only 4.8% presented a MHD ≥ 4 Gy versus 22.4% for patients treated with FB-GRT and 35.2% in FB.

Table 6 shows no difference in MHD and $MHD_{Fx}$ values comparing RNI and no RNI in a group of patients without gating procedure applied. The biggest difference was observed for DIBH (MHD 2.45 *vs*. 1.89, $p < 0.0001$, $MHD_{Fx}$ 2.58 *vs*. 2.15, $p = 0.0026$ respectively). MHD and $MHD_{Fx}$ did not differ significantly in patients with BMI below and above 30 if DIBH was used (Table 6). The difference was significant if FB and FB-GRT was used and MHD and $MHD_{Fx}$ were higher for patients with BMI above 30 (Table 6).

## Discussion

The present study was performed to evaluate the influence of DIBH on mean heart doses in patients with left breast cancer. Overall, the MHD in patients with left breast cancer was 3.37 Gy. Patients treated with DIBH had significantly lower MHD values than patients treated with FB or FB-GRT techniques (2.1 Gy *vs*. 3.48 and 3.38 Gy, respectively, $p < 0.0001$). The lowest MHD values were obtained in the last year of this study (2017), when nearly 85% of left breast cancer patients were treated with DIBH. Moreover, of the patients with MHD values > 4Gy, the smallest proportion was observed in the DIBH group. These data confirm that DIBH reduces the mean radiation dose to the heart in patients with left breast cancer. Drost *et al*.

**TABLE 4.** Comparison of mean $V_{40\%}$, $V_{60\%}$, $V_{80\%}$, $V_{100\%}$ values obtained from 2014 to 2017 and between radiation techniques

| Year | $V_{100}$ cm³ | $V_{80}$ cm³ | $V_{60}$ cm³ | $V_{40}$ cm³ |
|---|---|---|---|---|
| **2014** | 0.75 (0.46–1.03) | 7.21 (5.6–8.82) | 16.75 (13.98–19.51) | 33.02 (28.22–37.82) |
| **2015** | 0.54 (0.22–0.87) | 4.31 (3.3–5.32) | 9.56 (7.9–11.21) | 40.68 (3.03–78.33) |
| **2016** | 0.20 (0.02–0.38) | 2.73 (2.04–3.42) | 7.91 (6.56–9.26) | 16.9 (14.49–19.30) |
| **2017** | 0.08 (-0.0096–0.16) | 1.13 (0.32–1.94) | 3.13 (1.93–4.32) | 9.1 (4.44–13.76) |
| | 2014 *vs.* 2015: NS | 2014 *vs.* 2015: p = 0.0018 | 2014 *vs.* 2015: p < 0.001 | 2014 *vs.* 2015: NS |
| | 2015 *vs.* 2016: NS | 2015 *vs.* 2016: p = 0.0096 | 2015 *vs.* 2016: NS | 2015 *vs.* 2016: NS |
| | 2016 *vs.* 2017: NS | 2016 *vs.* 2017: p = 0.0029 | 2016 *vs.* 2017: p < 0.0001 | 2016–2017: p = 0.0027 |
| **FB** | 0.37 (0.22–0.52) | 4.46 (3.67–5.25) | 11.2 (9.9–12.5) | 33.13 (16.22–50.03) |
| **FB-GRT** | 0.76 (0.36–1.17) | 4.7 (3.61–5.79) | 9.87 (7.83–11.9) | 17.75 (13.95–21.56) |
| **DIBH** | 0.06 (-0.02–0.14) | 0.71 (0.37–1.05) | 2.3 (1.48–3.13) | 7.47 (2.71–12.23) |
| | FB *vs.* FB-GRT: p = 0.0274 | FB *vs.* FB-GRT: NS | FB *vs.* FB-GRT: NS | FB *vs.* FB-GRT: NS |
| | FB *vs.* DIBH: p = 0.0107 | FB *vs.* DIBH: p < 0.0001 | FB *vs.* DIBH: p < 0.0001 | FB *vs.* DIBH: p = 0.0529 |
| | FB-GRT *vs.* DIBH: p < 0.0001 | FB-GRT *vs.* DIBH: p < 0.0001 | FB-GRT *vs.* DIBH: p < 0.0001 | FB-GRT *vs.* DIBH: p = 0.0019 |

DIBH = deep inspiration breath hold; FB = free breathing; FB-GRT = free-breathing gated radiotherapy; $V_{40\%}$, $V_{60\%}$, $V_{80\%}$, $V_{100\%}$ = absolute heart volume (in cubic centimetres) covered by percentage of delivered dose (40%–100%);

Mean values (95% Confidence Interval in brackets)

analysed studies published between 2014 and 2017, reporting MHD 3.6 Gy in left breast cancer patients and 1.7 Gy if any breathing control technique was used (19). The data from 20 sites in United States show that median MHD decreased from 2.19 Gy in 2012 to 1.65 Gy in 2015 (20). Comparable values were observed for left breast cancer patients with median MHD 1.5 Gy for gated radiotherapy.[26] In our study the reported values are higher. It might be explained be differences in 3D planning systems used in different centres, as mean values for right breast cancer patients in our study are twice higher than in other studies (1.51 Gy *vs*. 0.7 Gy).[26] Testolin *et al*. presented data on 280 left breast cancer patients who underwent DIBH combined with IMRT. The mean MHD was 0.94 Gy in DIBH group and 2.14 Gy in those with no gating.[27] Those values are lower than the ones we present, but on the other hand in mentioned trial only 11% of patients were after mastectomy and only 11.4% patients underwent RNI comparing to 44% and 31% in 2017 in our study. Nevertheless in our study mean MHD without RNI was 1.89 Gy.

There is a large body of evidence on the negative impact of excessive radiation doses to the heart. Darby *et al*.[28] showed that every 1 Gy increase in MHD increases the risk of CVD-related mortality by 7.4%. Those authors estimated the risk of developing CVD according to increases in the MHD, as follows: 10% increased risk for MHD < 2 Gy; 30% for MHD 2–4 Gy; and 40% for MHD at 5–9 Gy. Taylor *et al*. estimated that every additional 1 Gy in MHD is associated with a 4% increase in CVD mortality[29], estimating no increase in CVD mortality risk for MHD values < 4 Gy, but an increase in risk of up to 25% for doses ranging from 4–8 Gy.

In our cohort, MHD and $MHD_{Fx}$ values – which indicate a lower risk of CVD – trended downwards over time as radiotherapy and gating techniques improved. In 2017, most of the left breast cancer patients in our study received MHD doses below 2–4 Gy, and none were exposed to a MHD > 8 Gy. Relevantly, the only factor that changed in this period was the introduction of DIBH irradiation in October 2016.

**TABLE 5.** Mean heart dose (MHD) and fractionation corrected MHD ($MHD_{fx}$) according to radiation technique

| | | FB | FB-GRT | DIBH | p |
|---|---|---|---|---|---|
| **Patients, n** | | 540 | 183 | 252 | |
| **MHD** | < 4 Gy | 350 | 142 | 240 | < 0.0001 |
| | ≥ 4 Gy | 190 | 41 | 12 | |
| **$MHD_{fx}$** | < 4 Gy | 340 | 137 | 237 | < 0.0001 |
| | ≥ 4 Gy | 200 | 46 | 15 | |

DIBH = deep inspiration breath hold; FB = free breathing; FB-GRT = free-breathing gated radiotherapy

**TABLE 6.** Mean heart dose (MHD) and fractionation-corrected MHD ($MHD_{fx}$) according to radiation technique and regional nodal irradiation, body mass index

| MHD | | FB | FB-GRT | DIBH |
|---|---|---|---|---|
| RNI | No | 3.5 (3.23–3.77) | 3.07 (2.75–3.39) | 1.89 (1.75–2.04) |
| | Yes | 3.62 (3.42–3.83) | 4.59 (3–6.19) | 2.45 (2.21–2.69) |
| | p | NS | 0.003 | < 0.0001 |
| BMI | < 30 | 2.72 (2.52–2.93) | 2.78 (2.4–3.15) | 1.92 (1.69–2.16) |
| | ≥ 30 | 4.04 (2.83–4.25) | 3.7 (3.14–4.27) | 2.19 (2.03–2.34) |
| | p | < 0.0001 | 0.0103 | NS |
| $MHD_{fx}$ | | FB | FB-GRT | DIBH |
| RNI | No | 3.71 (3.44–3.99) | 3.25 (2.94–3.57) | 2.15 (1.99–2.3) |
| | Yes | 3.69 (3.48–3.88) | 4.66 (3.05–6.27) | 2.58 (2.33–2.82) |
| | p | NS | 0.0061 | 0.0026 |
| BMI | < 30 | 2.83 (2.62–3.03) | 2.96 (2.57–3.35) | 2.12 (1.89–2.36) |
| | ≥ 30 | 4.16 (3.95–4.37) | 3.86 (3.3–4.42) | 2.4 (2.23–2.57) |
| | p | < 0.0001 | 0.0125 | NS |

BMI = body mass index; DIBH = deep inspiration breath hold; FB = free breathing; FB-GRT = free-breathing gated radiotherapy; NS = not significant; RNI = lymph node radiotherapy; Side = indicates right *vs.* left location;

Mean values (95% Confidence Interval in brackets)

Sardaro *et al*. suggested the following planning dose constraints to achieve a low risk (< 1%) of CVD-related mortality: $V_{30Gy} < 20$ cm$^3$, $V_{40Gy} < 10$ cm$^3$, and $V_{50Gy} < 2$ cm$^3$.[30] These constraints depend only on the heart volume exposed to a given radiation dose and do not depend on the quality of organ contouring. The values reflecting those constraints in our analysis were $V_{60\%}$, $V_{80\%}$, and $V_{100\%}$. In 2017, only 11 patients did not fulfil those criteria, and only 5 of those patients were treated with DIBH. In other words, 97.8% of breast cancer patients treated with DIBH radiotherapy had a less than 1% increased risk of CVD-related mortality. The largest improvement in $V_{80\%}$, $V_{60\%}$, $V_{40\%}$ values was observed in 2017, when DIBH was introduced. Data presented by Testolin *et al*. suggest that there is still possibility to improve the results as they presented mean $V_{80\%}$, $V_{60\%}$, $V_{40\%}$ values below 1 cm$^3$ with combined DIBH and IMRT.[27]

In our cohort, gated radiotherapy during FB modestly decreased the cardiac dose compared to non-gated FB, possibly due to more stringent qualification criteria, such as the expected benefit from gated radiotherapy during FB and the patients' ability to cooperate with the procedure. Thus, the non-gated FB group included patients whose heart was optimally located in relation to the chest wall. However, compared to gated and non-gated FB, DIBH resulted in significantly better heart sparing on nearly all parameters. These findings are consistent with other studies that have compared non-gated FB to DIBH, which have shown that DIBH decreases the MHD by 33%–66% from the initial value compared to non-gated FB.[12-16,22,31-36] However, those studies are limited by the type of analyses performed: the authors created plans based on CT scans obtained during FB and DIBH, and then calculated the estimated (i.e., theoretical) benefit from gated radiotherapy techniques. By contrast, we present real-world data from routine clinical practice, confirming the findings reported by Eldredge *et al*. in a prospective trial that demonstrated that radiotherapy with the Active Breathing Coordinator (ABC) reduced MHD values by ≥ 20% in 88% of patients.[15]

In 2017, 86% of left side breast cancer patients successfully underwent radiotherapy with DIBH. Comparable results presented Testolin *et al*., but Eldredge *et al*. reported that 72% patients successfully underwent radiotherapy with DIBH using a different gating system (Active Breath Coordinator System, Elekta Instrument AB, Stockholm, Sweden).[15,27] Surface monitoring systems seem to be more comfortable for patients.

MHD and $MHD_{Fx}$ were higher for RNI comparing to no RNI in those who underwent either FB-GRT or DIBH. DIBH offers the best sparing in both clinical scenarios. RNI leads to higher MHD[20,27,38], with the strongest impact if internal mammary lymph nodes are irradiated.[37] In our study 33% of left breast cancer patients were irradiated to internal mammary lymph nodes. It may explain higher MHD values reported in our study comparing to other series.[19,20,27]

In our cohort, MHD and $MHD_{Fx}$ were higher in patients with BMI > 30 if FB or FB-GRT was used but not DIBH. The correlation between BMI and MHD was also reported by Finazzi *et al*.[37]

### Study strengths and limitations

The main limitation of this study is the retrospective design. By contrast, an important strength is the large sample size (> 1000 patients). The study clinically demonstrates that DIBH reduces the risk of cardiotoxicity versus FB and FB-GRT.

## Conclusions

Our results show that the DIBH technique lowers the mean heart dose in patients with left breast can-

cer treated with radiotherapy, minimising the risk of radiation-induced CVD. Although the clinical impact of these findings remains unknown due to the long latency period, it seems highly probable that lower radiation doses to the heart will reduce radiation-induced CVD in these patients. The data from our study, considered in the context of other published studies, suggest that DIBH should be offered to every patient with left breast cancer to reduce treatment-related morbidity and mortality.

## Authors' contributions and acknowledgments

MF – study design, data collection, statistical analysis, manuscript edition; BM – study design, statistical analysis, manuscript edition; AM – data collection; MŁ – data collection; PW – manuscript edition; JM – manuscript edition.

We wish to thank Bradley Londres for professional editing of the final draft and for his invaluable suggestions to improve the text. We also thank Libby Cone from Edanz Group Japan for correcting spelling and grammar in the initial draft.

## References

1. EBCTCG (Early Breast Cancer Trialists' Collaborative Group); McGale P, Taylor C, Correa C, D Cutter, F Duane, M Ewertz, et al. Effect of radiotherapy after mastectomy and axillary surgery on 10-year recurrence and 20-year breast cancer mortality: meta-analysis of individual patient data for 8135 women in 22 randomised trials. *Lancet* 2014; **383:** 2127-35. doi: 10.1016/S0140-6736(14)60488-8
2. EBCTCG (Early Breast Cancer Trialists' Collaborative Group); Darby S, McGale P, Correa C, Taylor C, Arriagada R, Clarke M, et al. Effect of radiotherapy after breast-conserving surgery on 10-year recurrence and 15-year breast cancer death: meta-analysis of individual patient data for 10,801 women in 17 randomised trials. *Lancet* 2011; **378:** 1707-16. doi: 10.1016/S0140-6736(11)61629-2
3. Overgaard M, Hansen PS, Overgaard J, Rose C, Andersson M, Bach F, et al. Postoperative radiotherapy in high-risk premenopausal women with breast cancer who receive adjuvant chemotherapy. Danish Breast Cancer Cooperative Group 82b Trial. *N Engl J Med* 1997; **337:** 949-55. doi: 10.1056/NEJM199710023371401
4. Ragaz J, Jackson SM, Le N, Plenderleith IH, Spinelli JJ, Basco VE, et al. Adjuvant radiotherapy and chemotherapy in node-positive premenopausal women with breast cancer. *N Engl J Med* 1997; **337:** 956-62. doi: 10.1056/NEJM199710023371402
5. Overgaard M, Jensen MB, Overgaard J, Hansen PS, Rose C, Andersson M, et al. Postoperative radiotherapy in high-risk postmenopausal breast-cancer patients given adjuvant tamoxifen: Danish Breast Cancer Cooperative Group DBCG 82c randomised trial. *Lancet* 1999; **353:** 1641-8. doi: 10.1016/S0140-6736(98)09201-0
6. Cuzick J, Stewart H, Rutqvist L, Houghton J, Edwards R, Redmond C, et al. Cause-specific mortality in long-term survivors of breast cancer who participated in trials of radiotherapy. *J Clin Oncol* 1994; **12:** 447-53. doi: 10.1200/JCO.1994.12.3.447
7. Bouillon K, Haddy N, Delaloge S, Garbay JR, Garsi JP, Brindel P, et al. Long-term cardiovascular mortality after radiotherapy for breast cancer. *J Am Coll Cardiol* 2011; **57:** 445-52. doi: 10.1016/j.jacc.2010.08.638
8. Darby SC, McGale P, Taylor CW, Peto R. Long-term mortality from heart disease and lung cancer after radiotherapy for early breast cancer: prospective cohort study of about 300,000 women in US SEER cancer registries. *Lancet Oncol* 2005; **6:** 557-65. doi: 10.1016/S1470-2045(05)70251-5
9. Rehammar JC, Jensen MB, McGale P, Lorenzen EL, Taylor C, Darby SC, et al. Risk of heart disease in relation to radiotherapy and chemotherapy with anthracyclines among 19,464 breast cancer patients in Denmark, 1977-2005. *Radiother Oncol* 2017; **123:** 299-305. doi: 10.1016/j.radonc.2017.03.012
10. Rutter CE, Chagpar AB, Evans SB. Breast cancer laterality does not influence survival in a large modern cohort: implications for radiation-related cardiac mortality. *Int J Radiat Oncol Biol Phys* 2014; **90:** 329-34. doi: 10.1016/j.ijrobp.2014.06.030
11. Soumarová R, Rušinová L. Cardiotoxicity of breast cancer radiotherapy – overview of current results. *Rep Pract Oncol Radiother* 2020; **25:** 182-6. doi: 10.1016/j.rpor.2019.12.008
12. Czeremszyńska B, Drozda S, Górzyński M, Kępka L. Selection of patients with left breast cancer for deep-inspiration breath-hold radiotherapy technique: results of a prospective study. *Rep Pract Oncol Radiother* 2017; **22:** 341-8. doi: 10.1016/j.rpor.2017.05.002
13. Joo JH, Kim SS, Ahn SD, Kwak J, Jeong C, Ahn SH, et al. Cardiac dose reduction during tangential breast irradiation using deep inspiration breath hold: a dose comparison study based on deformable image registration. *Radiat Oncol* 2015; **10:** 264. doi: 10.1186/s13014-015-0573-7
14. Schönecker S, Walter F, Freislederer P, Marisch C, Scheithauer H, Harbeck N, et al. Treatment planning and evaluation of gated radiotherapy in left-sided breast cancer patients using the CatalystTM/SentinelTM system for deep inspiration breath-hold (DIBH). *Radiat Oncol* 2016; **11:** 143. doi: 10.1186/s13014-016-0716-5
15. Eldredge-Hindy H, Lockamy V, Crawford A, Eldredge-Hindy H, Lockamy V, Crawford A, et al. Active Breathing Coordinator reduces radiation dose to the heart and preserves local control in patients with left breast cancer: report of a prospective trial. *Pract Radiat Oncol* 2015; **5:** 4-10. doi: 10.1016/j.prro.2014.06.004
16. Al-Hammadi N, Caparrotti P1, Naim C, Hayes J, Benson KR, Vasic A, et al. Voluntary deep inspiration breath-hold reduces the heart dose without compromising the target volume coverage during radiotherapy for left-sided breast cancer. *Radiol Oncol* 2018; **52:** 112-20. doi: 10.1515/raon-2018-0008
17. Smyth LM, Knight KA, Aarons YK, Wasiak J. The cardiac dose-sparing benefits of deep inspiration breath-hold in left breast irradiation: a systematic review. *J Med Radiat Sci* 2015; **62:** 66-73. doi: 10.1002/jmrs.89
18. Boero IJ, Paravati AJ, Triplett DP, Hwang L, Matsuno RK, Gillespie EF, et al. Modern radiation therapy and cardiac outcomes in breast cancer. *Int J Radiat Oncol Biol Phys* 2016; **94:** 700-8. doi: 10.1016/j.ijrobp.2015.12.018
19. Drost L, Yee C, Lam H, Zhang L, Wronski M, McCann C, et al. A systematic review of heart dose in breast radiotherapy. *Clin Breast Cancer* 2018; **18:** e819-24. doi: 10.1016/j.clbc.2018.05.010
20. Pierce L, Feng M, Griffith KA, Jagsi R, Boike T, Dryden D, et al. Recent time trends and predictors of heart dose from breast radiation therapy in a large quality consortium of radiation oncology practices. *Int J Radiat Oncol Biol Phys* 2017; **99:** 1154-61. doi: 10.1016/j.ijrobp.2017.07.022
21. Rong Y, Walston S, Welliver MX, Chakravarti A, Quick AM. Improving intrafractional target position accuracy using a 3D surface surrogate for left breast irradiation using the respiratory-gated deep-inspiration breath-hold technique. *PLoS One* 2014; **9:** e97933. doi: 10.1371/journal.pone.0097933
22. Walston S, Quick AM, Kuhn K, Rong Y. Dosimetric considerations in respiratory-gated deep inspiration breath-hold for left breast irradiation. *Technol Cancer Res Treat* 2017; **16:** 22-32. doi: 10.1177/1533034615624311
23. Offersen BV, Boersma LJ, Kirkove C, Hol S, Aznar MC, Biete Sola A, et al. ESTRO consensus guideline on target volume delineation for elective radiation therapy of early stage breast cancer. *Radiother Oncol* 2015; **114:** 3-10. doi: 10.1016/j.radonc.2014.11.030
24. Feng M, Moran JM, Koelling T, Chughtai A, Chan JL, Freedman L, et al. Development and validation of a heart atlas to study cardiac exposure to radiation following treatment for breast cancer. *Int J Radiat Oncol Biol Phys* 2011; **79:** 10-8. doi: 10.1016/j.ijrobp.2009.10.058
25. Fogliata A, Seppälä J, Reggiori G, Lobefalo F, Palumbo V, De Rose F, et al. Dosimetric trade-offs in breast treatment with VMAT technique. *Br J Radiol* 2017; **90:** 20160701. doi: 10.1259/bjr.20160701

26. Berg M, Lorenzen EL, Jensen I, Thomsen MS, Lutz CM, Refsgaard L, et al. The potential benefits from respiratory gating for breast cancer patients regarding target coverage and dose to organs at risk when applying strict dose limits to the heart: results from the DBCG HYPO trial. *Acta Oncol* 2018; **57:** 113-9. doi: 10. 1080/ 0284186X. 2017. 1406139

27. Testolin A, Ciccarelli S, Vidano G, Avitabile R, Dusi F, Alongi F. Deep inspiration breath-hold intensity modulated radiation therapy in a large clinical series of 239 left-sided breast cancer patients: a dosimetric analysis of organs at risk doses and clinical feasibility from a single center experience. *Br J Radiol* 2019; **92:** 20190150. doi: 10.1259/bjr.20190150

28. Darby SC, Ewertz M, McGale P, Bennet AM, Blom-Goldman U, Brønnum D, et al. Risk of ischemic heart disease in women after radiotherapy for breast cancer. *N Engl J Med* 2013; **368:** 987-98. doi: 10.1056/NEJMoa1209825

29. Taylor C, Correa C, Duane FK, Aznar MC, Anderson SJ, Bergh J, et al. Estimating the risks of breast cancer radiotherapy: evidence from modern radiation doses to the lungs and heart and from previous randomized trials. *J Clin Oncol* 2017; **35:** 1641-9. doi: 10.1200/JCO.2016.72.0722

30. Sardaro A, Petruzzelli MF, D'Errico MP, Grimaldi L, Pili G, Portaluri M. Radiation-induced cardiac damage in early left breast cancer patients: risk factors, biological mechanisms, radiobiology, and dosimetric constraints. *Radiother Oncol* 2012; **103:** 133-42. doi: 10.1016/j.radonc.2012.02.008

31. Darapu A, Balakrishnan R, Sebastian P, Hussain MRK, Ravindran P, John S. Is the deep inspiration breath-hold technique superior to the free breathing technique in cardiac and lung sparing while treating both left-sided post-mastectomy chest wall and supraclavicular regions? *Case Rep Oncol* 2017; **10:** 37-51. doi: 10.1159/000453607

32. Edvardsson A, Nilsson MP, Amptoulach S, Ceberg S. Comparison of doses and NTCP to risk organs with enhanced inspiration gating and free breathing for left-sided breast cancer radiotherapy using the AAA algorithm. *Radiat Oncol* 2015; **10:** 84. doi: 10.1186/s13014-015-0375-y

33. Kügele M, Edvardsson A, Berg L, Alkner S, Andersson Ljus C, Ceberg S. Dosimetric effects of intrafractional isocenter variation during deep inspiration breath-hold for breast cancer patients using surface-guided radiotherapy. *J Appl Clin Med Phys* 2018; **19:** 25-38. doi: 10.1002/acm2.12214

34. Swanson T, Grills IS, Ye H, Entwistle A, Teahan M, Letts N, et al. Six-year experience routinely using moderate deep inspiration breath-hold for the reduction of cardiac dose in left-sided breast irradiation for patients with early-stage or locally advanced breast cancer. *Am J Clin Oncol* 2013; **36:** 24-30. doi: 10.1097/COC.0b013e31823fe481

35. Jensen CA1, Abramova T1, Frengen J, Lund JÅ. Monitoring deep inspiration breath hold for left-sided localized breast cancer radiotherapy with an in-house developed laser distance meter system. *J Appl Clin Med Phys* 2017; **18:** 117-23. doi: 10.1002/acm2.12137

36. Zhao F, Shen J, Lu Z, Luo Y, Yao G, Bu L, et al. Abdominal DIBH reduces the cardiac dose even further: a prospective analysis. *Radiat Oncol* 2018; **13:** 116. doi: 10.1186/s13014-018-1062-6

37. Finazzi T, Nguyen VT, Zimmermann F, Papachristofilou A. Impact of patient and treatment characteristics on heart and lung dose in adjuvant radiotherapy for left-sided breast cancer. *Radiat Oncol* 2019; **14:** 153. doi: 10.1186/s13014-019-1364-3

*research article*

# The outcome of IVF/ICSI cycles in male cancer patients: retrospective analysis of procedures from 2004 to 2018

Tanja Burnik Papler[1], Eda Vrtacnik-Bokal[1], Saso Drobnic[1], Martin Stimpfel[1]

[1] Department of Human Reproduction, Division of Gynaecology, University Medical Centre Ljubljana, Ljubljana, Slovenia

Radiol Oncol 2021; 55(2): 221-228.

Received 18 August 2020
Accepted 25 January 2021

Correspondence to: Assist. Martin Stimpfel, Ph.D., Department of Human Reproduction, Division of Gynaecology, University Medical Centre Ljubljana, Slajmerjeva 3. 1000-Ljubljana, SI-Slovenia. E-mail: martin.stimpfel@gmail.com, martin.stimpfel@kclj.si

Disclosure: No potential conflicts of interest were disclosed.

**Introduction.** Fertility preservation is an important aspect of quality of life in oncological patients, and in men is achieved by semen cryopreservation prior to treatment. Results of *in vitro* fertilization (IVF) procedures in healthy infertile couples are comparable, regardless of whether fresh or cryopreserved semen is used, but are scarce in male oncological patients.

**Patients and methods.** We performed a retrospective analysis of IVF/intracytoplasmic sperm injection (IVF/ICSI) procedures in infertile couples where men had been treated for cancer in the past. We additionally compared the results of IVF/ICSI procedures with respect to the type of semen used (fresh, cryopreserved).

**Results.** We compared the success rates of 214 IVF/ICSI cycles performed in the years 2004–2018. Pregnancy (30.0% *vs.* 21.4%; p = 0.12) and live-birth rates (22.3% *vs.* 17.9%; p = 0.43) per oocyte aspiration were similar between the groups in fresh cycles; however embryo utilization (48.9% *vs.* 40.0%; p = 0.006) and embryo cryopreservation rates (17.3% *vs.* 12.7%; p = 0.048) were significantly higher in the cryopreserved semen group. The cumulative pregnancy rate (60.6% *vs.* 37.7%; p = 0.012) was significantly higher, and the live-birth rate (45.1% *vs.* 34.0%; p = 0.21) non-significantly higher, in the cryopreserved semen group.

**Conclusions.** The success of IVF/ICSI procedures in couples where the male partner was treated for cancer in the past are the same in terms of pregnancies and live-births in fresh cycles regardless of the type of semen used. However, embryo utilization and embryo cryopreservation rates are significantly higher when cryopreserved semen is used, leading to a significantly higher cumulative number of couples who achieved at least one pregnancy.

Key words: assisted reproduction techniques; infertility; fertility preservation; sperm cryopreservation; pregnancy

## Introduction

The life expectancy of cancer patients has significantly improved during the past decade due to improved oncological treatment, and it has therefore become important to enable them to have a quality life after the oncological treatment has finished. The ability to have your own biological children is one of the most important aspects of quality of life.

It is well known that oncological treatment, as well as cancer itself, can cause male infertility. Testicles are sensitive to chemotherapy and radiotherapy, which can cause a disruption of spermatogenesis.[1,2] It has been estimated that approximately 15–30% of male cancer patient survivors become infertile after oncological treatment.[3,4] Whether or not sperm production is disrupted depends on several factors: type of cancer; semen quality prior to treatment; type, dosage and duration of oncological treatment.[2,5] For instance, most of the alkylating agents (*e.g.* chlorambucil, cyclophosphamide, melphalan), ionizing radiation (causes DNA breaks) and cisplatin (causes DNA cross-link) can cause prolonged azoospermia; nitrosoureas can cause

azoospermia in adulthood when used for treatment prior to puberty; while other agents cause permanent or prolonged azoospermia only when applied in combination with other gonadotoxic agents (*e.g* busulfan).[6] Despite the fact that spermatogenesis can be reinstated after prolonged azoospermia and semen quality can be reduced[7,8], it doesn't seem that intensified chemotherapy is the most important predictor for reducing fertility.[9] It is therefore crucial that we explain the possible negative impact of oncological treatment on fertility, and offer the possibility of fertility preservation to male cancer patients prior to treatment.[10] Data in literature show that semen cryopreservation before the start of oncological treatment is a highly successful method for male fertility preservation.[11,12] This method can be used from puberty onwards. It has been shown that the success rate of *in vitro* fertilization (IVF) procedures in healthy men is comparable when fresh or cryopreserved semen is used.[13,14] Before puberty, only testicular tissue can be cryopreserved for later re-transplantation or *in vitro* manipulation after the end of treatment.[15] This procedure, however, is still experimental and has only been successfully used in animal models[16,17] and monkeys.[18]

The aim of the present study was to retrospectively analyze the success rates of IVF procedures that were performed with the semen of men who had been treated for cancer in the past. We determined whether there are differences in IVF/intracytoplasmic sperm injection (IVF/ICSI) success rates when fresh or cryopreserved semen is used.

## Patients and methods

We performed a retrospective analysis of IVF/ICSI cycles in couples where the male partner had previously been treated for cancer. All consecutive cycles performed at our IVF center at the University Medical Centre in Ljubljana, in the period between January 2004 and December 2018, were included. First, we analyzed all cycles together, regardless of whether fresh or frozen semen was used for oocyte fertilization. We then divided the couples into two groups: one group in which cryopreserved semen was used for oocyte fertilization, and one group where fresh semen, obtained on the day of oocyte aspiration, was used. In all cases included in this retrospective study, the semen was cryopreserved before oncological treatment. Cryopreserved semen was used for IVF/ICSI in all azoospermic and aspermic patients. Fresh semen was used when the semen was of proper quality, so that high fertilization rates were expected. The decision on which sperm to use was made for each patient/sperm sample individually. If fertilization rates in cycles using fresh semen were low, frozen thawed semen was used in the next IVF/ICSI cycle. Similarly, if the development of embryos was poor in the previous cycle, we changed the type of semen to be used for the next IVF/ICSI procedure, where possible. Fresh semen was also used in patients where semen was not cryopreserved prior to oncological treatment.

In the majority of cases, embryo transfer was performed on day 5. However, in cases where there were only 1 or 2 embryos available for ET, or there was poor embryo development until day 5 in the previous cycle, embryos were transferred on day 3. In cases of poor embryo development, the rest of the embryos were cultured until day 5/6, and cryopreserved if developed to blastocysts of appropriate quality, according to Gardner *et al.*[19] The same criteria for the cryopreservation of supernumerary embryos were considered when all embryos were cultured until day 5/6.

To determine the differences between the groups, data were analyzed by using Pearson's chi-square test, Fisher's exact test and a Student's t-test. A p value of less than 0.05 was considered as statistically significant.

The study did not have to be notified in the Ethics Committee according to Slovene law, as it was a register-based study where all the participants signed individual personal approval and permission before starting the treatment (Personal Data Protection Act, Official Gazette of the Republic of Slovenia No 94/07, 2004). Additionally, by Slovenian law, the healthcare providers are obligated to collect data about assisted reproduction procedures and follow the success rates (Healthcare Databases Act, Official Gazette of the Republic of Slovenia No 65/00, 2000; No 47/15, 2015; 31/18, 2018).

## Results

We retrospectively analyzed the outcome of IVF/ICSI cycles where cryopreserved or fresh semen from male oncological patients was used for oocyte fertilization. Table 1 presents types of cancer, and the number of cases for each cancer type in the cryopreserved and fresh semen groups. There were 214 such IVF/ICSI cycles performed in 115 couples between January 2004 and December 2018. This represents 1.5% of all cycles performed during this

period. The mean female age was 31.9 ± 4.6 years. Altogether, 2,102 oocytes were retrieved (9.8 ± 5.8 per cycle). After fertilization (the results are for conventional IVF and ICSI together), 1,007 oocytes (47.9%) were fertilized, 363 (17.3%) were immature, 262 (12.5%) degenerated and 26 (1.2%) were incorrectly fertilized (polyploidies). Nine hundred and sixty-three fertilized oocytes (95.6%) developed into embryos, resulting in 4.5 ± 3.6 embryos per cycle. On the third day after oocyte aspiration, 63 (6.5%) of the embryos were transferred to the uterus, and the remaining embryos (900; 93.5%) were cultured until the fifth or sixth day of development. Of these embryos, 289 (32.1%) developed to blastocysts, and at least one blastocyst was obtained in 121 IVF/ICSI cycles (56.5%). Altogether, fresh embryo transfer (ET) was performed in 176 cycles; in 32 cycles (15.0%) there were no embryos of appropriate quality for transfer. Cryopreservation of all embryos was conducted in 6 cycles. Supernumerary embryos were cryopreserved (148; 15.4%) and cryopreservation was performed in 55 cycles (25.7%). Embryo utilization rate (the number of transferred embryos plus the number of cryopreserved) was 45.2%. Pregnancy rate per ET (with mean number of transferred embryos 1.6 ± 0.5) was 32.4% and 26.6% per oocyte aspiration. Miscarriage occurred in 12 pregnancies (21.1%). There were 44 deliveries

**TABLE 1.** Types of cancer in male patients, and the number of cases for each cancer type in the cryopreserved and fresh semen groups

| | Cryopreserved semen (N) | Fresh semen(N) |
|---|---|---|
| Testicular cancer | 39 | 36 |
| Hodgkin lymphoma | 16 | 7 |
| Non-Hodgkin lymphoma | 0 | 1 |
| Burkitt lymphoma | 1 | 0 |
| Leukemia | 7 | 5 |
| Plasmacytoma | 3 | 1 |
| Rectal cancer | 1 | 2 |
| Brain tumor | 1 | 0 |
| Malignant melanoma | 1 | 0 |
| Prostate cancer | 1 | 0 |
| Epipharynx tumor | 0 | 1 |
| Together | 70 | 53 |

**TABLE 2.** The baseline characteristics of patients and *in vitro* fertilization / intracytoplasmic sperm injection (IVF/ICSI) cycles. Statistically significant differences are marked with an asterisk (p value < 0.05)

| | Cryopreserved semen | Fresh semen | p values |
|---|---|---|---|
| **Causes of female infertility** | | | |
| Tubal factor | 2 (1.5%) | 1 (1.2%) | 1 |
| Endometriosis | 2 (1.5%) | 2 (2.4%) | 1 |
| Endocrine disorders | 16 (12.3%) | 2 (2.4%) | 0.011* |
| Uterine factor | 9 (6.9%) | 11 (13.1%) | 0.13 |
| Cervical factor | 0 | 5 (6.0%) | 0.009* |
| Multiple causes of female infertility | 15 (11.5%) | 20 (23.8%) | 0.018* |
| No cause of female infertility | 86 (66.2%) | 43 (51.2%) | 0.029* |
| **Ovarian stimulation protocols** | | | |
| Long agonist protocol | 74 (56.9%) | 53 (63.1%) | 0.37 |
| Short antagonist protocol | 55 (42.3%) | 30 (35.7%) | 0.33 |
| Others | 1 (0.8%) | 1 (1.2%) | 1 |
| **Number of cycles** | 130 | 84 | |
| **Number of couples** | 71 | 53 | |
| **Female mean age (± SD)** | 31.7±4.8 | 32.3±4.3 | 0.31 |
| **Number and rate of ICSI cycles** | 122 (93.8%) | 40 (84.5%) | 0.025* |
| **Oocyte number** (mean number per cycle) | 1273 (9.8±5.2) | 829 (9.9±6.7) | 0.93 |
| **Number of MII oocytes** (ICSI cycles only) | 974 | 568 | |

MII = metaphase II

**TABLE 3.** The outcome of the *in vitro* fertilization / intracytoplasmic sperm injection (IVF/ICSI) cycles in terms of oocytes and embryos according to the type of semen used. Statistically significant differences are marked with an asterisk (p value < 0.05)

| | Cryopreserved semen | Fresh semen | p value |
|---|---|---|---|
| Rate of normally fertilized oocytes (per COC, IVF and ICSI together) | 46.3% | 50.4% | 0.06 |
| Rate of normally fertilized oocytes (per MII oocytes number) | 55.6% | 59.3% | 0.16 |
| Number and rate of immature oocytes (%) | 225 (17.7%) | 138 (16.6%) | 0.54 |
| Number and rate of degenerated oocytes (% per COC, IVF and ICSI together) | 171 (13.4%) | 91 (11.0%) | 0.10 |
| Number and rate of degenerated oocytes (% per MII oocytes number) | 166 (17.0%) | 88 (15.5%) | 0.43 |
| Number and rate of polyploidies (% per all COC retrieved) | 13 (1.0%) | 13 (1.6%) | 0.27 |
| Number and proportion of embryos (% per normally fertilized oocytes) | 560 (95.1%) | 403 (96.4%) | 0.31 |
| Mean number of embryos per cycle (mean number ± SD) | 4.3 ± 3.4 | 4.8 ± 3.8 | 0.33 |
| Number of embryos cultured until day 5/6 | 518 (92.5%) | 382 (94.8%) | 0.16 |
| Number and rate of blastocysts (% per embryos cultured until day 5/6) | 177 (34.2%) | 112 (29.3%) | 0.12 |
| Number and rate of embryo utilization (transferred plus frozen embryos) | 274 (48.9%) | 161 (40.0%) | 0.006* |
| Number of cycles with at least one blastocyst | 74 (56.9%) | 47 (56.0%) | 0.89 |
| Number and rate of cryopreserved embryos (% of all embryos) | 97 (17.3%) | 51 (12.7%) | 0.048* |
| Number and proportion of cycles with embryo cryopreservation | 39 (30.0%) | 16 (19.0%) | 0.07 |
| Number and proportion of cycles with freezing/without ET | 4 (3.1%) | 2 (2.4%) | 1 |
| Number and proportion of cycles without freezing/without ET | 17 (13.1%) | 15 (17.9%) | 0.34 |

COC = cumulus oocyte complex; ET = embryo transfer; MII = metaphase II

leading to a 25.0% live-birth rate per ET and 20.6% per oocyte aspiration. Twins were born in three cases, representing 6.8% of all births.

Due to the nature of the oncological disease and its treatment, it is sometimes necessary to use the semen that has been cryopreserved prior to the start of the treatment in IVF/ICSI procedures. Therefore, we further analyzed whether there was a difference in the outcome of IVF/ICSI cycles, depending on whether fresh or cryopreserved semen was used. We summarized the types of cancer in male patients and the number of cases in Table 1, while the baseline characteristics of analyzed IVF/ICSI cycles are presented in Table 2. In the analyzed period, cryopreserved semen was used in 130 IVF/ICSI cycles, and fresh semen, obtained on the day of oocytes aspiration, was used in 84 IVF/ICSI cycles. Detailed results of these procedures are shown in Tables 3 and 4. Briefly, the cryopreserved semen and fresh semen groups were comparable for mean female's age (31.7 ± 4.8 *vs.* 32.3 ± 4.3), mean number of oocytes retrieved per aspiration (9.8 ± 5.2 *vs.* 9.9 ± 6.7), fertilization rate per retrieved cumulus-oocyte complexes (46.3% *vs.* 50.4%), and mean number of embryos obtained per cycle (4.3 ± 3.4 *vs.* 4.8 ± 3.8). There was a significant difference in some causes of female infertility. Briefly, significantly more women had an endocrinological cause of infertility, and a significantly higher number of couples did not have any female's cause of infertility in the cryopreserved semen group (Table 2). In the fresh semen group, a significantly higher number of women had more than one cause of infertility. In the cryopreserved semen group, a statistically significant higher rate of cryopreserved embryos (17.3% *vs.* 12.7%; p = 0.048) and a higher embryo utilization rate (48.9 % *vs.* 40.0%; p = 0.006) were observed. Furthermore, ICSI was performed more often (93.8% *vs.* 84.5%; p = 0.025) in the cryopreserved semen group. ICSI was performed only in cases of impaired semen quality, (oligo-, astheno-, or teratozoospermia, or a combination of these conditions).

In terms of the clinical outcomes of IVF/ICSI cycles, there were no differences in pregnancy rate per ET (35.8% *vs.* 26.9%), live birth rate per fresh ET (26.6% *vs.* 22.4%) and miscarriage rate per pregnancy (25.6% *vs.* 11.1%) between the cryopreserved and fresh semen groups. As presented in Table 4, the proportion of day 3 ETs was similar between the analyzed groups. However, when we analyzed cumulative pregnancy rate per couple (fresh and frozen-thawed cycles together), the results showed that at least one pregnancy was achieved in 60.6%

**TABLE 4.** Clinical outcome of *in vitro* fertilization / intracytoplasmic sperm injection (IVF/ICSI) cycles according to the type of semen used. Statistically significant difference is marked with an asterisk (p value < 0.05)

| | Cryopreserved semen | Fresh semen | p values |
|---|---|---|---|
| Number of all ETs | 109 | 67 | 0.45 |
| Number of ETs on day 3 (% per all ETs) | 27 (24.8%) | 15 (22.4%) | 0.72 |
| Mean number of transferred embryos (± SD) | 1.6 ± 0.5 | 1.6 ± 0.5 | 0.81 |
| Number of pregnancies (% per ET) | 39 (35.8%) | 18 (26.9%) | 0.22 |
| Number of pregnancies (% per oocyte aspiration) | 39 (30.0%) | 18 (21.4%) | 0.12 |
| Live births (% per ET) | 29 (26.6%) | 15 (22.4%) | 0.53 |
| Live births (% per aspiration) | 29 (22.3%) | 15 (17.9%) | 0.43 |
| Miscarriages | 10 (25.6%) | 2 (11.1%) (+1 x EU) | 0.21 |
| Gestational age (all births) | 38.4 ± 2.6 | 36.0 ± 5.1 | 0.14 |
| Gestational age for singletons | 38.5 ± 2.7 | 36.6 ± 4.9 | 0.18 |
| Birth weight of singletons (g) | 3300 ± 589 | 2959 ± 672 | 0.12 |
| Twins | 2 (6.9%) | 1 (6.7%) | 1 |
| Cumulative number and rate of couples with at least one pregnancy | 43 (60.6%) | 20 (37.7%) | 0.012* |
| Cumulative number and rate of couples with at least one live birth | 32 (45.1%) (+4 ongoing pregnancies) | 18 (34.0%) | 0.21 |

EU = extrauterine pregnancy; ET = embryo transfer

of couples in the cryopreserved semen group, and in 37.7% of couples in the fresh semen group. The difference was statistically significant (p = 0.012). Despite this difference, the proportion of couples achieving at least one birth was similar on a cumulative level, with 45.1% in the cryopreserved group and 34.0% in the fresh semen group (p = 0.21).

There were 9 couples who underwent 33 cycles (16 cycles with cryopreserved semen and 17 cycles with fresh semen) and used both cryopreserved and fresh semen for the IVF/ICSI procedure. Four couples started the treatment with cryopreserved semen, five with fresh semen, and in 7 of these couples, the treatment led to live birth. One couple had two children, the first one conceived with cryopreserved semen, and second one with fresh semen.

The mean duration of cryopreservation of semen was 6.6 ± 4.4 years (minimum 1 year and maximum 19 years), and the mean semen volume per sample prior to cryopreservation was 3.1 ± 1.5 ml. The mean sperm concentration was 31.2 ± 30.7 million/ml, mean sperm motility 34.7 ± 10.3%, and the proportion of morphologically normal spermatozoa was 16.3 ± 14.3%. The mean number of cryopreserved straws per cryopreservation procedure was 8.1 ± 3.8; however, some patients underwent more than just one cryopreservation procedure, and the mean number of cryopreserved straws per patient was 11.2 ± 5.6. Until now, 40.0% of these samples have been used for IVF/ICSI procedures, and 14.1% of patients included in this analysis have used all of their cryopreserved semen. After the thawing of the samples, and before using them for the IVF/ICSI procedure, the mean sperm motility was 30.9 ± 19.9%, the proportion of morphologically normal spermatozoa was 20.1 ± 16.5%, and the mean sperm concentration was 18.8 ± 22.0 million/ml. This concentration is lower than in fresh samples, but this is to be expected because sperm samples are diluted in a 1:1 ratio with freezing solution before cryopreservation. In the group of patients where fresh semen was used, the mean sperm concentration was 34.7 ± 43.7 million/ml, mean sperm motility 50.0 ± 23.2%, and the proportion of morphologically normal spermatozoa was 16.2 ± 13.4%.

## Discussion

In the present study, we performed a retrospective analysis of 214 IVF/ICSI procedures where fresh or cryopreserved semen of men, who were treated for cancer in the past, was used. We found that the success of the IVF/ICSI procedures, in terms of pregnancies and live-births after fresh embryo transfer, was the same regardless of the type of semen used. However, embryo utilization and cryopreservation rates were significantly higher when cryopreserved

semen was used, which led to a significantly higher cumulative number of couples who achieved at least one pregnancy. Despite this, the difference in cumulative number of live-births was not statistically significant. One reason for this could be in the non-significant higher number of miscarriages in the cryopreserved semen group.

Altogether, success rates of IVF/ICSI procedures in couples where men were treated for cancer in the past were comparable with success rates of IVF/ICSI procedures in the general population of infertile couples treated in our clinic, and also on a European level. Analyses of all IVF/ICSI cycles (combined data for cryopreserved and fresh semen and for IVF and ICSI) have shown that pregnancy rate per oocyte aspiration was 26.6%, which is similar to the pregnancy rate of infertile patients treated in our center in the same time period (2004–2018), 25.5% respectively, and the latest pregnancy rate reported for the general population in the European IVF Monitoring (EIM) data from 2016.[20] EIM collects data on the performance of IVF procedures in European Union Member States (https://www.eshre.eu/Data-collection-and-research/Consortia/EIM). According to EIM data, in 2016, the proportion of pregnancy rate per oocyte aspiration was 28.0% for classical IVF and 25.0% for ICSI procedures.[20]

If we compare the remaining results (oocyte fertilization, embryo development) with which we evaluate the success of IVF/ICSI procedures, with criteria that determine the recommended minimum values[21], we can see that not all of them reach these values. The desired proportion of fertilized oocytes according to these criteria is 65% for ICSI and 60% for classical IVF. In the present analysis, where we did not separate the data according to the type of IVF procedure used for oocyte fertilization, the proportion of fertilized oocytes was 47.9%, and when only ICSI was analyzed this proportion was 57.0%. This proportion is similar to the one reported in one of the very rare studies similar to ours, where 49% of oocytes were fertilized with classical IVF and 51% with ICSI.[22] A similar thing is seen with the desired minimum proportion of embryos that develop to blastocysts. In our study, 32.1% of embryos cultured until day 5/6 developed to blastocysts, which is lower than the desirable 40%. It is important to note, however, that the minimum criteria are determined on the basis of the general population of "healthy" couples attending IVF. In our study, however, semen obtained from male oncological patients was used, and such semen has been shown to be of poorer quality.[23,24] Therefore, the observed differences in our study are somewhat expected and most likely cannot be considered significant. In addition to the negative impact of the disease itself or oncological gonadotoxic treatment on the basic criteria of semen quality (number, motility, morphology), the negative impact of the disease is also reflected in increased sperm DNA fragmentation.[25,26] Meta-analyses have shown that increased sperm DNA fragmentation negatively affects IVF/ICSI outcomes even in the healthy male population.[27,28]

Since a part of the IVF/ICSI procedures was performed with cryopreserved semen which was stored before oncological treatment, and a part of the procedures with fresh semen obtained on the day of oocyte aspiration, after oncological treatment was completed, we checked whether there were any differences in the success rates of IVF procedures according to the type of semen used. The literature shows that the success of IVF/ICSI procedures in healthy men is the same regardless of the type of semen (fresh, cryopreserved) used.[13,14] However, relatively little data are available in men who have been treated for cancer. In part, the problem is that a relatively small proportion of men who cryopreserve semen before treatment also use it later. It is estimated that semen is used by 1.5% to 16.3% of men.[11,22,29-35] Studies by van Casteren *et al*.[11] and Botchan *et al*.[30] showed that the proportion of births (per oocyte aspiration) after the use of cryopreserved semen in cancer patients was 24% and 25%, respectively, which is similar to our results (22.3%). The study of van Casteren *et al*.[11] states that in 20% of IVF/ICSI procedures no suitable embryo was obtained for transfer. This is more than in our study, where in 15.0% of procedures (cryopreserved and fresh semen) there were no embryos suitable for transfer. There are also studies that report higher (29% for IVF and 32% for ICSI)[22] and much higher (50%)[36] percentage of births per oocyte aspiration. The reason for such a large difference with our results may be in the higher average number of embryos transferred per transfer. At our department, a maximum of two embryos are transferred to the uterus at the same time. In the study of Hourvitz *et al*.[36], the average number of embryos transferred to the uterus was 3.0 ± 1.1, which is significantly more than in our study (1.6 ± 0.5).

Interestingly, as mentioned above, our data have shown that in the group of couples where cryopreserved semen was used, embryo utilization and cryopreservation rates were significantly higher compared to couples where fresh semen was used. This finding implies that semen qual-

ity deteriorates after the oncological treatment. Data of currently published studies, however, are conflicting. Trottmann *et al*.[37] stated that semen quality deteriorated drastically after oncological treatment. Weibring *et al*.[38] reported similar observations, but further noted that semen quality improves 12 months after the end of treatment. Di Bisceglie *et al*.[39] also found that semen quality starts to improve 18 months after the end of treatment. In addition, there is evidence of an improvement of sperm DNA fragmentation after the end of some oncological treatments.[40] Despite these data, it is highly recommended that semen is cryopreserved in all oncological patients before treatment, even in those undergoing low-risk gonadotoxic treatment. This way, semen of better quality can be chosen to perform IVF/ICSI, if needed.

In the present study, a significantly higher number of women in the cryopreserved semen group did not have any cause of infertility, and IVF was only needed due to the male factor. One would assume that this is the cause of the significantly higher embryo cryopreservation rates in the cryopreserved semen. However, analysis of 121,744 women undergoing their first IVF/ICSI cycles has shown that IVF/ICSI success rates are most significantly affected by female's age and not by female's cause of infertility.[41] No significant difference in women's age was found in the present study.

As this is a retrospective study, there are some limitations in our data. We included cycles from a long time period, and some changes in our work have been introduced into clinical practice since then. For instance, in 2004, long GnRH agonist protocol was mostly used for controlled ovarian hyperstimulation, and it has been mostly replaced with short GnRH antagonist protocol since 2010. There have also been some changes in embryo culture approach, and embryos have been cultured in lower oxygen concentration (5%) since 2008. Prior to 2008, they were cultured in an atmospheric concentration of oxygen (21%). Additionally, there have been a few changes of manufacturers and types of embryo culture media. Despite these limitations, this shouldn't impair the conclusions drawn from our results, as the described changes were applied for all couples (cryopreserved and fresh semen groups).

## Conclusions

Semen cryopreservation before the start of oncological treatment is a widely accepted and successful method to maintain the fertility of men with cancer, as oncological treatment can negatively affect spermatogenesis. The results of our retrospective study show that the results of IVF/ICSI procedures in terms of pregnancies and live-birth rates after fresh embryo transfer are comparable regardless of whether we use fresh or cryopreserved semen from male cancer patients. Additionally, while the embryo utilization and embryo cryopreservation rates are higher if cryopreserved semen is used, this leads to a higher cumulative pregnancy rate and possibly to a higher cumulative birth rate. Overall results also show that the success rates of IVF/ICSI procedures where fresh or cryopreserved semen of male cancer patients was used are comparable with the results of IVF/ICSI procedures in the general population of infertile couples at European level, as well as with the population of couples treated at our clinic in the same time period.

## Acknowledgments

The authors would like to thank all gynecologists, clinical embryologists, medical nurses and other staff at the Department of Human Reproduction, Division of Gynaecology, University Medical Centre Ljubljana, Slovenia, for their support.

## References

1. Ragheb AM, Sabanegh ES Jr. Male fertility-implications of anticancer treatment and strategies to mitigate gonadotoxicity. *Anticancer Agents Med Chem* 2010; **10:** 92-102. doi: 10.2174/1871520611009010092
2. Howell SJ, Shalet SM. Testicular function following chemotherapy. *Hum Reprod Update* 2001; **7:** 363-9. doi: 10.1093/humupd/7.4.363
3. Johnson MD, Cooper AR, Jungheim ES, Lanzendorf SE, Odem RR, Ratts VS. Sperm banking for fertility preservation: a 20-year experience. *Eur J Obstet Gynecol Reprod Biol* 2013; **170:** 177-82. doi: 10.1016/j.ejogrb.2013.06.021
4. Reebals JF, Brown R, Buckner EB. Nurse practice issues regarding sperm banking in adolescent male cancer patients. *J Pediatr Oncol Nurs* 2006; **23:** 182-8. doi: 10.1177/1043454206289868
5. Giwercman A, Petersen PM. Cancer and male infertility. *Baillieres Best Practice Res Clin Endo Metab* 2000; **14:** 453-71. doi: 10.1053/beem.2000.0091
6. Meistrich ML. Effects of chemotherapy and radiotherapy on spermatogenesis in humans. *Fertil Steril* 2013; **100:** 1180-6. doi: 10.1016/j.fertnstert.2013.08.010
7. Neal MS, Nagel K, Duckworth J, Bissessar H, Fischer MA, Portwine C, et al. Effectiveness of sperm banking in adolescents and young adults with cancer: a regional experience. *Cancer* 2007; **110:** 1125-9. doi: 10.1002/cncr.22889
8. Tournaye H, Goossens E, Verheyen G, Frederickx V, De Block G, Devroey P, et al. Preserving the reproductive potential of men and boys with cancer: current concepts and future prospects. *Hum Reprod Update* 2004; **10:** 525-32. doi: 10.1093/humupd/dmh038
9. Boltežar L, Pintarić K, Jezeršek Novaković B. Fertility in young patients following treatment for Hodgkin's lymphoma: a single center survey. *J Assist Reprod Genet* 2016; **33:** 325-33. doi:10.1007/s10815-015-0636-6

10. Loren AW, Mangu PB, Beck LN, Brennan L, Magdalinski AJ, Partridge AH, et al. Fertility preservation for patients with cancer: American Society of Clinical Oncology clinical practice guideline update. *J Clin Oncol* 2013; **31:** 2500-10. doi: 10.1200/JCO.2013.49.2678

11. van Casteren NJ, van Santbrink EJ, van Inzen W, Romijn JC, Dohle GR. Use rate and assisted reproduction technologies outcome of cryopreserved semen from 629 cancer patients. *Fertil Steril* 2008; **90:** 2245-50. doi: 10.1016/j.fertnstert.2007.10.055

12. Depalo R, Falagario D, Masciandaro P, Nardelli C, Vacca MP, Capuano P, et al. Fertility preservation in males with cancer: 16-year monocentric experience of sperm banking and post-thaw reproductive outcomes. *Ther Adv Med Oncol* 2016; **8:** 412-20. doi: 10.1177/1758834016665078

13. Englert Y, Delvigne A, Vekemans M, Lejeune B, Henlisz A, de Maertelaer G, et al. Is fresh or frozen semen to be used in in vitro fertilization with donor sperm? *Fertil Steril* 1989; **51:** 661-4. doi: 10.1016/S0015-0282(16)60617-9

14. Eastick J, Venetis C, Cooke S, Storr A, Susetio D, Chapman M. Is early embryo development as observed by time-lapse microscopy dependent on whether fresh or frozen sperm was used for ICSI? A cohort study. *J Assist Reprod Genet* 2017; **34:** 733-40. doi: 10.1007/s10815-017-0928-0

15. Tournaye H, Dohle GR, Barratt CL. Fertility preservation in men with cancer. *Lancet* 2014; **384:** 1295-301. doi: 10.1016/S0140-6736(14)60495-5

16. Honaramooz A, Snedaker A, Boiani M, Schöler H, Dobrinski I, Schlatt S. Sperm from neonatal mammalian testes grafted in mice. *Nature* 2002; **418:** 778-81. doi: 10.1038/nature00918

17. Rodriguez-Sosa JR, Dobrinski I. Recent developments in testis tissue xenografting. *Reproduction* 2009; **138:** 187-94. doi: 10.1530/REP-09-0012

18. Fayomi AP, Peters K, Sukhwani M, Valli-Pulaski H, Shetty G, Meistrich ML, et al. Autologous grafting of cryopreserved prepubertal rhesus testis produces sperm and offspring. *Science* 2019; **363:** 1314-9. doi: 10.1126/science.aav2914. Erratum in: *Science* 2019; **364:** eaax4999. doi: 10.1126/science.aax4999

19. Gardner DK, Lane M, Stevens J, Schlenker T, Schoolcraft WB. Blastocyst score affects implantation and pregnancy outcome: towards a single blastocyst transfer. *Fertil Steril* 2000; **73:** 1155-8. doi: 10.1016/s0015-0282(00)00518-5

20. European IVF-monitoring Consortium (EIM) for the European Society of Human Reproduction and Embryology (ESHRE), Wyns C, Bergh C, Calhaz-Jorge C, De Geyter Ch, Kupka MS, Motrenko T, et al. ART in Europe, 2016: results generated from European registries by ESHRE. *Hum Reprod Open* 2020; **2020:** hoaa032. doi: 10.1093/hropen/hoaa032

21. ESHRE Special Interest Group of Embryology and Alpha Scientists in Reproductive Medicine. The Vienna consensus: report of an expert meeting on the development of ART laboratory performance indicators. *Reprod Biomed Online* 2017; **35:** 494-510. doi: 10.1016/j.rbmo.2017.06.015

22. Muller I, Oude Ophuis RJ, Broekmans FJ, Lock TM. Semen cryopreservation and usage rate for assisted reproductive technology in 898 men with cancer. *Reprod Biomed Online* 2016; **32:** 147-53. doi: 10.1016/j.rbmo.2015.11.005

23. Auger J, Sermondade N, Eustache F. Semen quality of 4480 young cancer and systemic disease patients: baseline data and clinical considerations. *Basic Clin Androl* 2016; **26:** 3. doi: 10.1186/s12610-016-0031-x

24. Degl'Innocenti S, Filimberti E, Magini A, Krausz C, Lombardi G, Fino MG, et al. Semen cryopreservation for men banking for oligospermia, cancers, and other pathologies: prediction of post-thaw outcome using basal semen quality. *Fertil Steril* 2013; **100:** 1555-63. doi: 10.1016/j.fertnstert.2013.08.005

25. Tamburrino L, Cambi M, Marchiani S, Manigrasso I, Degl'Innocenti S, Forti G, et al. Sperm DNA fragmentation in cryopreserved samples from subjects with different cancers. *Reprod Fertil Dev* 2017; **29:** 637-45. doi: 10.1071/RD15190

26. Said TM, Tellez S, Evenson DP, Del Valle AP. Assessment of sperm quality, DNA integrity and cryopreservation protocols in men diagnosed with testicular and systemic malignancies. *Andrologia* 2009; **41:** 377-82. doi: 10.1111/j.1439-0272.2009.00941.x

27. Osman A, Alsomait H, Seshadri S, El-Toukhy T, Khalaf Y. The effect of sperm DNA fragmentation on live birth rate after IVF or ICSI: a systematic review and meta-analysis. *Reprod Biomed Online* 2015; **30:** 120-7. doi: 10.1016/j.rbmo.2014.10.018

28. Deng C, Li T, Xie Y, Guo Y, Yang QY, Liang X, et al. Sperm DNA fragmentation index influences assisted reproductive technology outcome: a systematic review and meta-analysis combined with a retrospective cohort study. *Andrologia* 2019; **51:** e13263. doi: 10.1111/and.13263

29. Machen GL, Harris SE, Bird ET, Brown ML, Ingalsbe DA, East MM, et al. Utilization of cryopreserved sperm cells based on the indication for storage. *Investig Clin Urol* 2018; **59:** 177-81. doi: 10.4111/icu.2018.59.3.177

30. Botchan A, Karpol S, Lehavi O, Paz G, Kleiman SE, Yogev L, et al. Preservation of sperm of cancer patients: extent of use and pregnancy outcome in a tertiary infertility center. *Asian J Androl* 2013; **15:** 382-6. doi: 10.1038/aja.2013.3

31. Lass A, Akagbosu F, Brinsden P. Sperm banking and assisted reproduction treatment for couples following cancer treatment of the male partner. *Hum Reprod Update* 2001; **7:** 370-7. doi: 10.1093/humupd/7.4.370

32. Kelleher S, Wishart SM, Liu PY, Turner L, Di Pierro I, Conway AJ, et al. Long-term outcomes of elective human sperm cryostorage. *Hum Reprod* 2001; **16:** 2632-9. doi: 10.1093/humrep/16.12.2632

33. Agarwal A, Ranganathan P, Kattal N, Pasqualotto F, Hallak J, Khayal S, et al. Fertility after cancer: a prospective review of assisted reproductive outcome with banked semen specimens. *Fertil Steril* 2004; **81:** 342-8. doi: 10.1016/j.fertnstert.2003.07.021

34. Meseguer M, Molina N, García-Velasco JA, Remohí J, Pellicer A, Garrido N. Sperm cryopreservation in oncological patients: a 14-year follow-up study. *Fertil Steril* 2006; **85:** 640-5. doi: 10.1016/j.fertnstert.2005.08.022

35. Ragni G, Somigliana E, Restelli L, Salvi R, Arnoldi M, Paffoni A. Sperm banking and rate of assisted reproduction treatment: insights from a 15-year cryopreservation program for male cancer patients. *Cancer* 2003; **97:** 1624-9. doi: 10.1002/cncr.11229

36. Hourvitz A, Goldschlag DE, Davis OK, Gosden LV, Palermo GD, Rosenwaks Z. Intracytoplasmic sperm injection (ICSI) using cryopreserved sperm from men with malignant neoplasm yields high pregnancy rates. *Fertil Steril* 2008; **90:** 557-63. doi: 10.1016/j.fertnstert.2007.03.002

37. Trottmann M, Becker AJ, Stadler T, Straub J, Soljanik I, Schlenker B, et al. Semen quality in men with malignant diseases before and after therapy and the role of cryopreservation. *Eur Urol* 2007; **52:** 355-67. doi: 10.1016/j.eururo.2007.03.085

38. Weibring K, Nord C, Ståhl O, Eberhard J, Sandberg K, Johansson H, et al. Sperm count in Swedish clinical stage I testicular cancer patients following adjuvant treatment. *Ann Oncol* 2019; **30:** 604-11. doi: 10.1093/annonc/mdz017

39. Di Bisceglie C, Bertagna A, Composto ER, Lanfranco F, Baldi M, Motta G, et al. Effects of oncological treatments on semen quality in patients with testicular neoplasia or lymphoproliferative disorders. *Asian J Androl* 2013; **15:** 425-9. doi: 10.1038/aja.2012.171

40. Smit M, van Casteren NJ, Wildhagen MF, Romijn JC, Dohle GR. Sperm DNA integrity in cancer patients before and after cytotoxic treatment. *Hum Reprod* 2010; **25:** 1877-83. doi: 10.1093/humrep/deq104

41. Bhattacharya S, Maheshwari A, Mollison J. Factors associated with failed treatment: an analysis of 121,744 women embarking on their first IVF cycles. *PLoS One* 2013; **8:** e82249. doi: 10.1371/journal.pone.0082249

*research article*

# Multicatheter interstitial brachytherapy versus stereotactic radiotherapy with CyberKnife for accelerated partial breast irradiation: a comparative treatment planning study with respect to dosimetry of organs at risk

András Herein[1,2], Gábor Stelczer[1,2], Csilla Pesznyák[1,2], Georgina Fröhlich[1,3], Viktor Smanykó[1], Norbert Mészáros[1,4], Csaba Polgár[1,4], Tibor Major[1,4]

[1] National Institute of Oncology, Radiotherapy Centre, Budapest, Hungary
[2] Budapest University of Technology and Economic, Institute of Nuclear Techniques, Budapest, Hungary
[3] Eötvös Loránd University, Faculty of Science, Budapest, Hungary
[4] Semmelweis University, Department of Oncology, Budapest, Hungary

Radiol Oncol 2021; 55(2): 229-239.

Received 27 August 2020
Accepted 2 February 2021

Correspondence to: András Herein, National Institute of Oncology, Centre of Radiotherapy, Ráth György Street 7-9., H-1122 Budapest, Hungary. E-mail: hereina@gmail.com

Disclosure: No potential conflicts of interest were disclosed.

**Background.** The aim of the study was to dosimetrically compare multicatheter interstitial brachytherapy (MIBT) and stereotactic radiotherapy with CyberKnife (CK) for accelerated partial breast irradiation (APBI) especially concerning the dose of organs at risk (OAR-s).

**Patients and methods.** Treatment plans of thirty-two MIBT and CK patients were compared. The OAR-s included ipsilateral non-target and contralateral breast, ipsilateral and contralateral lung, skin, ribs, and heart for left-sided cases. The fractionation was identical (4 x 6.25 Gy) in both treatment groups. The relative volumes (e.g. V100, V90) receiving a given relative dose (100%, 90%), and the relative doses (e.g. D0.1cm$^3$, D1cm$^3$) delivered to the most exposed small volumes (0.1 cm$^3$, 1 cm$^3$) were calculated from dose-volume histograms. All dose values were related to the prescribed dose (25 Gy).

**Results.** Regarding non-target breast CK performed slightly better than MIBT (V100: 0.7% *vs.* 1.6%, V50: 10.5% *vs.* 12.9%). The mean dose of the ipsilateral lung was the same for both techniques (4.9%), but doses irradiated to volume of 1 cm$^3$ were lower with MIBT (36.1% *vs.* 45.4%). Protection of skin and rib was better with MIBT. There were no significant differences between the dose-volume parameters of the heart, but with MIBT, slightly larger volumes were irradiated by 5% dose (V5: 29.9% *vs.* 21.2%). Contralateral breast and lung received a somewhat higher dose with MIBT (D1cm$^3$: 2.6% *vs.* 1.8% and 3.6% *vs.* 2.5%).

**Conclusions.** The target volume can be properly irradiated by both techniques with similar dose distributions and high dose conformity. Regarding the dose to the non-target breast, heart, and contralateral organs the CK was superior, but the nearby organs (skin, ribs, ipsilateral lung) received less dose with MIBT. The observed dosimetric differences were small but significant in a few parameters at the examined patient number. More studies are needed to explore whether these dosimetric findings have clinical significance.

Key words: multicatheter interstitial brachytherapy; CyberKnife; APBI; dosimetric comparison

## Introduction

Breast radiotherapy after breast-conserving surgery reduces the risk of breast cancer recurrence by half and related mortality by one-sixth in early-stage breast cancer patients.[1] Today, the accelerated partial breast irradiation (APBI) for treating early-stage breast cancer has been a widely accepted technique among radiation oncologists.[2] APBI can be used because most of the local recurrences develop near the tumour bed requiring irradiation of the surroundings of the removed tumour, only.[2] During APBI, a smaller volume needs to be irradiated compared to whole breast irradiation (WBI), so patients can tolerate an accelerated regimen of irradiation with higher fraction doses. In the case of APBI, the total treatment time is only 4–5 days instead of the few weeks of conventional WBI, and therefore, APBI is a preferred treatment option by patients. Because of the smaller irradiated volume, there are decreased doses to healthy tissues compared to WBI, which is another advantage of the APBI, and this is an important issue among long time survivors of breast cancer.[3,4] In planning studies, and also in phantom measurements, it was verified that with smaller target volume the adjacent organs received less dose.[5,6]

There are numerous techniques available for APBI.[7] The first one was the multicatheter interstitial brachytherapy (MIBT), having the longest patient follow-up with excellent clinical results.[8-15] Furthermore, recommendations for patient selection[16], target volume definition[17,18] have been published, and practical guidelines are also available for MIBT[19,20] ensuring appropriate quality assurance for this technique. Brachytherapy (BT) also performs well when it is used for boost irradiation following WBI.[21,22] Other BT modalities have also been introduced, such as single/multichannel balloon therapy, non-invasive BT, and seed implantation. The external beam radiotherapy (EBRT) methods include 3D conformal radiotherapy (3D-CRT), intensity modulated radiotherapy (IMRT), volume modulated arc therapy (VMAT), CyberKnife therapy (CK), proton therapy and intraoperative methods with electrons or 50 kV photons.[23]

Dosimetric studies for APBI with CK are rare in the literature, and mainly focus on comparisons between different external beam techniques. CK dosimetry has been compared to 3D-CRT[24-31], IMRT[25,29,31], VMAT[28,29], and tomotherapy.[27] A dosimetric assessment of conformal and several different IMRT techniques for APBI is also available in the literature.[32] Treatment plans of MIBT were also assessed against 3D-CRT[33], IMRT[34] and VMAT.[35] Three years ago, a CK was installed at our institution, and very soon we started using it for APBI. Since we had lots of experience in interstitial BT we were interested in seeing how much the CK can imitate the BT, and whether it can be an alternative to BT.

Having surveyed the literature on APBI, we observed that the target volume can be irradiated properly with any technique, but differences exist in dosimetric issues of the organs at risk (OAR-s). In another study we compared plans of patients treated by CK with virtual MIBT plans based on CT images and contours of CK plans.[36]

The goal of this study was to dosimetrically compare the multicatheter interstitial brachytherapy and stereotactic irradiation with CyberKnife for APBI using separate patient cohorts with a special focus on dose to OAR-s. We believe that our results provide radiation oncologists and physicists with information on dosimetric advantages and disadvantages of these two image guided treatment techniques.

## Patients and methods

Treatment plans of thirty-two MIBT patients and thirty-two CK patients consecutively treated at our institute between June 2017 and May 2020 were selected for a dosimetric comparison. Mostly, all patients were candidate for both techniques, and the treatment option was primarily chosen by the patient. All the patients were treated according to our institutional protocol, and in this dosimetric study we retrospectively collected and evaluated the treatment planning data, so no ethical approval was needed.

### Multicatheter interstitial brachytherapy

The patients were treated with a high-dose-rate afterloader (microSelectron V3, Elekta, Brachytherapy, Veenendaal, The Netherlands) with Ir-192 stepping source. For patient selection and target volume definitions the GEC-ESTRO guidelines were followed.[16,18] The number of implanted catheters ranged between 7 and 28, with a mean of 14. The catheters were placed into the breast with a template in a triangle pattern with 1.3 cm catheter separation, and the source step size was 2.5 mm. The positions of the catheters were planned with image guidance using pre-implant CT imaging.[37] The patients were treated according to plans made with an inverse planning method (Hybrid Planning

Optimization, HIPO). For treatment planning the Oncentra Brachy v4.3 planning system (Elekta, Brachytherapy, Veenendaal, The Netherlands) was used. The calculation algorithm was based on the TG-43 formalism.[38] After the catheter implantation, CT scans with a 3 mm slice distance were acquired. First, the lumpectomy cavity was outlined with the help of surgical clips placed into the cavity wall during the lumpectomy. To get the clinical target volume (CTV), a safety margin was added to the cavity according to the surgical tumour-free margin in all six main directions. The surgical and radiation margin together was always 20 mm.[18] The CTV was limited to skin, thoracic wall, and pectoral muscles. No additional margin was added to the CTV to create the planning target volume (PTV), so the PTV was always equal to the CTV. The outlined OAR-s were as follows: the ipsilateral and contralateral lungs and breasts, heart, skin, and ribs. The skin was defined as a 5 mm layer below the skin surface. The non-target ipsilateral breast was created from the ipsilateral breast and the PTV with a subtraction. After contouring all structures, the catheter reconstruction was carried out, and the dwell time optimization was performed. The source positions were activated within the PTV, and for selection an isodose line for prescription the aim was to achieve at least 90% target coverage by the prescribed dose (PD) while keeping the dose distribution relatively homogenous. A higher isodose line was selected if a proper dose homogeneity was maintained. Dose-nonuniformity ratio (DNR) was used to measure the dose homogeneity. DNR is the ratio of volumes irradiated by 1.5 times of PD and PD ($V_{1.5xPD}/V_{PD}$). The required value for DNR was less or equal to 0.35. When coverage and homogeneity constraints could not be fulfilled at the same time, the target coverage was prioritized. For the OAR-s no dose-volume constraints were used, the parameters were only recorded. The PD was 25 Gy with a fractionation of 4 x 6.25 Gy, which is an accepted fractionation regime in the GEC-ESTRO VAPBI study.[39] The treatment time of one fraction ranged between 5 and 15 minutes according to the volume of the PTV and the source strength.

## CyberKnife treatments

The patients were treated with a CyberKnife M6 stereotactic system (Accuray, Sunnyvale, CA, USA) using InCise 2™ multileaf collimators (MLC-s) with step-and-shoot IMRT technique.[40] The patient selection was the same as for MIBT. The mean monitor unit number was 2498.8 (range, 1578.7–4142.2), and the median segment number was 57 (range, 39–75). One week before the planning CT, four gold markers were implanted around the lumpectomy cavity with ultrasound guidance by an experienced interventional radiologist. The gold markers were used for real-time tracking during irradiation (Synchrony Respiration Tracking). Although surgical titanium clips were placed into the cavity wall during the lumpectomy, they do not provide enough contrast on X-ray images, and therefore they cannot be reliably tracked. That is why we used gold markers. The CT slice thickness for treatment planning was 1.25 mm, and the images were acquired in exhalation breath-hold. The CT scans included both breasts and both sides of the lung. Metal artifact reduction CT scans were obtained to decrease the scattering effect of gold markers. The contouring protocol for CK was the same as for MIBT. However, to generate the PTV, a 2 mm margin was added to the CTV in each direction. With frequent intra-fraction imaging and correction by the robotic arm, the 2 mm margin seems to be enough to account for the non-rigid components of composite errors.[41] For evaluation purpose, PTV_EVAL was created from PTV with the subtraction of the 5 mm skin layer. The prescribed dose was 25 Gy with fractionation of 4 x 6.25 Gy, exactly the same as in MIBT.

For planning, the Precision 1.1.1.1 (Accuray, Sunnyvale, CA, USA) software was used with a finite size pencil beam (FSPB) dose calculation algorithm for optimization and Monte Carlo algorithm with 0.5% uncertainty for plan evaluation. Regarding beam orientations, the contralateral breast and lung were allowed with "exit only" direction for optimization. Sequential optimization method was applied with the parameters of maximum 400 MU/segments, 650 MU/node, and for beam shaping all three types of segments (eroded, perimeter, random shape) were used with a 2.5 mm leaf margin. The aim was to achieve at least 99.5% of V95 for PTV_EVAL and keep the maximum point dose under 120% of the PD. Regarding doses to OAR-s no constraints were used, only the orientation of the beams was optimized. Time reduction was used to reach the optimal treatment time without compromising the optimal dose distribution. The mean estimated treatment time was 33.3 min (range, 27–40 min).

## Dosimetric evaluation and statistical analysis

The treatment plan evaluation was performed using dose-volume histograms (DVH-s) (Figure 1).

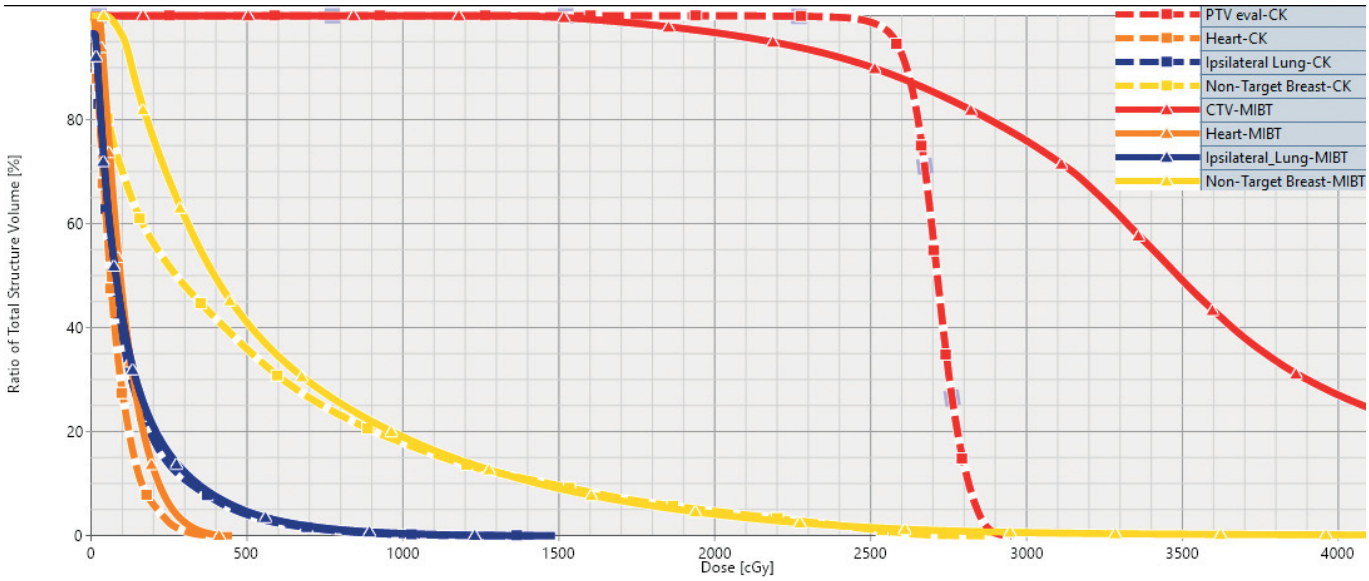


**FIGURE 1.** Representative dose-volume histograms (DVH-s) for multicatheter interstitial brachytherapy (MIBT) (solid line) and CyberKnife (CK) treatment (dashed line) for accelerated partial breast irradiation. The prescribed dose was 25 Gy. The target volume is indicated with red, the non-target breast with yellow, the ipsilateral lung with blue and the heart with orange. The solid red line clearly shows that with MIBT volumes irradiated by high doses (> 25 Gy) develop within the target volume.

All treatment plans and patient's data were anonymized for the dosimetric comparison. Quality parameters were derived as relative (e.g. V100, V90) or absolute volumes (e.g. V100 ($cm^3$), V50 ($cm^3$)) receiving a percentage of the PD. Relative doses in percentage of the PD to relative volumes (e.g. D5, D50) and to small absolute volumes (e.g. D0.1$cm^3$, D1$cm^3$) were calculated, too. The conformity of dose distribution was characterized by COIN.[42] Most of these parameters are published in dosimetric studies what makes the intercomparison possible. Descriptive statistics were calculated to describe the treatment plans. Shapiro-Wilk W test was used on the distribution of dose-volume parameters to test normality. Since almost none of the parameters followed Gaussian distribution, the Mann-Whitney U test was used for every comparison with the Statistica 10.0 software (StatSoft, Inc., Tulsa, OK, USA) and $p < 0.05$ was considered statistically significant.

**TABLE 1.** Tumour localization according to breast quadrants in patients treated by multicatheter interstitial brachytherapy (MIBT) and CyberKnife (CK)

| Method of treatment | Laterality | Upper outer | Lower outer | Upper inner | Lower inner | Central |
|---|---|---|---|---|---|---|
| MIBT | right | 3 | 1 | 3 | 2 | 4 |
| | left | 3 | 3 | 4 | 1 | 8 |
| CK | right | 6 | 6 | 2 | 1 | 2 |
| | left | 2 | 4 | 1 | 3 | 5 |

**TABLE 2.** Absolute volumes of the body irradiated by 100%, 50% and 20% of the prescribed dose for multicatheter interstitial brachytherapy (MIBT) and CyberKnife (CK) treatments

| Body | MIBT | CK | p-value* |
|---|---|---|---|
| V100 ($cm^3$) | 66.4 (28.9–193.8) | 77.1 (18.3–141.5) | 0.0356 |
| V50 ($cm^3$) | 159.0 (73.4–444.2) | 189.3 (58.6–397.6) | 0.0184 |
| V20 ($cm^3$) | 470.7 (253.4–1078.1) | 609.1 (326.7–1160.8) | 0.0013 |

*Mann-Whitney U test

## Results

Thirteen MIBT patients (41%) had right-sided and nineteen (59%) left-sided tumours, and seventeen CK patients (53%) had right-sided and fifteen (47%) left-sided lesions. The distribution of tumour localization is shown in Table 1.

The mean volume of the ipsilateral breast was 825.7 $cm^3$ (range, 386.9–2097.5 $cm^3$) and 984.4 $cm^3$ (range, 372.7–2437.1 $cm^3$) for the MIBT and CK patients, respectively ($p = 0.4400$). The mean volume of the PTV was 58.2 $cm^3$ (range, 26.6–173.6 $cm^3$) for

MIBT patients and 71.7 $cm^3$ (range, 17.1–129.1 $cm^3$) for CK patients, which was significantly higher ($p = 0.0101$). The mean volume of the CTV was 51.9 $cm^3$ (range, 10.2–96.4 $cm^3$) for CK, which did not differ significantly from the volume of the CTV for MIBT (58.2 $cm^3$, $p = 0.8456$). For MIBT the V100 for PTV was 91.4% (range, 83.1–96.4%) meanwhile the DNR was 0.35 (range, 0.24–0.44). For PTV_EVAL of CK patients, the V100 and V95 were 97.5% (range, 95.2–99.3%) and 99.7% (range, 97.7–100%), respectively, and the mean of the maximum doses was 116.5% (range, 113.6–125%). Because of the smaller target volumes, the V100, V50, and the V20 absolute volume parameters calculated for the whole body were significantly smaller for MIBT than for CK as it is presented in Table 2.

But, by relating these mean volumes to mean PTV volumes, it can be observed that the CK irradiated relatively less normal tissues, especially at higher dose levels. For MIBT and CK, the ratio of $V100_{BODY}/V_{PTV}$ is 1.14 *vs*. 1.08, and for $V50_{BODY}/V_{PTV}$ it is 2.73 *vs*. 2.64. Only the $V20_{BODY}/V_{PTV}$ is smaller for MIBT (8.09 *vs*. 8.5).

The conformity of the dose distributions was very high for both techniques (Figure 2), and the dosimetric parameters for ipsilateral breast were very similar (Table 3). Only the PD irradiated significantly less volume of the non-target breast at CK (0.7% *vs*. 1.6%, $p < 0.0001$). For lower dose values, the CK resulted in slightly smaller volumes, but without statistical significance. Large conformity indices (COIN-s) demonstrate the high dose conformity for both techniques. The COIN was 0.74 for MIBT and 0.88 for CK patients ($p < 0.001$).

The mean dose of the ipsilateral lung was exactly the same (4.9%) for both techniques (Table 4). All other parameters were smaller for MIBT, and the doses to the most exposed low volumes (0.1 $cm^3$, 1 $cm^3$) were significantly less.

Heart dosimetry was examined only for left-sided cases. The results are shown in Table 5. For each parameter, larger values were obtained with MIBT, but none of the differences was significant.

The protection of skin and ribs was better with MIBT. The differences were significant for all parameters, as shown in Table 6. The maximal dose to the ribs never exceeded the PD in MIBT cases ($V100(cm^3) = 0$). The mean value for $V100(cm^3)$ in CK patients was small, only 0.2 $cm^3$, and the maximal dose exceeded the PD in 11 cases.

For contralateral breast and lung, volumetric dose parameters were very low for both techniques, but CK resulted in significantly lower values in each parameter, as it is shown in Table 7.

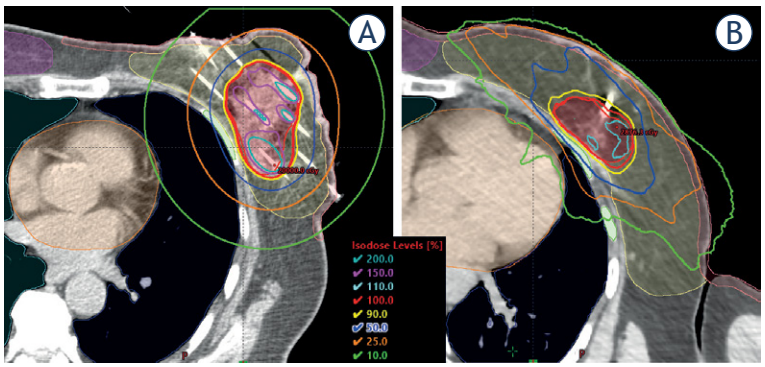


**FIGURE 2.** Representative dose distribution for multicatheter interstitial brachytherapy (MIBT) **(A)** and CyberKnife (CK) treatment **(B)**. PTV: red, ipsilateral breast: yellow, contralateral breast: pink, ribs: green, heart: orange, ipsilateral lung: dark blue, contralateral lung: light blue.

## Discussion

As a result of the technological development during the last decade, a number of new techniques have been introduced for APBI, and the question

**TABLE 3.** Dosimetry of ipsilateral breast for multicatheter interstitial brachytherapy (MIBT) and CyberKnife (CK) treatments. The values are given in percentages

| | MIBT | CK | p-value* |
|---|---|---|---|
| **Whole breast** | | | |
| V100 | 9.7 (2.2–29.7) | 9.6 (0.9–20.4) | 0.9381 |
| V50 | 23.2 (5.1–68.0) | 23.3 (2.7–47.1) | 0.9822 |
| **Non-target breast** | | | |
| V100 | 1.6 (0.4–4.2) | 0.7 (0.0–2.0) | < 0.0001 |
| V90 | 2.8 (0.6–8.1) | 2.3 (0.0–4.4) | 0.7019 |
| V50 | 12.9 (3.1–35.4) | 10.5 (1.7–18.9) | 0.5501 |
| V25 | 31.8 (9.4–68.4) | 29.9 (7.6–55.2) | 0.8772 |

*Mann-Whitney U test

**TABLE 4.** Dosimetry of ipsilateral lung for multicatheter interstitial brachytherapy (MIBT) and CyberKnife (CK) treatments. The values are given in percentages

| Ipsilateral lung | MIBT | CK | p-value* |
|---|---|---|---|
| Mean lung dose | 4.9 (1.9–11.1) | 4.9 (1.6–11.8) | 0.9946 |
| $D0.1cm^3$ | 41.0 (10.1–61.5) | 52.2 (15.6–90.5) | 0.0068 |
| $D1cm^3$ | 36.1 (8.7–55.8) | 45.4 (14.4–84.5) | 0.0162 |
| $D2cm^3$ | 33.6 (8–52.5) | 42.2 (13.7–80.5) | 0.0198 |
| D2 | 21.2 (7.4–32.9) | 24 (8.8–46.4) | 0.2454 |
| V5 | 30.6 (5.1–50.0) | 30.7 (5.8–63.2) | 0.9357 |

*Mann-Whitney U test

now arises whether which technique is the most advantageous for the patients. Based on large trials, at selected patients, the non-inferiority of APBI against WBI was confirmed, but between the various APBI techniques, only minor differences exist.[11] Dosimetric analysis can explore these differences providing some guidance for clinicians in selecting the appropriate method for a patient. Papers have been published on dosimetric comparisons between different APBI techniques[24,43-46]; and a few papers are available about the comparison of CyberKnife and other external beam techniques.[26-29] However, to our knowledge, this analysis is the first one which compares the dosimetric differences between the multicatheter interstitial brachytherapy and CyberKnife treatments for partial breast irradiation using clinical plans.

A couple of studies have investigated the feasibility of APBI with CK. The treatment characteristics with the dosimetric data from the literature are shown in Table 8. In most of the studies, cones or the Iris applicator were used, and the most frequent fractionation scheme was 5 x 6 Gy, but clinical results of dose escalation up to 5 x 8 Gy are also available now.[47] In the studies, the CTV-PTV margin ranged between 0 and 5 mm. With the introduction of the MLC, the treatment time remarkably decreased, compared to using cones or the Iris applicator. It is difficult to make quantitative dosimetric comparisons between studies because the reported parameters are too diverse. The first report on using stereotactic radiotherapy for breast tumours was published in 2009.[48] The study showed the feasibility of irradiation with CK, but dosimetric details were not reported. The earliest study with dosimetry was performed by Vermeulen *et al*.[49], and based on their results, the authors recommend the CK as a suitable treatment method for APBI.

They compared their dosimetric data with the constraints of 3D-CRT used in the NSABP-39/RTOG 0413 protocol.[50] On average, 11% of the ipsilateral breast received the PD (V100), and 23% (for two patients) and 26% (for seven patients) were irradiated by the half of the PD (V50). These values are well below the constraints of the NSABP-39/RTOG 0413 protocol and are in good agreement with our CK results (V100 = 9.6%, V50 = 23.3%). We note that for MIBT patients, we obtained practically the same values (V100 = 9.7%, V50 = 23.2%). In 2014, the same group published dosimetric data of twenty-one patients, but those basically did not differ from the previous ones.[51] In a retrospective planning study published by Xu *et al*.[25] for fourteen patients previously treated with 3D-CRT, additional CK plans were created and compared with 3D-CRT and IMRT plans. Since in CK plans very homogenous dose distributions were created, the mean V100 parameter was 95.7%, which is lower than the value in our study (97.5%). The maximum dose in PTV was kept on 104% which is much lower than presented in this study (116.5%). The mean V100 and V50 parameters of the uninvolved normal breast were 9% and 23.1%, which are much higher than our values (0.7% and 10.5%). Probably, because of the relatively homogenous dose distribution, the dose gradient was not steep enough to achieve very low V100 parameters for the breast. Another explanation for our better dose conformity can be the use of MLC-s with step-and-shoot IMRT technique. For the median V5 parameter of ipsilateral lung, their analysis resulted in 31.4%, which is very similar to our 30.7%. In another retrospective study, Obayomi *et al*.[52] analyzed the dosimetric results of 10 CK treated patients. The mean PTV volume was 70 $cm^3$, very similar to ours (71.7 $cm^3$). The fractionation was 5 x 6 Gy (30 Gy), and the authors reported the maximum doses of skin and ribs as 32 Gy (107% of PD) and 26 Gy (87% of PD), consecutively. In our assessment, for skin and ribs, the D0.1$cm^3$ value was 88.8% and 78.9%. In the paper of Lozza *et al*.[53], mainly the clinical results from 20 CK treated patients were reported. Among 20 patients, the mean volume of PTV was 88.1 $cm^3$, and the V5 value of heart for left-sided cases was 14.0%, which is lower than in our study (21.2%). For skin, they examined the Dmax parameter, which was 98.2% of the PD. In our study, the D0.1$cm^3$ was 88.8%. In a recent paper, Lee *et al*.[54] published their first experience in Korea of partial breast irradiation with CK. In their study, on average, 35.5% of ipsilateral breast volume received 50% of the PD, while in our case, only 23.3%. The mean volume of PTV was similar (73.6 $cm^3$ *vs*. 71.7 $cm^3$), although they did not use any CTV-PTV margin. But, the ipsilateral breast volume of their patients was less than half compared to ours (481.1 $cm^3$ *vs*. 984.4 $cm^3$). Despite the fact, that Korean women have smaller breast the authors consider the CK technique as a feasible method for APBI. They found that the mean maximal skin dose was 89%, while in our case, the D0.1$cm^3$ was 89%. The mean dose to heart for left-sided lesions was also similar (2.3% *vs*. 3.3%).

APBI treatment with CyberKnife is feasible and compared to other external beam techniques the CK plans produce better dosimetric parameters regarding the OAR-s. Xu *et al*.[25] found CK plans more

conformal and observed better dose sparing of the critical structure except for the extremely low dose region (for example, V1 for ipsilateral lung) compared to IMRT and 3D-CRT. In a quantitative analysis with ten patients, Lee *at al*.[29] compared CK with 3D-CRT, IMRT and VMAT for APBI. They only examined patients with left-sided lesions and had a very similar conclusion about conformity of dose distribution as Xu *et al*. 25.[25] Rault *et al*.[27] examined the dosimetric effect of respiratory tracking at CK treatments against Tomotherapy and 3D-CRT. The authors stated that the non-coplanarity of the CK resulted in significantly less dose to the normal tissue of ipsilateral breast, in case of the 2 mm CTV-PTV margin. A very profound analysis was performed by Goggin *et al*.[26] in comparing different CK treatment plans (Iris, MLC) with 3D-CRT ones. Based on the analysis of nine patients, they found that CK-MLC technique resulted in lower dose to the ipsilateral lung than CK-Iris and comparable treatment time with 3D-CRT. In an examination with ten patients, Bonfantini *et al*.[28] compared CK with 3D-CRT and VMAT. Based on their analysis, 3D-CRT gives a reduction of the dose to OAR-s except for ipsilateral breast.

Major *et al*.[34] reported results of MIBT against co-planar IMRT. They found that MIBT generally spares normal tissues and organs at risk (except for heart) better than IMRT. They found significant differences in non-target breast dosimetry parameters in favour of MIBT. Inverse planning can improve the plan quality of breast implants, better homogeneity and a few percent less dose to OAR-s can be achieved at identical target coverage.[55,56] In this way we made a comparison between the treatment plans of the most advanced inverse optimized BT and a high-tech stereotactic EBRT technique.

In a recent publication our group reported a comparative dosimetry between CK and MIBT, but in that work ideal implant geometry was assumed in the hypothetical BT plans.[36] Therefore, the strength of the conclusion is weaker than in case of comparison between real clinical plans. Anyway, the findings regarding the dose to OAR-s are very similar to the ones observed in current study.

Comparing the dose distributions between MIBT and EBRT techniques, the CK seems most similar to the MIBT regarding the shapes of the isodose lines between 50–100% of PD. The explanation can be the use of lots of non-isocentric beams entering from different directions, not limited from one plane, which results in more focused 3D dose delivery to the PTV. This is presented in Figure 2, where the isodose lines between 50–100% of PD following the shape of the PTV are very similar for both techniques. But, differences exist because volumes irradiated by high doses always develop in BT, which is shown in Figure 2 by the 150 and 200% isodose lines. However, the low isodoses around BT implant become nearly circular, while in CK case, they are irregular due to the multiple

**TABLE 5.** Dosimetry of heart for multicatheter interstitial brachytherapy (MIBT) and CyberKnife (CK) treatments. The values are given in percentages

| Heart | MIBT | CK | p-value* |
|---|---|---|---|
| Mean heart dose | 4.1 (1.0–7.7) | 3.3 (1.3–6.9) | 0.1706 |
| D0.1cm³ | 21.4 (4.0–47.2) | 18.9 (8.4–43.2) | 0.2822 |
| D1cm³ | 18.2 (3.2–42.3) | 16.6 (7.3–40.3) | 0.4878 |
| D2cm³ | 17 (3.0–40.0) | 15.6 (6.8–38.3) | 0.5324 |
| D2 | 13.3 (4.3–26.4) | 12.5 (5.2–31.5) | 0.5098 |
| V5 | 29.9 (0.0–62.5) | 21.2 (6.1–41.0) | 0.1653 |

*Mann-Whitney U test

**TABLE 6.** Dosimetry of skin and ribs for multicatheter interstitial brachytherapy (MIBT) and CyberKnife (CK) treatments. The values are given in percentages except for V100 and V50

| Skin | MIBT | CK | p-value* |
|---|---|---|---|
| D0.1cm³ | 75.3 (18.0–164.2) | 88.8 (27.6–112.4) | 0.0080 |
| D0.2cm³ | 70.3 (17.4–140.7) | 86.8 (21.1–111.1) | 0.0053 |
| D1cm³ | 58.4 (15.0–97.1) | 79 (22.8–106.0) | 0.0007 |
| **Ribs** | | | |
| D0.1cm³ | 53.7 (8.1–92.7) | 78.9 (17.6–108.4) | 0.0003 |
| D1cm³ | 43.1 (5.3–76.4) | 69.1 (16.4–105) | 0.0004 |
| V100 (cm³) | 0 (0–0) | 0.2 (0.0–3.0) | 0.0101 |
| V50 (cm³) | 2 (0.0–16.4) | 4.2 (0.0–13.4) | 0.0105 |

*Mann-Whitney U test

**TABLE 7.** Dosimetry of contralateral breast and lung for multicatheter interstitial brachytherapy (MIBT) and CyberKnife (CK) treatments. The values are given in percentages

| Contralateral breast | MIBT | CK | p-value* |
|---|---|---|---|
| D0.1cm³ | 4 (0.0–9.8) | 2.1 (0.3–11.2) | 0.0039 |
| D1cm³ | 2.6 (0.0–6.4) | 1.8 (0.3–9.9) | 0.0378 |
| **Contralateral lung** | | | |
| D0.1cm³ | 5.5 (0.0–11.7) | 3 (1.0–5.6) | 0.0000 |
| D1cm³ | 3.6 (0.0–8.3) | 2.5 (0.6–4.8) | 0.0228 |

*Mann-Whitney U test

**TABLE 8.** Treatment characteristics and mean dosimetric parameters in publications for accelerated partial breast irradiation (APBI) with CyberKnife

| Publication | Xu 2012[25] | Vermeulen 2014[51] | Goggin 2015[26] | Rault 2016[27] | Obayomi 2016[52] | Lozza 2018[53] | Bonfantini 2018[28] | Lee 2018[29] | Lee 2020[54] | Fröhlich 2020[36] | Current study |
|---|---|---|---|---|---|---|---|---|---|---|---|
| Patient number | 14 | 21 | 9 | 10 | 10 | 20 | 10 | 10 | 103 | 25 | 32 |
| Applicator | Cones | - | Iris, MLC | Iris | - | Iris | Iris | Cones | - | MLC | MLC |
| Beam number | - | 151 | - , - | - | 155 | 180 | 122 | - | - | - | 40 (57)[@] |
| Fractionation | 10 x 3.85 Gy | 10 x 3.4 Gy | 5 x 6 Gy | 10 x 4 Gy | 5 x 6 Gy | 5 x 6 Gy | 5 x 6 Gy | 5 x 6 Gy | 5 x 6 Gy | 4 x 6.25 Gy | 4 x 6.25 Gy |
| Treatment Time (min) | - | 46 | 28, 14.7 | 40 | - | 60 | 60 | 60 | 33[#] | - | 33.3 |
| CTV-PTV margin (mm) | 2 | 2 | 2 | 3 | 5 | 5 | 5 | 2 | 0 | 2 | 2 |
| Mean PTV volume (cm$^3$) | - | 114 | - | - | 70 | 88.1 | 121.6 | 37.7 | 73.6 | 71.6 | 71.7 |
| Ipsilateral breast | | | | | | | | | | | |
| V100 (%) | 7[#] | 12 | 12.5, 12.2 | - | 14 | 28.7 | - | 10 | - | - | 9.6 |
| V50 (%) | 22.4[#] | 26 | 25.8, 24.2 | - | 31 | 75 | - | 24 | 35.5[#] | - | 23.3 |
| Ipsilateral non-target breast | | | | | | | | | | | |
| V100 (%) | 9 | - | - | - | - | - | 1.7 | - | - | | 0.7 |
| V50 (%) | 23.1 | - | - | 17.6 | - | - | 16.3 | - | - | 10.5 | 10.5 |
| Ipsilateral lung | | | | | | | | | | | |
| V30 (%) | 1.3 | 3 | 1.9, 1.6 | - | 3 | 2.3 | 2.1 | 3 | 2.2[#] | - | 1.0 |
| V5 (%) | 31.4[#] | - | 39.4, 17.9 | - | - | - | - | - | - | - | 30.7 |
| mean dose (%) | - | - | - | - | - | - | 6 | - | - | - | 4.9 |
| D0.1cm$^3$ | - | - | - | - | - | - | - | - | - | 57.5 | 52.2 |
| D1cm$^3$ | - | - | - | - | - | - | - | - | - | 45 | 45.4 |
| Heart | | | | | | | | | | | |
| V5 (%) | 9.4 | 10 | - | 3.9 | 31 | 14 | 23.2 | 23 | - | - | 21.2 |
| mean dose (%) | - | - | - | - | - | - | - | - | 2.3[#] | - | 3.3 |
| D0.1cm$^3$ | - | - | - | - | - | - | - | - | - | 12.1 | 18.9 |
| D1cm$^3$ | - | - | - | - | - | - | - | - | - | 10.5 | 16.6 |
| Skin | | | | | | | | | | | |
| Dmax (%) | - | 108.8 | - | - | 106.6 | 98.2 | 94.7 | 103.3 | 88.7[#] | 99.6* | 88.8* |
| Contralateral breast | | | | | | | | | | | |
| Dmax (%) | 1.6 | 3 | - | - | 10 | - | - | 10 | 2.7[#] | 3.8* | 2.1* |

* = D0.1cm$^3$; [#] = median value; [@] = segment number in parentheses; CTV = clinical target volume; MLC = multileaf collimator; PTV = planning target volume

non-coplanar beam entries. The absolute volumes encompassed by 100%, 50%, and 20% isodose surfaces are 16%, 19%, and 29% larger at CK compared to MIBT (Table 2). The volume of the ipsilateral breast was slightly larger in the CK group (984.4 cm$^3$ *vs*. 825.7 cm$^3$), but the PTV was also bigger (71.7 cm$^3$ *vs*. 58.2 cm$^3$), and this explains why the relative volumes of ipsilateral breast irradiated by the 100% and 50% dose for the two techniques were nearly identical (Table 3). There was no difference between the mean lung doses and the volumes irradiated by low dose (V5) for the two techniques (Table 4). However, the other examined dose parameters were significantly smaller with MIBT (D0.1cm$^3$: 41.0% *vs*. 52.2%, D1cm$^3$: 36.1% *vs*. 45.4%). The heart was better protected with CK, since all dosimetric parameters were smaller, but without statistical significance (Table 5). This observation is similar to the findings of Major *et al*.[34] when MIBT was compared to IMRT. In our CK group, almost half of the tumours located in one of the upper quadrants, and in these cases, the heart protection was better maintained because the beams could avoid the heart directly. In most cases, the skin and ribs are close to the PTV, sometimes they are contacting, and that is why the MIBT performs better for these two organs. In close proximity to the implant, due to inverse square law, the dose gradient is high resulting in proper protection of adjoining organs. In our study, all dose parameters for skin and ribs were significantly lower for MIBT than for CK (Table 6). We note that the TG-43 formalism overestimates the skin dose because it assumes a full scattering condition, which is not fulfilled at all in breast BT.[34,57] From this follows that the real differences are even higher in favour of MIBT. The contralateral breast and lung receive low doses at both techniques, but the values were smaller with CK (Table 7). These organs are usually far from the PTV, and therefore in MIBT there is no way to lessen the dose without compromising the target coverage. In contrast, with proper selection

of beam orientations, such as choosing 'exit only' option for these volumes at optimization, the dose can be kept lower at CK. Both techniques require invasive intervention, but with different degrees of invasiveness. At MIBT sometimes quite a lot of catheters are implanted, but at CK the gold markers are inserted with 2–3 needles, only. The overall treatment times of CK and MIBT treatments were similar, every patient finished the therapy in four days.

The limitation of our study is that the dosimetric evaluation was performed on two separate patient populations. However, the patient selection, target volume definition, and organ delineations in the two patient cohorts were performed using the same rules by three experienced radiotherapists providing appropriate consistency. The volumes of ipsilateral breasts and CTV-s were similar in the two groups meaning a proper balance with respect to base-line dosimetry. The differences in patient characteristics and individual anatomy in two patient cohorts may cause some uncertainties regarding dosimetric comparison. However, this serves the purpose of assessment of real treatments. Using the same CT-data with identical contours to compare the two treatment techniques would decrease the uncertainties, but in that case real treatments are compared with hypothetical ones which can never be realized.[36] In contrast, the advantage of our current analysis is that both investigated treatment methods reflect reality, as in the study of Weed *et al*.[24], in which MIBT against MammoSite™ and 3D-CRT techniques was compared for three different patient cohorts. Our investigated two techniques are routinely used in our clinical practice, therefore the obtained results are realistic. However, whether the observed small dosimetric differences translate into different clinical outcomes requires further investigations with an assessment of more data.

## Conclusions

In APBI, the dose distributions of MIBT and CK are similar with high dose conformity and comparable isodose lines between 50–100 % of PD, but at MIBT regions in the target volume irradiated by very high doses develop due to unique feature of the BT. The low dose isodose lines are nearly circular at MIBT and irregular at CK cases. Regarding the PD the CK treatments mimic well the BT irradiation with taking advantage of non-coplanar beam entries and management of organ motion. OAR-s close to tumour bed (skin, ribs, ipsilateral lung) can be better protected with MIBT, but CK performs better for other organs (heart, contralateral breast, and lung). The advantage of CK is its less invasiveness, but its accessibility is very limited. BT is an easily accessible technique in almost all radiotherapy departments, but it demands proper skills with good dexterity.

## Acknowledgements

This study was supported by the Hungarian Thematic Excellence Programme (TKP2020-NKA-26).

## References

1. Darby S, Mc Gale P, Correa C, Taylor C, Arriagada R, Clarke M, et al; Early Breast Cancer Trialists' Collaborative Group (EBCTCG). Effect of radiotherapy after breast-conserving surgery on 10-year recurrence and 15-year breast cancer death: meta-analysis on individual patient data for 10,801 women in 17 randomised trials. *Lancet* 2011; **378:** 1707-16. doi: 10.1016/S0140-6736(11)61629-2

2. Bennion NR, Baine M, Granatowicz A, Wahl AO. Accelerated partial breast radiotherapy: a review of the literature and future directions. *Gland Surg* 2018; **7:** 596-610. doi: 10.21037/gs.2018.11.05

3. Grantzau T, Overgaard J. Risk of second non-breast cancer after radiotherapy for breast cancer: a systematic review and meta-analysis of 762,468 patients. *Radiother Oncol* 2015; **114:** 56-65. doi:10.1016/j.radonc.2014.10.004

4. Marcu LG, Santos A, Bezak E. Risk of second primary cancer after breast cancer treatment. *Eur J Cancer Care* 2014; **23:** 51-64. doi: 10.1111/ecc.12109

5. Lara TRM, Fleury E, Mashouf S, Helou J, McCann C, Ruschin M, et al. Measurement of mean cardiac dose for various breast irradiation techniques and corresponding risk of major cardiovascular event. *Front Oncol* 2014; **4:** 284. doi: 10.3389/fonc.2014.00284

6. Duma MN, Baumann R, Budach W, Dunst J, Feyer P, Fietkau R, et al. Heart-sparing radiotherapy techniques in breast cancer patients: a recommendation of the breast cancer expert panel of the German Society of Radiation Oncology (DEGRO). *Strahlenther Onkol* 2019; **195:** 861-71. doi: 10.1007/s00066-019-01495-w

7. Forster T, Köhler CVK, DebusJ, Hörner-Rieber J. Accelerated partial breast irradiation: a new standard of care? *Breast Care* 2020; **15:** 136-47. doi: 10.1159/000506254

8. Polgár Cs, Major T, Fodor J Sulyok Z, Somogyi A, Lövey K, et al. Accelerated partial breast irradiation using high-dose-rate interstitial brachytherapy: 12-year update of a prospective clinical study. *Radiother Oncol* 2010; **94:** 274-79. doi: 10.1016/j.radonc.2010.01.019

9. Polgár Cs, Fodor J, Major T, Sulyok Z, Kásler M. Breast-conserving therapy with partial or whole breast irradiation: ten-year results of the Budapest randomized trial. *Radiother Oncol* 2013; **108:** 197-202. doi: 10.1016/j.radonc.2013.05.008

10. Polgár Cs, Ott OJ, Hildebrant G, Kauer-Dorner D, Knauerhase H, Major T, et al. Late side-effects and cosmetic results of accelerated partial breast irradiation with interstitial brachytherapy versus whole-breast irradiation after breast-conserving surgery for low-risk invasive and in-situ carcinoma of the female breast: 5-year results of a randomised, controlled, phase 3 trial. *Lancet Oncol* 2017; **18:** 259-68. doi: 10.1016/S1470-2045(17)30011-6

11. Strnad V, Ott OJ, Hildebrandt G, Kauer-Dorner D, Knauerhase H, Major T, et al. 5-year results of accelerated partial breast irradiation using sole interstitial multicatheter brachytherapy versus whole-breast irradiation with boost after breast-conserving surgery for low-risk invasive and in-situ carcinoma of the female breast: a randomized, phase 3, non-inferiority trial. *Lancet* 2016; **387:** 229-38. doi: 10.1016/S0140-6736(15)00471-7

12. Ott OJ, Strnad V, Hildebrant G, Kauer-Dorner D, Knauerhase H, Major T, et al. GEC-ESTRO multicenter phase 3-trial: accelerated partial breast irradiation with interstitial multicatheter brachytherapy versus external beam whole breast irradiation: early toxicity and patient compliance. *Radiother Oncol* 2016; **120:** 119-23. doi: 10.1016/j.radonc.2016.06.019

13. Soror T, Kovács G, Seibold N, Melchert C, Baumann K, Wenzel E, et al. Cosmetic changes following surgery and accelerated partial breast irradiation using HDR interstitial brachytherapy. *Strahlenther Onkol* 2017; **193;** 367-74. doi: 10.1007/s00066-016-1093-6

14. Schafer R, Strnad V, Polgár Cs, Uter W, Hildebrandt G, Ott OJ, et al. Quality-of-life results for accelerated partial breast irradiation with interstitial brachytherapy versus whole-breast irradiation in early breast cancer after breast conserving surgery (GEC-ESTRO): 5-year results of a randomised, phase 3 trial. *Lancet Oncol* 2018; **19:** 834-44. doi: 10.1016/S1470-2045(18)30195-5

15. Vicini F, Cecchini R, White J, Arthur DW, Julian TB, Rabinovitch RA, et al. Long-term primary results of accelerated partial breast irradiation after breast-conserving surgery for early-stage breast cancer: a randomised, phase 3, equivalence trial. *Lancet* 2019; **394:** 2155-64. doi: 10.1016/S0140-6736(19)32514-0

16. Polgár Cs, van Limbergen E, Pötter R, Kovács Gy, Polo A, Lyczek J, et al. Patient selection for accelerated partial breast irradiation (APBI) after breast conserving surgery: recommendations of the Groupe Européen de Curiethérapie-European Society for Therapeutic Radiology and Oncology (GEC-ESTRO) Breast Cancer Working Group based on clinical evidence (2009). *Radiother Oncol* 2010; **94:** 264-73. doi: 10.1016/j.radonc.2010.01.014

17. Strnad V, Hannoun-Levi JM, Guinot JL, Lössl K, Kauer-Dorner D, Resch A, et al. Recommendations from GEC ESTRO breast cancer working group (I): target definition and target delineation for accelerated or boost partial breast irradiation using multicatheter interstitial brachytherapy after breast conserving closed cavity surgery. *Radiother Oncol* 2015; **115:** 342-8. doi: 10.1016/j.radonc.2015.06.010

18. Major T, Gutiérrez C, Guix B, Van Limbergen E, Strnad V, Polgár Cs, et al; on behalf of Breast Cancer Working Group of GEC-ESTRO. Recommendations from GEC ESTRO Breast Cancer Working Group (II): target definition and target delineation for accelerated or boost partial breast irradiation using multicatheter interstitial brachytherapy after breast conserving open cavity surgery. *Radiother Oncol* 2016; **18:** 199-204. doi: 10.1016/j.radonc.2015.12.006

19. Strnad V, Major T, Polgár Cs, Lotter M, Guinot JL, Gutierrez-Miguelez C, et al. ESTRO-ACROP guideline: interstitial multi-catheter breast brachytherapy as accelerated partial breast irradiation alone or as boost – GEC-ESTRO breast cancer working group practical recommendations. *Radiother Oncol* 2018; **128:** 411-20. doi: 10.1016/j.radonc.2018.04.009

20. Strnad V, Krug D, Sedlmayer F, Piroth MD, Budach W, Baumann R, et al. DEGRO practical guideline for partial-breast irradiation. *Strahlenther Onkol* 2020; **196:** 749-63. doi: 10.1007/s00066-020-01613-z

21. Kindts I, Laenen A, Christiansen M, Janssen H, Van Limbergen E, Weltens C. Comparison of brachytherapy and external beam radiotherapy boost in breast-conserving therapy: patient-reported outcome measures and aesthetic outcome. *Strahlenther Onkol* 2019; **195:** 21-31. doi: 10.1007/s00066-018-1346-7

22. Kindts I, Verhoeven K, Laenen A, Christiaens M, Janssen H, Van der Vorst A, et al. A comparison of a brachytherapy and an external beam radiotherapy boost in breast-conserving therapy for breast cancer: local and any recurrences. *Strahlenther Onkol* 2019; **195;** 310-7. doi: 10.1007/s00066-018-1413-0

23. Njeh CF, Saunders MW, Langton CM. Accelerated partial breast irradiation (APBI): a review of available techniques. *Radiat Oncol* 2010; **5:** 90. doi: 10.1186/1748-717X-5-90

24. Weed DW, Edmundson GK, Vicini FA, Chen PY, Martinez AA. Accelerated partial breast irradiation: a dosimetric comparison of three different techniques. *Brachytherapy* 2005; **4:** 121-9. doi: 10.1016/j.brachy.2004.12.005

25. Xu Q, Chen Y, Grimm J, Fan J, An L, Xue J, et al. Dosimetric investigation of accelerated partial breast irradiation (APBI) using CyberKnife. *Med Phys* 2012; **39:** 6621-8. doi: 10.1118/1.4757616

26. Goggin LM, Descovich M, McGuinness C, Shiao S, Pouliot J, Park C. Dosimetric bomparison between 3-dimensional conformal and robotic SBRT treatment plans for accelerated partial breast radiotherapy. *Technol Cancer Res Treatm* 2016; **15:** 437-45. doi: 10.1177/1533034615601280

27. Rault E, Lacornerie T, Dang H, Crop F, Lartigau E, Reynaert N, et al. Accelerated partial breast irradiation using robotic radiotherapy: a dosimetric comparison with tomotherapy and three-dimensional conformal radiotherapy. *Radiat Oncol* 2016; **11:** 29. doi: 10.1186/s13014-016-0607-9

28. Bonfantini F, De Martin E, Giandini T, Fumagalli ML, Cavallo A, Pinzi V, et al. A dosimetric comparison between three different external photon beam techniques for accelerated partial breast irradiation. *Clin Oncol* 2018; **3:** 1501.

29. Lee CY, Kim WC, Kim HJ, Lee J, Park S, Huh HD. Dosimetric plan comparison of accelerated partial breast irradiation (APBI) Using CyberKnife. *Prog Med Phys* 2018; **29:** 73-80. doi: 10.14316/pmp.2018.29.2.73

30. Shahbazian H, Bakhshali R, Shamsi A, Bagheri A. Dosimetric analysis of breast cancer tumor bed boost: an interstitial brachytherapy vs. external beam radiation therapy comparison for deeply seated tumors. *Brachytherapy* 2020; **19:** 264-74. doi: 10.1016/j.brachy.2019.10.008

31. Fan J, Hayes S, Freedman G, Anderson P, Li J, Wang L, et al. Planning the breast boost: dosimetric comparison of CyberKnife, photon mini tangents, IMRT, and electron techniques. *Int J Radiat Oncol Biol Phys* 2010; **78(3 Suppl):** S788-9. doi: 10.1016/j.ijrobp.2010.07.1826

32. Stelczer G, Major T, Mészáros N, Polgár Cs, Pesznyák Cs. External beam accelerated partial breast irradiation: dosimetric assessment of conformal and three different intensity modulated techniques. *Radiol Oncol* 2019; **53:** 123-30. doi:10.2478/raon-2019-0001

33. Anbumani S, Palled SR, Prabhakara GS, Nambiraj NA, Pichandia A. Accelerated partial breast irradiation using external beam radiotherapy – a feasibility study based on dosimetric analysis. *Rep Pract Onc Radiother* 2012; **7:** 200-6. doi: 10.1016/j.rpor.2012.04.002

34. Major T, Stelczer G, Pesznyák Cs, Mészáros N, Polgár Cs. Multicatheter interstitial brachytherapy versus intensity modulated external beam therapy for accelerated partial breast irradiation: a comparative treatment planning study with respect to dosimetry of organs at risk. *Radiother Oncol* 2017; **122:** 17-23. doi: 10.1016/j.radonc.2016.08.003

35. Charaghvandi RK, den Hartogh MD, van Ommen ALN, de Vries WJH, Scholten V, Moerland MA, et al. MRI-guided single fraction ablative radiotherapy for early-stage breast cancer: a brachytherapy versus volumetric modulated arc therapy dosimetry study. *Radiother Oncol* 2015; **117:** 477-82. doi: 10.1016/j.radonc.2015.09.023

36. Fröhlich G, Mészáros N, Smanykó V, Stelczer G, Herein A, Polgár Cs, et al. Is stereotactic CyberKnife radiotherapy or multicatheter HDR brachytherapy the better option dosimetrically for accelerated partial breast irradiation? *Brachytherapy* Nov 19, 2020; [Ahead of print]. doi: 10.1016/j.brachy.2020.10.003

37. Major T, Polgár Cs, Lövey K, Fröhlich G. Dosimetric characteristics of accelerated partial breast irradiation with CT image-based multicatheter interstitial brachytherapy: a single institution's experience. *Brachytherapy* 2011; **10:** 421-6. doi: 10.1016/j.brachy.2010.12.006

38. Nath R, Anderson LL, Luxton G, Weaver KA, Williamson JF, Meigooni AS. Dosimetry of interstitial brachytherapy sources: Recommendations of the AAPM Radiation Therapy Committee Task Group No. 43. *Med Phys* 1995; **22:** 209-34.

39. Guinot JL, Gonzalez-Perez V, Meszaros N, Major T, Najjari-Jamal D, Gutierrez-Miguelez C, et al; GEC-ESTRO Breast Working Group2. Very accelerated partial breast irradiation Phase I–II multicenter trial (VAPBI): feasibility and early results. *Brachytherapy* 2020; Nov 19, 2020; [Ahead of print]. doi: 10.1016/j.brachy.2020.10.010

40. Mészáros N, Smanykó V, Major T, Stelczer G, Jánváry L, Kovács E, et al. Implementation of stereotactic accelerated partial breast irradiation using cyber-knife – technical considerations and early experiences of a phase II clinical study. *Pathol Oncol Res* 2020; **26:** 2307-13. doi: 10.1007/s12253-020-00821-3

41. Zhen X, Zhao B, Wang Z, Timmerman R, Spangler A, Kim N, et al. Comprehensive target geometric errors and margin assessment in stereotactic partial breast irradiation. *Radiat Oncol* 2017; **12:** 151. doi: 10.1186/s13014-017-0889-6

42. Baltas D, Kolotas C, Geramani K, Mould RF, Ioannidis G, Kekchidi M, et al. A conformal index (COIN) to evaluate implant quality and dose specification in brachytherapy. *Int J Radiat Oncol Biol Phys* 1998; **40:** 515-24. doi: 10.1016/S0360-3016(97)00732-3

43. Rusthoven KE, Carter DL, Howell K, Kercher JM, Henkenberns P, Hunter KL, et al. Accelerated partial-breast intensitymodulated radiotherapy results in improved dose distribution when compared with three-dimensional treatment-planning techniques. *Int J Radiat Oncol Biol Phys* 2008; **70:** 296-302. doi: 10.1016/j.ijrobp.2007.08.047

44. Moon SH, Shin KH, Kim TH, Yoon M, Park S, Lee DH, et al. Dosimetric comparison of four different external beam partial breast irradiation techniques: three-dimensional conformal radiotherapy, intensity-modulated radiotherapy, helical tomotherapy, and proton beam therapy. *Radiother Oncol* 2009; **9:** 66-73. doi: 10.1016/j.radonc.2008.09.027

45. Qiu JJ, Chang Z, Horton JK, Wu QRJ, Yoo S, Yin FF. Dosimetric comparison of 3D conformal, IMRT, and V-MAT techniques for accelerated partial-breast irradiation (APBI). *Med Dosim* 2014; **39:** 152-8. doi: 10.1016/j.meddos.2013.12.001

46. Major T, Niehoff P. Kovács Gy, Fodor J, Polgár Cs. Dosimetric comparisons between high dose rate interstitial and MammoSite™ balloon brachytherapy for breast cancer. *Radiother Oncol* 2006; **79:** 321-8. doi: 10.1016/j.radonc.2006.05.005

47. Rahimi A, Thomas K, Spangler A, Rao R, Leitch M, Wooldridge R, et al. Preliminary results of a phase 1 dose-escalation trial for early-stage breast cancer using 5-fraction stereotactic body radiation therapy for partial-breast irradiation. *Int J Radiat Oncol Biol Phys* 2017; **98:** 196-205.e2. doi: 10.1016/j.ijrobp.2017.01.020

48. Bondiau PY, Bahadoran P, Lallement M, Birtwisle-Peyrottes I, Chapellier C, Chamorey E, et al. Robotic stereotactic radioablation concomitant with neoadjuvant chemotherapy for breast tumors. *Int J Radiat Oncol Biol Phys* 2009; **75:** 1041-7. doi: 10.1016/j.ijrobp.2008.12.037

49. Vermeulen S, Cotrutz C, Morris A, Meier R, Buchanan C, Dawson P, et al. Accelerated partial breast irradiation: using the CyberKnife as the radiation delivery platform in the treatment of early breast cancer. *Front Oncol* 2011; **1:** 43. doi: 10.3389/fonc.2011.00043

50. NSABP PROTOCOL B-39, RTOG PROTOCOL 0413. [internet]. [cited 2020 May 27]. Available at: http://rpc.mdanderson.org/rpc/credentialing/files/B39_Protocol1.pdf

51. Vermeulen SS, Haas JA. CyberKnife stereotactic body radiotherapy and CyberKnife accelerated partial breast irradiation for the treatment of early breast cancer. *Transl Cancer Res* 2014; **3:** 295-302. doi: 10.3978/j.issn.2218-676X.2014.07.06

52. Obayomi-Davies O, Kole TP, Oppong B, Rudra S, Makariou EV, Campbell LD, et al. Stereotactic accelerated partial breast irradiation for early-stage breast cancer: rationale, feasibility, and early experience using the cyberknife radiosurgery delivery platform. *Front Oncol* 2016; **6:** 129. doi: 10.3389/fonc.2016.00129

53. Lozza L, Fariselli L, Sandri M, Rampa M, Pinzi V, Carmen De Santis M, et al. Partial breast irradiation with CyberKnife after breast conserving surgery: a pilot study in early breast cancer. *Radiat Oncol* 2018; **13:** 49. doi: 10.1186/s13014-018-0991-4

54. Lee WH, Chang JS, Kim MJ, Park VY, Yoon JH, Kim SY, et al. First experience in Korea of stereotactic partial breast irradiation for low-risk early-stage breast cancer. *Front Oncol* 2020; **10:** 672. doi: 10.3389/fonc.2020.00672

55. Fröhlich G, Geszti Gy, Vízkeleti J, Ágoston P, Polgár Cs, Major T. Dosimetric comparison of inverse optimisation methods versus forward optimisation in HDR brachytherapy of breast, cervical and prostate cancer. *Strahlenther Onkol* 2019; **195:** 991-1000. doi: 10.1007/s00066-019-01513-x

56. Major T, Fröhlich G, Mészáros N, Smanykó V, Polgár CS. Does inverse planning improve the plan quality in interstitial high dose rate breast brachytherapy? *J Contemp Brachytherapy* 2020; **12:** 166-74. doi: 10.5114/jcb.2020.94584

57. Sanjay R, Jaiteerth SA, Moonseong MS, Harish KM, Wainwright J, Michael RK, et al. Quantifying IOHDR brachytherapy underdosage resulting from an incomplete scatter environment. *Radiat Oncol Biol Phys* 2005; **61:** 1582-6. doi: 10.1016/j.ijrobp.2004.10.002

research article

# Typical air kerma area product values for trauma orthopaedic surgical procedures

Damijan Skrk[1], Katja Petek[2], Dean Pekarovic[2], Nejc Mekis[3]

[1] Slovenian Radiation Protection Administration, Ljubljana, Slovenia
[2] University Medical Centre Ljubljana, Ljubljana, Slovenia
[3] Faculty of Health Sciences, University of Ljubljana, Ljubljana, Slovenia

Radiol Oncol 2021; 55(2): 240-246.

Received 12 June 2020
Accepted 28 September 2020

Correspondence to: Assist. Prof. Damijan Škrk, Ph.D., Slovenian Radiation Protection Administration, Ajdovščina 4, SI-1000 Ljubljana, Slovenia. E-mail: damijan.skrk@gov.si

Disclosure: No potential conflicts of interest were disclosed.

**Background.** The aim of study was to establish the typical radiation quantity values for the most common trauma orthopaedic surgical procedures and to compare them with reference values of equivalent procedures performed in other institutions. In addition, we assess the impact of image intensifier and flat panel detector technology used for fluoroscopically guidance on patient exposure.

**Materials and methods.** Five most frequently performed fluoroscopically guided trauma orthopaedic procedures in University Medical Centre Ljubljana were analysed. Data on 199 cases over a 6 months period from December 2016 to June 2017 were gathered retrospectively. Study covered 40 dynamic hip screw fixations (DHS), 23 proximal femoral nail insertions (PFN), 20 proximal humeral nail insertions (PHN), 77 partial hip endoprosthesis implantations (PEP) and 39 percutaneous posterior spine fixations (PPS). The median and average along with the first and third quartile values of air kerma area product (KAP) for each procedure type were calculated as well as median and average value of fluoroscopy screening time.

**Results.** Typical KAP value for dynamic hip screw fixation was set at 0.52 Gycm$^2$; for proximal femoral nail insertion at 0.53 Gycm$^2$ and for proximal humeral nail insertion at 0.26 Gycm$^2$. For implantation of partial endoprosthesis typical KAP value utilizing flat panel technology was set at 0.08 Gycm$^2$ and at 0.21 Gycm$^2$ when the image intensifier technology was used. Typical KAP value for percutaneous posterior spine fixation was set at 1.26 Gycm$^2$, using flat panel technology and at 3.98 Gycm$^2$ using image intensifier technology.

**Conclusions.** Established typical KAP levels of surgical orthopaedic procedures in traumatology will serve as a valuable tool for further radiation exposure optimization.

Key words: typical value; fluoroscopy; air kerma-area product; trauma orthopaedic procedures

## Introduction

The use of fluoroscopy in orthopaedic theatres has significantly increased over the past decade.[1] Benefits of intra-operative fluoroscopy include the indirect visualisation of anatomy, which enables many orthopaedic procedures to be performed using minimally invasive techniques, thus reducing morbidity and patient hospital stay. Using fluoroscopy guidance procedures are performed with greater ease, in less time and with less traumatisation of patient tissues.[2,3] Fluoroscopy guidance is performed by employing conventional image intensifier (II) or flat panel detector (FPD) for x-ray detection. Improvements in technology of C-arms give more opportunities for optimisation and call for additional skills of operator. In addition well known practical tool for optimization of diagnostic radiological procedures are diagnostic reference levels (DRL).[4] DRLs are values of radiation quantities used to indicate whether, in routine conditions, the amount of radiation used for a specified radiological procedure is unusually high or low for that procedure. To assist the implementation of op-

timisation process in a single facility, typical values of radiation quantity might be introduced. A typical value is defined as the median of the radiation quantity distribution and can be used as a guide to encourage further optimisation in a facility by providing a local comparator, in a similar manner to local DRLs. Typical values may be set also to provide a comparator linked to a new technology or technique for a single facility. Due to advances in technology and techniques DRL or typical values should be regularly updated.[5]

## Materials and methods

The primary objective of our research was to establish typical KAP values for five the most commonly fluoroscopically guided trauma orthopaedic procedures performed in University Medical Centre Ljubljana:

- dynamic hip screw fixation (DHS),
- proximal femoral nail insertion (PFN),
- proximal humeral nail insertion (PHN),
- partial hip endoprosthesis implantation (PEP) and
- percutaneous posterior spine fixation (PPS).

Procedures were guided by fluoroscopy units equipped with either image intensifier (II) based or flat panel detector (FPD) based technology. DHS fixations and PFN insertions were guided by FPD-based unit, while PHN insertions were guided by II - based unit. Also, the performance of both technologies were compared for PEP implantation and PPS fixation. Data in this retrospective study was acquired in a time interval from December 2016 to June 2017 from University Medical Centre Ljubljana. To establish the typical values for each procedure we gathered data of patient age, patient body weight, air kerma area product (KAP) and fluoroscopic screening time (FT) for each of 199 procedures. The inclusion criterion was body weight 60–90kg. Median, average and third quartile values for KAP and median and average values for FT were calculated for five listed fluoroscopically guided trauma orthopaedic procedures. Statistical analysis was performed using IBM SPSS Statistics, version 23. Mann-Whitney U test was applied to test the significant differences in KAP and FT. A p-value < 0.05 was used to indicate statistical significance. Established typical values were compared to reference levels of similar procedures presented in literature. National Ethics Committee approval for study performance was not required, due to the retrospective nature of the study of anonymized data and prior consent of Clinical Institute of Radiology, University Medical Centre Ljubljana.

## Results

Radiation exposure parameters of 199 trauma orthopaedic surgical procedures were analysed. Study covered 40 DHS fixations, 23 PFN insertions, 20 PHN insertions 77 PEP implantations and 39 PPS fixations. The median and average along with the first and third quartile values of KAP for each procedure type were calculated, as well as median and average value of fluoroscopy screening time. Statistical data of patient body weight (BW), KAP and FT are displayed in Table 1, while KAP distributions are shown in Figure 1.

Average age of patients who underwent the DHS fixations, PFN insertions and PHN insertions were 78, 87 and 67 years, respectively. Out of 77 partial hip endoprosthesis implantations a group of 22 patients underwent procedure which was fluoroscopically guided with FPD, while for the other group of 55 patients II was used. Average age of the patients was 78 years and 77 years for first and second group of patients, respectively. Mann-Whitney U test confirmed that no statistical differences between body mass distributions for two groups of patients who underwent procedures using different fluoroscopy detection technology exist (p = 0.308). Mann-Whitney U test showed statistically significant difference in KAP values (p < 0.001) as well as in FT (p < 0.001) between two groups of procedures using different fluoroscopy technologies (FPD and II) in favour of FPD.

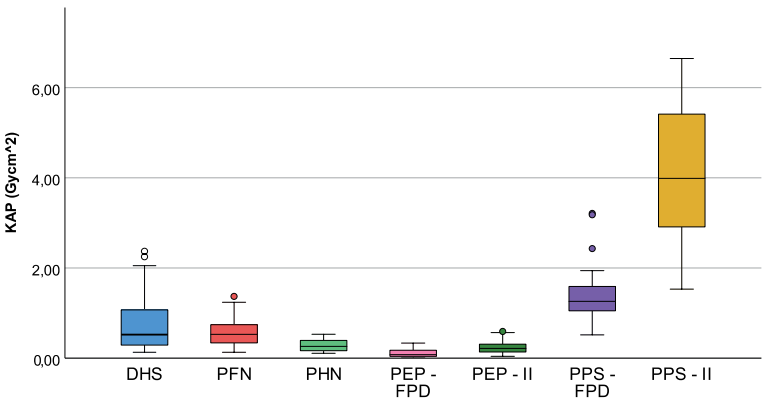


**FIGURE 1.** Distribution of kerma area product (KAP) data (minimum, first quartile, median, third quartile, and maximum) for 40 dynamic hip screw fixations (DHS), 23 proximal femoral nail insertions (PFN), 20 proximal humeral nail insertions (PHN), 77 partial hip endoprosthesis implantations utilizing flat panel detector (FPD) (22) and image intensifier (II) (55) for fluoroscopically guidance and 39 percutaneous posterior spine fixations (PPS) utilizing FPD (21) and II (18) for fluoroscopically guidance.

**TABLE 1.** Statistical data of patient body weight, KAP and fluoroscopy screening time for 40 DHS fixations, 23 PFN insertions, 20 PHN insertions, 77 PEP implantations utilizing FPD (22) and II (55) for fluoroscopically guidance and 39 PPS fixations utilizing FPD (21) and II (18) for fluoroscopically guidance

| | Min | Q1 | Median | Average ± SD | Q3 | Max |
|---|---|---|---|---|---|---|
| **DYNAMIC HIP SCREW FIXATIONS (DHS)** | | | | | | |
| **BW [kg]** | 60 | | 70 | 72 ± 9 | | 90 |
| **KAP(FPD)[Gycm²]** | 0.13 | 0.29 | **0.52** | 0.71 ± 0.56 | 1.07 | 2.37 |
| **FT [s]** | 17 | | 43 | 46 ± 20 | | 96 |
| **PROXIMAL FEMORAL NAIL INSERTIONS (PFN)** | | | | | | |
| **BW [kg]** | 60 | | 70 | 73 ± 9 | | 90 |
| **KAP(FPD)[Gycm²]** | 0.13 | 0.34 | **0.53** | 0.60 ± 0.34 | 0.74 | 1.37 |
| **FT [s]** | 26 | | 45 | 48 ± 18 | | 96 |
| **PROXIMAL HUMERAL NAIL INSERTIONS (PHN)** | | | | | | |
| **BW [kg]** | 60 | | 80 | 78 ± 8 | | 90 |
| **KAP(II) [Gycm²]** | 0.11 | 0.16 | **0.26** | 0.28 ± 0.14 | 0.41 | 0.53 |
| **FT [s]** | 19 | | 55.5 | 66.7 ± 37.9 | | 175 |
| **PARTIAL HIP ENDOPROSTHESIS IMPLANTATIONS (PEP)** | | | | | | |
| **BW(FPD) [kg]** | 60 | | 77.5 | 76 ± 7 | | 90 |
| **BW(II) [kg]** | 60 | | 80 | 78 ± 7 | | 90 |
| **KAP(FPD)[Gycm²]** | 0.03 | 0.04 | **0.08** | 0.12 ± 0.09 | 0.17 | 0.33 |
| **KAP(II)[Gycm²]** | 0.04 | 0.13 | **0.21** | 0.24 ± 0.14 | 0.31 | 0.60 |
| **FT(FPD) [s]** | 1.0 | | 3.0 | 4.0 ± 3.6 | | 19.0 |
| **FT(II) [s]** | 1.0 | | 5.0 | 6.9 ± 4.4 | | 21.0 |
| **PERCUTANEOUS POSTERIOR SPINE FIXATIONS (PPS)** | | | | | | |
| **BW(FPD) [kg]** | 60 | | 75 | 75 ± 6 | | 90 |
| **BW(II) [kg]** | 60 | | 75 | 76 ± 10 | | 90 |
| **KAP(FPD)[Gycm²]** | 0.52 | 0.91 | **1.26** | 1.44 ± 0.74 | 1.63 | 3.21 |
| **KAP(II) [Gycm²]** | 1.53 | 2.80 | **3.98** | 4.12 ± 1.69 | 5.53 | 6.65 |
| **FT(FPD) [s]** | 28 | | 71 | 80 ± 40 | | 182 |
| **FT(II) [s]** | 42 | | 110 | 115 ± 54 | | 215 |

BW = body weight; FPD = flat panel detector; FT = fluoroscopic screening time; II = image intensifier; KAP = kerma area product; Q1 = first quartile; Q3 = third quartile

Out of 39 percutaneous posterior spine fixation a group of 21 patients underwent procedure which was fluoroscopically guided with FPD while for the other group of 18 patients II was used. Average age of the patients was 65 years and 64 years for first and second group of patients, respectively. Mann-Whitney U test confirmed that no statistical differences between body mass distributions for two groups of patients who underwent procedures utilizing different detector technologies exist ($p = 0.922$). Mann-Whitney U test showed statistically significant difference in KAP values ($p < 0.001$) as well as in FT ($p = 0.040$) between two groups of procedures using different fluoroscopy technology (FPD and II) in favour of FPD.

## Discussion

The purpose of this study was to establish the typical KAP values for chosen trauma orthopaedic surgical procedures and to compare them with reference values of equivalent procedures performed in other institutions. In addition, the impact on patient exposure of two different image detector technologies used for fluoroscopy guidance were analysed for PEP implantation and PPS fixations.

### Dynamic hip screw fixation

For DHS fixations we established the median and average KAP values at 0.52 Gycm², and 0.71 Gycm²,

**TABLE 2.** Comparison of diagnostic reference levels (DRL) with literature - dynamic hip screw fixations (DHS)

| DYNAMIC HIP SCREW FIXATIONS (DHS) | Median KAP (Gycm²) | Average KAP (Gycm²) | Median FT (s) | Average FT (s) | BW (kg) |
|---|---|---|---|---|---|
| Our study | 0.52 | 0.71 | 43 | 45.6 | 73 |
| Hardman *et al.*, (2015)[6] 1. hospital | / | 0.65 | | 46.1 | 70 |
| Hardman *et al.*, (2015)[6] 2. hospital | / | 1.01 | | 55.3 | 70 |
| Hardman *et al.*, (2015)[6] 3. hospital | / | 3.94 | | 92.4 | 70 |
| Hardman *et al.*, (2015)[6] 4. hospital | / | 1.24 | | 61.5 | 70 |
| Hardman *et al.*, (2015)[6] – all | / | 1.57 | | 60.4 | 70 |
| Rashid *et al.*, (2017)[7] | 0.67 | | 36 | | |

BW = body weight; FT = fluoroscopic screening time; KAP = kerma area product

respectively, while median and average FT duration was 43.0 s and 45.6 s, respectively. Patient's average body weight was 73 kg. Table 2 shows the comparison of our results with results from the literature.

We compared the results of our study with similar study, performed by Hardman *et al.* performed in four major reference hospitals in London.[6] Our average KAP value was similar to value set in first reference hospital, while in others their values were higher. To broaden the analysis, we performed the comparison of FT durations. Only in the first reference hospital the FT was similar to ours, while in the others their FT were longer. The results are in line with the findings based on average KAP values comparison.

Hardman *et al.* also established average KAP value using data from all four institutions and set the value at 1.57 Gycm², while our average KAP value was set at 0.71 Gycm².

In addition, findings of the study performed by Rashid *et al.*[7] were compared to our results. Their median value of KAP is slightly higher while FT is shorter. Most probable reasons for differences are chosen exposure parameters, pulse frequency, collimation, use of fixed exposure parameters when metal implant is in field of view or patient's constitution. Due to unavailability of data from literature we were not able to evaluate the impact.

## Proximal femoral nail insertion

For PFN insertion we established the median and average KAP value at 0.53 Gycm² and 0.60 Gycm², respectively, median and average FT were set at 45 s and 48 s respectively. Average patients BW was 73 kg. Table 3 shows the comparison of our results with results from literature.[8-10]

The results of our study were compared to research conducted by Roux *et al.*[8], in one of the French hospitals, utilizing conventional II detector. Despite the shorter FT, their average KAP value was higher. This effect could most probably be attributed to different detector technologies, while we used FPD. Unfortunately, they did not report patients BW data, so we could not perform any further comparison or establish the reasons for differences in KAP values.

Pillai and Jain[9] completed their research in a major Scottish hospital, employing conventional

**TABLE 3.** Comparison of proximal femoral nail insertions (PFN) median and average kerma area product (KAP) values and average fluoroscopic screening time (FT) with literature

| PROXIMAL FEMORAL NAIL INSERTIONS (PFN) | Median KAP (Gycm²) | Average KAP (Gycm²) | Average FT (s) | BW (kg) |
|---|---|---|---|---|
| Our study | 0.53 | 0.60 | 48 | 73 |
| Roux *et al.* (2011)[8] | / | 0.79 | 32 | / |
| Pillai and Jain (2004)[9] | 0.69 | / | 34 | / |
| Salvia *et al.* (2011)[10] | / | / | 60 | / |

BW = body weight

**TABLE 4.** Comparison of proximal humeral nail insertions (PHN) average fluoroscopic screening time (FT) with literature

| PROXIMAL HUMERAL NAIL INSERTIONS | Median KAP (Gycm²) | Average KAP (Gycm²) | Average FT (s) | BW (kg) |
|---|---|---|---|---|
| Our study | 0.26 | 0.28 | 67 | 75 |
| Salvia *et al.*, (2011)[10] | / | / | 42 | / |

BW = body weight; FT = fluoroscopic screening time; KAP = kerma area product

**TABLE 5.** Comparison of partial hip endoprosthesis implantations (PEP) exposure parameters using flat panel detectors (FPD) and image intensifier technology for fluoroscopy guidance

| PARTIAL HIP ENDOPROSTHESIS IMPLANTATIONS | Median KAP ($Gycm^2$) | Average KAP ($Gycm^2$) | Median FT (s) | Average FT (s) | BW (kg) |
|---|---|---|---|---|---|
| Our research – FPD | 0.08 | 0.12 | 3.0 | 4.0 | 75.7 |
| Our research - II | 0.21 | 0.24 | 5.0 | 6.9 | 77.7 |

BW = body weight; FT = fluoroscopic screening time; KAP = kerma area product

**TABLE 6.** Comparison of percutaneous posterior spine fixations (PPS) exposure parameters using flat panel detectors (FPD) and image intensifier (II) technology for fluoroscopy guidance

| PERCUTANEOUS POSTERIOR SPINE FIXATIONS | Median KAP ($Gycm^2$) | Average KAP ($Gycm^2$) | Median FT (s) | Average FT (s) | BW (kg) |
|---|---|---|---|---|---|
| Our study - FPD | 1.26 | 1.44 | 71 | 80 | 75 |
| Our study - II | 3.98 | 4.12 | 110 | 115 | 78 |
| Roux *et al.*, (2011)[8] | / | 10.35 | / | 158 | / |

BW = body weight; FT = fluoroscopic screening time; KAP = kerma area product

II detector. They established median KAP value at 0.69 $Gycm^2$, while we set median KAP value at 0.53 $Gycm^2$. Our average FT is longer compared to Scottish study. The comparison of results exhibited similar circumstances as seen in study by Roux *et al.*[8] Again, we attributed this outcome to difference in used detector technologies. Longer fluoroscopy duration in our institution could be the result of less experienced operators or different methodology of radiological practice.

Salvia *et al.*[10], performed their study in Santa Clara hospital, USA, using conventional II detector. They established the average FT for the procedure, which is longer, than the one in our study. Regrettably, any other parameters, such as KAP or patient constitution descriptors are not reported.

## Proximal humeral nail insertion

For PHN insertion we established the median and average KAP values at 0.26 $Gycm^2$, and 0.28 $Gycm^2$, respectively, while median and average FT duration was 55.5 s and 66.7 s, respectively. Patient's average body weight was 75 kg. The comparison of our results with results from literature are shown in Table 4.

Salvia *et al.*[10] performed their study in Santa Clara hospital, USA, using conventional II detector. They established the average FT duration for procedure, which is much shorter, than the one in our study. Regrettably, they did not report any other parameters, such as KAP values or patient constitution descriptors. Due to the lack of comparable data, we can only conclude, that the reason for shorter duration of examination is probably the result of different method or more experienced staff.

## Partial hip endoprosthesis implantation

For PEP implantation guided by fluoroscopy unit with FPD detector we established the median, and average KAP values at 0.08 $Gycm^2$ and 0.12 $Gycm^2$, respectively, while median and average FT duration was 3 s and 4 s, respectively. Patient's average body weight was 75.7 kg.

For procedures performed by fluoroscopy unit equipped with II, we established the median and average KAP values at 0.21 $Gycm^2$ and 0.24 $Gycm^2$, respectively, while median and average FT duration was 5 s and 6.9 s, respectively. Patient's average body weight was 77.7 kg. Table 5 shows the exposure levels for PEP implantation for both detector technologies.

Applying the Mann Whitney U test, we showed that statistically significant difference in average KAP as well as in average FT exist between the two groups of procedures with different fluoroscopy technology used for guidance ($p < 10^{-3}$).

In procedures using II technology compared to procedures where FPD were employed KAP values were higher and FT were longer. One reason for higher KAP in procedures guided with fluoros-

copy unit equipped with II is longer FT, however, it stands to reason, that the observed difference is due to the impact of improved FPD technology. In our study the x-ray generator maximum power output for II type was 2.3 kW, while for FPD type was 15 kW. It is worth to note that comparison is limited because quality of fluoroscopic image was not taken into consideration.

### Percutaneous posterior spine fixation

For PPS fixations guided by fluoroscopy unit with FPD detector we established the median and average KAP values at 1.26 Gycm$^2$ and 1.44 Gycm$^2$, respectively, while median and average FT duration was 71 s and 80 s, respectively. Patient's average body weight was 75.0 kg.

For procedures performed by fluoroscopy unit equipped with II, we established the median and average KAP values at 3.98 Gycm$^2$ and 4.12 Gycm$^2$, respectively, while median and average FT duration was 110 s and 115 s, respectively. Patient's average body weight was 76 kg. Table 6 shows the exposure levels for PEP implantation for both detector technologies.

Applying the Mann Whitney U test we showed that statistically significant difference in average KAP as well as in average FT exist between the two groups of procedures using with different fluoroscopy technology for guidance ($p < 0.001$).

In procedures using II technology compared to procedures where FPD were employed KAP values were nearly three times higher while FT values were only one third longer. Besides shorter FT, FPD technology advantages compared to II technology has predominantly impact on KAP values. Consideration of fluoroscopy image quality would enable more specific findings.

We also compared our results with earlier mentioned study by Roux *et al.*[8], which conducted their research in one of the French hospitals, utilizing conventional II. Nearly three times lower average KAP in our sample and 1.5 times shorter FT duration were observed when comparing data obtained with II. This points to advantage of our method, however the conclusion may be misleading, because we were not able to evaluate impact of other procedure parameters, as they were not presented.

## Conclusions

Based on retrospective study, typical KAP values were established for most frequently performed fluoroscopy guided trauma orthopaedic surgeries performed in University Medical Centre Ljubljana, Slovenia. Typical KAP values were set for DHS fixation using FPD technology for fluoroscopy at 0.52 Gycm$^2$, PFN insertion using FPD technology for fluoroscopy at 0.53 Gycm$^2$, PHN insertion using II technology for fluoroscopy at 0.26 Gycm$^2$. For PEP implantation we set DRLs at 0.08 Gycm$^2$ and 0.21 Gycm$^2$ for FPD and II technology used for guidance, respectively, as well as for PPS fixation at 1.26 Gycm$^2$ and 3.98 Gycm$^2$ for FPD and II technology used for guidance, respectively.

In addition, we showed that radiation exposure parameters are deceased if FPD technology for fluoroscopy guidance is used, which could be accredited to advanced performance characteristics of FPD compared to II.

Established typical KAP values were compared to values set in other institutions and reported in literature. Analysis showed that our typical values are mostly lower than those set in other hospitals, while fluoroscopy FT durations are sometimes marginally longer. This aspect indicates the direction for additional optimisation.

For further research we recommend the acquirement of additional data to get larger samples and improve the statistical parameters. Moreover, a more detailed description of exposure parameters, pulse frequency, collimation, filtration and patient's constitution, such as diameter of observed body part and patient body height for body mass index calculations as well as comparison of fluoroscopic image quality, would enable even more specific findings and conclusions.

It is important to be aware that typical values for fluoroscopy guided trauma orthopaedic surgeries are one of the steps in the overall process of optimization and can act as standards for clinical audits.

## Acknowledgement

The authors would like to express gratitude to Clinical Institute of Radiology, University Medical Centre Ljubljana in Slovenia for making the data of trauma orthopaedic surgical procedures available for publication.

## References

1. Tsalafoutas IA, Tsapaki V, Kaliakmanis A, Pneumaticos S, Tsoronis F, Koulentianos ED, et al. Estimation of radiation doses to patients and surgeons from various fluoroscopically guided orthopaedic surgeries. *Radiat Prot Dosimetry* 2008; **128:** 112-9. doi: 10.1093/rpd/ncm234

2. Tunçer N, Kuyucu E, Sayar Ş, Polat G, Erdil İ, Tuncay İ. Orthopedic surgeons' knowledge regarding risk of radiation exposition: a survey analysis. *Sicot-J* 2017; **3:** 29. doi: 10.1051/sicotj/2017008

3. Miller DL. Interventional fluoroscopy: reducing radiation risks for patients and staff. *J Vasc Interv Radiol* 2009; **20(7 Suppl):** S274. doi: 10.1016/j.jvir.2009.04.057

4. Vassileva J, Rehani M. Diagnostic reference levels. *AJR Am J Roentgenol* 2015; **204:** W1-3. doi: 10.2214/AJR.14.12794

5. Vano E, Miller DL, Martin CJ, Rehani MM, Kang K, Rosenstein M, et al. *ICRP, 2017. Diagnostic reference levels in medical imaging. ICRP Publication 135. Ann ICRP 46(1).* London: SAGE, published for the International Commission on Radiological Protection; 2017.

6. Hardman J, Elvey M, Shah N, Simson N, Patel S, Anakwe R. Defining reference levels for intra-operative radiation exposure in orthopaedic trauma: a retrospective multicentre study. *Injury* 2015; **46:** 2457-60. doi: 10.1016/j.injury.2015.10.010

7. Rashid MS, Aziz S, Haydar S, Fleming SS, Datta A. Intra-operative fluoroscopic radiation exposure in orthopaedic trauma theatre. *Eur J Orthop Surg Traumatol* 2018; **28:** 9-14. doi: 10.1007/s00590-017-2020-y

8. Roux A, Bronsard N, Blanchet N, de Peretti F. Can fluoroscopy radiation exposure be measured in minimally invasive trauma surgery? *Orthop Traumatol Surg Res* 2011; **97:** 662-7. doi: 10.1016/j.otsr.2011.03.024

9. Pillai A, Jain M. Dose area product measurement in orthopaedic trauma. An attempt at establishing a local diagnostic reference level. *Radiography* 2004; **10:** 103-7. doi: 10.1016/j.radi.2004.02.002

10. Salvia JC La, de Moraes PR, Ammar TY, Schwartsmann CR. Fluoroscopy duration in orthopedic surgery. *Revista Brasileira de Ortopedia (English Edition)* 2011; **46:** 136-8. doi: 10.1016/s2255-4971(15)30228-7

Radiol Oncol 2021; 55(2): 121-129.
doi:10.2478/raon-2021-0010

# Okužba s COVID-19 pri bolnikih z rakom. Obravnava bolnikov v diagnostični enoti

Granata V, Fusco R, Izzo F, Setola SV, Coppola M, Grassi R, Reginelli A, Cappabianca S, Grassi R, Petrillo A

**Izhodišča.** Pri ranljivih bolnikih, kot so bolniki z rakom, je okužba s COVID-19 še posebej agresivna. Za obravnavo onkoloških bolnikov je zato bolj primeren multidisciplinarni pristop. Ta omogoča prepoznavanje bolnikov, ki potrebujejo bolnišnično obravnavo, bolnikov, ki jih lahko obravnavamo ambulantno, in bolnikov, pri katerih je mogoče zdravljenje odložiti.

**Zaključki.** Vloga radiologa je ključnega pomena, saj moramo pri vsakem bolniku z rakom, ki potrebuje slikovno diagnostiko, uporabiti najprimernejše slikovne preiskave. Te omogočajo odgovoriti na klinično vprašanje, še posebno pozornost pa je treba nameniti ohranjanju javnega zdravja. Za pravilno organizacijo delovanja radiološke enote so potrebne smernice za obravnavo bolnikov s sumom na okužbo ali s potrjeno okužbo s COVID-19. Če je le mogoče, bi bilo za zmanjšanje tveganja prenosa okužbe potrebno uporabljati satelitski radiografski center z namensko opremo.

Radiol Oncol 2021; 55(2): 130-143.
doi:10.2478/raon-2021-0004

# Pregled jetrnoceličnega raka z atipičnim vzorcem obarvanja. Spekter najdb pri magnetoresonančnem slikanju in korelacija s patološkim izvidom

Djokić Kovač J, Ivanović A, Milovanović T, Mićev M, Alessandrino F, Gore RM

**Izhodišča.** Pri bolnikih z jetrno cirozo lahko diagnozo jetrnoceličnega raka (HCC) dokončno ugotovimo že s slikovnimi metodami. Lezije so večje od 1 cm, imajo tipičen izgled, ki vključuje hipervaskularnost v arterijski fazi, ki ji sledi izplavljanje v venski faz. Vendar pa zaradi kompleksnosti hepatokarcinogeneze nimajo vsi HCC tipičnega videza. Atipične oblike kot hipervaskularen HCC brez izplavljanja, izovaskularen ali pa celo hipovaskularen HCC lahko predstavljajo diagnostične dileme. V teh primerih je pomembno tudi upoštevati izgled nodulov pri difuzijskem slikanju in v hepatobiliarni fazi. Za malignom je sumljivo, če sta prisotni restrikcija difuzije in hipointenzivnost v hepatobiliarni fazi. Če sta prisotna oba znaka, je pri bolniku z jetrno cirozo, kljub atipičnemu obarvanju, potrebno pomisliti na HCC. V prid diagnozi HCC lahko govorijo tudi pomožni znaki, kot prisotnost kapsule, vsebnost maščobe in signal na obteženih sekvencah T2. Obliko atipičnega HCC predstavljajo tudi lezije, ki so hiperintenzivne v hepatobiliarni fazi. Namen pričujoče raziskave je bil pripraviti pregled HCC-jev z atipičnim obarvanjem ter njihovga izgleda pri magnetnoresonančnem slikanju.

**Zaključki.** Da bi pravilno opredelili atipične HCC v cirotičnih jetrih, je ob načinu obarvanja nodula potrebno upoštevati tudi pomožne znake, kot so restrikcija difuzije, hipointenzivnost v hepatobiliarni fazi in hiperintenzivnost na obteženih sekvencah T2. Tudi vsebnost maščobe, okolno obarvanje v obliki krone in mozaična zgradba so magnetnoresonančni znaki, ki tudi ob odsotnosti tipičnega obarvanja govorijo v prid HCC.

Radiol Oncol 2021; 55(2): 144-149.
doi:10.2478/raon-2021-0009

# Kirurško zdravljenje in ohranitev plodnosti pri bolnicah z rakom endometrija

Kovačević N

**Izhodišča.** Rak endometrija predstavlja tako v Sloveniji kot po svetu veliko zdravstveno breme. Njegova incidenca narašča zaradi staranje prebivalstva ter tveganega življenjskega sloga, kot so neprimerno hranjenje s posledično debelostjo, kajenje, izpostavljenost estrogenom. Najpogosteje rak endometrija odkrijemo v zgodnji fazi zaradi očitnih znakov in simptomov. Standardno zdravljenje je operacija z ali brez dopolnilne terapije, odvisno od razširjenosti bolezni in tveganja za ponovitev. Vendar pa so se načini zdravljenja v zadnjih desetletjih precej spremenili, predvsem v obsegu limfadenektomije.

**Zaključki.** Zlati standard zdravljenja raka endometrija v začetnem stadiju in z nizkim histološkim gradusom je izključno kirurški. Priporočljiv je minimalno invaziven pristop z biopsijo varovalne bezgavke. Konservativen pristop s hormonalnim zdravljenjem uvedemo, ko želimo ohraniti plodnost. Če je rak endometrija lokalno napredoval ali gre za histološki tip visokega gradusa, svetujemo dopolnilno zdravljenje z radioterapijo, kemoterapijo ali kombinacijo obeh.

Radiol Oncol 2021; 55(2): 150-157.
doi:10.2478/raon-2021-0005

# Odnos med analitičnimi parametri ADC histograma in izražanjem PD-L1 pri rakih glave in vratu. Preliminarna raziskava

Meyer HJ, Höhn AK, Surov A

**Izhodišča.** Temelj sodobnega zdravljenja raka v zadnjem času vse bolj predstavlja imunoterapija. Ocena izražanja liganta 1 za programirano celično smrt (PD-L1) z neinvazivnimi metodami slikovne diagnostike bi lahko bila pomembna. V pričujoči raziskavi smo uporabili difuzijski poudarek slikanja (*angl. diffusion weighted imaging*, DWI) magnetne resonance in tako pridobili vrednost difuzijskega koeficienta (*angl. apparent diffusion coefficient*, ADC) celotne lezije za osvetlitev povezave z izražanjem PD-L1 pri bolnikih s ploščatoceličnim rakom glave in vratu.

**Bolniki in metode.** V preiskavo smo zajeli 29 bolnikov, ki so imeli na različnih mestih primarni ploščatocelični rak glave in vratu. Uporabili smo magnetnoresonančno napravo 3T z b-vrednostmi 0 in 800 s/mm2 sekvenc DWI. Vrednosti ADC smo ocenili s pomočjo histograma v področju celotnih lezij. Izražanje PD-L1 smo ocenili iz bioptičnih vzorcev lezij pred terapijo s pomočjo treh točkovnikov, točkovnika pozitivnosti tumorja (TPS), točkovnika imunskih celic (ICS) in skupega pozitivnega točkovnika (CPS).

**Rezultati.** Ugotovili smo inverzno korelacijo med vrednostmi ADC in ICS ($r = -0,38$; $p = 0,04$). Vrednost $ADC_{max}$ se je nagibala h korelaciji z ICS ($r = -0,35$; $p = 0,06$). Povezave ostalih parametrov ADC z izračunanimi točkovniki ni bilo opaziti.

**Zaključki.** Ugotovili smo zgolj šibko povezavo med koeficientom simetrije pri vrednostnih ADC in izraženostjo PD-L1 pri bolnikih s ploščatoceličnim rakom glave in vratu. Možno je, da ta način ugotavljanja izražanja PD-L1 ne bi bil primeren za klinično prakso. Vrednosti ADC so verjetno pod večjim vplivom kompleksnih histopatoloških dogajanj v tumorju, tako celičnih kot medceličnih in na njih ne vplivajo samo različne vrste tumorskih celic.

Radiol Oncol 2021; 55(2): 158-163.
doi:10.2478/raon-2021-0007

# Konfiguracija mehkotkivnih sarkomov pri slikanju z MRI je povezana s stopnjo malignosti

Sedaghat S, Salehi Ravesh M, Sedaghat M, Both M, Jansen O

**Izhodišča.** Cilj raziskave je bil oceniti, ali je konfiguracija primarnih mehkotkivnih sarkomov pri slikanju z magnetno resonanco (MRI) povezana s stopnjo malignosti.

**Bolniki in metode.** V raziskavo smo vključili 71 bolnikov s histološko potrjenim mehkotkivnim sarkomom. Na slikah MRI smo določili konfiguracijo ter meje in prostornino primarnega tumorja. Glede na klasifikacijski sistem Francoske nacionalne zveze centrov za rake (FNCLCC), skupine za sarkome, so bili tumorji razdeljeni na sarkome visokega (G3), srednjega (G2) in nizkega gradusa (G1).

**Rezultati.** Potrdili smo 30 primarnih mehkotkivnih sarkomov visokega, 22 srednjega in 19 nizkega gradusa. Mehkotkivni sarkomi visokega in srednjega gradusa (G3/2) so bili najpogosteje policiklični ($p < 0,001$) ali multilobularni ($p = 0,002$). Mehkotkivni sarkomi nizkega gradusa (G1) pa so bili večinoma anovoidni/nodularni ali pa so imeli progasto konfiguracijo ($p = 0,008$) in dobro omejene meje (95 %). Podoba mehkotkivnih sarkomov z visokim, srednjim in nizkim gradusom ter z ovoidno/nodularno konfiguracijo je bila na MRI podobna. Vsi mehkotkivni sarkomi višjega gradusa (G3/2) in progasto konfiguracijo ter policiklični/multilobulirani sarkomi visokega gradusa (G3) 17 od 20 bolnikov so kazali znake infiltracije. Mehkotkivni sarkomi s progasto konfiguracijo in policiklični/multilobularni sarkomi visokega gradusa so imeli v primerjavi s tumorji srednjega in nizkega gradusa večjo prostornino.

**Zaključki.** Konfiguracija primarnih mehkotkivnih sarkomov na slikah MRI lahko kaže na stopnjo malignosti. Tumorji višjega gradusa (G2/3) so imeli najpogosteje policiklično/multilobularno konfiguracijo, medtem ko so bili tumorji nizkega gradusa večinoma ovoidni/nodularni ali progasti. Znaki infiltracije lahko kažejo na višji gradus pri mehkotkivnih sarkomih s progasto konfiguracijo in pri policikličnih/multilobuliranih sarkomih.

Radiol Oncol 2021; 55(2): 164-171.
doi:10.2478/raon-2021-0006

# Primerjava transjugularnega intrahepatičnega portosistemskega odvoda in endoskopskega zdravljenja pri preprečevanju ponavljajočih se krvavitev iz varic. Dolgoročno spremljanje 126-ih bolnikov

Koršič Š, Štabuc B, Skok P, Popovič P

**Izhodišča.** Ponavljajoče krvavitve iz varic požiralnika in želodca so najpogostejši življenje ogrožujoči zapleti portalne hipertenzije. V smernicah transjugularni intrahepatični portosistemski odvod (*angl. transjugular intrahepatic portosystemic shunt,* TIPS) ni zdravljenje izbora ponavljajočih se krvavitev iz varic. Naredili bi ga naj le pri krvavitvah, ki so odporne na farmakološko in endoskopsko zdravljenje. V dostopni literaturi so redke dolgoročne raziskave, ki primerjajo varnost in učinkovitost TIPS-a in endoskopskega zdravljenja za preprečevanje ponavljajočih se krvavitev iz varic.

**Bolniki in metode.** Retrospektivno smo analizirali 70 bolnikov, ki smo jih zdravili s TIPS-om, in 56-ih bolnikov, ki smo jih zdravili endoskopsko. Bolnike smo spremljali od vključitve v raziskavo do njihove smrti, ali presaditve jeter, zadnje kontrole ali do konca raziskave.

**Rezultati.** Ponavljajoče krvavitve so bile statistično značilno pogostejše v skupini endoskopsko zdravljenih v primerjavi s skupino TIPS (66,1 % proti 21,4 %, $p < 0,001$; $\chi 2$-test). Incidenca smrti zaradi ponavljajoče krvavitve je bila višja v skupini endoskopsko zdravljenih (28,6 % proti 10 %). 1-, 2- in 5-letno preživetje v skupini TIPS v primerjavi s skupino endoskopsko zdravljenih je bilo 85 % proti 83 %, 73 % proti 67 % and 41 % proti 35 %. Jetrna odpoved je bil najpogostejši vzrok smrti pri bolnikih s preživetjem daljšim od dveh let. Srednji čas spremljanja v skupini TIPS je bil 47 mesecev (razpon; 2–194 mesecev) in v skupini endoskopsko zdravljenih 40 mesecev (razpon; 1–168 mesecev).

**Zaključki.** TIPS je bil v primerjavi z endoskopsko zdravljenimi bolj učinkovit pri preprečevanju ponavljajočih se krvavitev iz varic in po njem je bila smrtnost zaradi krvavitev nižja.

Radiol Oncol 2021; 55(2): 172-178.
doi: 10.2478/raon-2021-0014

# Analiza urgentne preiskave CT glave pri kritično bolnih onkoloških bolnikih

Pristavu C, Martin A, Irina Ristescu A, Patrascanu E, Gavril L, Lundu O, Manole M, Rusu D, Grigoras I

**Izhodišča.** Kritično bolni bolniki imajo povečano tveganje za razvoj akutnih nevroloških znakov. Namen raziskave je bil oceniti uporabo in uporabnost urgentne preiskave CT glave pri takšnih bolnikih.

**Bolniki in metode.** V retrospektivno kohortno raziskavo posamičnega centra smo vključili bolnike z urgentno preiskavo CT glave, ki smo jo naredili med hospitalizacijo v enoti intenzivne terapije v obdobju treh let. Želeli smo prepoznati diagnostično dobrobit in soodvisnost med abnormalnimi najdbami na posnetkih CT-ja, tumorskim tipom in stopnjo smrtnosti, zato smo ocenili indikacije, najdbe na posnetkih in izid zdravljenja.

**Rezultati.** Našli smo 64 urgentnih preiskav CT glave pri 54 kritično bolnih bolnikih; 32 posnetkov (50 %) je prikazalo predhodno neznane lezije in smo jih upoštevali kot pozitivne ugotovitve. Najpogostejše abnormalne najdbe so bile ishemične (pri 15 preiskavah, 47 %) in hemoragične (pri 13 preiskavah, 40 %) lezije. Indikacije za 38 urgentnih preiskav CT glave (59 %) so bile spremenjeno mentalno stanje s 50 % pozitivnih posnetkov. 18 urgentnih preiskav CT glave (48 %) smo naredili pri bolnikih s hematološkimi raki: 9 posnetkov (50 %) je bilo pozitivnih, 8/9 (89 %) s hemoragičnimi lezijami. Pri bolnikih s solidnimi raki smo naredili 20 urgentnih CT preiskav glave: 10 (50 %) je bilo pozitivnih in pri 9/10 (90 %) smo našli ishemične lezije. Izmed 54 bolnikov je med hospitalizacijo v enoti intenzivne terapije umrlo 30 bolnikov (55 %). Stopnja smrtnosti je bila višja pri bolnikih s hematološkimi raki in pozitivnimi najdbami z urgentnim CT glave (78 % proti 58 %).

**Zaključek.** Diagnostična dobrobit urgentne preiskave CT glave pri kritično bolnih bolnikih je mnogo višja kot pri drugih kategorijah bolnikov v enoti intenzivne terapije. Priporočamo sistematično uporabo te preiskave pri kritično bolnih, predvsem pri hemato-onkoloških bolnikih z nespecifično nevrološko okvaro, saj lahko prispeva k zgodnji prepoznavi intrakranialnih zapletov.

Radiol Oncol 2021; 55(2): 179-186.
doi:10.2478/raon-2021-0002

# Vloga genskih polimorfizmov, povezanih z glutationom, pri azbestnih boleznih

Franko A, Goričar K, Dodič Fikfak M, Kovač V, Dolžan V

**Izhodišča.** V raziskavi smo preučevali vpliv polimorfizmov *GCLC, GCLM, GSTM1, GSTT1* in *GSTP1*, kot tudi vpliv interakcij med polimorfizmi ter interakcij med polimorfizmi in izpostavljenostjo azbestu na tveganje za razvoj plevralnih plakov, azbestoze in malignega mezotelioma.

**Preiskovanci in metode.** V raziskavo smo vključili 940 preiskovancev, ki so bili izpostavljeni azbestu, med njimi 390 preiskovancev s plevralnimi plaki, 147 z azbestozo, 225 z malignom mezoteliomom ter 178 preiskovancev, ki niso imeli nobene bolezni, povezane z izpostavljenostjo azbestu. Genotipe *GCLC* rs17883901, *GCLM* rs41303970, nični *GSTM1*, nični *GSTT1* ter *GSTP1* rs1695 in *GSTP1* rs1138272 smo določili z metodami, ki so temeljile na polimerazni verižni reakciji. V statistični analizi smo uporabili metodo logistične regresije.

**Rezultati.** Nični genotip *GSTT1* je bil povezan z manjšim tveganjem za razvoj plevralnih plakov (razmerje obetov [RO] = 0,63; 95 % interval zaupanja [IZ] = 0,40–0,98; p = 0,026) in azbestoze (RO = 0,51; 95 % IZ = 0,28–0,93; p = 0,028), ni pa bil povezan z malignim mezoteliomom. Pozitivno povezavo smo ugotovili med genotipi *GSTP1* rs1695 AG + GG *vs*. AA za maligni mezoteliom v primerjavi s plevralnimi plaki (RO = 1,39; 95 % IZ = 1,00–1,94; p = 0,049). Interakcije med različnimi polimorfizmi niso vplivale na tveganje za razvoj preučevanih bolezni, povezanih z izpostavljenostjo azbestu. Interakcija med ničnim polimorfizmom *GSTT1* in izpostavljenostjo azbestu je znižala tveganje za maligni mezoteliom (RO = 0,17; 95 % IZ = 0,03–0,85; p = 0,031).

**Zaključki.** Rezultati raziskave kažejo, da bi bil nični genotip *GSTT1* lahko povezan z manjšim tveganjem za razvoj plevralnih plakov in azbestoze. Lahko modificira povezavo med izpostavljenostjo azbestu in malignim mezoteliomom ter lahko posledično deluje protektivno na tveganje za razvoj malignega mezotelioma. Ugotovili smo tudi protektivni učinek interakcije med polimorfizmom *GSTP1* rs1695 in izpostavljenostjo azbestu za tveganje za nastanek malignega mezotelioma.

Radiol Oncol 2021; 55(2): 187-195.
doi:10.2478/raon-2021-0001

# Dolgoročno sledenje po samoodvzemu vzorca za HPV z odvzemnikoma Qvintip in HerSwab pri neodzivnicah presejalnega programa za raka maternične vratu

Bokan T, Ivanuš U, Jerman T, Takač I, Arko D

**Izhodišča.** Prvič predstavljamo rezultate pilotne raziskave s samoodvzemom vzorca za test HPV pri ženskah v okviru Nacionalnega presejalnega programa ZORA, ki smo jih pregledali v kolposkopski ambulanti. Navajamo rezultate enoletnega in štiriletnega sledenja pri uporabi dveh različnih samoodvzemnikov.

**Bolniki in metode.** Vključili smo 209 žensk iz kolposkopske ambulante. Pred ginekološkim pregledom so si same iz nožnice odvzele vzorec za test na humani papilomavirus (HPV); 111 s samoodvzemnikom Qvintip in 98 s samoodvzemnikom HerSwab. Po samoodvzemu je ginekolog odvzel dva vzorca s površine maternične vratu, enega za standardno citološko preiskavo in enega za test na HPV. Pri vseh smo opravili kolposkopijo in biopsijo maternične vratu, če je bila indicirana. Primerjali smo občutljivost, specifičnost in napovedne vrednosti citologije (mejna vrednost atipične ploščate celice, neopredeljene; APC-N) in testa na HPV (pri samoodvzetem vzorcu in vzorcu, ki ga je odvzel ginekolog) za odkrivanje intraepiteliske neoplazije gradus 2 ali več (CIN2+) po enem in štirih letih sledenja. Za analizo vzorca na okužbo s HPV smo uporabili *Hybride Capture 2* (HC2).

**Rezultati.** Povprečna starost vseh 209 žensk je bila 37,6 let, HPV je bil pozitiven pri 67,0 % (140/209). V skupini Qvintip je bila povprečna starost 36,9 let, pri 70,3 % (78/111) je bil HPV pozitiven, v skupini HerSwab pa 38,4 let in pri 63,3 % (62/98) HPV pozitiven. Odstotek skupnega ujemanja med samoodvzetim vzorcem in vzorcem, ki ga je odvzel ginekolog, je bil 81,8 % (kappa 0,534) v skupini Qvintip in 77,1 % (kappa 0,456) v skupini HerSwab. V skupini Qvintip so bile longitudinalna občutljivost, specifičnost, pozitivna in negativna napovedna vrednost za citologijo: 71,8 %, 75,0 %, 83,6 %, 60,0 %; za samoodvzet HPV: 83,1 %, 51,3 %, 75,6 % in 62,5 % ter za test HPV, ki ga je odvzel ginekolog: 94,4 %, 57,5 %, 79,8 % in 85,2 %. V skupini HerSwab so bili rezultati istih vrednosti: 71,7 %, 46,7 %, 61,3 %, 58,3 % za citologijo; 75,0 %, 47,7 %, 62,9 % in 61,8 % za samoodvzet HPV in 94,3 %, 44,4 %, 66,7 % in 87,0 % za test HPV, ki ga je odvzel ginekolog.

**Zaključki.** Rezultati so potrdili, da je samoodvzet vzorec za test na HPV, določen s HC2, manj zanesljiv od vzorca, ki ga odvzame zdravnik. Vsi HPV testi so pokazali višjo občutljivost v odkrivanju CIN2+ v primerjavi s citologijo. Glede na primerljivo občutljivost samoodvzetega HPV s citologijo, bi bil samoodvzem morda lahko možnost za neodzivnice v nacionalnem presejalnem programu.

Radiol Oncol 2021; 55(2): 196-202.
doi: 10.2478/raon-2020-0072

# Ocena uspešnosti spremljanja bolnikov z rakom sečnega mehurja s testom *Xpert BC monitor* glede na citološko preiskavo urina

Smrkolj T, Čegovnik Primožič U, Fabjan T, Šterpin S, Osredkar J

**Izhodišča.** Cistoskopija in citološka preiskava urina sta zlati standard pri spremljanju bolnikov z rakom sečnega mehurja. V raziskavi smo ovrednotili pomen novega urinskega testa Xpert BC monitor *(angl. Xpert bladder cancer monitor;* XBC) pri sledenju teh bolnikov.

**Bolniki in metode.** Na vzorcih urina bolnikov, ki so bili zdravljeni zaradi raka sečnega mehurja, smo izvedli XBC in citološko preiskavo. Rezultate smo primerjali z izvidom cistoskopije ter histopatološkim izvidom po transuretralni resekciji tumorjev sečnega mehurja.

**Rezultati.** Za napovedovanje malignega histopatološkega izvida so bile občutljivost, specifičnost in negativna napovedna vrednost 76,9 %; 97,5 % in 93,0 % za test XBC ter 38,4 %; 97,5 %; 83.3 % za citološko preiskavo urina. Za napovedovanje sumljivega cistoskopskega izvida so bile občutljivost, specifičnost in negativna napovedna vrednost 75,0 %; 95,2 % in 93;0 % za test XBC ter 41,7 %; 97,6 %; 85,4 % za citološko preiskavo urina. Občutljivost testa XBC za papilarni urotelialni tumor nizkega malignega potenciala, za tumorje nizkega in za tumorje visokega gradusa je bila 0,0 %; 66,7 % in 100,0 %, občutljivost citološke preiskave urina pa 0,0 %; 66,7 % in 42,9 %.

**Zaključki.** Test XBC ima pomembno višjo skupno občutljivost in negativno napovedno vrednost kot citološka preiskava urina. Tako omogoča povečanje časovnega razmika med kontrolnimi cistoskopijami. Kombinacija testa XBC in citološke preiskave urina ne izboljša napovedne vrednosti testa XBC.

Radiol Oncol 2021; 55(2): 203-211.
doi: 10.2478/raon-2021-0017

# Napovedni dejavniki pri pooperativni radioterapiji raka prostate. Izkušnje terciarnega centra

Miszczyk M, Majewski W, Stawiski K, Rasławski K, Rajwa P, Jabłońska I, Magrowski L, Masri O, Paradysz A, Miszczyk L

**Izhodišča.** Namen raziskave je bil analizirati napovedne dejavnike pri pooperativni radioterapiji raka prostate in izdelati nomogram za preživetje brez bolezni.

**Bolniki in metode.** V retrospektivno raziskavo smo med leti 2009 in 2014 vključili 236 zaporednih bolnikov iz terciarne ustanove. Vsi bolniki so imeli rak prostate ter smo jih zdravili z radikalno prostatektomijo, ki ji je sledila radioterapija. Osnovni cilj je bil ugotoviti preživetje brez bolezni, naredili smo uni- in mulitvariatno analizo, preživetvene krivulje po Kaplan-Meireju, test log-rank, analizo rekurzivno podanih zaporedij ter izdelali nomogram.

**Rezultati.** Srednji čas sledenja bolnikov je bil 62,3 mesecev (interkvartilni razmik 38,1–79 mesecev). Neodvisni klinični dejavniki, ki so v mulitvariatni analizi prispevali k povišanemu tveganju za ponovitev ali napredovanje bolezni, so bili vrednost PSA pred radioterapijo, stadij pT3 in lokalni recidiv kot indikacija za rešilno zdravljenje. Velikost padca vrednosti PSA je imela pomemben vpliv na tveganje za biokemični neuspeh zdravljenja. Biokemična kontrola bolezni in preživetje brez bolezni sta se pomembno razlikovala glede na indikacijo za zdravljenje ($p < 0,0001$). Analiza rekurzivno podanih zaporedij je izpostavila pomen vrednosti PSA pred radioterapijo, stopnje po Gleasonu, padca vrednosti PSA in lokalnega recidiva kot indikacije za rešilno zdravljenje. Razvili smo nomogram za preživetje brez bolezni, ki je dosegljiv na https://apps.konsta.com.pl/app/prostate-salvage-dfs/.

**Zaključki.** Vrednost PSA pred radioterapijo, stadij pT3 in lokalni recidiv kot indikacija za rešilno zdravljenje so najpomembnejši napovedni dejavniki, ki zvišujejo tveganje za ponovitev ali napredovanje bolezni. Stopnja po Gleasonu 4–5 in padec vrednosti PSA dovoljujeta nadaljnjo stratifikacijo tveganja. Rezultati zdravljenja s pooperativnim obsevanjem raka prostate se pomembno razlikujejo glede na indikacijo za zdravljenje. Izdelali smo spletni nomogram, ki omogoča vpogled v spreminjanje napovedi poteka bolezni v odvisnosti od kliničnih podatkov.

Radiol Oncol 2021; 55(2): 212-220.
doi:10.2478/raon-2021-0008

# Globoki zadržani vdih zmanjša srednjo sevalno dozo na srce pri obsevanju raka leve dojke

Falco M, Masojć B, Macała A, Łukowiak M, Woźniak P, Malicki J

**Izhodišča.** Pri bolnice z rakom leve dojke, ki smo jih obsevali, je nevarnost, da se bo razvila z obsevanjem povzročena srčno-žilna bolezen, dokaj resna. Skušamo se ji izogniti z izboljšanimi protokoli za načrtovanjem obsevanja, tehnikami dihalnega proženja, vključno z globokim zadržanim vdihom. Več dozimetričnih raziskav je pokazalo, da globoki zadržani vdih zmanjša sevalno dozo na srce, vendar so klinični podatki skopi. Namen pričujoče raziskave je bil primerjati srednjo dozo na srce pri bolnicah z rakom leve dojke, ki smo jih obsevali ob neproženem prostem dihanju, proženem prostem dihanju ali globokem zadržanem vdihu.

**Bolniki in metode.** V retrospektivno raziskavo smo vključili 2022 bolnic, ki smo jih zaradi raka dojke obsevali na Onkološkem centru Zahodnega Pomeranja od 1. januarja 2014 do 31. decembra 2017. Primerjali smo srednjo sevalno dozo na srce glede na obdobje, ko smo bolnice obsevali, in glede na obsevalno tehniko.

**Rezultati.** Srednja sevalna doza na srce pri vseh bolnicah z rakom leve dojke je bila 3,37 Gy. Srednja doza na srce je bila pri bolnicah obsevanimi ob globokem zadržanem vdihu značilno nižja kot pri bolnicah obsevanimi ob neproženem prostem dihanju (2,1 *vs.* 3,48 Gy; $p < 0,0001$) ali ob proženem prostem dihanju (3,28 Gy: $p < 0,0001$). Najnižjo srednjo sevalno dozo na srce smo ugotovili v 4-letnem obdobju (do leta 2017), ko smo skoraj 85 % bolnic obsevali ob globokem zadržanem vdihu. Delež bolnic, ki je bil izpostavljen visoki srenji sevalni dozi na srce (> 4 Gy) se je vsako leto zmanjševal, od 40 % v letu 2014 do 7,9 % v letu 2017, med tem ko se je delež bolnic obsevanih ob globokem zadržanem vdihu povečeval.

**Zaključki.** Primerjava obsevanja ob neproženem in proženem prostem dihanju ter obsevanja ob globokem zadržanem vdihu je pokazala, da smo s slednjo tehniko zmanjšali srednjo sevalno dozo na srce pri bolnicah z rakom leve dojke. Tako podpira uvedbo in uporabo tehnike obsevanja ob globokem zadržanem vdihu v klinično prakso.

Radiol Oncol 2021; 55(2): 221-228.
doi:10.2478/raon-2021-0011

# Rezultati postopkov IVF/ICSI pri moških onkoloških bolnikih. Retrospektivna analiza postopkov iz obdobja 2004–2018

Burnik Papler T, Vrtačnik-Bokal E, Drobnič S; Štimpfel M

**Izhodišča.** Ohranjanje plodnosti predstavlja pomemben vidik kakovosti življenja onkoloških bolnikov po koncu zdravljenja. Pri moških plodnost ohranjamo z zamrzovanjem semena pred pričetkom zdravljenja. Izidi postopkov zunajtelesne oploditve so pri zdravih neplodnih parih primerljivi, ne glede na to ali uporabimo sveže ali odmrznjeno seme. Podatkov o izidih postopkov zunajtelesne oploditve pri moških onkoloških bolnikih ni veliko.

**Bolniki in metode.** V retrospektivni raziskavi smo analizirali izide postopkov zunajtelesne oploditve (angl. *in vitro* fertilization / intracytoplasmic sperm injection; IVF/ICSI) pri neplodnih parih, katerih moški je bil v preteklosti zdravljen zaradi raka. Nadalje smo primerjali izide postopkov zunajtelesne oploditve glede na uporabljeno vrsto semena.

**Rezultati.** Analizirali smo 214 postopkov zunajtelesne oploditve opravljenih v letih 2004–2018. Stopnja zanositve (zamrznjeno *vs*. sveže seme; 30,0 % *vs*. 21,4 %; p = 0,12) in stopnja porodov (22,3 % *vs*. 17,9 %; p = 0,43) izračunana na aspiracijo jajčnih celic se nista razlikovali. Deleža uporabnih (48,9 % *vs*. 40,0 %; p = 0,006) in zamrznjenih zarodkov (17,3 % *vs*. 12,7 %; p=0,048) sta bila statistično pomembno višja v skupini bolnikov, kjer smo uporabili zamrznjeno seme. Kumulativna stopnja zanositve je bila statistično pomembno višja v skupini bolnikov z uporabljenim zamrznjenim semenom (60,6 % *vs*. 37,7 %; p = 0,012). Kumulativna stopnja porodov se med skupinama ni statistično pomembno razlikovala (45,1 % *vs*. 34,0 %; p = 0,21).

**Zaključki.** Izhod (zanositev, porod) svežih postopkov zunajtelesne oploditve je podoben ne glede na to ali uporabimo odmrznjeno ali sveže seme moških, ki so bili v preteklosti zdravljeni zaradi raka. Deleža uporabnih in zamrznjenih zarodkov sta bila statistično pomembno višja, če je bilo uporabljeno zamrznjeno seme, kar je tudi vodilo v večje število parov, ki so po takem postopku prišli vsaj do ene zanositve.

Radiol Oncol 2021; 55(2): 229-239.
doi: 10.2478/raon-2021-0016

# Primerjava večkatetrne intersticijske brahiterapije in CyberKnifa pri pospešenem delnem obsevanju dojk. Načrtovanje obsevanj z upoštevanjem sevalne doze na rizične organe

Herein A, Stelczer G, Pesznyák C, Fröhlich G, Smanykó V, Mészáros N, Polgár C, Major T

**Izhodišča.** Namen raziskave je bil dozimetrično primerjati večkatetrno intersticijsko brahiterapijo in stereotaktično radioterapijo s CyberKnifom pri pospešenem delnem obsevanju dojk in upoštevanju sevalne doze na rizične organe.

**Materiali in metode.** Pri 32 bolnicah smo primerjali obsevalne načrte za dvoje obsevalnih tehnik, za večkatetrno intersticijsko brahiterapijo in za CyberKnif. Bolnicam smo obsevali levo dojko. Med rizične organe smo vključili istostransko dojko (predele dojke izven načrtovalnega volumna) in nasprotno dojko, istostranske in nasprotne dele pljuč, predele kože, reber in srca. Obsevalni režim je bil enak pri obeh obsevalnih tehnikah (4 x 6,25 Gy). Iz dozno-volumskih histogramov smo izračunali relativne volumne (V100 in V90), ki so prejeli 100 % in 90 % predpisane doze ter relativno dozo (D0,1 $cm^3$ in D1 $cm^3$), ki so jo prejeli najbolj izpostavljeni deli tkiva majhnih volumnov (0,1 $cm^3$ in 1 $cm^3$). Vse dozne vrednosti smo izračunali relativno glede na predpisano dozo 25 Gy.

**Rezultati.** Pri istostranski dojki (deli izven načrovalnega volumna) so bili rezultati s CyberKnifom nekoliko boljši kot pri obsevanju z večkatetrno intersticijsko brahiterapijo: V100 = 0,7 % in V50 = 10,5 % *vs.* V100 = 1,6 % in V50 = 12,9 %. Povprečna doza istostranskih delov pljuč je bila enaka (4,9 %) ne glede na uporabljeno obsevalno tehniko, medtem ko so bile doze na majhne volumne nižje pri večkatetrni intersticijski brahiterapiji (36,1 %) v primerjavi s CyberKnifom (45,4 %). Varovanje kože in reber je bilo boljše pri tehniki večkatetrne intersticijske brahiterapije. Pri dozno-volumskih parametrih za srce nismo našli pomembnih razlik med obema tehnikama, je pa bil nekoliko večji volumen obsevan s 5 % dozo pri večkatetrni intersticijski brahiterapiji. Nasprotna dojka in nasprotni deli pljuč so prejeli višjo dozo z večkatetrno intersticijsko brahiterapijo (D1 $cm^3$ = 2,6 % *vs.* D1 $cm^3$ = 3,6 %) v primerjavi s CyberKnifom (D1 $cm^3$ = 1,8 % *vs.* D1 $cm^3$ = 2,5 %).

**Zaključki.** Tarčne volumne pri dojki lahko dobro obsevamo z obema obsevalnima tehnikama. Z njima dosežemo podobno dozno porazdelitev in visoko konformnost. Doza v delih istostranske dojke, v srcu in v nasprotno ležečih organih je bila ugodnejša pri obsevalni tehniki s CyberKnifom, medtem ko so bližnji organi (koža, rebra, istostranski deli pljuč) prejeli nižjo dozo ob uporabi večkatetrne intersticijske brahiterapije. Čeprav so bile dozimetrične razlike pri opazovanih parametrih majhne, so bile statistično pomembne. Za oceno klinične relevantnosti dozimetričnih razlik med obema obsevalnima tehnika so potrebne dodatne raziskave.

Radiol Oncol 2021; 55(2): 240-246.
doi: 10.2478/raon-2020-0066

# Vzpostavitev tipičnih vrednosti produkta kerme in ploščine slikovnega polja za travmatološke operacijske posege

Škrk D, Petek K, Pekarovič D, Mekiš N

**Izhodišča.** Namen raziskave je bil vzpostavitev tipičnih vrednosti produkta kerme in ploščine slikovnega polja za najbolj pogoste travmatološke operacijske posege in primerjava le teh s tipičnimi vrednostmi primerljivih raziskav. Prav tako smo primerjali izpostavljenost pacientov glede na uporabljeno tehnologijo za zajem diaskopske slike (klasičen ojačevalnik slike ali ploski detektor).

**Materiali in metode.** V analizo so bili vključeni podatki petih najbolj pogostih travmatoloških operacijskih posegov, ki so bili izvedeni v Univerzitetnem kliničnem centru Ljubljana. Skupno smo zbrali podatke za 199 operacij, izvedenih v časovnem obdobju od decembra 2016 do junija 2017. Zbrali smo podatke za naslednje posege: vstavitev dinamičnega kolčnega vijaka – DHS (n=40), vstavitev proksimalnega stegneničnega žeblja – PFN (n=23), vstavitev proksimalnega nadlahtičnega žeblja – PHN (n=20), vstavitev delne kolčne endorpoteze – PEP (n=77) in perkutana posteriorna fiksacija hrbtenice – PPS (n=39). Na podlagi pridobljenih podatkov smo izračunali mediano in povprečje za vrednosti produkta kerme v zraku in ploščine slikovnega polja (KAP) ter povprečje in mediano za čas diaskopije.

**Rezultati.** Ugotovili smo da srednja vrednost (mediana) KAP-a pri vstavitvi dinamičnega kolčnega vijaka znaša 0,52 Gycm$^2$, za vstavitev proksimalnega stegneničnega žeblja je mediana znašala 0,53 Gycm$^2$. Mediana je pri operacijskem posegu vstavitve proksimalnega nadlahtičnega žeblja znašala 0,26 Gycm$^2$. Za operativni poseg vstavitve delne kolčne endoproteze in perkutano posteriorno fiksacija hrbtenice smo rezultate predstavili za vsako uporabljeno tehnologijo posebej. Za PEP je bila vrednost mediane pri uporabi ploskega detektorja 0,08 Gycm$^2$, pri uporabi klasičnega ojačevalnika slike pa je mediana znašala 0,21 Gycm$^2$. Pri operacijskem posegu PPS pa je bila vrednost mediane pri uporabi ploskega detektorja 1.26 Gycm$^2$, pri uporabi klasičnega ojačevalnika slike pa je bila vrednost mediane 3,98 Gycm$^2$.

**Zaključki.** Postavitev tipičnih vrednosti sevalnih veličin za travmatološke operacijske posege so pomembno orodje pri postopkih optimizacije izpostavljenosti pacientov kot tudi pri izvedbi kliničnih presoj.

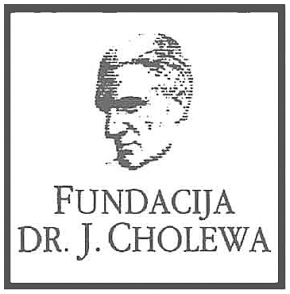


Fundacija "Docent dr. J. Cholewa"
je neprofitno, neinstitucionalno in nestrankarsko
združenje posameznikov, ustanov in organizacij, ki želijo
materialno spodbujati in poglabljati raziskovalno
dejavnost v onkologiji.

Dunajska 106
1000 Ljubljana
IBAN: SI56 0203 3001 7879 431

TANTUM VERDE®

benzidaminijev klorid


# Za lajšanje bolečine in oteklin v ustni votlini in žrelu, ki so posledica radiomukozitisa

**Bistvene informacije iz Povzetka glavnih značilnosti zdravila**

**Tantum Verde 1,5 mg/ml oralno pršilo, raztopina**
**Tantum Verde 3 mg/ml oralno pršilo, raztopina**
**Sestava 1,5 mg/ml:** 1 ml raztopine vsebuje 1,5 mg benzidaminijevega klorida, kar ustreza 1,34 mg benzidamina. V enem razpršku je 0,17 ml raztopine. En razpršek vsebuje 0,255 mg benzidaminijevega klorida, kar ustreza 0,2278 mg benzidamina. **Sestava 3 mg/ml:** 1 ml raztopine vsebuje 3 mg benzidaminijevega klorida, kar ustreza 2,68 mg benzidamina. V enem razpršku je 0,17 ml raztopine. En razpršek vsebuje 0,51 mg benzidaminijevega klorida, kar ustreza 0,4556 mg benzidamina. **Terapevtske indikacije:** Samozdravljenje: Lajšanje bolečine in oteklin pri vnetju v ustni votlini in žrelu, ki so lahko posledica okužb in stanj po operaciji. Po nasvetu in navodilu zdravnika: Lajšanje bolečine in oteklin v ustni votlini in žrelu, ki so posledica radiomukozitisa. **Odmerjanje in način uporabe:** Odmerjanje 1,5 mg/ml: Odrasli: 4 do 8 razpršk 2- do 6-krat na dan (vsake 1,5 do 3 ure). Pediatrična populacija: Mladostniki, stari od 12 do 18 let: 4-8 razpršk 2- do 6-krat na dan. Otroci od 6 do 12 let: 4 razprški 2- do 6-krat na dan. Otroci, mlajši od 6 let: 1 razpršek na 4 kg telesne mase; do največ 4 razprške 2- do 6-krat na dan. Odmerjanje 3 mg/ml: Uporaba 2- do 6-krat na dan (vsake 1,5 do 3 ure). Odrasli: 2 do 4 razprški 2- do 6-krat na dan. Pediatrična populacija: Mladostniki, stari od 12 do 18 let: 2 do 4 razprški 2- do 6-krat na dan. Otroci od 6 do 12 let: 2 razprška 2- do 6-krat na dan. Otroci, mlajši od 6 let: 1 razpršek na 8 kg telesne mase; do največ 2 razprška 2- do 6-krat na dan. Starejši bolniki, bolniki z jetrno okvaro in bolniki z ledvično okvaro: Uporabo oralnega pršila z benzidaminijevim kloridom se svetuje pod nadzorom zdravnika. Način uporabe: Za orofaringealno uporabo. Zdravilo se razpriši v usta in žrelo. **Kontraindikacije:** Preobčutljivost na učinkovino ali katero koli pomožno snov. **Posebna opozorila in previdnostni ukrepi:** Če se simptomi v treh dneh ne izboljšajo, se mora bolnik posvetovati z zdravnikom ali zobozdravnikom, kot je primerno. Benzidamin ni priporočljiv za bolnike s preobčutljivostjo nasalicilno kislino ali druga nesteroidna protivnetna zdravila. Pri bolnikih, ki imajo ali so imeli bronhialno astmo, lahko pride do bronhospazma, zato je potrebna previdnost. To zdravilo vsebuje majhne količine etanola (alkohola), in sicer manj kot 100 mg na odmerek. To zdravilo vsebuje metilparahidroksibenzoat (E218). Lahko povzroči alergijske reakcije (lahko zapoznele). Zdravilo z jakostjo 3 mg/ml vsebuje makrogolglicerol hidroksistearat 40. Lahko povzroči želodčne težave in drisko. **Medsebojno delovanje z drugimi zdravili in druge oblike interakcij:** Študij medsebojnega delovanja niso izvedli. **Nosečnost in dojenje:** O uporabi benzidamina pri nosečnicah in doječih ženskah ni zadostnih podatkov. Uporaba zdravila med nosečnostjo in dojenjem ni priporočljiva. **Vpliv na sposobnost vožnje in upravljanja strojev:** Zdravilo v priporočenem odmerku nima vpliva na sposobnost vožnje in upravljanja strojev. **Neželeni učinki:** Neznana pogostnost (ni mogoče oceniti iz razpoložljivih podatkov): anafilaktične reakcije, preobčutljivostne reakcije, odrevenelost, laringospazem, suha usta, navzea in bruhanje, angioedem, fotosenzitivnost, pekoč občutek v ustih. Neposredno po uporabi se lahko pojavi občutek odrevenelosti v ustih in v žrelu. Ta učinek se pojavi zaradi načina delovanja zdravila in po kratkem času izgine. **Način in režim izdaje zdravila:** BRp-Izdaja zdravila je brez recepta v lekarnah in specializiranih prodajalnah.

**Imetnik dovoljenja za promet:** Aziende Chimiche Riunite Angelini Francesco – A.C.R.A.F. S.p.A., Viale Amelia 70, 00181 Rim, Italija **Datum zadnje revizije besedila:** 14. 10. 2019

Pred svetovanjem ali izdajo preberite celoten Povzetek glavnih značilnosti zdravila.

Samo za strokovno javnost.

Datum priprave informacije: november 2019

Odgovoren za trženje: Bonifar d.o.o.

ANGELINI

PR/BSI/BEN/2019/012

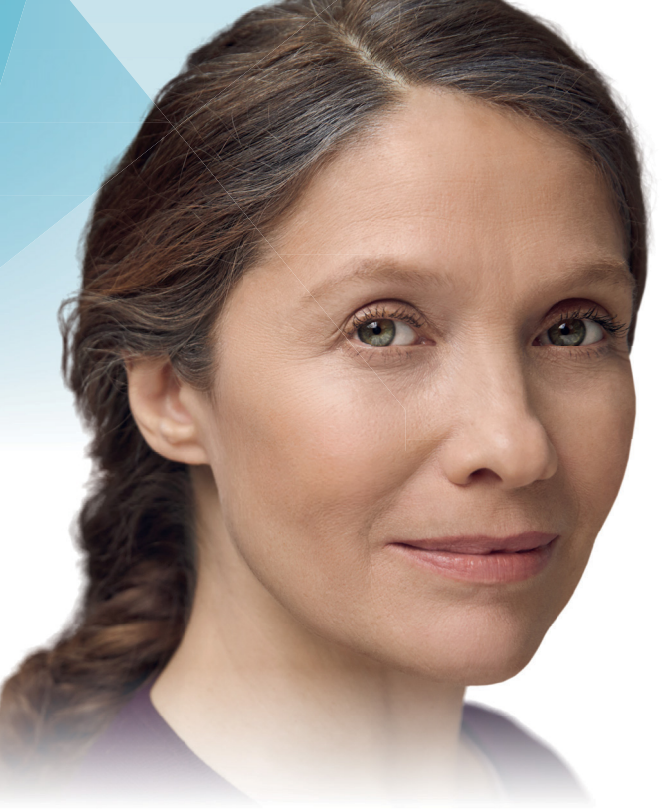

vsak dan

Verzenios®

abemaciklib

dvakrat na dan

# EDINI

## zaviralec CDK4 & 6, ki se jemlje NEPREKINJENO VSAK DAN, 2x NA DAN[1, 2, 3]

**SKRAJŠAN POVZETEK GLAVNIH ZNAČILNOSTI ZDRAVILA**

▼Za to zdravilo se izvaja dodatno spremljanje varnosti. Tako bodo hitreje na voljo nove informacije o njegovi varnosti. Zdravstvene delavce naprošamo, da poročajo o katerem koli domnevnem neželenem učinku zdravila. Glejte poglavje 4.8, kako poročati o neželenih učinkih.
**IME ZDRAVILA:** Verzenios 50 mg/100 mg/150 mg filmsko obložene tablete **KAKOVOSTNA IN KOLIČINSKA SESTAVA:** Ena filmsko obložena tableta vsebuje 50 mg/100 mg/150 mg abemaciklib. Ena filmsko obložena tableta vsebuje 14 mg/28 mg/42 mg laktoze (v obliki monohidrata). **Terapevtske indikacije:** Zdravilo Verzenios je indicirano za zdravljenje žensk z lokalno napredovalim ali metastatskim, na hormonske receptorje (HR – *Hormone Receptor*) pozitivnim in na receptorje humanega epidermalnega rastnega faktorja 2 (HER2 – *Human Epidermal Growth Factor Receptor 2*) negativnim rakom dojk v kombinaciji z zaviralcem aromataze ali s fulvestrantom kot začetnim endokrinim zdravljenjem ali pri ženskah, ki so prejele predhodno endokrino zdravljenje. Pri ženskah v pred- in perimenopavzi je treba endokrino zdravljenje kombinirati z agonistom gonadoliberina (LHRH – *Luteinizing Hormone–Releasing Hormone*). **Odmerjanje in način uporabe:** Zdravljenje z zdravilom Verzenios mora uvesti in nadzorovati zdravnik, ki ima izkušnje z uporabo zdravil za zdravljenje rakavih bolezni. *Zdravilo Verzenios v kombinaciji z endokrinim zdravljenjem:* Priporočeni odmerek abemaciklib je 150 mg dvakrat na dan, kadar se uporablja v kombinaciji z endokrinim zdravljenjem. Zdravilo Verzenios je treba jemati, dokler ima bolnica od zdravljenja klinično korist ali do pojava nesprejemljive toksičnosti. Če bolnica bruha ali izpusti odmerek zdravila Verzenios, ji je treba naročiti, da naj naslednji odmerek vzame ob predvidenem času; dodatnega odmerka ne sme vzeti. Obvladovanje nekaterih neželenih učinkov lahko zahteva prekinitev in/ali zmanjšanje odmerka. Zdravljenje z abemaciklibom prekinite v primeru povišanja vrednosti AST in/ali ALT >3 x ZMN SKUPAJ s celokupnim bilirubinom > 2,0 x ZMN v odsotnosti holestaze ter pri bolnicah z intersticijsko pljučno boleznijo (ILD)/pnevmonitis stopnje 3 ali 4. Sočasni uporabi močnih zaviralcev CYP3A4 se je treba izogibati. Če se uporabi močnih zaviralcev CYP3A4 ni mogoče izogniti, je treba odmerek abemaciklib znižati na 100 mg dvakrat na dan. Pri bolnicah, pri katerih je bil odmerek znižan na 100 mg abemaciklib dvakrat na dan in pri katerih se sočasnemu dajanju močnega zaviralca CYP3A4 ni mogoče izogniti, je treba odmerek abemaciklib dodatno znižati na 50 mg dvakrat na dan. Pri bolnicah, pri katerih je bil odmerek znižan na 50 mg abemaciklib dvakrat na dan in pri katerih se sočasnemu dajanju močnega zaviralca CYP3A4 ni mogoče izogniti, je mogoče z odmerkom abemaciklib nadaljevati ob natančnem spremljanju znakov toksičnosti. Alternativno je mogoče odmerek abemaciklib znižati na 50 mg enkrat na dan ali prekiniti dajanje abemaciklib. Če je uporaba zaviralca CYP3A4 prekinjena, je treba odmerek abemaciklib povečati na odmerek, kakršen je bil pred uvedbo zaviralca CYP3A4 (po 3–5 razpolovnih časih zaviralca CYP3A4). Prilagajanje odmerka glede na starost in pri bolnicah z blago ali zmerno ledvično okvaro ter z blago (Child Pugh A) ali zmerno (Child Pugh B) jetrno okvaro ni potrebno. Pri dajanju abemaciklib bolnicam s hudo ledvično okvaro sta potrebna previdnost in skrbno spremljanje glede znakov toksičnosti. Način uporabe: Zdravilo Verzenios je namenjeno za peroralno uporabo. Odmerek se lahko vzame s hrano ali brez nje. Zdravilo se ne sme jemati z grenivko ali grenivkinim sokom. Bolnice naj odmerke vzamejo vsak dan ob približno istem času. Tableto je treba zaužiti celo (bolnice je pred zaužitjem ne smejo gristi, drobiti ali deliti). **Kontraindikacije:** Preobčutljivost na učinkovino ali katero koli pomožno snov. **Posebna opozorila in previdnostni ukrepi:** Pri bolnicah, ki so prejemale abemaciklib, so poročali o nevtropeniji, o večji pogostnosti okužb kot pri bolnicah, zdravljenih s placebom in endokrinim zdravljenjem, o povečanih vrednostih ALT in AST. Pri bolnicah, pri katerih se pojavi nevtropenija stopnje 3 ali 4, je priporočljivo prilagoditi odmerek. Bolnice je treba spremljati za znake in simptome globoke venske tromboze in pljučne embolije ter jih zdraviti, kot je medicinsko utemeljeno. Glede na povečanje vrednosti ALT ali AST je mogoče potrebna prilagoditev odmerka. Driska je najpogostejši neželeni učinek. Bolnice je treba ob prvem znaku tekočega blata začeti zdraviti z antidiaroiki, kot je loperamid, povečati vnos peroralnih tekočin in obvestiti zdravnika. Sočasni uporabi induktorjev CYP3A4 se je treba izogibati zaradi tveganja za zmanjšano učinkovitost abemaciklib. Bolnice z redkimi dednimi motnjami, kot so intoleranca za galaktozo, popolno pomanjkanje laktaze ali malapsorpcija glukoze/galaktoze, tega zdravila ne smejo jemati. Bolnice spremljajte glede pljučnih simptomov, ki kažejo na ILD/pnevmonitis, in jih ustrezno zdravite. Glede na stopnjo ILD/pnevmonitisa je morda potrebno prilagajanje odmerka abemaciklib. **Medsebojno delovanje z drugimi zdravili in druge oblike interakcij:** Abemaciklib se primarno presnavlja s CYP3A4. Sočasna uporaba abemaciklib in zaviralcev CYP3A4 lahko poveča plazemsko koncentracijo abemaciklib. Uporabi močnih zaviralcev CYP3A4 sočasno z abemaciklibom se je treba izogibati. Če je močne zaviralce CYP3A4 treba dajati sočasno, je treba odmerek abemaciklib zmanjšati, nato pa bolnico skrbno spremljati glede toksičnosti. Pri bolnicah, zdravljenih z zmernimi ali šibkimi zaviralci CYP3A4, ni potrebno prilagajanje odmerka, vendar jih je treba skrbno spremljati za znake toksičnosti. Sočasni uporabi močnih induktorjev CYP3A4 (vključno, vendar ne omejeno na: karbamazepin, fenitoin, rifampicin in šentjanževko) se je treba izogibati zaradi tveganja za zmanjšano učinkovitost abemaciklib. Abemaciklib in njegovi glavni aktivni presnovki zavirajo prenašalce v ledvicah, in sicer kationski organski prenašalec 2 (OCT2) ter prenašalca MATE1. *In vivo* lahko pride do medsebojnega delovanja abemaciklib in klinično pomembnih substratov teh prenašalcev, kot je dofelitid ali kreatinin. Trenutno ni znano, ali lahko abemaciklib zmanjša učinkovitost sistemskih hormonskih kontraceptivov, zato se ženskam, ki uporabljajo sistemske hormonske kontraceptive, svetuje, da hkrati uporabljajo tudi mehansko metodo. **Neželeni učinki:** Najpogostejši neželeni učinki so driska, okužbe, nevtropenija, anemija, utrujenost, navzea, bruhanje in zmanjšanje apetita. *Zelo pogosti:* okužbe, nevtropenija, levkopenija, anemija, trombocitopenija, driska, bruhanje, navzea, zmanjšanje apetita, disgevzija, omotica, alopecija, pruritus, izpuščaj, utrujenost, pireksija, povečana vrednost alanin-aminotransferaze, povečana vrednost aspartat-aminotransferaze *Pogosti:* limfopenija, povečano solzenje, venska trombembolija, intersticijska pljučna bolezen (ILD)/pnevmonitis, suha koža, mišična šibkost *Občasni:* febrilna nevtropenija **Rok uporabnosti:** 3 leta **Posebna navodila za shranjevanje:** Za shranjevanje zdravila niso potrebna posebna navodila. **Imetnik dovoljenja za promet z zdravilom**: Eli Lilly Nederland B.V., Papendorpseweg 83, 3528BJ, Utrecht, Nizozemska. Datum prve odobritve dovoljenja za promet: 27. september 2018 **Datum zadnje revizije besedila**: 16.1.2020 **Režim izdaje:** Rp/Spec - Predpisovanje in izdaja zdravila je le na recept zdravnika specialista ustreznega področja medicine ali od njega pooblaščenega zdravnika.


**Reference:**
**1.** Povzetek glavnih značilnosti zdravila Verzenios. Datum zadnje revizije besedila: 16.1.2020. **2.** Povzetek glavnih značilnosti zdravila Ibrance. Dostop preverjen 10.4.2020.
**3.** Povzetek glavnih značilnosti zdravila Kisqali. Dostop preverjen 10.4.2020.


**Pomembno:** Predpisovanje in izdaja zdravila je le na recept zdravnika specialista ustreznega področja medicine ali od njega pooblaščenega zdravnika. Pred predpisovanjem zdravila Verzenios si preberite zadnji veljavni Povzetek glavnih značilnosti zdravil. Podrobne informacije o zdravilu so objavljene na spletni strani Evropske agencije za zdravila http://www.ema.europa.eu


Eli Lilly farmacevtska družba, d.o.o., Dunajska cesta 167, 1000 Ljubljana, telefon 01 / 580 00 10, faks 01 / 569 17 05
PP-AL-SI-0059, 20.04.2020, Samo za strokovno javnost.


Lilly

# KEYTRUDA®
(pembrolizumab, MSD)


Referenca: 1. Keytruda EU SmPC

**SKRAJŠAN POVZETEK GLAVNIH ZNAČILNOSTI ZDRAVILA • Pred predpisovanjem, prosimo, preberite celoten Povzetek glavnih značilnosti zdravila! • Ime zdravila:** KEYTRUDA 25 mg/ml koncentrat za raztopino za infundiranje vsebuje pembrolizumab. **Terapevtske indikacije:** Zdravilo KEYTRUDA je kot samostojno zdravljenje indicirano za zdravljenje: napredovalega (neoperabilnega ali metastatskega) melanoma pri odraslih; za adjuvantno zdravljenje odraslih z melanomom v stadiju III, ki se je razširil na bezgavke, po popolni kirurški odstranitvi; metastatskega nedrobnoceličnega pljučnega raka (NSCLC) v prvi liniji zdravljenja pri odraslih, ki imajo tumorje z ≥ 50 % izraženostjo PD-L1 (TPS) in brez pozitivnih tumorskih mutacij EGFR ali ALK; lokalno napredovalega ali metastatskega NSCLC pri odraslih, ki imajo tumorje z ≥ 1 % izraženostjo PD-L1 (TPS) in so bili predhodno zdravljeni z vsaj eno shemo kemoterapije, bolniki s pozitivnimi tumorskimi mutacijami EGFR ali ALK so pred prejemom zdravila KEYTRUDA morali prejeti tudi tarčno zdravljenje; odraslih in pediatričnih bolnikov, starih 3 leta ali več, s ponovljenim ali neodzivnim klasičnim Hodgkinovim limfomom (cHL), pri katerih avtologna presaditev matičnih celic (ASCT) ni bila uspešna, ali po najmanj dveh predhodnih zdravljenjih kadar ASCT ne pride v poštev kot možnost zdravljenja; lokalno napredovalega ali metastatskega urotelijskega raka pri odraslih, predhodno zdravljenih s kemoterapijo, ki je vključevala platino; lokalno napredovalega ali metastatskega urotelijskega raka pri odraslih, ki niso primerni za zdravljenje s kemoterapijo, ki vsebuje cisplatin in imajo tumorje z izraženostjo PD-L1 ≥ 10, ocenjeno s kombinirano pozitivno oceno (CPS); ponovljenega ali metastatskega ploščatoceličnega raka glave in vratu (HNSCC) pri odraslih, ki imajo tumorje z ≥ 50 % izraženostjo PD-L1 (TPS), in pri katerih je bolezen napredovala med zdravljenjem ali po zdravljenju s kemoterapijo, ki je vključevala platino in za prvo linijo zdravljenja metastatskega kolorektalnega raka z visoko mikrosatelitsko nestabilnostjo (MSI-H – microsatellite instability-high) ali s pomanjkljivim popravljanjem neujemanja pri podvojevanju DNA (dMMR - mismatch repair deficient) pri odraslih. Zdravilo KEYTRUDA je kot samostojno zdravljenje ali v kombinaciji s kemoterapijo s platino in 5-fluorouracilom (5-FU) indicirano za prvo linijo zdravljenja metastatskega ali neoperabilnega ponovljenega ploščatoceličnega raka glave in vratu pri odraslih, ki imajo tumorje z izraženostjo PD-L1 s CPS ≥ 1. Zdravilo KEYTRUDA je v kombinaciji s pemetreksedom in kemoterapijo na osnovi platine indicirano za prvo linijo zdravljenja metastatskega neploščatoceličnega NSCLC pri odraslih, pri katerih tumorji nimajo pozitivnih mutacij EGFR ali ALK; v kombinaciji s karboplatinom in bodisi paklitakselom bodisi nab-paklitakselom je indicirano za prvo linijo zdravljenja metastatskega ploščatoceličnega NSCLC pri odraslih; v kombinaciji z aksitinibom je indicirano za prvo linijo zdravljenja napredovalega raka ledvičnih celic (RCC) pri odraslih. **Odmerjanje in način uporabe:** Testiranje PD-L1 pri bolnikih z NSCLC, urotelijskim rakom ali HNSCC: Za samostojno zdravljenje z zdravilom KEYTRUDA je priporočljivo opraviti testiranje izraženosti PD-L1 tumorja z validirano preiskavo, da izberemo bolnike z NSCLC ali predhodno nezdravljenim urotelijskim rakom. Bolnike s HNSCC je treba za samostojno zdravljenje z zdravilom KEYTRUDA ali v kombinaciji s kemoterapijo s platino in 5-fluorouracilom (5-FU) izbrati na podlagi izraženosti PD-L1, potrjene z validirano preiskavo. Testiranje MSI-H/dMMR pri bolnikih s CRC: Za samostojno zdravljenje z zdravilom KEYTRUDA je priporočljivo opraviti testiranje MSI-H/dMMR statusa tumorja z validirano preiskavo, da se izbere bolnike s CRC. Odmerjanje: Priporočeni odmerek zdravila KEYTRUDA za samostojno zdravljenje pri odraslih je bodisi 200 mg na 3 tedne ali 400 mg na 6 tednov, apliciran z intravensko infuzijo v 30 minutah. Priporočeni odmerek zdravila KEYTRUDA za samostojno zdravljenje pri pediatričnih bolnikih s cHL, starih 3 leta ali več, je 2 mg/kg telesne mase (do največ 200 mg) na 3 tedne, apliciran z intravensko infuzijo v 30 minutah. Priporočeni odmerek za kombinirano zdravljenje pri odraslih je 200 mg na 3 tedne, apliciran z intravensko infuzijo v 30 minutah. Za uporabo v kombinaciji glejte povzetke glavnih značilnosti sočasno uporabljenih zdravil. Če se uporablja kot del kombiniranega zdravljenja skupaj z intravensko kemoterapijo, je treba zdravilo KEYTRUDA aplicirati prvo. Bolnike je treba zdraviti do napredovanja bolezni ali nesprejemljivih toksičnih učinkov. Pri adjuvantnem zdravljenju melanoma je treba zdravilo uporabljati do ponovitve bolezni, pojava nesprejemljivih toksičnih učinkov oziroma mora zdravljenje trajati do enega leta. Če je aksitinib uporabljen v kombinaciji s pembrolizumabom, se lahko razmisli o povečanju odmerka aksitiniba nad začetnih 5 mg v presledkih šest tednov ali več. Pri bolnikih starih ≥ 65 let, bolnikih z blago do zmerno okvaro ledvic, bolnikih z blago okvaro jeter prilagoditev odmerka ni potrebna. Odložitev odmerka ali ukinitev zdravljenja: Zmanjšanje odmerka zdravila KEYTRUDA ni priporočljivo. Za obvladovanje neželenih učinkov je treba uporabo zdravila KEYTRUDA zadržati ali ukiniti, prosimo, glejte celoten Povzetek glavnih značilnosti zdravila. **Kontraindikacije:** Preobčutljivost na učinkovino ali katero koli pomožno snov. **Povzetek posebnih opozoril, previdnostnih ukrepov, interakcij in neželenih učinkov:** Imunsko pogojeni neželeni učinki (pnevmonitis, kolitis, hepatitis, nefritis, endokrinopatije, neželeni učinki na kožo in drugi): Pri bolnikih, ki so prejemali pembrolizumab, so se pojavili imunsko pogojeni neželeni učinki, vključno s hudimi in smrtnimi primeri. Večina imunsko pogojenih neželenih učinkov, ki so se pojavili med zdravljenjem s pembrolizumabom, je bila reverzibilnih in so jih obvladali s prekinitvami uporabe pembrolizumaba, uporabo kortikosteroidov in/ali podporno oskrbo. Pojavijo se lahko tudi po zadnjem odmerku pembrolizumaba in hkrati prizadanejo več organskih sistemov. V primeru suma na imunsko pogojene neželene učinke je treba poskrbeti za ustrezno oceno za potrditev etiologije oziroma izključitev drugih vzrokov. Glede na izrazitost neželenega učinka je treba zadržati uporabo pembrolizumaba in uporabiti kortikosteroide – za natančna navodila, prosimo, glejte Povzetek glavnih značilnosti zdravila Keytruda. Zdravljenje s pembrolizumabom lahko poveča tveganje za zavrnitev pri prejemnikih presadkov čvrstih organov. Pri bolnikih, ki so prejemali pembrolizumab, so poročali o hudih z infuzijo povezanih reakcijah, vključno s preobčutljivostjo in anafilaksijo. Pembrolizumab se iz obtoka odstrani s katabolizmom, zato presnovnih medsebojnih delovanj zdravil ni pričakovati. Uporabi sistemskih kortikosteroidov ali imunosupresivov pred uvedbo pembrolizumaba se je treba izogibati, ker lahko vplivajo na farmakodinamično aktivnost in učinkovitost pembrolizumaba. Vendar pa je kortikosteroide ali druge imunosupresivne mogoče uporabiti za zdravljenje imunsko pogojenih neželenih učinkov. Kortikosteroide je mogoče uporabiti tudi kot premedikacijo, če je pembrolizumab uporabljen v kombinaciji s kemoterapijo, kot antiemetično profilakso in/ali za ublažitev neželenih učinkov, povezanih s kemoterapijo. Ženske v rodni dobi morajo med zdravljenjem s pembrolizumabom in vsaj še 4 mesece po zadnjem odmerku pembrolizumaba uporabljati učinkovito kontracepcijo, med nosečnostjo in dojenjem se ga ne sme uporabljati. Varnost pembrolizumaba pri samostojnem zdravljenju so v kliničnih študijah ocenili pri 6.185 bolnikih z napredovalim melanomom, kirurško odstranjenim melanomom v stadiju III (adjuvantno zdravljenje), NSCLC, cHL, urotelijskim rakom, HNSCC ali CRC s štirimi odmerki (2 mg/kg na 3 tedne, 200 mg na 3 tedne in 10 mg/kg na 2 ali 3 tedne). V tej populaciji bolnikov je mediani čas opazovanja znašal 7,6 mesece (v razponu od 1 dneva do 47 mesecev), najpogostejši neželeni učinki zdravljenja s pembrolizumabom so bili utrujenost (32 %), navzea (21 %) in diareja (21 %). Večina poročanih neželenih učinkov pri samostojnem zdravljenju je bila po izrazitosti 1. ali 2. stopnje. Najresnejši neželeni učinki so bili imunsko pogojeni neželeni učinki in hude z infuzijo povezane reakcije. Varnost pembrolizumaba pri kombiniranem zdravljenju s kemoterapijo so ocenili pri 1.067 bolnikih NSCLC ali HNSCC, ki so v kliničnih študijah prejemali pembrolizumab v odmerkih 200 mg, 2 mg/kg ali 10 mg/kg na vsake 3 tedne. V tej populaciji bolnikov so bili najpogostejši neželeni učinki naslednji: anemija (50 %), navzea (50 %), utrujenost (37 %), zaprtost (35%), diareja (30 %), nevtropenija (30 %), zmanjšanje apetita (28 %) in bruhanje (25 %). Pri kombiniranem zdravljenju s pembrolizumabom je pri bolnikih z NSCLC pojavnost neželenih učinkov 3. do 5. stopnje znašala 67 %, pri zdravljenju samo s kemoterapijo pa 66 %, pri kombiniranem zdravljenju s pembrolizumabom pri bolnikih s HNSCC 85 % in pri zdravljenju s kemoterapijo v kombinaciji s cetuksimabom 84 %. Varnost pembrolizumaba v kombinaciji z aksitinibom so ocenili v klinični študiji pri 429 bolnikih z napredovalim rakom ledvičnih celic, ki so prejemali 200 mg pembrolizumaba na 3 tedne in 5 mg aksitiniba dvakrat na dan. V tej populaciji bolnikov so bili najpogostejši neželeni učinki diareja (54 %), hipertenzija (45 %), utrujenost (38 %), hipotiroidizem (35 %), zmanjšan apetit (30 %), sindrom palmarno-plantarne eritrodisestezije (28 %), navzea (28 %), zvišanje vrednosti ALT (27 %), zvišanje vrednosti AST (26 %), disfonija (25 %), kašelj (21 %) in zaprtost (21 %). Pojavnost neželenih učinkov 3. do 5. stopnje je bila med kombiniranim zdravljenjem s pembrolizumabom 76 % in pri zdravljenju s sunitinibom samim 71 %. Za celoten seznam neželenih učinkov, prosimo, glejte celoten Povzetek glavnih značilnosti zdravila. **Način in režim izdaje zdravila:** H – Predpisovanje in izdaja zdravila je le na recept, zdravilo se uporablja samo v bolnišnicah. **Imetnik dovoljenja za promet z zdravilom:** Merck Sharp & Dohme B.V. , Waarderweg 39, 2031 BN Haarlem, Nizozemska.

MSD **Merck Sharp & Dohme inovativna zdravila d.o.o.,**
Šmartinska cesta 140, 1000 Ljubljana,
tel: +386 1/ 520 42 01, fax: +386 1/ 520 43 50;
Pripravljeno v Sloveniji, april 2021; SI-KEY-00231 EXP: 04/2023
**Samo za strokovno javnost.**
**H - Predpisovanje in izdaja zdravila je le na recept, zdravilo pa se uporablja samo v bolnišnicah. Pred predpisovanjem, prosimo, preberite celoten Povzetek glavnih značilnosti zdravila Keytruda, ki je na voljo pri naših strokovnih sodelavcih ali na lokalnem sedežu družbe.**

Roche

TECENTRIQ▼ + AVASTIN®

# UČINKOVITOST, KI OMOGOČA DALJŠE ŽIVLJENJE

Prva in edina odobrena kombinacija z zaviralcem imunskih nadzornih točk za zdravljenje bolnikov z neresektabilnim hepatocelularnim karcinomom, ki je dokazala izboljšanje preživetja v primerjavi s sorafenibom.

TECENTRIQ®
atezolizumab
POVEZANI Z NAMENOM

▼Za to zdravilo se izvaja dodatno spremljanje varnosti.
Tako bodo hitreje na voljo nove informacije o njegovi varnosti. Zdravstvene delavce naprošamo, da poročajo o katerem koli domnevnem neželenem učinku zdravila.
Kako poročati o neželenih učinkih, si poglejte skrajšani povzetek glavnih značilnosti zdravila pod "Poročanje o domnevnih neželenih učinkih".

**Ime zdravila:** Tecentriq 1200 mg koncentrat za raztopino za infundiranje. **Kakovostna in količinska sestava:** ena 20-ml viala s koncentratom vsebuje 1200 mg atezolizumaba. Po redčenju je končna koncentracija razredčene raztopine med 3,2 mg/ml in 16,8 mg/ml. Atezolizumab je humanizirano monoklonsko protitelo IgG1 z inženirsko obdelano domeno Fc, ki je pridobljeno iz celic jajčnika kitajskega hrčka s tehnologijo rekombinantne DNA in deluje na ligand za programirano celično smrt 1 (PD-L1). **Terapevtske indikacije:** Urotelijski karcinom: Zdravilo Tecentriq je kot monoterapija indicirano za zdravljenje odraslih bolnikov z lokalno napredovalim ali razsejanim urotelijskim karcinomom, ki: so bili predhodno zdravljeni s kemoterapijo na osnovi platine ali niso primerni za zdravljenje s cisplatinom in katerih tumorji izražajo PD-L1 v ≥ 5 %. Nedrobnocelični rak pljuč: Zdravilo Tecentriq je v kombinaciji z bevacizumabom, paklitakselom in karboplatinom indicirano kot prva linija zdravljenja odraslih bolnikov z razsejanim nepleščatoceličnim nedrobnoceličnim rakom pljuč (NDRP). Pri bolnikih z EGFR mutiranim ali ALK pozitivnim NDRP je zdravilo Tecentriq v kombinaciji z bevacizumabom, paklitakselom in karboplatinom indicirano le, ko so izčrpana ustrezna tarčna zdravljenja. Zdravilo Tecentriq je kot monoterapija indicirano za zdravljenje odraslih bolnikov z lokalno napredovalim ali razsejanim NDRP, ki so bili predhodno zdravljeni s kemoterapijo. Bolniki z EGFR mutiranim ali ALK pozitivnim NDRP morajo pred uvedbo zdravila Tecentriq prejeti tudi tarčna zdravljenja. Zdravilo Tecentriq je v kombinaciji z nab-paklitakselom in karboplatinom indicirano kot prva linija zdravljenja odraslih bolnikov z razsejanim nepleščatoceličnim NDRP, ki ni EGFR mutiran ali ALK pozitiven. Drobnocelični rak pljuč: Zdravilo Tecentriq je v kombinaciji s karboplatinom in etopozidom indicirano kot prva linija zdravljenja odraslih bolnikov z razsejanim drobnoceličnim rakom pljuč (DRP). Hepatocelularni karcinom: Zdravilo Tecentriq je v kombinaciji z bevacizumabom indicirano za zdravljenje odraslih bolnikov z neresektabilnim hepatocelularnim karcinomom (HCC), ki predhodno še niso prejemali sistemskega zdravljenja. **Odmerjanje in način uporabe:** Zdravilo Tecentriq morajo uvesti in nadzorovati zdravniki z izkušnjami pri zdravljenju raka. Testiranje PD-L1 pri bolnikih z urotelijskim karcinomom: bolnike s predhodno nezdravljenim urotelijskim karcinomom je treba za zdravljenje izbrati na podlagi tumorskega izražanja PD-L1, potrjenega z validirano preiskavo. Odmerjanje: *Zdravilo Tecentriq v monoterapiji:* priporočeni odmerek zdravila Tecentriq je 1200 mg intravensko na vsake tri tedne. *Zdravilo Tecentriq v kombinaciji: Prva linija zdravljenja neploščatoceličnega NDRP: Zdravilo Tecentriq v kombinaciji z bevacizumabom, paklitakselom in karboplatinom:* Med uvodno fazo je priporočeni odmerek zdravila Tecentriq 1200 mg v intravenski infuziji, čemur sledijo bevacizumab, paklitaksel in nato karboplatin na tri tedne, skupno štiri ali šest ciklov. Uvodni fazi zdravljenja sledi faza vzdrževanja brez kemoterapije, med katero se na tri tedne uporabi zdravilo Tecentriq v odmerku 1200 mg v intravenski infuziji, ki mu sledi bevacizumab. *Zdravilo Tecentriq v kombinaciji z nab-paklitakselom in karboplatinom:* Med uvodno fazo je priporočeni odmerek zdravila Tecentriq 1200 mg v intravenski infuziji, čemur sledijo nab-paklitaksel in nato karboplatin na vsake tri tedne, skupno štiri ali šest ciklov. Uvodni fazi zdravljenja sledi faza vzdrževanja brez kemoterapije, med katero se zdravilo Tecentriq v odmerku 1200 mg v intravenski infuziji aplicira na tri tedne. *Prva linija zdravljenja razsejanega DRP: Zdravilo Tecentriq v kombinaciji s karboplatinom in etopozidom:* Med uvodno fazo je 1. dan cikla priporočeni odmerek zdravila Tecentriq 1200 mg v intravenski infuziji, čemur sledita najprej karboplatin in nato etopozid v intravenski infuziji. Etopozid v intravenski infuziji se aplicira tudi 2. in 3. dan. Ta shema se aplicira na vsake tri tedne v skupno štirih ciklih. Uvodni fazi sledi faza vzdrževanja brez kemoterapije, med katero se zdravilo Tecentriq v odmerku 1200 mg v intravenski infuziji aplicira na tri tedne. *Hepatocelularni karcinom: Zdravilo Tecentriq v kombinaciji z bevacizumabom:* Priporočeni odmerek zdravila Tecentriq je 1200 mg, ki mu sledi bevacizumab 15 mg/kg telesne mase, dan z intravensko infuzijo vsake 3 tedne. *Trajanje zdravljenja:* zdravljenje z zdravilom Tecentriq je priporočljivo nadaljevati, dokler je klinično koristno ali dokler se ne pojavijo neobvladljivi toksični učinki. *Prilagoditev odmerka med zdravljenjem:* odmerkov zdravila Tecentriq ni priporočljivo zmanjševati. *Zapoznitev odmerka ali prenehanje uporabe* glede na neželeni učinek je opisano v SmPC. Način uporabe: zdravilo Tecentriq je namenjeno za intravensko uporabo. Infuzij se ne sme dajati kot hiter intravenski odmerek ali bolus. Začetni odmerek zdravila Tecentriq je treba dati v 60 minutah. Če bolnik prvo infuzijo dobro prenese, je mogoče vse nadaljnje infuzije dati v 30 minutah. **Kontraindikacije:** Preobčutljivost na atezolizumab ali katero koli pomožno snov. **Posebna opozorila in previdnostni ukrepi:** Sledljivost: Za izboljšanje sledljivosti bioloških zdravil je treba lastniško ime in številko serije uporabljenega zdravila jasno zabeležiti v bolnikovi dokumentaciji. Imunsko pogojeni neželeni učinki: Večina imunsko pogojenih neželenih učinkov, ki so se pojavili med zdravljenjem z atezolizumabom, je bila po prekinitvi atezolizumaba in uvedbi kortikosteroidov in/ali podpornega zdravljenja reverzibilna. Opazili so imunsko pogojene neželene učinke, ki vplivajo na več kot en organski sistem. Imunsko pogojeni neželeni učinki, povezani z atezolizumabom, se lahko pojavijo po zadnjem odmerku atezolizumaba. Pri sumu na imunsko pogojene neželene učinke je treba opraviti temeljito oceno za potrditev etiologije oziroma izključitev drugih vzrokov. Glede na izrazitost neželenega učinka je treba uporabo atezolizumaba odložiti in uvesti kortikosteroide. Atezolizumab je treba trajno prenehati uporabljati pri vseh imunsko pogojenih neželenih učinkih 3. stopnje, ki se ponovijo, in pri vseh imunsko pogojenih neželenih učinkih 4. stopnje, z izjemo endokrinopatij, ki jih je mogoče nadzorovati z nadomestnimi hormoni. Bolnike je treba spremljati glede znakov in simptomov pnevmonitisa ter izključiti druge možne vzroke, razen imunsko pogojenega pnevmonitisa. Bolnike je treba spremljati glede znakov in simptomov hepatitisa. Vrednosti AST, ALT in bilirubina je treba spremljati pred začetkom zdravljenja z atezolizumabom, redno med zdravljenjem in kot je potrebno glede na klinično oceno. Bolnike je treba spremljati glede znakov in simptomov kolitisa in endokrinopatij, meningitisa ali encefalitisa. V primeru meningitisa ali encefalitisa je treba zdravljenje z atezolizumabom trajno ukiniti ne glede na njuno stopnjo. Bolnike je treba spremljati glede znakov in simptomov motoričnе in senzorične nevropatije. V primeru miastenijskega sindroma/miastenije gravis ali Guillain-Barrejevega sindroma je treba zdravljenje z atezolizumabom trajno prekiniti ne glede na njihovo stopnjo. Bolnike je treba nadzorovati glede znakov in simptomov, ki kažejo na akutni pankreatitis. Bolnike je treba nadzorovati glede znakov in simptomov, ki kažejo na miokarditis. Imunsko pogojeni nefritis: Bolnike je treba nadzorovati glede sprememb v delovanju ledvic. Bolnike je treba nadzorovati glede znakov in simptomov, ki kažejo na miozitis. Z infundiranjem povezane reakcije: pri zdravljenju z atezolizumabom so opažali z infundiranjem povezane reakcije. Pri bolnikih, ki imajo z infundiranjem povezane reakcije 1. ali 2. stopnje, je treba hitrost infundiranja zmanjšati ali zdravljenje prekiniti. Pri bolnikih, ki imajo z infundiranjem povezane reakcije 3. ali 4. stopnje, je treba zdravljenje z atezolizumabom trajno ukiniti. Bolniki, ki imajo z infundiranjem povezane reakcije 1. ali 2. stopnje, lahko še naprej prejemajo atezolizumab pod natančnim nadzorom; v poštev pride premedikacija z antipiretikom in antihistaminikom. Pri bolnikih, ki so prejemali atezolizumab, so poročali o imunsko pogojenih hudih kožnih neželenih učinkih, vključno s primeri Stevens-Johnsonovega sindroma (SJS) in toksične epidermalne nekrolize (TEN). Bolnike je treba spremljati glede sumov na hude kožne neželene učinke in izključiti druge vzroke. V primeru suma na hude kožne neželene učinke je treba bolnike napotiti k specialistu po nadaljnjo diagnozo in zdravljenje. Uporabo atezolizumaba je treba odložiti pri bolnikih s sumom na SJS ali TEN. Pri potrjenem SJS ali TEN je treba trajno prenehati z uporabo atezolizumaba. Bolniki, ki niso bili vključeni v klinična preskušanja: v klinična preskušanja niso bili vključeni bolniki z naslednjimi stanji: z anamnezo avtoimunske bolezni, pnevmonitisa, simptomatskimi možganskimi zasevki, okužbo z virusom HIV, hepatitisom B ali hepatitisom C, pomembnimi srčno-žilnimi boleznimi ter bolniki z nezadostnim hematološkim delovanjem in delovanjem končnih organov. Prav tako v klinična preskušanja niso bili vključeni bolniki, ki so bili v obdobju 28 dni pred vključitvijo v študijo cepljeni z živim ostabljenim cepivom, ki so v obdobju 4 tednov pred vključitvijo v študijo dobili sistemska imunostimulacijska sredstva ali v obdobju 2 tednov sistemska imunosupresivna zdravila ali so v obdobju 2 tednov pred začetkom Študijskega zdravljenja prejemali zdravljenje s peroralnimi ali intravenskimi antibiotiki. Kartica za bolnika: Zdravnik, ki predpiše zdravilo, se mora z bolnikom pogovoriti o tveganjih zdravljenja z zdravilom Tecentriq. Bolniku je treba dati kartico za bolnika in mu naročiti, naj jo ima vedno pri sebi. **Medsebojno delovanje z drugimi zdravili in druge oblike interakcij:** Formalnih študij farmakokinetičnega medsebojnega delovanja zdravil z atezolizumabom niso izvedli. Ker se atezolizumab odstrani iz obtoka s katabolizmom, ni pričakovati presnovnih medsebojnih delovanj med zdravili. Uporabi sistemskih kortikosteroidov ali imunosupresivov se je pred uvedbo atezolizumaba treba izogibati, ker tako vplivajo na farmakodinamično aktivnost in učinkovitost atezolizumaba. Vendar pa se sistemske kortikosteroide ali druge imunosupresive lahko uporabi po začetku zdravljenja z atezolizumabom za zdravljenje imunsko pogojenih neželenih učinkov. **Neželeni učinki:** *Informacije o varnosti atezolizumaba v monoterapiji:* najpogostejši neželeni učinki (> 10 %) so bili utrujenost, zmanjšan apetit, navzea, zvišana telesna temperatura, diareja, kašelj, izpuščaj, dispneja, mišično-skeletna bolečina, bolečina v hrbtu, bruhanje, srbenje, astenija, artralgija, okužba sečil in glavobol. *Varnost atezolizumaba v kombinaciji z drugimi učinkovinami:* najpogostejši neželeni učinki (> 20 %) so bili anemija, nevtropenija, navzea, utrujenost, trombocitopenija, diareja, izpuščaj, alopecija, zaprtost, zmanjšan apetit in periferna nevropatija. Poročanje o domnevnih neželenih učinkih: Poročanje o domnevnih neželenih učinkih zdravila po izdaji dovoljenja za promet je pomembno. Omogoča namreč stalno spremljanje razmerja med koristmi in tveganji zdravila. Od zdravstvenih delavcev se zahteva, da poročajo o katerem koli domnevnem neželenem učinku zdravila na: Javna agencija Republike Slovenije za zdravila in medicinske pripomočke, Sektor za farmakovigilanco, Nacionalni center za farmakovigilanco, Slovenčeva ulica 22, SI-1000 Ljubljana, Tel: +386 (0)8 2000 500, Faks: +386 (0)8 2000 510, e-pošta: h-farmakovigilanca@jazmp.si, spletna stran: www.jazmp.si. Za zagotavljanje sledljivosti zdravila je pomembno, da pri izpolnjevanju obrazca o domnevnih neželenih učinkih zdravila navedete številko serije biološkega zdravila. **Režim izdaje zdravila:** H. **Imetnik dovoljenja za promet:** Roche Registration GmbH, Emil-Barell-Strasse 1, 79639 Grenzach-Wyhlen, Nemčija. **Verzija: 2.0/21**

**Ime zdravila:** Avastin 25 mg/ml koncentrat za raztopino za infundiranje. **Kakovostna in količinska sestava:** En ml koncentrata vsebuje 25 mg bevacizumaba. Ena 4-ml viala vsebuje 100 mg bevacizumaba. Ena 16-ml viala vsebuje 400 mg bevacizumaba. **Terapevtske indikacije:** v kombinaciji s kemoterapijo na osnovi fluoropirimidina za zdravljenje odraslih bolnikov z metastatskim rakom debelega črevesa in danke; v kombinaciji s paklitakselom za prvo linijo zdravljenja odraslih bolnikov z metastatskim rakom dojk; v kombinaciji s kapecitabinom za prvo linijo zdravljenja odraslih bolnikov z metastatskim rakom dojk, pri katerih zdravljenje z drugimi možnostmi kemoterapije, vključno s taksani ali antraciklini, ni primerno. Bolniki, ki so v okviru adjuvantnega zdravljenja v zadnjih 12 mesecih prejeli sheme, ki so vsebovale taksan ali antraciklin, se ne smejo zdraviti z zdravilom Avastin v kombinaciji s kapecitabinom; kot dodatek kemoterapiji, osnovani na platini, za prvo linijo zdravljenja odraslih bolnikov z inoperabilnim, napredovalim, metastatskim ali ponavljajočim se nedrobnoceličnim rakom pljuč (NDRP), ki nima prevladujoče ploščatocelične histologije; v kombinaciji z erlotinibom za prvo linijo zdravljenja odraslih bolnikov z inoperabilnim, napredovalim, metastatskim ali ponavljajočim se neskvamoznim NDRP z EGFR-aktivirajočimi mutacijami; v kombinaciji z interferonom alfa-2a za prvo linijo zdravljenja odraslih bolnikov z napredovalim in/ali metastatskim rakom ledvičnih celic; v kombinaciji s karboplatinom in paklitakselom za prvo zdravljenje odraslih bolnic z napredovalim epiteljskim rakom jajčnikov (Klasifikacija FIGO: stadij III B, III C in IV), karcinomom jajcevodov ali primarnim peritonealnim karcinomom; v kombinaciji s karboplatinom in gemcitabinom ali v kombinaciji s karboplatinom in paklitakselom za zdravljenje odraslih bolnic, pri katerih je prišlo do prve ponovitve epitelijskega raka jajčnikov, karcinoma jajcevodov ali primarnega peritonealnega karcinoma, občutljivega na platino, ki se še niso zdravile z bevacizumabom ali drugimi zaviralci VEGF ali zdravili, ki delujejo na receptor VEGF; v kombinaciji s paklitakselom, topotekanom ali pegiliranim liposomalnim doksorubicinom za zdravljenje odraslih bolnic s ponovitvijo epitelijskega raka jajčnikov, karcinoma jajcevodov ali primarnega peritonealnega karcinoma, rezistentnega na platino, ki so predhodno prejele največ dve shemi kemoterapije, z bevacizumabom ali drugimi zaviralci VEGF ali zdravili, ki delujejo na receptor VEGF, pa se še niso zdravile; za zdravljenje odraslih bolnic z rakom materničnega vratu, pri katerih je bolezen prisotna tudi po zaključenem primarnem zdravljenju, se je ponovila ali je metastatska, v kombinaciji s paklitakselom in cisplatinom ali, alternativno, s paklitakselom in topotekanom pri bolnicah, ki ne morejo dobivati zdravljenja s platino. **Odmerjanje in način uporabe:** Zdravilo Avastin je treba dajati pod nadzorom zdravnika z izkušnjami pri uporabi zdravil za zdravljenje novotvorb. Zmanjšanje odmerka zaradi neželenih učinkov ni priporočljivo. Če je indicirano, zdravljenje dokončno ukinemo ali začasno prekinemo. *Način uporabe:* Začetni odmerek je treba dajati v obliki intravenske infuzije 90 minut. Če je bolnik prvi odmerek dobro prenesel, lahko naslednje infuzije dajemo 60 minut. Če je bolnik tudi 60-minutno infuzijo dobro prenesel, lahko vse naslednje infuzije dajemo 30 minut. Zdravila se ne sme dajati kot hitro infuzijo ali bolus. Infuzije zdravila Avastin se ne sme dajati ali mešati skupaj z raztopinami glukoze. *Metastatski rak debelega črevesa ali danke:* Priporočeni odmerek zdravila Avastin je 5 mg/kg ali 10 mg/kg telesne mase v enkratnem odmerku vsaka 2 tedna ali 7,5 mg/kg ali 15 mg/kg telesne mase v enkratnem odmerku vsake 3 tedne. *Metastatski rak dojk:* Priporočeni odmerek zdravila Avastin je 10 mg/kg telesne mase v enkratnem odmerku vsaka 2 tedna ali 15 mg/kg telesne mase v enkratnem odmerku vsake 3 tedne. *Neskvamozni NDRP v prvi liniji zdravljenja: al v kombinaciji s kemoterapijo na osnovi platine:* Zdravilo Avastin dodajamo k kemoterapiji, osnovani na platini, do 6 ciklov, nato pa ga dajemo samostojno. Priporočeni odmerek zdravila Avastin je 7,5 mg/kg ali 15 mg/kg telesne mase v enkratnem odmerku na 3 tedne. *b) z EGFR-aktivirajočimi mutacijami v kombinaciji z erlotinibom:* Pred začetkom zdravljenja je treba opraviti testiranje za določanje mutacij EGFR. Priporočeni odmerek zdravila Avastin je 15 mg/kg telesne mase v enkratnem odmerku na 3 tedne. *Napredovali ali/ali metastatski rak ledvičnih celic:* Priporočeni odmerek zdravila Avastin je 10 mg/kg telesne mase v enkratnem odmerku vsaka 2 tedna. *Epiteljski rak jajčnikov, karcinom jajcevodov in primarni peritonealni karcinom: Prvo zdravljenje:* Zdravilo Avastin dodajamo karboplatinu in paklitakselu do 6 ciklov, nato pa ga dajemo samostojno do napredovanja bolezni ali do največ 15 mesecev oziroma do nesprejemljive toksičnosti, kar od tega nastopi prej. Priporočeni odmerek zdravila Avastin je 15 mg/kg telesne mase v enkratnem odmerku na 3 tedne. *Zdravljenje ponovitve bolezni, občutljive na platino:* zdravilo Avastin dajemo v kombinaciji bodisi s karboplatinom in gemcitabinom od 6 do največ 10 ciklov ali v kombinaciji s karboplatinom in paklitakselom od 6 do največ 8 ciklov, nato pa nadaljujemo z dajanjem zdravila Avastin samostojno do napredovanja bolezni. Priporočeni odmerek zdravila Avastin je 15 mg/kg telesne mase v enkratnem odmerku na 3 tedne. *Zdravljenje ponovitve bolezni, ki je rezistentna na platino:* zdravilo Avastin dajemo v kombinaciji z enim od naslednjih zdravil: paklitakselom, topotekanom ali pegiliranim liposomalnim doksorubicinom. Priporočeni odmerek zdravila Avastin je 10 mg/kg telesne mase v enkratnem odmerku na 2 tedna. Kadar zdravilo Avastin dajemo v kombinaciji s topotekanom, je priporočeni odmerek zdravila Avastin 15 mg/kg telesne mase v enkratnem odmerku na 3 tedne. *Rak materničnega vratu:* Zdravilo Avastin se uporablja v kombinaciji z eno od naslednjih shem kemoterapije: paklitakselom in cisplatin ali paklitakselom in topotekan. Priporočeni odmerek zdravila Avastin je 15 mg/kg telesne mase v enkratnem odmerku na 3 tedne. *Pediatrična populacija:* Zdravilo Avastin ni odobreno za uporabo pri bolnikih, mlajših od 18 let. Priporočil o odmerjanju ni mogoče dati. **Kontraindikacije:** Preobčutljivost na učinkovino ali katerokoli pomožno snov, preobčutljivost za produkte ovarijskih celic kitajskega hrčka ali na druga rekombinantna humana ali humanizirana protitelesa, nosečnost. **Posebna opozorila in previdnostni ukrepi:** *Sledljivost:* z namenom izboljšanja sledljivosti bioloških zdravil, je treba jasno zabeležiti ime in številko serije uporabljenega zdravila. *Perforacije in fistule prebavil:* Bolniki so lahko izpostavljeni večjemu tveganju za nastanek perforacije prebavil in žolčnika, če se zdravijo z zdravilom Avastin. Vnetni proces znotraj trebušne votline je lahko dejavnik tveganja za perforacijo prebavil pri bolnikih z metastatskim rakom debelega črevesa ali danke, zato je med zdravljenjem teh bolnikov potrebna previdnost. Predhodno obsevanje je dejavnik tveganja za perforacije prebavil pri bolnicah z rakom materničnega vratu, pri katerih je bolezen prisotna tudi po zaključenem primarnem zdravljenju, se je ponovila ali je metastatska, in se zdravijo z zdravilom Avastin. Zdravljenje opustimo pri bolnikih, pri katerih se je pojavila perforacija prebavil. *Fistule med prebavili in nožnico:* Bolnice z rakom materničnega vratu, pri katerih je bolezen prisotna tudi po zaključenem primarnem zdravljenju, se je ponovila ali je metastatska, in se zdravijo z zdravilom Avastin, imajo večje tveganje za nastanek fistule med nožnico in katerim koli delom prebavil. Predhodno obsevanje je velik dejavnik tveganja za nastanek fistule med prebavili in nožnico. Ponoviter raka v območju predhodnega obsevanja je dodaten pomemben dejavnik tveganja za nastanek fistule med prebavili in nožnico. *Fistule izven prebavil:* Bolniki so lahko izpostavljeni večjemu tveganju za nastanek fistule, če se zdravijo z zdravilom Avastin. *Zapleti pri celjenju ran:* Zdravilo Avastin lahko neugodno vpliva na proces celjenja ran. Zdravljenja ne smemo začeti, če je od večje operacije minilo manj kot 28 dni ali dokler se kirurška rana popolnoma ne zaceli. Zdravljenje z zdravilom Avastin je treba pri bolnikih, pri katerih se razvije nekrotizirajoči fasciitis, nemudoma prekiniti in takoj začeti z ustreznim zdravljenjem. *Hipertenzija:* Incidenca hipertenzije je bila večja pri bolnikih zdravljenih z zdravilom Avastin. Zdravilo Avastin dokončno opustimo, če klinično pomembne hipertenzije ni mogoče ustrezno uravnati z antihipertenzivnimi zdravili, ali če se je pri bolniku pojavila hipertenzivna kriza ali hipertenzivna encefalopatija. *Sindrom posteriorne reverzibilne encefalopatije:* Pri bolnikih, ki so se zdravili z zdravilom Avastin, so redko poročali o pojavu znakov in simptomov, povezanih s sindromom posteriorne reverzibilne encefalopatije. *Proteinurija:* Bolnike z anamnezo hipertenzije spremljа večje tveganje za razvoj proteinurije, če jih zdravimo z zdravilom Avastin. *Arterijska trombembolija:* Bolniki, ki prejemajo zdravilo Avastin skupaj s kemoterapijo in imajo arterijske trombembolične nedelene učinke v anamnezi, sladkorno bolezen ali so stari nad 65 let, imajo med zdravljenjem povečano tveganje za razvoj arterijskih trombemboličnih nedelenih učinkov. Pri zdravljenju teh bolnikov je zato potrebna previdnost. *Venska trombembolija:* Med zdravljenjem z zdravilom Avastin so bolniki lahko podvrženi povečanemu tveganju za razvoj venskih trombemboličnih nedelenih učinkov, vključno s pljučno embolijo. Bolnice z rakom materničnega vratu, pri katerih je bolezen prisotna tudi po zaključenem primarnem zdravljenju, se je ponovila ali je metastatska, in se zdravijo z zdravilom Avastin v kombinaciji s paklitakselom in cisplatinom, imajo lahko večje tveganje za venske trombembolične dogodke. *Krvavitev:* Bolnike, zdravljene z zdravilom Avastin, spremlja večje tveganje za krvavitev, še posebej za krvavitev, povezano s tumorjem. Bolniki z nezdravljenimi zasevki v osrednjem živčevju so bili rutinsko izključeni iz kliničnih preskušanj z zdravilom Avastin. Bolnike je treba spremljati za znake ali simptome krvavitev v osrednjem živčevju in zdravljenje z zdravilom Avastin v primerih intrakranialne krvavitve prekiniti. Varnostni profil zdravila Avastin pred njegovo uvedbo pri bolnikih, ki imajo kongenitalno hemoragično diatezo ali pridobljeno koagulopatijo ali če prejemajo polni odmerek antikoagulantov za zdravljenje trombembolije, ni poznan, ker le-ti niso bili vključeni v klinična preskušanja. Zato je pred začetkom zdravljenja pri teh bolnikih potrebna previdnost. *Krvavitev v pljučih/hemoptize:* Pri bolnikih z nedrobnoceličnim rakom pljuč, ki se zdravijo z zdravilom Avastin, lahko obstaja tveganje za resno in v nekaterih primerih smrtno krvavitev v pljučih/hemoptizo. *Anevrizme in disekcije arterij:* Uporaba zaviralcev poti VEGF pri bolnikih s hipertenzijo ali brez nje lahko spodbudi nastanek anevrizem in/ali disekcij arterij. Pred uvedbo zdravila Avastin je treba to tveganje skrbno preučiti pri bolnikih z dejavniki tveganja, kot sta hipertenzija ali anamneza anevrizme. *Kongestivno srčno popuščanje:* Pri zdravljenju z zdravilom Avastin je pri bolnikih s klinično pomembno kardiovaskularno boleznijo, kot je predhodno obstoječa bolezen koronarnih arterij ali kongestivno srčno popuščanje, potrebna previdnost. *Nevtropenija in okužbe:* Pri bolnikih, zdravljenih z nekaterimi mielotoksičnimi kemoterapevtskimi shemami in zdravilom Avastin, so v primerjavi s samo kemoterapijo opazili večji pojav hude nevtropenije, febrilne nevtropenije ali okužbe s hudo nevtropenijo ali brez nje (vključno s smrtnimi primeri). *Preobčutljivostne reakcije/reakcije pri infundiranju:* Priporočljivo je, da se bolnika med ter po dajanju bevacizumaba skrbno spremlja. Če pride do reakcije, je treba infundiranje prekiniti ter uvesti ustrezno zdravljenje. Sistematska premedikacija ni potrebna. *Ösofagealna/traheoezofagealna fistula:* Pri bolnikih, ki so prejemali zdravljenje na osnovi platine ali taksanov pri NDRP ter metastatskemu raku dojk. *Radioterapija:* Varnost in učinkovitost sočasnega zdravljenja z radioterapijo in zdravilom Avastin nista bili ugotovljeni. *Monoklonska protitelesa z delovanjem na EGFR, v kombinaciji s kemoterapevtskimi shemami, ki vključujejo bevacizumab:* Študij medsebojnega delovanja niso izvedli. Monoklonska protitelesa z delovanjem na EGFR se za zdravljenje metastatskega raka debelega črevesa in danke, ne smejo dajati v kombinaciji s kemoterapevtsko shemo, ki vključuje bevacizumab. **Neželeni učinki:** *Želo pogosti:* febrilna nevtropenija, levkopenija, trombocitopenija, nevtropenija, anoreksija, hipomagneziemija, hiponatriemija, periferna senzorična nevropatija, disartrija, glavobol, disgevzija, bolezni oči, povečano solzenje, hipertenzija, (venska) trombembolija, dispneja, rinitis, epistaksa, kašelj, rektalna krvavitev, stomatitis, konstipacija, diareja, navzea, bruhanje, bolečine v trebuhu, zapleti pri celjenju ran, eksfoliativni dermatitis, suha koža, obarvanje kože, artralgija, mialgija, proteinurija, okvara jajčnikov, astenija, utrujenost, pireksija, bolečina, vnetje sluznic in zmanjšanje telesne mase. Poročanje o domnevnih neželenih učinkih: Poročanje o domnevnih neželenih učinkih zdravila po izdaji dovoljenja za promet je pomembno. Omogoča namreč stalno spremljanje razmerja med koristmi in tveganji zdravila. Od zdravstvenih delavcev se zahteva, da poročajo o katerem koli domnevnem neželenem učinku zdravila na: Javna agencija Republike Slovenije za zdravila in medicinske pripomočke, Sektor za farmakovigilanco, Nacionalni center za farmakovigilanco, Slovenčeva ulica 22, SI-1000 Ljubljana, Tel: +386 (0)8 2000 500, Faks: +386 (0)8 2000 510, e-pošta: h-farmakovigilanca@jazmp.si, spletna stran: www.jazmp.si. Za zagotavljanje sledljivosti zdravila je pomembno, da pri izpolnjevanju obrazca o domnevnih neželenih učinkih zdravila navedete številko serije biološkega zdravila. **Režim izdaje zdravila:** H. **Imetnik dovoljenja za promet:** Roche Registration GmbH, Emil-Barell-Strasse 1, 79639 Grenzach-Wyhlen, Nemčija. **Verzija: 1.0/21**



M-SI-00000181 (v4.0)

# Lonsurf®

trifluridin/tipiracil

# Več časa za trenutke, ki štejejo

## Kolorektalni rak

Zdravilo Lonsurf je indicirano v monoterapiji za zdravljenje odraslih bolnikov z metastatskim kolorektalnim rakom (KRR), ki so bili predhodno že zdravljeni ali niso primerni za zdravljenja, ki so na voljo. Ta vključujejo kemoterapijo na osnovi fluoropirimidina, oksaliplatina in irinotekana, zdravljenje z zaviralci žilnega endotelijskega rastnega dejavnika (VEGF – Vascular Endothelial Growth Factor) in zaviralci receptorjev za epidermalni rastni dejavnik (EGFR – Epidermal Growth Factor Receptor).

## Rak želodca

Zdravilo Lonsurf je indicirano v monoterapiji za zdravljenje odraslih bolnikov z metastatskim rakom želodca vključno z adenokarcinomom gastro-ezofagealnega prehoda, ki so bili predhodno že zdravljeni z najmanj dvema sistemskima režimoma zdravljenja za napredovalo bolezen.

Družba Servier ima licenco družbe Taiho za zdravilo Lonsurf®. Pri globalnem razvoju zdravila sodelujeta obe družbi in ga tržita na svojih določenih področjih.

SERVIER

**Skrajšan povzetek glavnih značilnosti zdravila: Lonsurf 15 mg/6,14 mg filmsko obložene tablete in Lonsurf 20 mg/8,19 mg filmsko obložene tablete**
**SESTAVA*: Lonsurf 15 mg/6,14 mg:** Ena filmsko obložena tableta vsebuje 15 mg trifluridina in 6,14 mg tipiracila (v obliki klorida). **Lonsurf 20 mg/8,19 mg**: Ena filmsko obložena tableta vsebuje 20 mg trifluridina in 8,19 mg tipiracila (v obliki klorida). **TERAPEVTSKE INDIKACIJE*:** Kolorektalni rak – v monoterapiji za zdravljenje odraslih bolnikov z metastatskim kolorektalnim rakom, ki so bili predhodno že zdravljeni ali niso primerni za zdravljenja, ki so na voljo. Ta vključujejo kemoterapijo na osnovi fluoropirimidina, oksaliplatina in irinotekana, zdravljenje z zaviralci žilnega endotelijskega rastnega dejavnika (VEGF – Vascular Endothelial Growth Factor) in zaviralci receptorjev za epidermalni rastni dejavnik (EGFR – Epidermal Growth Factor Receptor). Rak želodca – v monoterapiji za zdravljenje odraslih bolnikov z metastatskim rakom želodca vključno z adenokarcinomom gastro-ezofagealnega prehoda, ki so bili predhodno že zdravljeni z najmanj dvema sistemskima režimoma zdravljenja za napredovalo bolezen. **ODMERJANJE IN NAČIN UPORABE*:** Priporočeni začetni odmerek zdravila Lonsurf pri odraslih je 35 mg/m$^2$/odmerek peroralno dvakrat dnevno na 1. do 5. dan in 8. do 12. dan vsakega 28-dnevnega cikla zdravljenja, najpozneje 1 uro po zaključku jutranjega in večernega obroka (20 mg/m$^2$/odmerek dvakrat dnevno pri bolnikih s hudo ledvično okvaro). Odmerek, izračunan glede na telesno površino, ne sme preseči 80 mg/odmerek. Možne prilagoditve odmerka glede na varnost in prenašanje zdravila: dovoljena so zmanjšanja odmerka na najmanjši odmerek 20 mg/m$^2$ dvakrat dnevno (oz. 15 mg/m$^2$ dvakrat dnevno pri bolnikih s hudo ledvično okvaro). Potem ko je bil odmerek zmanjšan, povečanje ni dovoljeno. **KONTRAINDIKACIJE*:** Preobčutljivost na učinkovini ali katero koli pomožno snov. **OPOZORILA IN PREVIDNOSTNI UKREPI*:** Supresija kostnega mozga: Pred uvedbo zdravljenja in po potrebi za spremljanje toksičnosti zdravila, najmanj pred vsakim ciklom zdravljenja, je treba pregledati celotno krvno sliko. Zdravljenja ne smete začeti, če je absolutno število nevtrofilcev < 1,5 x 10$^9$/l, če je število trombocitov < 75 x 10$^9$/l ali če se je pri bolniku zaradi predhodnih zdravljenj pojavila klinično pomembna nehematološka toksičnost 3. ali 4. stopnje, ki še traja. Bolnike je treba skrbno spremljati zaradi morebitnih okužb, uvesti je treba ustrezne ukrepe, kot je klinično indicirano. Toksičnost za prebavila: Potrebna je uporaba antiemetikov, antidiaroikov ter drugih ukrepov, kot je klinično indicirano. Če je potrebno, prilagodite odmerke. Ledvična okvara: Uporaba zdravila ni priporočljiva pri bolnikih s končno stopnjo ledvične okvare. Bolnike z ledvično okvaro je potrebno med zdravljenjem skrbno spremljati; bolnike z zmerno ali hudo ledvično okvaro je treba zaradi hematološke toksičnosti bolj pogosto spremljati. Jetrna okvara: Uporaba zdravila Lonsurf pri bolnikih z obstoječo zmerno ali hudo jetrno okvaro ni priporočljiva. Proteinurija: Pred začetkom zdravljenja in med njim je priporočljivo spremljanje proteinurije z urinskimi testnimi lističi. Pomožne snovi: Zdravilo vsebuje laktozo. **INTERAKCIJE*:** Previdnost: Zdravila, ki medsebojno delujejo z nukleozidnimi prenašalci CNT1, ENT1 in ENT2, zaviralci OCT2 ali MATE1, substrati humane timidin-kinaze (npr. zidovudin), hormonski kontraceptivi. **PLODNOST*. NOSEČNOST IN DOJENJE*:** Ni priporočljivo. **KONTRACEPCIJA*:** Ženske in moški morajo uporabljati zelo učinkovite metode kontracepcije med zdravljenjem in do 6 mesecev po zaključku zdravljenja. **VPLIV NA SPOSOBNOST VOŽNJE IN UPRAVLJANJA STROJEV*:** Med zdravljenjem se lahko pojavijo utrujenost, omotica ali splošno slabo počutje. **NEŽELENI UČINKI*:** *Zelo pogosti:* nevtropenija, levkopenija, anemija, trombocitopenija, zmanjšan apetit, diareja, navzea, bruhanje, utrujenost. *Pogosti:* okužba spodnjih dihal, febrilna nevtropenija, limfopenija, hipoalbuminemija, disgevzija, periferna nevropatija, dispneja, bolečina v trebuhu, zaprtje, stomatitis, bolezni ustne votline, hiperbilirubinemija, sindrom palmarne plantarne eritrodisestezije, izpuščaj, alopecija, pruritus, suha koža, proteinurija, pireksija, edem, vnetje sluznice, splošno slabo počutje, zvišanje jetrnih encimov, zvišanje alkalne fosfataze v krvi, zmanjšanje telesne mase. *Občasni:* septični šok, infekcijski enteritis, pljučnica, okužba žolčevoda, gripa, okužba sečil, gingivitis, herpes zoster, tinea pedis, okužba s kandido, bakterijska okužba, okužba, nevtropenična sepsa, okužba zgornjih dihal, konjunktivitis, bolečina zaradi raka, pancitopenija, granulocitopenija, monocitopenija, eritropenija, levkocitoza, monocitoza, dehidracija, hiperglikemija, hiperkaliemija, hipokaliemija, hipofosfatemija, hipernatriemija, hiponatriemija, hipokalciemija, protin, anksioznost, nespečnost, nevrotoksičnost, disestezija, hiperestezija, hipoestezija, sinkopa, parestezija, pekoč občutek, letargija, omotica, glavobol, zmanjšana ostrina vida, zamegljen vid, diplopija, katarakta, suho oko, vrtoglavica, neugodje v ušesu, angina pektoris, aritmija, palpitacije, embolija, hipertenzija, hipotenzija, vročinski oblivi, pljučna embolija, plevralni izliv, izcedek iz nosu, disfonija, orofaringealna bolečina, epistaksa, kašelj, hemoragični enterokolitis, krvavitev v prebavilih, akutni pankreatitis, ascites, ileus, subileus, kolitis, gastritis, refluksni gastritis, ezofagitis, moteno praznjenje želodca, abdominalna distenzija, analno vnetje, razjede v ustih, dispepsija, gastroezofagealna refluksna bolezen, proktalgija, bukalni polip, krvavitev dlesni, glositis, parodontalna bolezen, bolezen zob, siljenje na bruhanje, flatulenca, slab zadah, hepatotoksičnost, razširitev žolčnih vodov, luščenje kože, urtikarija, preobčutljivostne reakcije na svetlobo, eritem, akne, hiperhidroza, žulj, bolezni nohtov, otekanje sklepov, artralgija, bolečina v kosteh, mialgija, mišično-skeletna bolečina, mišična oslabelost, mišični krči, bolečina v okončinah, ledvična odpoved, neinfektivni cistitis, motnje mikcije, hematurija, levkociturija, motnje menstruacije, poslabšanje splošnega zdravstvenega stanja, bolečina, občutek spremembe telesne temperature, kseroza, nelagodje, zvišanje kreatinina v krvi, podaljšanje intervala QT na elektrokardiogramu, povečanje mednarodnega umerjenega razmerja (INR), podaljšanje aktiviranega parcialnega tromboplastinskega časa (aPTČ), zvišanje sečnine v krvi, zvišanje laktatne dehidrogenaze v krvi, znižanje celokupnih proteinov, zvišanje C-reaktivnega proteina, zmanjšan hematokrit. *Post-marketinške izkušnje:* intersticijska bolezen pljuč. **PREVELIKO ODMERJANJE*:** Neželeni učinki, o katerih so poročali v povezavi s prevelikim odmerjanjem, so bili v skladu z uveljavljenim varnostnim profilom. Glavni pričakovani zaplet prevelikega odmerjanja je supresija kostnega mozga. **FARMAKODINAMIČNE LASTNOSTI*:** *Farmakoterapevtska skupina:* zdravila z delovanjem na novotvorbe, antimetaboliti, oznaka ATC: L01BC59. Zdravilo Lonsurf sestavljata antineoplastični timidinski nukleozidni analog, trifluridin, in zaviralec timidin-fosforilaze (TPaze), tipiracilijev klorid. Po privzemu v rakave celice timidin-kinaza fosforilira trifluridin. Ta se v celicah nato presnovi v substrat deoksiribonukleinske kisline (DNA), ki se vgradi neposredno v DNA ter tako preprečuje celično proliferacijo. TPaza hitro razgradi trifluridin in njegova presnova po peroralni uporabi je hitra zaradi učinka prvega prehoda, zato je v zdravilo vključen zaviralec TPaze, tipiracilijev klorid. **PAKIRANJE*:** 20 filmsko obloženih tablet. **NAČIN PREDPISOVANJA IN IZDAJE ZDRAVILA:** Rp/Spec. **Imetnik dovoljenja za promet:** Les Laboratoires Servier, 50, rue Carnot, 92284 Suresnes cedex, Francija. Številka dovoljenja za promet z zdravilom: EU/1/16/1096/001 (Lonsurf 15 mg/6,14 mg), EU/1/16/1096/004 (Lonsurf 20 mg/8,19 mg). **Datum zadnje revizije besedila: december 2020. *Pred predpisovanjem preberite celoten povzetek glavnih značilnosti zdravila. Celoten povzetek glavnih značilnosti zdravila in podrobnejše informacije so na voljo pri: Servier Pharma d.o.o., Podmilščakova ulica 24, 1000 Ljubljana, tel: 01 563 48 11, www.servier.si.**

Datum priprave informacije: december 2020.
LON AD2 C1 2020-21. Samo za strokovno javnost.

# Instructions for authors

**The editorial policy**

Radiology and Oncology is a multidisciplinary journal devoted to the publishing original and high quality scientific papers and review articles, pertinent to diagnostic and interventional radiology, computerized tomography, magnetic resonance, ultrasound, nuclear medicine, radiotherapy, clinical and experimental oncology, radiobiology, medical physics and radiation protection. Therefore, the scope of the journal is to cover beside radiology the diagnostic and therapeutic aspects in oncology, which distinguishes it from other journals in the field.

The Editorial Board requires that the paper has not been published or submitted for publication elsewhere; the authors are responsible for all statements in their papers. Accepted articles become the property of the journal and, therefore cannot be published elsewhere without the written permission of the editors.

**Submission of the manuscript**

The manuscript written in English should be submitted to the journal via online submission system Editorial Manager available for this journal at: **www.radioloncol.com**.

In case of problems, please contact Sašo Trupej at **saso.trupej@computing.si** or the Editor of this journal at **gsersa@onko-i.si**

All articles are subjected to the editorial review and when the articles are appropriated they are reviewed by independent referees. In the cover letter, which must accompany the article, the authors are requested to suggest 3-4 researchers, competent to review their manuscript. However, please note that this will be treated only as a suggestion; the final selection of reviewers is exclusively the Editor's decision. The authors' names are revealed to the referees, but not vice versa.

Manuscripts which do not comply with the technical requirements stated herein will be returned to the authors for the correction before peer-review. The editorial board reserves the right to ask authors to make appropriate changes of the contents as well as grammatical and stylistic corrections when necessary. Page charges will be charged for manuscripts exceeding the recommended length, as well as additional editorial work and requests for printed reprints.

Articles are published printed and on-line as the open access (**https://content.sciendo.com/raon**).

All articles are subject to 900 EUR + VAT publication fee. Exceptionally, waiver of payment may be negotiated with editorial office, upon lack of funds.

Manuscripts submitted under multiple authorship are reviewed on the assumption that all listed authors concur in the submission and are responsible for its content; they must have agreed to its publication and have given the corresponding author the authority to act on their behalf in all matters pertaining to publication. The corresponding author is responsible for informing the coauthors of the manuscript status throughout the submission, review, and production process.

**Preparation of manuscripts**

Radiology and Oncology will consider manuscripts prepared according to the Uniform Requirements for Manuscripts Submitted to Biomedical Journals by International Committee of Medical Journal Editors (www.icmje.org). The manuscript should be written in grammatically and stylistically correct language. Abbreviations should be avoided. If their use is necessary, they should be explained at the first time mentioned. The technical data should conform to the SI system. The manuscript, excluding the references, tables, figures and figure legends, must not exceed 5000 words, and the number of figures and tables is limited to 8. Organize the text so that it includes: Introduction, Materials and methods, Results and Discussion. Exceptionally, the results and discussion can be combined in a single section. Start each section on a new page, and number each page consecutively with Arabic numerals. For ease of review, manuscripts should be submitted as a single column, double-spaced text.and must have continuous line numbering.

*The Title page* should include a concise and informative title, followed by the full name(s) of the author(s); the institutional affiliation of each author; the name and address of the corresponding author (including telephone, fax and E-mail), and an abbreviated title (not exceeding 60 characters). This should be followed by the abstract page, summarizing in less than 250 words the reasons for the study, experimental approach, the major findings (with specific data if possible), and the principal conclusions, and providing 3-6 key words for indexing purposes. Structured abstracts are required. Slovene authors are requested to provide title and the abstract in Slovene language in a separate file. The text of the research article should then proceed as follows:

*Introduction* should summarize the rationale for the study or observation, citing only the essential references and stating the aim of the study.

*Materials and methods* should provide enough information to enable experiments to be repeated. New methods should be described in details.

*Results* should be presented clearly and concisely without repeating the data in the figures and tables. Emphasis should be on clear and precise presentation of results and their significance in relation to the aim of the investigation.

*Discussion* should explain the results rather than simply repeating them and interpret their significance and draw conclusions. It should discuss the results of the study in the light of previously published work.

**Charts, Illustrations, Images and Tables**

Charts, Illustrations, Images and Tables must be numbered and referred to in the text, with the appropriate location indicated. Charts, Illustrations and Images, provided electronically, should be of appropriate quality for good reproduction. Illustrations and charts must be vector image, created in CMYK color space, preferred font "Century Gothic", and saved as .AI, .EPS or .PDF format. Color charts, illustrations and Images are encouraged, and are published without additional charge. Image size must be 2.000 pixels on the longer side and saved as .JPG (maximum quality) format. In Images, mask the identities of the patients. Tables should be typed double-spaced, with a descriptive title and, if appropriate, units of numerical measurements included in the column heading. The files with the figures and tables can be uploaded as separate files.

**References**

References must be numbered in the order in which they appear in the text and their corresponding numbers quoted in the text. Authors are responsible for the accuracy of their references. References to the Abstracts and Letters to the Editor must be identified as such. Citation of papers in preparation or submitted for publication, unpublished observations, and personal communications should not be included in the reference list. If essential, such material may be incorporated in the appropriate place in the text. References follow the style of Index Medicus, DOI number (if exists) should be included.

All authors should be listed when their number does not exceed six; when there are seven or more authors, the first six listed are followed by "et al.". The following are some examples of references from articles, books and book chapters:

Dent RAG, Cole P. In vitro maturation of monocytes in squamous carcinoma of the lung. *Br J Cancer* 1981; **43:** 486-95. doi: 10.1038/bjc.1981.71

Chapman S, Nakielny R. *A guide to radiological procedures*. London: Bailliere Tindall; 1986.

Evans R, Alexander P. Mechanisms of extracellular killing of nucleated mammalian cells by macrophages. In: Nelson DS, editor. *Immunobiology of macrophage.* New York: Academic Press; 1976. p. 45-74.

**Authorization for the use of human subjects or experimental animals**

When reporting experiments on human subjects, authors should state whether the procedures followed the Helsinki Declaration. Patients have the right to privacy; therefore the identifying information (patient's names, hospital unit numbers) should not be published unless it is essential. In such cases the patient's informed consent for publication is needed, and should appear as an appropriate statement in the article. Institutional approval and Clinical Trial registration number is required. Retrospective clinical studies must be approved by the accredited Institutional Review Board/Committee for Medical Ethics or other equivalent body. These statements should appear in the Materials and methods section.

The research using animal subjects should be conducted according to the EU Directive 2010/63/EU and following the Guidelines for the welfare and use of animals in cancer research (Br J Cancer 2010; 102: 1555 – 77). Authors must state the committee approving the experiments, and must confirm that all experiments were performed in accordance with relevant regulations.

These statements should appear in the Materials and methods section (or for contributions without this section, within the main text or in the captions of relevant figures or tables).

**Transfer of copyright agreement**

For the publication of accepted articles, authors are required to send the License to Publish to the publisher on the address of the editorial office. A properly completed License to Publish, signed by the Corresponding Author on behalf of all the authors, must be provided for each submitted manuscript.

The non-commercial use of each article will be governed by the Creative Commons Attribution-NonCommercial-NoDerivs license.

**Conflict of interest**

When the manuscript is submitted for publication, the authors are expected to disclose any relationship that might pose real, apparent or potential conflict of interest with respect to the results reported in that manuscript. Potential conflicts of interest include not only financial relationships but also other, non-financial relationships. In the Acknowledgement section the source of funding support should be mentioned. The Editors will make effort to ensure that conflicts of interest will not compromise the evaluation process of the submitted manuscripts; potential editors and reviewers will exempt themselves from review process when such conflict of interest exists. The statement of disclosure must be in the Cover letter accompanying the manuscript or submitted on the form available on **www.icmje.org/coi_disclosure.pdf**

**Page proofs**

Page proofs will be sent by E-mail to the corresponding author. It is their responsibility to check the proofs carefully and return a list of essential corrections to the editorial office within three days of receipt. Only grammatical corrections are acceptable at that time.

**Open access**

Papers are published electronically as open access on **https://content.sciendo.com/raon**, also papers accepted for publication as E-ahead of print.

# ZAUPANJE, ZGRAJENO NA MOČI

## Za zdravljenje lokalno napredovalega ali metastatskega HR+/HER2- raka dojk:

- v kombinaciji z zaviralcem aromataze,
- v kombinaciji s fulvestrantom pri ženskah, ki so prejele predhodno endokrino zdravljenje.

Pri ženskah v pred- in perimenopavzi je treba endokrino zdravljenje kombinirati z agonistom gonadoliberina (*LHRH – Luteinizing Hormone-Releasing Hormone*).

### BISTVENI PODATKI IZ POVZETKA GLAVNIH ZNAČILNOSTI ZDRAVILA

**IBRANCE 75 mg, 100 mg, 125 mg trde kapsule**[1]
**IBRANCE 75 mg, 100 mg, 125 mg filmsko obložene tablete**[2]

▼ Za to zdravilo se izvaja dodatno spremljanje varnosti. Tako bodo hitreje na voljo nove informacije o njegovi varnosti. Zdravstvene delavce naprošamo, da poročajo o kateremkoli domnevnem neželenem učinku zdravila. Glejte poglavje 4.8 povzetka glavnih značilnosti zdravila, kako poročati o neželenih učinkih.

**Sestava in oblika zdravila:** (1) Ena trda kapsula vsebuje 75 mg, 100 mg ali 125 mg palbocikliba in 56 mg, 74 mg ali 93 mg laktoze (v obliki monohidrata). (2) Ena filmsko obložena tableta vsebuje 75 mg, 100 mg ali 125 mg palbociklib. **Indikacije:** Zdravljenje lokalno napredovalega ali metastatskega na hormonske receptorje (HR – *Hormone Receptors*) pozitivnega in na receptorje humanega epidermalnega rastnega faktorja 2 (HER2 – *Human Epidermal growth factor Receptor 2*) negativnega raka dojk: v kombinaciji z zaviralcem aromataze ali v kombinaciji s fulvestrantom pri ženskah, ki so prejele predhodno endokrino zdravljenje. Pri ženskah v pred- in perimenopavzi je treba endokrino zdravljenje kombinirati z agonistom gonadoliberina. **Odmerjanje in način uporabe:** Zdravljenje mora uvesti in nadzorovati zdravnik, ki ima izkušnje z uporabo zdravil za zdravljenje rakavih bolezni. Priporočeni odmerek je 125 mg enkrat na dan 21 zaporednih dni, sledi 7 dni brez zdravljenja (shema 3/1), celotni cikel traja 28 dni. Zdravljenje je treba nadaljevati, dokler ima bolnik od zdravljenja klinično korist ali dokler se ne pojavi nesprejemljiva toksičnost. Pri sočasnem dajanju s palbociklibom je treba zaviralec aromataze dajati v skladu s shemo odmerjanja, ki je navedena v Povzetku glavnih značilnosti zdravila (PGZZ). Pri sočasnem dajanju s palbociklibom je priporočeni odmerek fulvestranta 500 mg intramuskularno 1., 15. in 29. dan ter nato enkrat na mesec, glejte PGZZ za fulvestrant. Prilagajanja odmerkov: Za prilagajanja odmerkov zaradi hematološke toksičnosti glejte preglednico 2, zaradi nehematološke toksičnosti pa preglednico 3 v PGZZ-ju. Pri bolnikih s hudo intersticijsko boleznijo pljuč (ILD)/pnevmonitisom je treba zdravljenje trajno prekiniti. Posebne skupine bolnikov: *Starejši:* Prilagajanje odmerka ni potrebno. *Okvara jeter ali ledvic*: Pri bolnikih z blago ali zmerno okvaro jeter ali blago, zmerno ali hudo okvaro ledvic prilagajanje odmerka ni potrebno. Pri bolnikih s hudo okvaro jeter je priporočeni odmerek 75 mg enkrat na dan po shemi 3/1. *Pediatrična populacija*: Varnost in učinkovitost pri otrocih in mladostnikih, starih < 18 let, nista bili dokazani. Način uporabe: Peroralna uporaba. (1) Jemanje s hrano, priporočljivo z obrokom. (2) Tablete se lahko jemlje s hrano ali brez nje. (1, 2) Ne smemo jemati z grenivko ali grenivkinim sokom. Kapsule oz. tablete zdravila je treba pogoltniti cele. **Kontraindikacije:** Preobčutljivost na učinkovino ali katerokoli pomožno snov. Uporaba pripravkov s šentjanževko. **Posebna opozorila in previdnostni ukrepi:** Ženske v pred- in perimenopavzi: Kadar zdravilo uporabljamo v kombinaciji z zaviralcem aromataze je obvezna ovarijska ablacija ali supresija z agonistom gonadoliberina. Hematološke bolezni: Pri nevtropeniji stopnje 3 ali 4 je priporočljiva prekinitev odmerjanja, zmanjšanje odmerka ali odložitev začetka ciklov zdravljenja, bolnike pa je treba ustrezno spremljati. ILD/pnevmonitis: Pri bolnikih se lahko pojavita huda, življenjsko ogrožajoča ali smrtna ILD in/ali pnevmonitis, kadar zdravilo jemljejo v kombinaciji z endokrinim zdravljenjem. Bolnike je treba spremljati glede pljučnih simptomov, ki kažejo na ILD/pnevmonitis (npr. hipoksija, kašelj, dispneja), in pri pojavu novih ali poslabšanju respiratornih simptomov oz. sumu na ILD/pnevmonitis zdravljenje prekiniti. Okužbe: Zdravilo lahko poveča nagnjenost k okužbam, zato je bolnike treba spremljati glede znakov in simptomov okužbe ter jih ustrezno zdraviti. Okvara jeter ali ledvic: Pri bolnikih z zmerno ali hudo okvaro jeter ali ledvic je treba zdravilo uporabljati previdno in skrbno spremljati znake toksičnosti. (1) Laktoza: Vsebuje laktozo. Bolniki z redko dedno intoleranco za galaktozo, odsotnostjo encima laktaze ali malabsorpcijo glukoze-galaktoze ne smejo jemati tega zdravila. **Medsebojno delovanje z drugimi zdravili in druge oblike interakcij:** Učinki drugih zdravil na farmakokinetiko palbociklibа: *Zaviralci CYP3A:* Sočasni uporabi močnih zaviralcev CYP3A, med drugim klaritromicina, indinavirja, itrakonazola, ketokonazola, lopinavirja/ritonavirja, nefazodona, nelfinavirja, posakonazola, sakvinavirja, telaprevirja, telitromicina, vorikonazola in grenivke ali grenivkinega soka, se je treba izogibati. *Induktorji CYP3A:* Sočasni uporabi močnih induktorjev CYP3A, med drugim karbamazepina, enzalutamida, fenitoina, rifampicina in šentjanževke, se je treba izogibati. Učinek zdravil za zmanjševanje kisline: (1) Če palbociklib zaužijemo s hrano, klinično pomembnega učinka na izpostavljenost palbociklibu ni pričakovati. (2) Klinično pomembnega učinka na izpostavljenost palbociklibu ni pričakovati. Učinki palbociklibа na farmakokinetiko drugih zdravil: Pri sočasni uporabi bo morda treba zmanjšati odmerek občutljivih substratov CYP3A z ozkim terapevtskim indeksom (npr. alfentanil, ciklosporin, dihidroergotamin, ergotamin, everolimus, fentanil, pimozid, kinidin, sirolimus in takrolimus), saj IBRANCE lahko poveča izpostavljenost tem zdravilom. Študije *in vitro* s prenašalci: Palbociklib lahko zavira prenos, posredovan s P-gp v prebavilih in beljakovino odpornosti pri raku dojk (BCRP). Uporaba palbociklibа z zdravili, ki so substrati P-gp (npr. digoksin, dabigatran, kolhicin) ali BCRP (npr. pravastatin, rosuvastatin, sulfasalazin) lahko poveča njihov terapevtski učinek in neželene učinke. Palbociklib lahko zavira privzemni prenašalec organskih kationov OCT1. **Plodnost, nosečnost in dojenje:** Med zdravljenjem in vsaj 3 tedne (ženske) oziroma 14 tednov (moški) po koncu zdravljenja je treba uporabljati ustrezne kontracepcijske metode. Zdravila ne uporabljajte pri nosečnicah in ženskah v rodni dobi, ki ne uporabljajo kontracepcije. Bolnice, ki prejemajo palbociklib, ne smejo dojiti. Zdravljenje s palbociklibom lahko ogrozi plodnost pri moških. Pred začetkom zdravljenja naj moški zato razmislijo o hrambi sperme. **Vpliv na sposobnost vožnje in upravljanja s stroji:** Ima blag vpliv na sposobnost vožnje in upravljanja strojev. Potrebna je previdnost. **Neželeni učinki:** Zelo pogosti: okužbe, nevtropenija, levkopenija, anemija, trombocitopenija, pomanjkanje teka, stomatitis, navzea, diareja, bruhanje, izpuščaj, alopecija, suha koža, utrujenost, astenija, pireksija, povečane vrednosti ALT/AST. **Način in režim izdaje:** Rp/Spec - Predpisovanje in izdaja zdravila je le na recept zdravnika specialista ustreznega področja medicine ali od njega pooblaščenega zdravnika. **Imetnik dovoljenja za promet:** Pfizer Europe MA EEIG, Boulevard de la Plaine 17, 1050 Bruxelles, Belgija. **Datum zadnje revizije besedila:** 09.11.2020

**Pred predpisovanjem se seznanite s celotnim povzetkom glavnih značilnosti zdravila.**

PP-IBR-EEP-0188 Datum priprave: januar 2021. Samo za strokovno javnost.
**HR+/HER2-** = pozitiven na hormonske receptorje in negativen na receptorje humanega epidermalnega rastnega faktorja 2.
**Literatura:** Povzetek glavnih značilnosti zdravila Ibrance, 9.11.2020.

Pfizer

Pfizer Luxembourg SARL, GRAND DUCHY OF LUXEMBOURG,
51, Avenue J. F. Kennedy, L-1855
Pfizer, podružnica Ljubljana, Letališka cesta 29a, Ljubljana

IBRANCE® palbociklib

Radiology and Oncology | Ljubljana | Slovenia | https://content.sciendo.com/raon

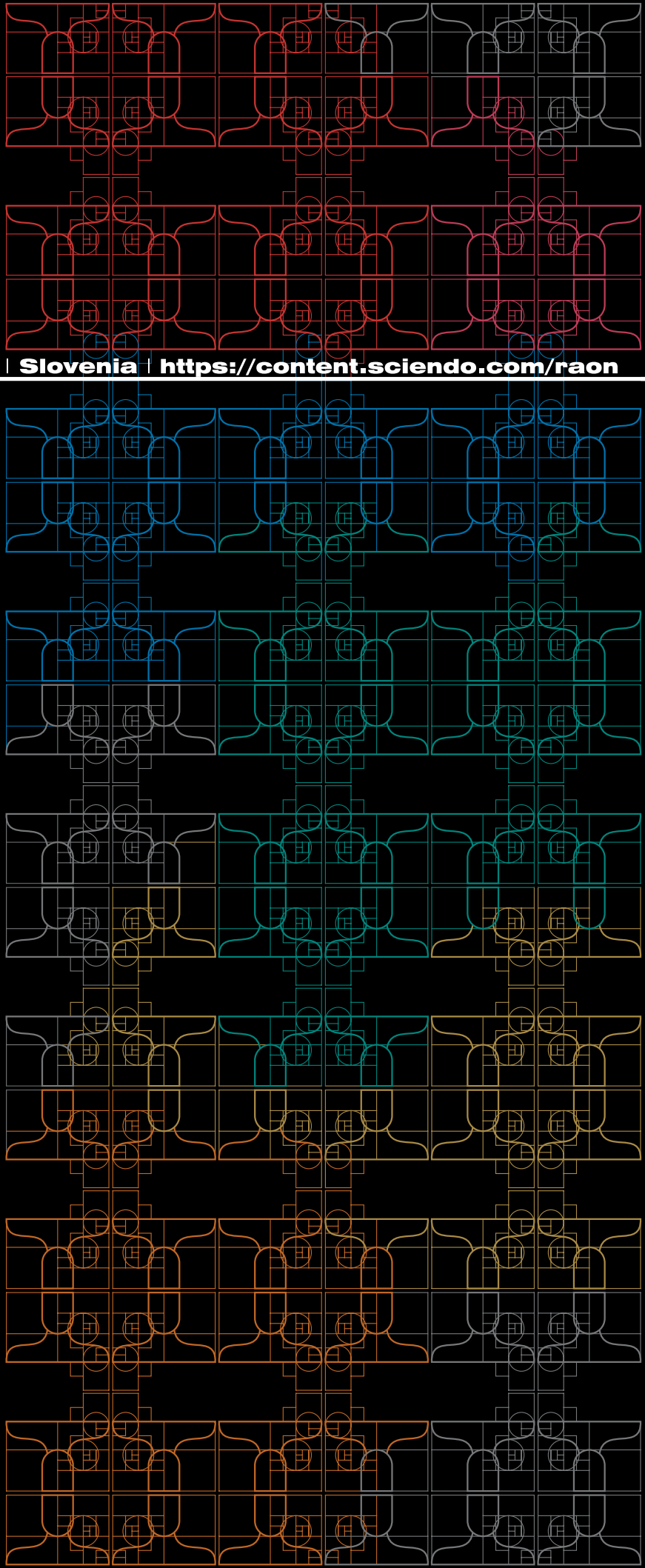

ISSN 1318 - 2099